МОРСКОЙ БИОЛОГИЧЕСКИЙ ЖУРНАЛ
MARINE BIOLOGICAL JOURNAL

включён в перечень рецензируемых научных изданий, рекомендованных ВАК Российской Федерации.
Журнал реферируется международной библиографической и реферативной базой данных Scopus (Elsevier),
международной информационной системой по водным наукам и рыболовству ASFA (ProQuest),
Всероссийским институтом научно-технической информации (ВИНИТИ),
а также Российским индексом научного цитирования (РИНЦ) на базе Научной электронной библиотеки elibrary.ru.
Все материалы проходят независимое двойное слепое рецензирование.

Адрес учредителя, издателя и редакции:
ФИЦ «Институт биологии южных морей имени А. О. Ковалевского РАН».
Пр. Нахимова, 2, Севастополь, 299011, РФ.
Тел.: +7 8692 54-41-10.
E-mail: *mbj@imbr-ras.ru*.
Сайт журнала: https://mbj.marine-research.org.

Адрес соиздателя:
Зоологический институт РАН.
Университетская наб., 1, Санкт-Петербург, 199034, РФ.

Founder, Publisher and Editorial Office address:
A. O. Kovalevsky Institute of Biology of the Southern Seas of Russian Academy of Sciences.
2 Nakhimov ave., Sevastopol, 299011, Russia.
Tel.: +7 8692 54-41-10.
E-mail: *mbj@imbr-ras.ru*.
Journal website: https://mbj.marine-research.org.

Co-publisher address:
Zoological Institute Russian Academy of Sciences.
Universitetskaya emb., 1, St.-Petersburg, 199034, Russia.

A. O. KOVALEVSKY INSTITUTE OF BIOLOGY OF THE SOUTHERN SEAS OF RAS
ZOOLOGICAL INSTITUTE OF RAS

МОРСКОЙ БИОЛОГИЧЕСКИЙ ЖУРНАЛ

MARINE BIOLOGICAL JOURNAL

2020 Vol. 5 no. 2

Established in February 2016 SCIENTIFIC JOURNAL *4 issues per year*

CONTENTS

Scientific communications

Notes

Chronicle and information

1871
ИнБЮМ – IBSS

Морской биологический журнал
Marine Biological Journal
2020, vol. 5, no. 2, pp. 3–11
https://mbj.marine-research.org

SCIENTIFIC COMMUNICATIONS

UDC 595.34:591.13:582.26/.27

PRODUCTION CHARACTERISTICS OF THE COPEPODS *ARCTODIAPTOMUS SALINUS* AND *CALANIPEDA AQUAEDULCIS* BEING FED WITH A MIXTURE OF MICROALGAE DINOPHYCEAE AND PRYMNESIOPHYCEA

© 2020 **L. O. Aganesova**

A. O. Kovalevsky Institute of Biology of the Southern Seas of RAS, Sevastopol, Russian Federation
E-mail: *la7risa@gmail.com*

Received by the Editor 03.09.2019; after revision 14.02.2020;
accepted for publication 26.06.2020; published online 30.06.2020.

The ubiquitous copepod species *Arctodiaptomus salinus* (Daday, 1885) and *Calanipeda aquaedulcis* (Krichagin, 1873) are important components of food chains of numerous fresh- and saltwater areas. These copepods are suitable for feeding larvae of both marine and freshwater fish species; however, influence of nutrition on the production characteristics of these species is not well understood. Previously we determined that monocultures of microalgae Dinophyceae and Prymnesiophyceae are optimal feeding objects for egg production by females of *A. salinus* and *C. aquaedulcis*, survival rate, and development time of these copepods throughout ontogenesis. The aim of this work was to determine the production characteristics of copepods *A. salinus* and *C. aquaedulcis* under optimal temperature conditions depending on the model of the feeding with a mixture of microalgae Dinophyceae and Prymnesiophyceae. The highest survival rates of *A. salinus* from the naupliar stage to the adult one (93–95 %) were observed when copepods were fed with a monoculture of microalga *Isochrysis galbana* (Parke, 1949) or a mixture *I. galbana* + *Prorocentrum cordatum* (Ostenfeld) J. D. Dodge, 1975; the shortest development time (19 days) – when copepods were fed with a mixture of three microalgae *I. galbana* + *P. cordatum* + *Prorocentrum micans* (Ehrenberg, 1834). The shortest development time of *C. aquaedulcis* from the naupliar stage to the adult one (13 days) was observed when copepods were fed with a mixture of microalgae *I. galbana* + *P. cordatum*. The shortest duration of the naupliar stage of development of both copepod species was observed when their diet included *I. galbana* as a monoculture or one of mixture components. During the copepodit stage, the pattern remains the same, only with *P. cordatum*. The maximum absolute fecundity of *C. aquaedulcis* reached 24 eggs per female (*I. galbana*), of *A. salinus* – 16 eggs per female (*P. cordatum*). Egg hatching of *C. aquaedulcis* when being fed with both monocultures of microalgae *P. cordatum* and *I. galbana* and with their mixture reached 100 %. The highest egg hatching rate for *A. salinus* was reached only when copepod females were fed with a mixture of microalgae *I. galbana* + *P. micans*.

Keywords: copepods, *Arctodiaptomus salinus*, *Calanipeda aquaedulcis*, survival, development, reproduction, microalgae, mixture of microalgae, Dinophyceae, Prymnesiophyceae

For this experimental work, two Calanoida representatives were selected as model species: brackish water copepods *Arctodiaptomus salinus* (Daday, 1885) and *Calanipeda aquaedulcis* (Krichagin, 1873). One of the main advantages of using these species as food objects in aquaculture is the possibility of using them for feeding both marine and freshwater larvae of valuable fish species, since both copepod species can withstand a wide range of salinity (up to 50–60 ‰) [4]. Among other technological advantages

it can be distinguished that, unlike marine Calanoida (for example, those of genus *Acartia*), these species lack cannibalism (neither their own eggs nor early naupliar stages are eaten by adult copepods). As a result, naupliar, copepodit, and adult stages can be grown together.

The main criteria for microalgae nutritional value for copepods are: development time of individuals when being fed with the same microalgae species; survival rate during embryonic development (egg hatching rate); success of moults during the transition from one life stage to another; success of metamorphosis during the transition from the last naupliar stage to the first copepodit one; time of reaching sexual maturity; female fecundity (egg production rate); survival rate before feeding naupliar stage, and successful transition of nauplii to exogenous nutrition.

The results of our previous studies [1 ; 3] showed that monocultures of microalgae Dinophyceae and Prymnesiophyceae are optimal food objects for egg production by *A. salinus* and *C. aquaedulcis* females, as well as copepod survival and development rates throughout ontogenesis. We identified temperature optimal values of copepod cultivation (+20…+22 °C for *A. salinus* and +20…+26 °C for *C. aquaedulcis* [2]), at which the overall development time significantly reduces and the highest values of survival rate and fecundity of individuals are obtained.

The aim of this work was to determine production characteristics of copepods *A. salinus* and *C. aquaedulcis* under optimal temperature conditions when being fed with a mixture of microalgae Dinophyceae and Prymnesiophyceae.

MATERIAL AND METHODS

The experiments were carried out on laboratory cultures of copepods *A. salinus* and *C. aquaedulcis* at a temperature of (21 ± 1.5) °C. As food for *A. salinus*, a mixture of microalgae was used: Prymnesiophyceae (*Isochrysis galbana* Parke, 1949, of 3–6 μm) and Dinophyceae (*Prorocentrum cordatum* (Ostenfeld) J. D. Dodge, 1975, of 12–14 μm; *Prorocentrum micans* Ehrenberg, 1834, of 28–42 μm). As food for *C. aquaedulcis*, a mixture of microalgae *I. galbana* + *P. cordatum* was used. Concentration of food was maintained at the level of 0.02–0.08 mg of dry weight per ml (microalgae ratio in a mixture was equalized by the dry weight of its components). The microalgae used in the experiments were grown in a cumulative mode on the basis of sterilized Black Sea water saturated with Walne's medium [7], at a temperature of (24 ± 1.5) °C and round-the-clock illuminance with an intensity of 5000 lx. Adaptation of copepods to nutrition with a specific microalgae mixture was carried out for at least 2 to 3 weeks.

Black Sea water [(17.8 ± 0.2) ‰] was used as a culture medium (microalgae suspension in sterilized seawater) for copepods; this water was subjected to rough purification, settled, then mechanically purified by sequential filtration through cartridge filters (with pore sizes of 10, 5, and 1 μm), sterilized by ultraviolet, and pasteurized twice. For the experiments, 50-ml glass cylindrical vessels were used, which were illuminated around the clock with an intensity of 2000 lx. Complete replacement of culture medium in the experimental vessels was carried out every 2–3 days.

To determine copepod development time, survival rate, and percentage of males and females, we transplanted from laboratory cultures of *C. aquaedulcis* and *A. salinus*, being adapted to nutrition with a specific microalgae mixture, 15 hatched N1 nauplii (see the explanation below) (6 replicates for each microalgae mixture) of each copepod species into 50-ml vessels with culture medium. The experiments were carried out at a copepod density in vessels of 0.3 ind. per ml.

Copepod survival rate was assessed as the percentage of individuals that survived all stages from the first naupliar (N1) to adult one (C6). Copepod development time was identified as an average time interval for the development of individuals from N1 to reaching C6.

In experiments to determine reproductive characteristics of *A. salinus* and *C. aquaedulcis* from laboratory cultures of copepods adapted for being fed with a specific mixture of microalgae, 1 female (of each copepod species) with eggs was transplanted in 50-ml cylindrical glass vessels (n = 25 for each microalgae mixture). The number of eggs in the laying (absolute fecundity) and hatched viable nauplii (egg hatching rate) were calculated. All observations of copepods (every 1–3 days) were carried out intravitally using MBS-12 microscope at a magnification of 2×8 and 4×8.

For comparison, the data on the reproductive characteristics of *A. salinus* and *C. aquaedulcis* were used when copepods were fed with monocultures of microalgae Dinophyceae and Prymnesiophyceae. Those data were obtained in previous works [1 ; 3].

For all the data obtained, arithmetic means (M), confidence interval (95 % CI), standard deviations (SD), and reliability (p) of differences in sample means using Student's t-test were calculated.

RESULTS

The survival rate of *C. aquaedulcis* and *A. salinus* throughout moults from stage N1 to C6 varied depending on microalgae species the copepods were fed with. The survival rate of *C. aquaedulcis* was of 92.5 % when being fed with *P. cordatum*; of 83 % – with *I. galbana*; of 89 % – with a mixture *I. galbana* + *P. cordatum* (Fig. 1). The minimum survival rate of *A. salinus* throughout all the moults from stage N1 to C6 (68.6 %) was observed when being fed with *P. cordatum*; the maximum survival rate – when being fed with *I. galbana* (94.5 %) and with a mixture of microalgae *I. galbana* + *P. cordatum* (93 %) (Fig. 1).

The influence of microalgae species on development time of copepod stages was identified (Fig. 2). When being fed with microalgae *I. galbana* and *P. cordatum*, development time of *C. aquaedulcis* was of 14 days; when being fed with a mixture *I. galbana* + *P. cordatum*, it was of 13 days. The shortest development time of naupliar stage (6 days) was obtained when copepods were fed with *I. galbana* and *I. galbana* + *P. cordatum*. The shortest development time of copepodit stage of *C. aquaedulcis* (C1–5) (7 days) was obtained when being fed with *P. cordatum* and *I. galbana* + *P. cordatum*.

Development time from the first naupliar stage to the adult one of another copepod species – *A. salinus* – turned out to be significantly longer than that of *C. aquaedulcis*, when being fed with all microalgae species proposed. The development time of *A. salinus* when being fed with monocultures *I. galbana* and *P. cordatum*, as well as a mixture *I. galbana* + *P. cordatum* was of 20 days. The shortest development time (19 days) was noted when copepods were fed with a mixture of three microalgae *I. galbana* + *P. cordatum* + *P. micans*. When being fed with a mixture *I. galbana* + *P. micans* and with a monoculture *P. micans*, the development time of copepods increased to 21 and 22 days, respectively. The longest development time (25 days) was observed when copepods were fed with a mixture *P. cordatum* + *P. micans*.

The shortest time of *A. salinus* naupliar stage of development was of 7 days (when being fed with *I. galbana* and mixtures of microalgae *I. galbana* + *P. cordatum* + *P. micans* and *I. galbana* + *P. micans*), and the longest was of 10 days (with *P. cordatum* + *P. micans*). The shortest time of *A. salinus* copepodit stage of development (C1–5) was of 12 days (when being fed with *P. cordatum* and mixtures of microalgae *I. galbana* + *P. cordatum* + *P. micans* and *I. galbana* + *P. cordatum*), and the longest was of 15 days (when being fed with *P. cordatum* + *P. micans*).

The percentage of males and females of *A. salinus* and *C. aquaedulcis* when reaching the adult stage of development also varied depending on microalgae species the copepods were fed with (Table 1). For *C. aquaedulcis*, the lowest percentage of males (21 %) was obtained (reliably) when copepods were fed with *I. galbana*; the proportion increased to 43 % when copepods were fed with *P. cordatum* and a mixture

I. galbana + *P. cordatum*. For *A. salinus*, the highest percentage of males (70 %) was obtained (unreliably) when copepods were fed with a mixture *I. galbana* + *P. micans*, and the lowest (45–48 %) – when being fed with monocultures *P. micans* and *P. cordatum*.

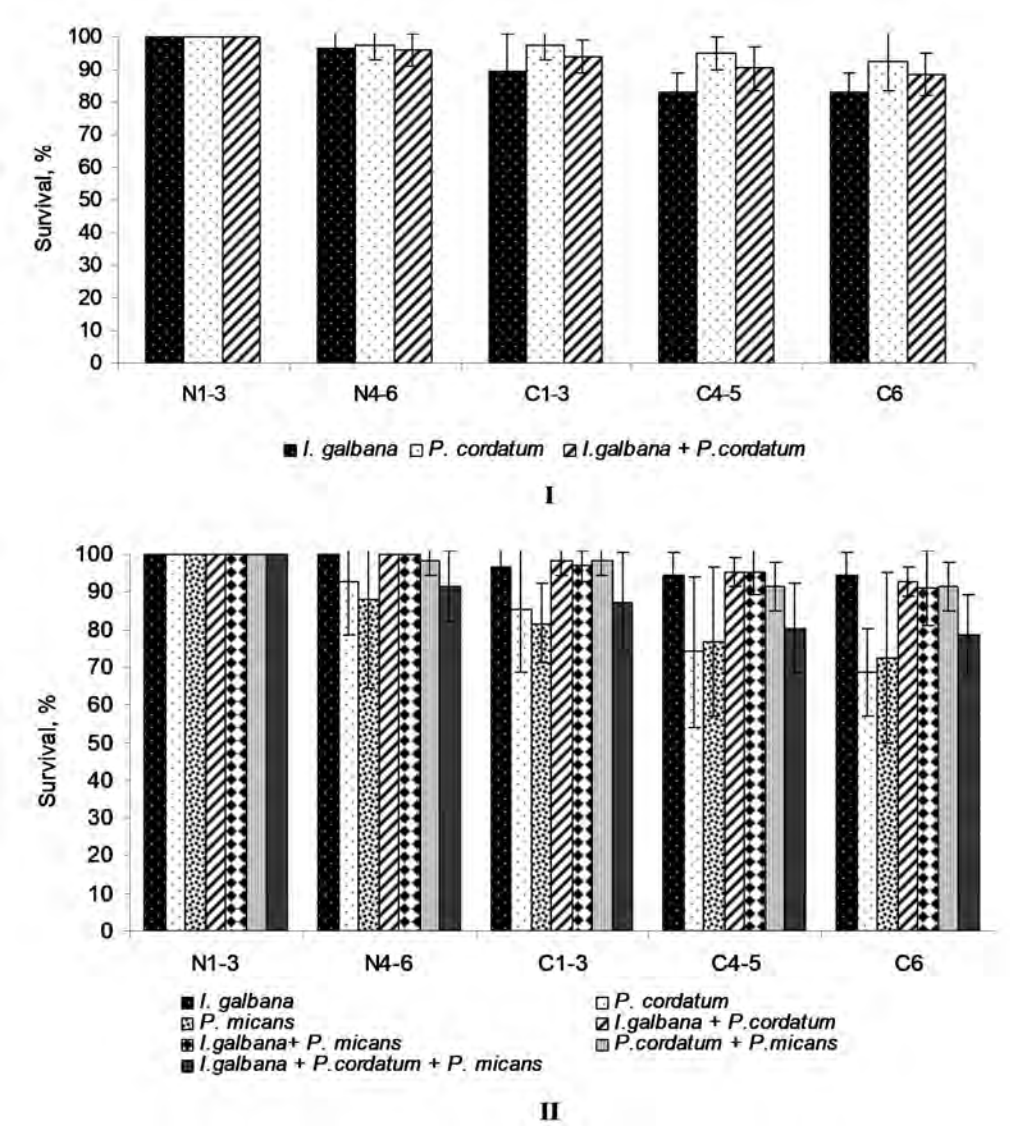

Fig. 1. Survival rate of *Calanipeda aquaedulcis* (I) and *Arctodiaptomus salinus* (II) in the experiment depending on being fed with various microalgae species (*M*; 95 % *CI*; *n* = 15)

Table 1. Percentage of males (M) and females (F) of copepods *Calanipeda aquaedulcis* and *Arctodiaptomus salinus* when being fed with various microalgae species ($M \pm SD$; $n = 15$) (95 % *CI*)

Microalgae	*C. aquaedulcis*		*A. salinus*	
	M, %	F, %	M, %	F, %
I. galbana	20.8 ± 8.3	79.2 ± 8.3	56.1 ± 12.7	43.9 ± 12.7
P. cordatum	42.7 ± 6.3	57.3 ± 6.3	47.7 ± 10	52.3 ± 10
P. micans	–	–	45 ± 2.3	55 ± 2.3
I. galbana + *P. cordatum*	43.3 ± 9.3	56.7 ± 9.3	61 ± 5.9	39 ± 5.9
I. galbana + *P. micans*	–	–	70.1 ± 12.3	29.9 ± 12.3
P. cordatum + *P. micans*	–	–	59.1 ± 12.4	40.9 ± 12.4
I. galbana + *P. cordatum* + *P. micans*	–	–	52.8 ± 12.7	47.2 ± 12.7

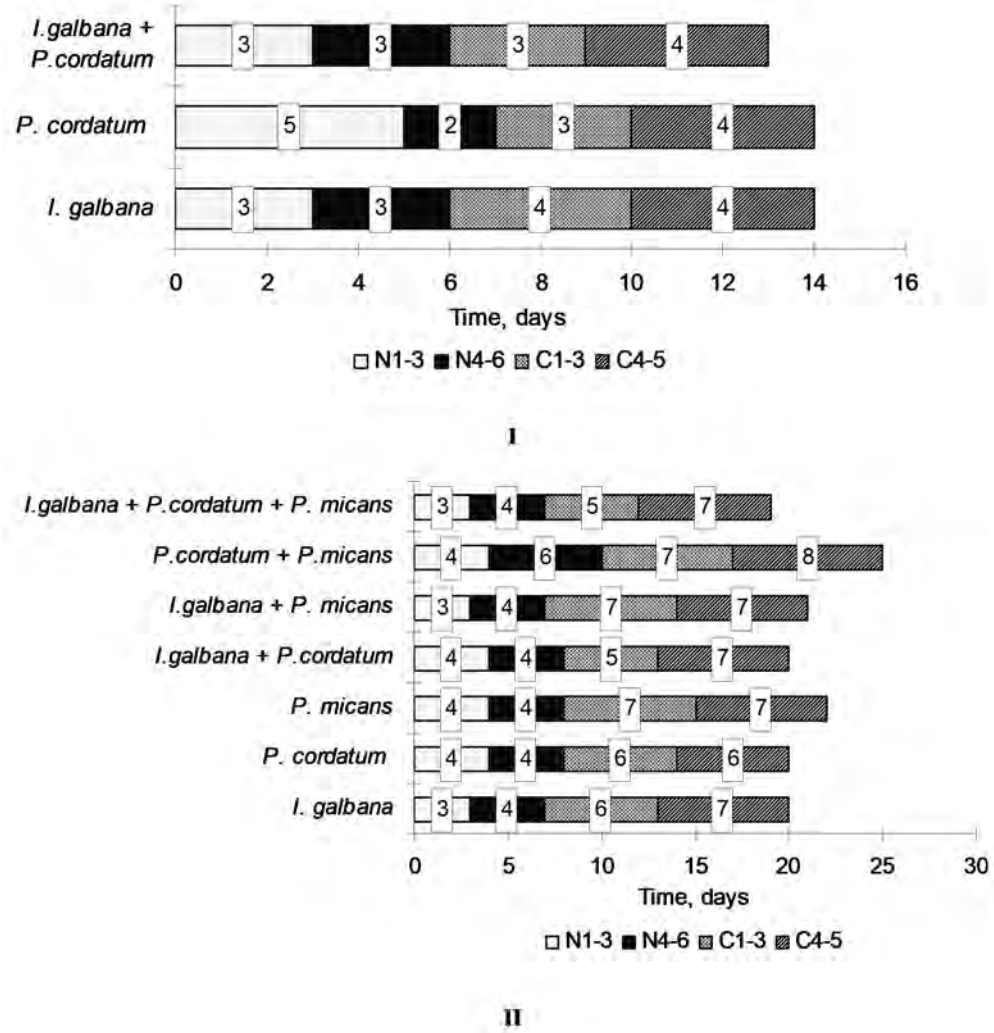

Fig. 2. Development time of *Calanipeda aquaedulcis* (I) and *Arctodiaptomus salinus* (II) in the experiment depending on being fed with various microalgae species (M; n = 15)

The average value of absolute fecundity of *C. aquaedulcis* slightly varied (19.3 ± 3.2) eggs per female (*I. galbana* + *P. cordatum*) to (24.2 ± 1.8) eggs per female (*I. galbana*). Egg hatching reached 100 % when copepods were fed with both monocultures of microalgae *P. cordatum* and *I. galbana* and with their mixture (Fig. 3).

Significant differences were identified in the effect of microalgae species on the absolute fecundity of *A. salinus*: the minimum [(8.8 ± 1.9) to (10.3 ± 1.3) eggs per female] was noted when copepods were fed with *P. cordatum* + *P. micans*; *I. galbana* + *P. cordatum* + *P. micans*; *I. galbana* + *P. micans*; *I. galbana*, and the maximum [(13.75 ± 2.3) to (16.4 ± 2.4) eggs per female] – when being fed with *P. micans*; *I. galbana* + *P. cordatum*; *P. cordatum*.

The trophic conditions (chemotaxonomic characteristics associated with a species and a class of microalgae which copepod females were fed with) had the most expressed effect on the embryonic development of *A. salinus*, the norm of which is characterized by the hatching rate from the eggs of viable nauplii. This index was reliably minimal [(62.63 ± 10) %] when *A. salinus* females were fed with *P. cordatum*. Then the value of the hatching rate of nauplii varied (unreliably) (84.9 ± 7.3) to (97.46 ± 2.7) %, reaching a maximum (100 %) when copepods were fed with *I. galbana* + *P. micans*.

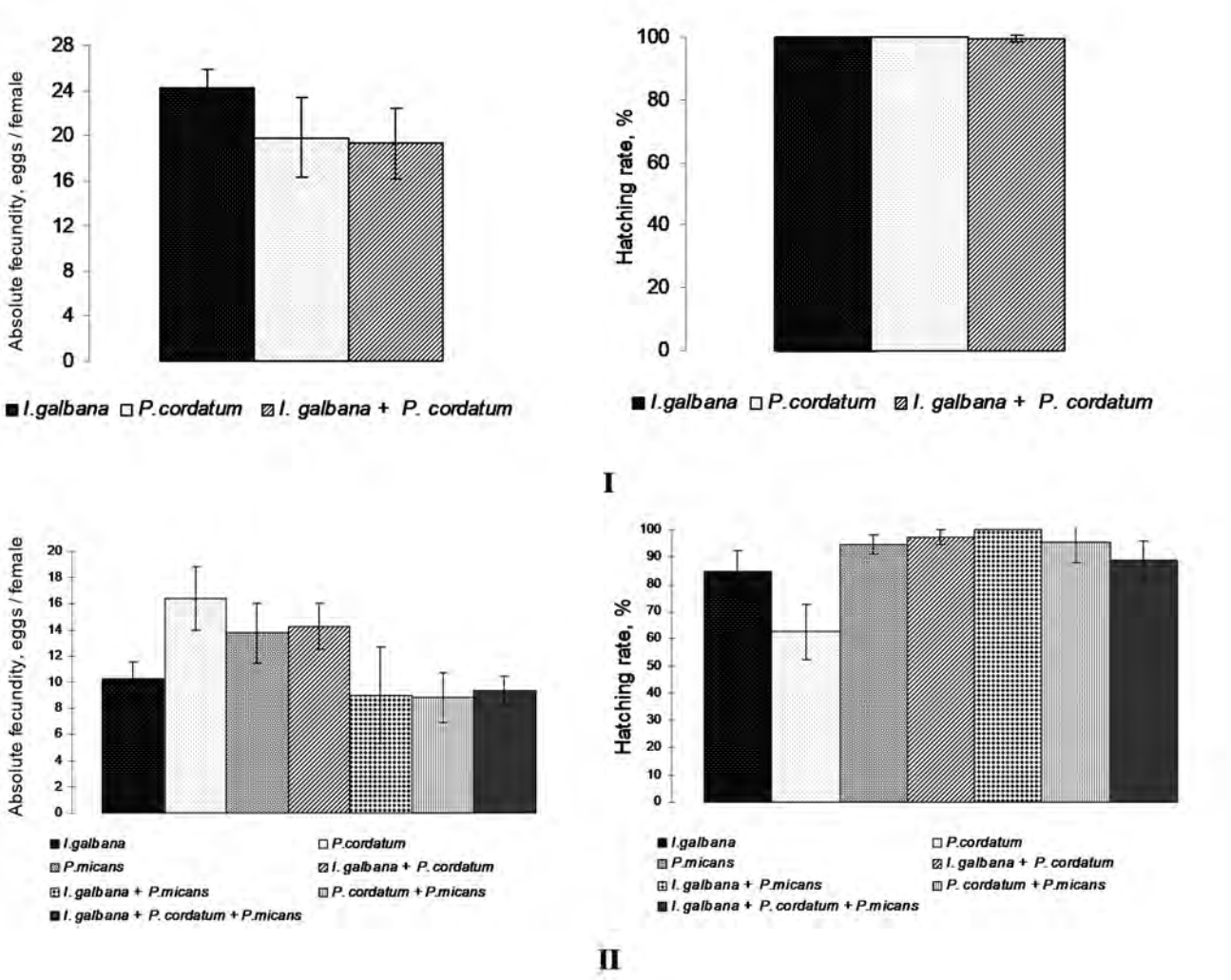

Fig. 3. Comparative diagrams of absolute fecundity and hatching rate of viable nauplii from the total number of eggs of females of copepods *Calanipeda aquaedulcis* (I) and *Arctodiaptomus salinus* (II) when being fed with various microalgae species ($M \pm SD$; $n = 15$) (95 % *CI*)

DISCUSSION

When comparing values of copepod survival rates and development time, a similarity of the influence of some microalgae species on indices of *C. aquaedulcis* and *A. salinus* is found. The shortest duration of the naupliar stage of development of both copepod species was observed when their diet included *I. galbana* as a monoculture or one of mixture components. During the copepodit stage, the pattern remains the same, only with *P. cordatum*.

Feeding with small-sized *I. galbana* turned out to be optimal for the development of copepod naupliar stages. Meanwhile, such nutrition delayed the development of copepodit stages compared to nutrition with large-sized *P. cordatum*. The shortened development time during the naupliar stage when copepods are fed with *I. galbana* is leveled out by the shortened development time during the copepodit stage when they are fed with *P. cordatum*. Thus, the total development time (naupliar stage plus copepodit stage) was the shortest for *C. aquaedulcis* when copepods were fed with a mixture *I. galbana* + *P. cordatum* (13 days), and for *A. salinus* – when they were fed with *I. galbana* + *P. cordatum* + *P. micans* (19 days).

It is known that in most Calanoida copepods, females are always larger than males; smaller sizes of Calanoida males are usually associated with their faster development [6]. According to hypothesis [11], under the influence of unfavorable environmental conditions, a shift in the sex ratio towards the predominance of males can be expected; when the conditions are favorable, a shift towards females can be expected. In case of *C. aquaedulcis* and *A. salinus*, males are smaller than females. Therefore, if the hypothesis is correct, then a shift in the sex ratio towards males can testify non-optimal environmental conditions: extreme temperatures and/or high salinity, or inadequate food availability. It is likely that food biochemical composition can also affect sex differentiation of developing copepods, as defined for other hydrobionts [13]. Concentration and quality of food affect numerical sex ratio of adult *Calanus* spp.: an increase in the proportion of females is observed with an increase in the concentration of food in the medium, in which copepods develop [8]. However, the data obtained on the supposed influence of microalgae chemotaxonomic characteristics on the sex ratio in copepod experimental populations require additional comprehensive studies of their biology, combined with studies of the biochemical composition of microalgae and copepods being fed with them.

The chemotaxonomic composition of microalgae, that female copepods are fed with, certainly affects their reproductive characteristics and especially viability of nauplii of both species throughout hatching. In our experiments, the maximum egg hatching rate (100 %) of nauplii was observed when female *C. aquaedulcis* were fed with monocultures *I. galbana* and *P. cordatum*, as well as a mixture of the same microalgae. However, for *A. salinus*, some differences were found in the influence of microalgae species on the survival rate of nauplii while hatching. Thus, the minimum hatching rate of *A. salinus* nauplii and their females' maximum absolute fecundity were obtained when copepods were fed with *P. cordatum*.

Microalgae Dinophyceae are characterized by a high content of highly unsaturated fatty acids with a predominance of docosahexaenoic acid (hereinafter DHA) over eicosapentaenoic one (hereinafter EPA) [12]. Prymnesiophyceae are characterized by an increased DHA content with a low EPA content [10]. Content and ratio of DHA and EPA in microalgae composition, supposedly, are among the main chemotaxonomic factors, which influence the reproductive characteristics of Calanoida copepods [5 ; 9]. Balanced EPA and DHA presence in microalgal nutrition throughout copepod ontogenesis has a positive effect on the development rate of *C. aquaedulcis* and *A. salinus*. At the same time, the nutrition of copepod females with a mixture of microalgae Dinophyceae and Prymnesiophyceae determines maximum nauplii hatching rate of both copepod species.

Conclusion. The highest survival rates of *A. salinus* from the naupliar stage of development to the adult one (93–95 %) were obtained when copepods were fed with a monoculture of microalga *I. galbana* and a mixture *I. galbana* + *P. cordatum*, and the shortest development rate (19 days) – when copepods were fed with a mixture of three microalgae *I. galbana* + *P. cordatum* + *P. micans*. The shortest development rate of *C. aquaedulcis* from the naupliar to the adult stage (13 days) was obtained when copepods were fed with a mixture of microalgae *I. galbana* + *P. cordatum*.

For *C. aquaedulcis*, the lowest percentage of males (21 %) was obtained reliably when copepods were fed with *I. galbana*; their proportion increased to 43 % when being fed with *P. cordatum* and a mixture *I. galbana* + *P. cordatum*. No significant differences in the percentage of *A. salinus* males and females when reaching the adult stage depending on microalgae species were identified.

The shortest duration of the naupliar stage of development of both copepod species was observed when their diet included *I. galbana* as a monoculture or one of mixture components. During the copepodit stage, the pattern remains the same, only with *P. cordatum*.

The maximum absolute fecundity of *C. aquaedulcis* reached 24 eggs per female (*I. galbana*); of *A. salinus* – 16 eggs per female (*P. cordatum*). Egg hatching reached 100 % when copepods were fed with both monocultures of microalgae *P. cordatum* and *I. galbana* and with their mixture. The highest egg hatching rate for *A. salinus* was reached only when females were fed with a mixture of microalgae *I. galbana* + *P. micans*.

Therefore, mixtures of microalgae *P. cordatum* + *I. galbana* (for *C. aquaedulcis*) and *I. galbana* + *P. cordatum* + *P. micans* (for *A. salinus*), due to balanced presence of eicosapentaenoic and docosahexaenoic acids, were determined as optimal food objects for copepod survival rate and development time throughout ontogenesis. Also, these microalgae mixtures determined the maximum hatching rate of viable nauplii.

This work was carried out within the framework of government research assignment of IBSS "Investigation of the mechanisms of controlling production processes in biotechnological complexes with the aim of developing the scientific foundations for the production of biologically active substances and technical products of marine genesis" (No. AAAA-A18-118021350003-6).

REFERENCES

1. Aganesova L. O. Survival and development times of the copepods *Calanipeda aquaedulcis* and *Arctodiaptomus salinus* depending on feeding microalgae of different taxonomic groups. *Morskoj ekologicheskij zhurnal*, 2011, vol. 10, iss. 2, pp. 27–33. (in Russ.)
2. Aganesova L. O. Development times of the copepods *Calanipeda aquaedulcis* and *Arctodiaptomus salinus* at different temperatures. *Morskoj ekologicheskij zhurnal*, 2013, vol. 12, no. 1, pp. 19–25. (in Russ.)
3. Aganesova L. O. Reproductive characteristics of females of the copepods *Calanipeda aquaedulcis* and *Arctodiaptomus salinus* fed microalgae from different taxonomic groups. *Morskoj ekologicheskij zhurnal*, 2011, spec. iss. no. 2, pp. 7–10. (in Russ.)
4. Hubareva E. S., Svetlichny L. S. Salinity tolerance of copepods *Calanipeda aquaedulcis* and *Arctodiaptomus salinus* (Calanoida, Copepoda). *Morskoj ekologicheskij zhurnal*, 2011, vol. 10, iss. 4, pp. 32–39. (in Russ.)
5. Khanaychenko A. N. The effect of microalgal diet on copepod reproduction parameters. *Ekologiya morya*, 1999, iss. 49, pp. 56–61. (in Russ.)
6. Corkett C. J., McLaren I. A., Sevighy J.-M. The rearing of the marine calanoid copepods *Calanus finmarchicus* (Gunnerus), *C. glacialis* Jaschnov, and *C. hyperboreus* Kroyer with comment on the equiproportional rule. *Sillogeus*, 1986, vol. 58, pp. 539–546.
7. Coutteau P. *Micro-Algae. Manual on the Production and Use of Live Food for Aquaculture* / P. Lavens, P. Sorgeloos (Eds). Rome : FAO, 1996, 300 p. (FAO Fisheries Technical Paper ; no. 361).
8. Irigoien X., Obermuller B., Head R. N., Harris R. P., Rey C., Hansen B. W., Hygum B. H., Heath M. R., Durbin E. G. The effect of food on the determination of sex ratio in *Calanus* spp.: Evidence from experimental studies and field data. *ICES Journal of Marine Science*, 2000, vol. 57, iss. 6, pp. 1752–1763. https://doi.org/10.1006/jmsc.2000.0960
9. Lacoste A., Poulet S. A., Cueff A., Kattner G., Ianora A., Laabir M. New evidence of the copepod maternal food effects on reproduction. *Journal of Experimental Marine Biology and Ecology*, 2001, vol. 259, iss. 1, pp. 85–107. https://doi.org/10.1016/S0022-0981(01)00224-6
10. Payne M. F., Rippengale R. J. Evaluation of diets for culture of the calanoid copepod *Gladioferens imparipes*. *Aquaculture*, 2000, vol. 187, iss. 1, pp. 85–96. https://doi.org/10.1016/S0044-8486(99)00391-9
11. Sapir Y., Mazer S. J., Holzapfel C. Sex ratio. *Jorgensen Encyclopedia of Ecology*, 2008, vol. 4, pp. 3243–3248. https://doi.org/10.1016/B978-008045405-4.00658-3

12. Zhukova N. V., Aizdaicher N. A. Fatty acid composition of 15 species of marine microalgae. *Phytochemistry*, 1995, vol. 39, iss. 2, pp. 351–356. https://doi.org/10.1016/0031-9422(94)00913-E

13. Zupo V. Influence of diet on sex differentiation of *Hippolyte inermis* Leach (Decapoda: Natantia) in the field. *Hydrobiologia*, 2001, vol. 449, iss. 1–3, pp. 131–140. https://doi.org/10.1007/978-94-017-0645-2_13

ПРОДУКЦИОННЫЕ ХАРАКТЕРИСТИКИ КОПЕПОД *ARCTODIAPTOMUS SALINUS* И *CALANIPEDA AQUAEDULCIS* ПРИ ПИТАНИИ СМЕСЬЮ МИКРОВОДОРОСЛЕЙ DINOPHYCEAE И PRYMNESIOPHYCEAE

Л. О. Аганесова

Федеральный исследовательский центр «Институт биологии южных морей имени А. О. Ковалевского РАН», Севастополь, Российская Федерация

E-mail: *la7risa@gmail.com*

Убиквитные виды копепод *Arctodiaptomus salinus* (Daday, 1885) и *Calanipeda aquaedulcis* (Krichagin, 1873) — важные компоненты пищевых цепей многочисленных пресных и солёных водоёмов. Данные копеподы пригодны для кормления личинок как морских, так и пресноводных видов рыб, однако влияние питания на продукционные характеристики этих видов копепод изучено недостаточно. Ранее нами было определено, что монокультуры микроводорослей Dinophyceae и Prymnesiophyceae являются оптимальными кормовыми объектами для продуцирования яиц самками *A. salinus* и *C. aquaedulcis*, выживаемости и скорости развития этих копепод на всём протяжении их онтогенеза. Цель данной работы заключалась в определении продукционных характеристик копепод *A. salinus* и *C. aquaedulcis* в оптимальных температурных условиях в зависимости от варианта питания смесью микроводорослей Dinophyceae и Prymnesiophyceae. Наиболее высокие значения выживаемости *A. salinus* от науплиальной до взрослой стадии развития (93–95 %) отмечены при питании копепод монокультурой микроводоросли *Isochrysis galbana* (Parke, 1949) и смесью *I. galbana* + *Prorocentrum cordatum* (Ostenfeld) J. D. Dodge, 1975; наименьшая продолжительность развития (19 суток) — при кормлении смесью из трёх микроводорослей *I. galbana* + *P. cordatum* + *Prorocentrum micans* (Ehrenberg, 1834). Наименьшая средняя продолжительность развития *C. aquaedulcis* от науплиальной до взрослой стадии развития (13 сут.) зафиксирована при питании смесью микроводорослей *I. galbana* + *P. cordatum*. Наименьшая продолжительность науплиального периода развития копепод обоих видов отмечена тогда, когда в состав их диеты входила *I. galbana* в качестве моно- или одного из компонентов смеси. Такая же закономерность сохраняется для копеподитного периода, только уже с *P. cordatum*. Максимальная абсолютная плодовитость *C. aquaedulcis* достигала 24 яиц на самку (*I. galbana*), *A. salinus* — 16 яиц на самку (*P. cordatum*). Выклев *C. aquaedulcis* при питании как монокультурами микроводорослей *P. cordatum* и *I. galbana*, так и их смесью достигал 100 %. Для *A. salinus* только питание самок смесью микроводорослей *I. galbana* + *P. micans* обуславливает максимальный процент выклева.

Ключевые слова: копеподы, *Arctodiaptomus salinus*, *Calanipeda aquaedulcis*, выживаемость, развитие, размножение, микроводоросли, смесь микроводорослей, Dinophyceae, Prymnesiophyceae

1871
ИнБЮМ – IBSS

Морской биологический журнал
Marine Biological Journal
2020, vol. 5, no. 2, pp. 12–18
https://doi.org/10.21072/mbj.2020.05.2.02

UDC 582.273:594.124:577.1

INFLUENCE OF MUSSEL *MYTILUS GALLOPROVINCIALIS* EXOMETABOLITES ON R-PHYCOERYTHRIN CONCENTRATION IN RED ALGA *GELIDIUM SPINOSUM* WHEN GROWN IN POLYCULTURE

© 2020 **B. N. Belyaev and N. M. Beregovaya[1]**

[1]A. O. Kovalevsky Institute of Biology of the Southern Seas of RAS, Sevastopol, Russian Federation
E-mail: *belyaevbob@yandex.ru*

Received by the Editor 10.10.2019; after revision 14.11.2019;
accepted for publication 26.06.2020; published online 30.06.2020.

To increase R-phycoerythrin concentration in red Black Sea alga *Gelidium spinosum* (S. G. Gmelin) P. C. Silva, 1996 (Rhodophyta), it was cultivated in laboratory conditions in polyculture microalga *Tetraselmis viridis* – mussel *Mytilus galloprovincialis* – *Gelidium*; the results of the study are presented. The positive effect of mussel exometabolites on R-phycoerythrin concentration in *Gelidium* in polyculture is described. The relevance of the work is determined by the value of R-phycoerythrin, which is used as a powerful antioxidant, as well as a marker in cytometry and microscopy. The aim of the study is to increase R-phycoerythrin concentration in *Gelidium* using the polyculture method. As a material, *Gelidium* from the fouling of rocks and coastal protection structures of Karantinnaya Bay (Sevastopol) was used; it was cultivated in a laboratory installation with eight working volumes, four of which contained mussels. Mussel decontamination, supplemented with mineral salts and biogens, was used as a nutrient medium for *Gelidium*. The combination of mussel exometabolites with previously developed nutrient medium, based on Black Sea water and enriched with nutrients and mineral salts, results in an increase in R-phycoerythrin concentration by more than 2 times, while the addition of exometabolites to pure filtered seawater increases it maximum by 35 %. Approximate ratios of polyculture elements in 1.5-L volumes, allowing to achieve the desired results in 2 weeks, are as follows: 2 g of *Gelidium* / 50–60 g of two-year-old mussels / 0.4–0.6 g of microalga wet weight.

Keywords: cultivation, polyculture, microalgae, molluscs, macrophytes, nutrient medium

Black Sea *Gelidium spinosum* (S. G. Gmelin) P. C. Silva, 1996 is a valuable raw material source of high-quality agar and R-phycoerythrin – phycobiliprotein pigment, which is widely used in immune diagnostics, microscopy, and cytometry [13]. Algae containing agar and R-phycoerythrin are cultivation objects in many countries of the Asia-Pacific [9 ; 14], and the cost of 1 g of purified R-phycoerythrin reaches $3250–14000 [12].

In previous years, we carried out studies to determine the optimal conditions for *Gelidium* growth and R-phycoerythrin accumulation in it: concentrations of mineral salts and biogens, light and temperature conditions, carbonation of the nutrient medium, as well as its circulation and flow rate [2].

It is known that under natural conditions, *Gelidium* is often found as an epibiont of molluscs-filtrators. Such symbiosis is caused by the positive effect of mollusc exometabolites on macrophyte growth, and that is why hydrobiont cultivation in polyculture has been developed [7 ; 14].

Previously, we obtained results on the beneficial effect of exometabolites of *Anadara kagoshimensis*, starving in pure Black Sea water for 15 days, on *Gelidium* growth and R-phycoerythrin content. With an increase in *Gelidium* biomass by 11.6 %, R-phycoerythrin concentration increased by 40 % compared with the control [4].

The aim of this work is to increase R-phycoerythrin concentration during *Gelidium* cultivation in polyculture. To achieve the aim, the following task is set: to determine the optimal ratio of polyculture elements microalga – mussel – macrophyte.

MATERIAL AND METHODS

As a material, *Gelidium spinosum* from the fouling of rocks and coastal protection structures in the area of Martynova and Karantinnaya bays (Sevastopol) was used. It was cultivated in a laboratory installation with eight working volumes [1] at a temperature range of +15…+27 °C and illumination of 10–25 klx in the mode of 18 h day : 6 h night. The nutrient medium was prepared on the basis of filtered Black Sea water with an increase in its salinity to 26 ‰ and addition of nitrogen, phosphorus, iron, magnesium, and manganese [3]. Mussels (*Mytilus galloprovincialis* Lamarck, 1819) of 45–50 mm were picked from farm collectors located south of the entrance to the Sevastopol Bay, opposite IBSS radiobiological building. Microalga was cultivated separately in a flat cultivator.

Four of eight working volumes of the installation with a right-angled bottom were modernized to contain mussels: they were blocked by left-angled perforated shelves for placing there 2 to 6 individuals with an average weight of 9.5 to 11.5 g. Constant bubbling of the working volumes with air was regulated so that mollusc feces did not stir up and remained in the deepened bottom part.

Mussels were fed with a suspension of *Tetraselmis viridis* (Rouchijajnen) R. E. Norris, Hori & Chihara, 1980 culture, taken from museum of IBSS biotechnology and phytoresources department, either once or twice a day or once every two days. Culture density was of 12–17 mg of microalga wet weight per 1 ml, ranging 5 to 35 ml per one working volume. The contents of the working volumes with mussels were completely poured into previously dried containers with *Gelidium* once every two days; in these containers, a set of minerals and biogens was added [2]. Measurements of R-phycoerythrin concentration in *Gelidium* were carried out by a standard method [10] once a week and at the end of the experiment. Macrophyte initial weight in each working volume was of (2.00 ± 0.05) g. Measurements were made using Sartorius L 220 S balance.

Experiments were carried out in autumn and winter. In the first experiment, decontamination was poured into the containers with *Gelidium* from the working volumes with mussels (4 ind. in each), maintained in clean filtered seawater with the salinity of 26 ‰ and fed with *Tetraselmis viridis* microalga. Thus, *Gelidium* was fed exclusively with mussel metabolites, without mineralization of the medium, the same as in the experiment with *Anadara* [4].

In the second experiment, the components of a previously developed nutrient medium were added to the poured decontamination: nitrogen (8.54 mg per L as KNO_3), phosphorus (1.77 mg per L as KH_2PO_4), iron (1.39 mg per L as $FeSO_4 \cdot 7H_2O$ in combination with 17 mg of Na_2EDTA per 1 g of salt), manganese (0.55 mg per L as $MnCl_2 \cdot 4H_2O$), and magnesium (120 mg per L as $MgSO_4 \cdot 7H_2O$) [2]. Four mussels with an average weight of 9.5–11.5 g were placed into each of four modernized working volumes, and (2 ± 0.05) g of *Gelidium* were placed into four other volumes. Mussels were fed with microalga: 5 to 20 ml of suspension per day.

The first two experiments were carried out according to our patent [3] with an element of *Gelidium* weekly "maturing" to increase R-phycoerythrin concentration. In the third experiment, this element was excluded because of weekly measuring of pigment concentration.

In the third experiment, the same as in the second one, *Gelidium* was grown on mussel decontamination with the addition of minerals and biogens. To identify the dynamics of pigment accumulation in *Gelidium* and to determine the optimal weight ratio of polyculture elements, different number of mussels were maintained in the containers: 3, 4, and 5 ind. with a total initial weight of 33.4, 41.4, and 57 g. They were fed with *Tetraselmis viridis* suspension in the amount of 15, 25, and 35 ml, respectively. Microalga culture density was of 17 mg of wet weight per 1 ml and was kept constant throughout the experiment. In two control working volumes (No. 1 and 5), *Gelidium* was cultivated on the medium mentioned above [2] without metabolites added; it was supplemented with minerals and biogens only. R-phycoerythrin concentration was determined after two, three, and four weeks of cultivation.

The peculiarity of the third experiment was as follows: *Gelidium* was cultivated in five working volumes (No. 1–5) with equal initial mass of 2 g. In three volumes (No. 2–4), the number of added metabolites increased consistently due to both different number of mussels (3; 4; 5) from the volumes No. 6–8 and increased diet of the molluscs (5; 6.25; 7 ml of culture per ind.).

RESULTS AND DISCUSSION

The results of the first two experiments are presented in Tables 1 and 2, of the third one – in Table 3 and in Fig. 1.

Table 1. R-phycoerythrin concentration in *Gelidium* grown on exometabolites of Black Sea mussels with different microalga diet

No. of the experiment	Volume of *Tetraselmis viridis* culture with the density of 12 mg of wet weight per ml	R-phycoerythrin concentration, mg per g
Control	0	5.8 ± 0.5
1	10	6.4 ± 0.9
2	15	5.6 ± 0.4
3	20	7.9 ± 0.8

Table 1 shows that R-phycoerythrin concentration in *Gelidium* increased within the range 10 to 35 % in the polyculture microalga *Tetraselmis viridis* – mussel *Mytilus galloprovincialis* – macrophyte *Gelidium spinosum*, when being fed with mussel exometabolites (if considering the result of the second experiment an artifact). The last figure shows the results close to that obtained in the experiment with *Anadara* [4].

Table 2 presents the results of the experiment, in which decontamination was completely poured into the working volumes with *Gelidium* from the volumes with mussels and enriched with a set of biogens and microelements. Four variants of mussel diet were tested; the maximum variant (20 ml per volume) contributed to an increase in R-phycoerythrin concentration in *Gelidium* by more than three times.

The results of the dynamics of weight growth and pigment concentration in the third experiment are presented in Table 3, and R-phycoerythrin accumulation – in Fig. 1.

The results of a 4-week experiment show that on the 12th day of cultivation in variants with the addition of metabolites from the working volumes with 3, 4 and 5 mussels, R-phycoerythrin accumulation exceeds the initial control value by 50–100 %, while in the containers with no metabolites added (volumes No. 1 and 5) – only by 16 %.

Table 2. R-phycoerythrin concentration in *Gelidium* grown on mussel exometabolites with the addition of nutrients and mineral salts into the culture medium

No. of the experiment	Volume of *Tetraselmis viridis* culture with the density of 12 mg of wet weight per ml	R-phycoerythrin concentration, mg per g
Control	0	7.9 ± 0.8
1	5	16.1 ± 1.5
2	10	20.3 ± 4.4
3	15	18.3 ± 2.2
4	20	28.8 ± 4.5

Table 3. Dynamics of weight growth and R-phycoerythrin concentration in *Gelidium* thalli at different number of mussels in the polyculture

No. of the volume	Number of mussels	V_{ma}, ml	*Gelidium* weight, g / R-phycoerythrin concentration, mg per g			
			30.01.2019	11.02.2019*	18.02.2019*	25.02.2019*
1; 5	0	0	2.0 / 6.9 ± 2.3	2.90 / 8.0 ± 2.3	3.00 / 9.6 ± 1.6	3.20 / 11.1 ± 1.2
2	3	15	2.0 / 6.9 ± 2.3	3.00 / 11.4 ± 2.4	2.55 / 8.7 ± 0.9	3.00 / 12.3 ± 1.2
3	4	25	2.0 / 6.9 ± 2.3	3.25 / 12.4 ± 1.8	3.10 / 10.6 ± 0.8	3.22 / 13.6 ± 0.9
4	5	35	2.0 / 6.9 ± 2.3	3.05 / 14.4 ± 1.4	2.85 / 14.9 ± 1.7	3.30 / 14.4 ± 0.1

Note: at the dates marked with an asterisk (*), samples were taken to measure R-phycoerythrin, and *Gelidium* weight was returned to W_0 = 2 g; V_{ma} indicates volume of microalga suspension.

At the end of the 3rd week of cultivation, there was a significant decrease in pigment concentration in *Gelidium* from the working volume No. 2, into which the decontamination was poured from the volume with 3 mussels. It is 24 % lower than the previous result and 29 % lower than the final one. Since algae were equally supplemented with minerals and biogens in all the volumes, it could result from a change in the physiological state of at least one of three mussels, which we did not monitor in our experiments.

This result can be considered an artifact, since nothing was found in this volume that distinguishes it from the rest ones. Meanwhile, in our other experiments, there were emissions of mussel sex products (such cases can be the reason for further separate studies of their effect on R-phycoerythrin concentration in *Gelidium*).

According to the results of 4 weeks of cultivation, it was noted, that pigment levels in *Gelidium* from the working volumes No. 2–4 were arranged in increasing order directly proportional to the expected increase in the number of exometabolites from 3, 4, and 5 mussels. If R-phycoerythrin level in *Gelidium*, cultivated by already known method [3] in the volumes No. 1 and 5, is taken as 100 %, then we can conclude that the increases from the use of mussel exometabolites are of 11, 12, and 30 %, respectively.

The maximum R-phycoerythrin content obtained in the second experiment (Table 2) was 2 times higher than the maximum pigment concentration in the third experiment (Table 3). This is explained by the facts that in the latter case, the algae were taken for measurements immediately after the end of the experiment and the element of “maturing”, in which the lag of phycoerythrin accumulation in rapidly growing biomass is eliminated in the dark and at a low temperature, was not used [3]. In this case, the specific rate of biomass weight growth was quite high: the biomass doubled in less than 10 days.

The change in R-phycoerythrin concentration in *Gelidium* with a different number of mussel individuals in the polyculture is clearly shown in Fig. 1. After two weeks of cultivation, when the macrophyte was fed with exometabolites of 5 mussels, we observed a 2-fold increase in R-phycoerythrin content.

After four weeks of cultivation, the difference with the control decreased and was approximately of 25 %. Exometabolites of 3 and 4 mussels also caused an increase in pigment concentration after two weeks of cultivation – by 30 and 40 %.

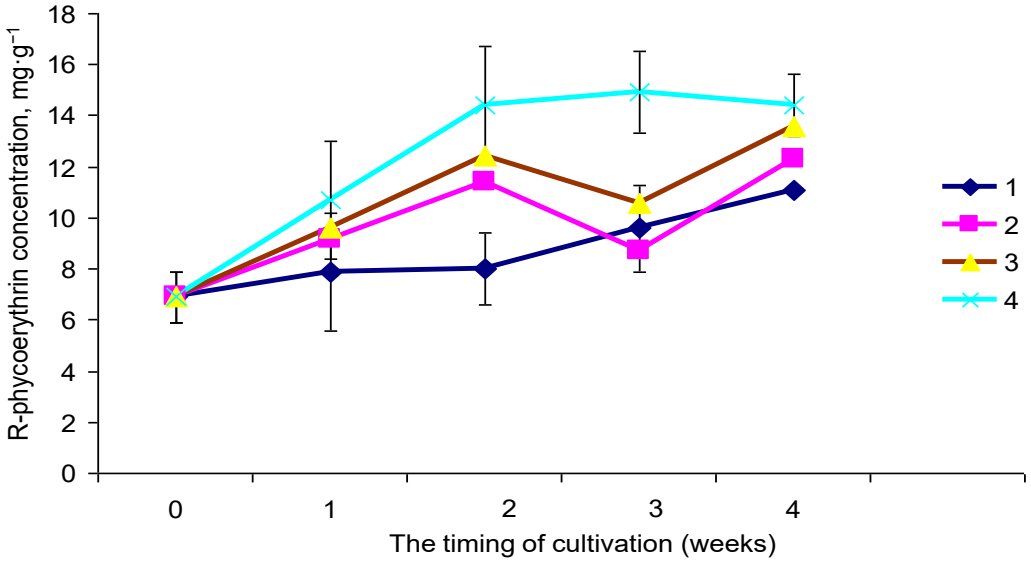

Fig. 1. Dynamics of R-phycoerythrin concentration in *Gelidium* with different number of mussels in the polyculture (1 – control; 2 – 3 mussels; 3 – 4 mussels; 4 – 5 mussels)

The average results of *Gelidium* growth in the volumes No. 2–4 for the last two weeks of the third experiment were of 1 g per week. Thus, a system, including microalga *Tetraselmis viridis* cultivator with a productivity of 600 mg of wet weight per day, a 1.5-L volume for maintaining 5 mussels with a total weight of 60 g, and a 1.5-L *Gelidium* cultivator, is quite capable of producing 14.4 mg of R-phycoerythrin in 7 days.

The advantages of macrophyte cultivation in polyculture in comparison with cultivation in monoculture are known from literature. Thus, macrophytes accumulate larger biomass and larger amount of protein [8 ; 14], and agar quality of *Gracilaria* improves due to creating an optimal diet resulting from exometabolite extraction by invertebrates [7].

Macroalgae can extract from water up to 60 % of nitrogen compounds, including up to 95 % of ammonium [14]. Mussels are known to release ammonium nitrogen into the medium [5]. The chromophore group of pigment (phycobilin) is covalently bound to a water-soluble protein such as globulin [13], the building of which requires nitrogen. In addition, phycobiliproteins are considered to be a “depot” of protein in algae cells. They are destroyed primarily by nitrogen starvation [6 ; 11]. Meanwhile, it is highly possible that not only the addition of nitrogen, but also the form of its compound affect R-phycoerythrin level. However, according to the results of previous studies, culture medium contained a sufficient amount of nitrogen [3]. It seems likely that in that case other interactions have an effect (for example, at the level of hormonal regulation). Thus, the use of metabolites, including in polyculture, creates a fundamentally new way of regulating natural processes [8].

Conclusion. A positive effect of mussel exometabolites on R-phycoerythrin synthesis in the polyculture microalga *Tetraselmis viridis* – mussel *Mytilus galloprovincialis* – macrophyte *Gelidium spinosum* was revealed. The addition of mollusc exometabolites into clean filtered seawater gave an increase in R-phycoerythrin concentration in *Gelidium* by 10–35 %, and the addition of exometabolites in combination

with a standard nutrient medium led to an increase in R-phycoerythrin content by more than 2 times. Approximate weight ratios of polyculture elements in 1.5-L working volumes, allowing to achieve the desired result after two weeks, were as follows: 2 g of *Gelidium* / 50–60 g of two-year-old mussels / 0.4–0.6 g of microalga raw weight.

This work was carried out within the framework of government research assignment of IBSS "Investigation of the mechanisms of controlling production processes in biotechnological complexes with the aim of developing the scientific foundations for the production of biologically active substances and technical products of marine genesis" (No. AAAA-A18-118021350003-6).

REFERENCES

1. Belyaev B. N. Tekhnicheskoe obespechenie kul'tivirovaniya makrofitov. *Rybnoe khozyaistvo Ukrainy*, 2001, no. 5, pp. 21–24. (in Russ.)
2. Belyaev B. N., Beregovaya N. M. The influence of culture medium on the quantity of agar, pigments, and growth of *Gelidium spinosum* from the Black Sea. *Morskoj biologicheskij zhurnal*, 2016, vol. 1, no. 4, pp. 3–11. (in Russ.). https://doi.org/10.21072/mbj.2016.01.4.01
3. Belyaev B. N., Beregovaya N. M. *Sposob kul'tivirovaniya chernomorskoi krasnoi vodorosli Gelidium spinosum (Grev.) Born. et Thur (Rhodophyta).* Patent RU 2691579 C2 MK *C12N 1/12 A01G 33/00*. Zayavlen FGBUN IMBI im. A. O. Kovalevskogo 09.11.2017, no. 2017139062. Opublikovan 14.06.2019. Bul. no. 14. (in Russ.)
4. Borodina A. V., Belyaev B. N., Beregovaya N. M. Vliyanie ekzometabolitov mollyuskov *Anadara kagoshimensis* (Tokunaga, 1906) na makrofity *Gelidium* sp. *Science, technology and life – 2014* : International scientific conference, Czech Republic, Karlovy Vary, 27–28 Dec., 2014. [Karlovy Vary], 2014, pp. 66–71. (in Russ.)
5. Vyalova O. Yu. *Osobennosti energeticheskogo i azotistogo metabolizma nepolovozrelykh midii Mytilus galloprovincialis Lam. v usloviyakh eksperimenta* : avtoref. dis. … kand. biol. nauk : 03.00.17 / NAN Ukrainy, In-t biologii yuzhnykh morei im. A. O. Kovalevskogo. Sevastopol, 2000, 17 p. (in Russ.)
6. Gudvilovich I. N. The influence of cultivation conditions on growth and the phycobiliprotein content in the red microalgae *Porphyridium purpureum*. *Ekologiya morya*, 2010, iss. 81, pp. 28–36. (in Russ.)
7. Evdokimov V. V. *Morfofunktsional'naya otsenka gamet i produktsionnye vozmozhnosti gidrobiontov pri razmnozhenii ikh v mono- i polikul'ture* : avtoref. dis. … d-ra biol. nauk : 03.00.11 ; 03.00.08 / Tikhookeanskii nauchno-issledovatel'skii institut rybnogo khozyaistva i okeanografii. Vladivostok, 1991, 39 p. (in Russ.)
8. Evdokimov V. V., Evdokimov A. V. Vzaimodeistvie gidrobiontov v polikul'ture pri vosproizvodstve v kontroliruemykh usloviyakh. *Izvestiya TINRO*, 2002, vol. 131, pp. 373–380. (in Russ.)
9. Kalugina A. A., Gryuner V. S., Sokolova N. N. Agar iz chernomorskoi vodorosli gelidium. *Rybnoe khozyaistvo*, 1964, no. 4, pp. 68–70. (in Russ.)
10. Krasnovskii A. A. Vydelenie fikoeritrina iz krasnykh vodoroslei, ego spektral'nye i fotokhimicheskie svoistva. *Doklady Akademii nauk SSSR*, 1952, vol. 82, no. 6, pp. 947–950. (in Russ.)
11. Los' S. I. Influence of urea on spectral properties of phycobilin pigments of algae. *Al'gologiya*, 2009, vol. 19, no. 1, pp. 25–33. (in Russ.)
12. Minyuk G. S., Drobetskaya I. V., Chubchikova I. N., Terent'eva N. V. Unicellular algae as renewable biological resource: A review. *Morskoj ekologicheskij zhurnal*, 2008, vol. 7, iss. 2, pp. 5–23. (in Russ.)
13. Stadnichuk I. N. *Fikobiliproteiny.* Moscow : VINITI, 1990, 193 p. (Itogi nauki i tekhniki, ser. biologicheskaya khimiya ; vol. 40). (in Russ.)
14. Titlyanov E. A., Titlyanova T. V. *Morskie rasteniya stran aziatsko-tikhookeanskogo regiona, ikh ispol'zovanie i kul'tivirovanie.* Vladivostok : "Dal'nauka", 2012, 362 p. (in Russ.)]

INFLUENCE OF MUSSEL *MYTILUS GALLOPROVINCIALIS* EXOMETABOLITES ON R-PHYCOERYTHRIN CONCENTRATION IN RED ALGA *GELIDIUM SPINOSUM* WHEN GROWN IN POLYCULTURE

B. N. Belyaev and N. M. Beregovaya[1]

[1]A. O. Kovalevsky Institute of Biology of the Southern Seas of RAS, Sevastopol, Russian Federation
E-mail: *belyaevbob@yandex.ru*

Приведены результаты исследований культивирования красной черноморской водоросли *Gelidium spinosum* (S. G. Gmelin) P. C. Silva, 1996 (Rhodophyta) в лабораторных условиях в поликультуре микроводоросль *Tetraselmis viridis* — мидия *Mytilus galloprovincialis* — гелидиум с целью повышения концентрации R-фикоэритрина в последнем. Описано положительное влияние экзометаболитов мидий на концентрацию R-фикоэритрина в гелидиуме в поликультуре. Актуальность работы определяется ценностью фикоэритрина, который используют как мощный антиоксидант, а также как метчик в цитометрии и микроскопии. Цель исследования — увеличить концентрацию R-фикоэритрина в гелидиуме с применением метода поликультуры. В качестве материала использовали гелидиум из обрастания скал и берегоукрепительных сооружений в районе бухты Карантинная (г. Севастополь); его культивировали в лабораторной установке с восемью рабочими объёмами, в четырёх из которых содержали мидий. Деконтат мидий, дополненный минеральными солями и биогенами, использовали как питательную среду для гелидиума. Сочетание экзометаболитов мидий с разработанной ранее питательной средой на основе черноморской воды, обогащённой биогенами и минеральными солями, приводит к увеличению содержания R-фикоэритрина более чем вдвое, в то время как внесение экзометаболитов в чистую профильтрованную черноморскую воду повышает его максимум на 35 %. Ориентировочные весовые соотношения элементов поликультуры в 1,5-литровых объёмах, позволяющие достичь желаемого результата уже через две недели, — это 2 г гелидиума / 50–60 г двухлетних мидий / 0,4–0,6 г сырого веса микроводорослей.

Ключевые слова: культивирование, поликультура, микроводоросли, моллюски, макрофиты, питательная среда

1871
ИнБЮМ – IBSS

Морской биологический журнал
Marine Biological Journal
2020, vol. 5, no. 2, pp. 19–37
https://doi.org/10.21072/mbj.2020.05.2.03

UDC 574.587.015(268.45)

BARENTS SEA MEGABENTHOS: SPATIAL AND TEMPORAL DISTRIBUTION AND PRODUCTION

© 2020 **D. V. Zakharov[1,2], L. L. Jørgensen[3], I. E. Manushin[1], and N. A. Strelkova[1]**

[1]Polar branch of VNIRO ("PINRO" named after N. M. Knipovich), Murmansk, Russian Federation
[2]Murmansk Marine Biological Institute RAS, Murmansk, Russian Federation
[3]Institute of Marine Research, Tromsø, Norway
E-mail: *zakharden@yandex.ru*

Received by the Editor 11.10.2019; after revision 07.05.2020;
accepted for publication 26.06.2020; published online 30.06.2020.

This long-term observation of the faunal composition within the Barents Sea provides a benchmark for monitoring community changes caused by oceanographic variability, fishery activities, and crab predators (*Chionoecetes opilio*, *Paralithodes camtschaticus*), whose populations have been rapidly growing and spreading in recent years. In the Arctic systems, megabenthic communities comprise a significant part of benthic biomass and play an important role in carbon cycling on continental shelves. The gradual accumulation of knowledge on megabenthos may make it possible to assess their role in the ecosystem and ultimately contribute to a more rational management of the Barents Sea resources. This article represents an important series of long-term megabenthic observations in the Barents Sea. The main goal of our research is to identify spatial patterns and temporal trends in the megabenthic part of communities, including changes in the biomass and production values. As a part of the joint Norwegian-Russian ecosystem surveys, benthic experts have been identifying the invertebrates (megafauna) collected by bottom trawls during annual assessments of commercial stocks, such as Atlantic cod (*Gadus morhua*) and northern shrimp (*Pandalus borealis*). The sampling equipment used was a Campelen 1800 bottom trawl, rigged with rockhopper ground gear and towed on double warps, and standardized to a fixed sampling effort (equivalent to a towing distance of 0.75 nautical miles (nm), or 1.4 km). The processing of the biological material was conducted in accordance with standardized procedures, following the retrieval of each trawl. This work represents data from 5016 stations from 2005 to 2017, with a total sampled biomass of 238.4 tons and 14.9 million individual organisms. In total, 694 megabenthic species (1058 taxa) have been recorded, with the greatest diversity observed in the depth range of 100–400 m, while the largest mean catches were taken between depths of 600–800 m. The biomass (B) and production (P) values of the benthic megafauna were approximately stable during the 9 years of investigation, although there was a decreasing trend after 2014. The annual production P/B ratio of megabenthos was calculated to be at 0.3. The distribution, contribution to production, and gross biomass values of the megabenthos had been underestimated in the previous studies of zoobenthos. The results from this research show that, in the current warm period, the majority of the Barents Sea is in an intermediate state between the Arctic and boreal regions due to the wide distribution of boreal species toward the north. The dynamics of the mean biogeographical index (the border between areas of the dominance of boreal and Arctic species) within the central-southern part of the Barents Sea suggests that a large part of the area can be characterized as predominantly boreal intermediate since 2013.

Keywords: Arctic, Barents Sea, megabenthos, climate, Atlantic Current, production, species distribution

The effects of global climate change have been particularly noticeable in the Arctic, causing a restructuring of Arctic ecosystem [19 ; 25 ; 33] and a northward shift of biogeographical boundaries as a consequence of warming [5 ; 6 ; 10 ; 12 ; 18 ; 21].

In the Arctic systems, megabenthic communities comprise a significant part of benthic biomass [7 ; 30] and play an important role in carbon cycling on continental shelves [23 ; 32]. Marine benthic communities are well-suited for long-term comparative investigations, as comprising species have a relatively long lifespan and either are sessile or have low motility. These traits make it possible to measure the effects of environmental change on communities over time. The potential impact of climate change on the marine environment may be acute, but it is difficult to register due to the lack of baseline data. A recent analysis showed that 34–59 % of Arctic megafauna taxa have yet to be documented [45].

The Barents Sea is a continental shelf sea with an average depth of 230 m (Fig. 1a); it is characterized by a transitional zone from warm Atlantic waters to cold Arctic ones (Fig. 1b) [43 ; 44]. Substantial climatic changes have been observed during the last four decades [8 ; 47]. Water temperatures in the subarctic Barents Sea during the past decade have reached the highest rates over the period observed [8]. Ice coverage has declined by about 10 % [4], while water temperature has risen by approximately 1.5 °C [35]. The area covered by the warmer Atlantic water has increased [28] due to northward shifts in the polar front, where Atlantic and Arctic water masses meet [43].

Analysis of Barents Sea benthic megafauna shows clear biogeographical patterns, with an Arctic productive community dominating in the northeast [11] and occasionally in the northwest, and an Atlantic warm water community in the southwest [29 ; 30]. A deep-cold-water community is found in the northwestern part of the Barents Sea shelf. A shallow bank community is predominant on the Spitsbergen Bank located southwards of Spitsbergen and in the southeastern Barents Sea. This shallow bank community is also found sporadically west and north of Spitsbergen [30].

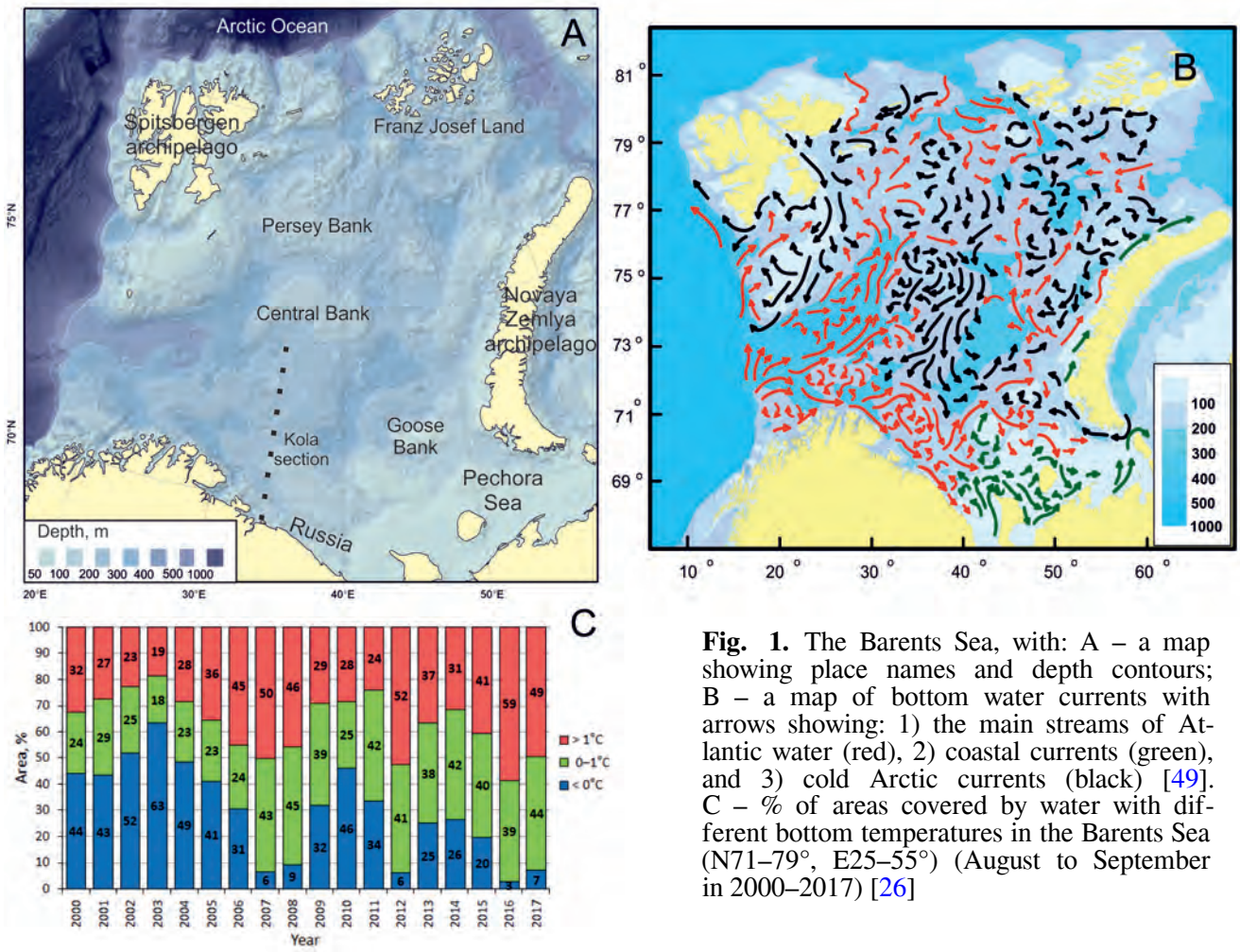

Fig. 1. The Barents Sea, with: A – a map showing place names and depth contours; B – a map of bottom water currents with arrows showing: 1) the main streams of Atlantic water (red), 2) coastal currents (green), and 3) cold Arctic currents (black) [49]. C – % of areas covered by water with different bottom temperatures in the Barents Sea (N71–79°, E25–55°) (August to September in 2000–2017) [26]

It has been suggested that climate change is causing a northward shift of biogeographical boundaries in the northern hemisphere due to the warming process [21]. The number of boreal species has increased, while the number of arctic species have declined [31]. The range of some species has expanded, and new boreal-subtropical species have appeared in the Arctic [52 ; 53].

The gradual accumulation of knowledge on megabenthos may make it possible to assess its role in the ecosystem and ultimately contribute to a more rational management of Barents Sea resources. This article presents an important series of long-term megabenthic observations in the Barents Sea. The main goal of our research is to identify spatial patterns and temporal trends in the megabenthic part of communities, including changes in biomass and production values.

MATERIAL AND METHODS

Benthos sampling. Norwegian and Russian ships were used to survey the Barents Sea annually August to November. Sampling stations were established at fixed positions along a regular grid (around 35 nautical miles between each station), covering an area of about 1.5 million km^2. The sampling equipment used was a Campelen 1800 bottom trawl, rigged with rockhopper ground gear, towed on double warps, and standardized to a fixed sampling effort (equivalent to a towing distance of 0.75 nautical miles, or 1.4 km). The horizontal opening was 15 m, and the vertical one was 5 m. The mesh size was 80 mm (stretched) in the front and 22 mm in the cod end, allowing capture and retention of vertebrates (fishes) and large invertebrates (megabenthos) from the seabed. All catch data presented in the article have been standardized to 1 nautical mile (hereinafter nm).

Data. Benthos specialists from the Polar branch of VNIRO (Russian and Norwegian ships), Institute of Marine Research, Murmansk Marine Biological Institute, and other international institutions (Norwegian ships) were involved in the processing and identification of benthos collected by the scientific trawl during the annual Norwegian-Russian Ecosystem Survey [1].

The processing of the biological material was conducted in accordance with standardized procedures, following the retrieval of each trawl [30]. The invertebrates were separated from the vertebrate catch in the onboard fish laboratory. Depending on catch weight, the material was processed in total or as a subsample. Records were made using paper datasheets, to be entered into a database afterward.

The total subsample weight was used to determine the adjustment factor in order to represent the full catch. All large (> 100 g) species, as well as rare megabenthic ones, were taken from the total catch, while the remaining species were extracted only from the subsample.

Most of the taxonomic processing was undertaken onboard to the lowest possible taxon. In cases of identification difficulties, the species were photographed and/or preserved for further processing by taxonomic specialists on land. In order to develop standardized species identification across all involved ships and throughout the entire research period, the naming of all the species was checked using photographs of each processed catch since 2013.

Following identification, the number of individuals of each species or taxon was counted, and wet weight was measured on electronic balances (± 0.5 g).

Totally, 5016 stations were sampled between 2005 and 2017 (Fig. 2). The total sampled biomass of benthic megafauna was 238.4 tons, consisting of over 14.9 million individuals. Some individuals were assigned to the genus or higher taxonomic level due to difficulties with their species identification. The final list included 1058 taxa, of which 694 were identified to species onboard (Table 1). As the Campelen trawl is designed to catch northern shrimp (Pandalidae family), this semipelagic shrimp could be overestimated

in the data, and therefore it was excluded from the analysis and used only for megabenthic data smoothing. Similarly, all pelagic species, such as jellies (Scyphozoa), were also excluded from the analysis. Values are presented as mean ± standard error (hereinafter *SE*) unless otherwise stated.

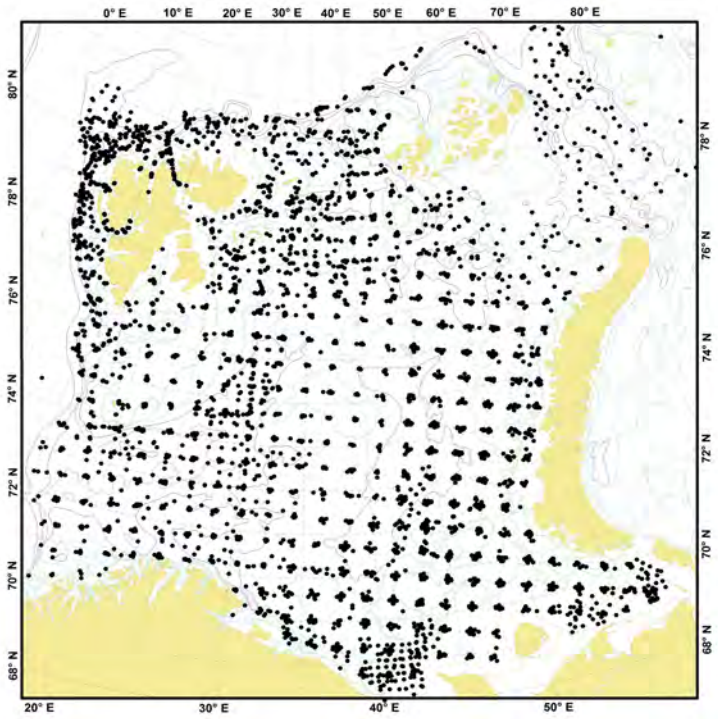

Fig. 2. Location of 5016 trawl stations covered during 2005–2017 by the joint Norwegian-Russian Ecosystem Survey

Table 1. Summary of the analyzed megafauna from the joint Norwegian-Russian Ecosystem Survey (2005–2017)

Year	Number of stations	Total		Average abundance (ind.·nm^{-1})	Average biomass (kg·nm^{-1})	Amount	
		Abundance (ind.)	Biomass (tons)			species	taxa
2005	224	107,114.0	2.6	522.5	12.7	142	218
2006	637	964,569.0	25.9	1576.0	42.1	261	388
2007	551	633,761.5	22.9	1240.2	44.6	222	351
2008	431	901,885.1	14.8	2183.7	35.7	157	244
2009	378	769,129.3	15.9	2056.4	42.2	283	391
2010	319	285,322.8	8.6	900.0	27.3	273	360
2011	391	1,333,887.2	13.4	3411.4	34.3	282	442
2012	443	4,345,807.4	55.6	9832.1	125.5	354	513
2013	487	1,888,138.0	34.8	3885.0	71.7	362	538
2014	165	463,108.6	6.0	2806.7	36.7	220	333
2015	334	606,272.4	6.6	1815.1	19.9	398	599
2016	317	1,340,958.8	11.5	4230.1	36.3	266	423
2017	339	1,277,828.3	19.8	3769.4	58.6	319	500
Total	5016	14,917,782.4	238.4	2940.7*	45.2*	694	1058

Note: * indicates the mean value across all years.

To determine whether there were any temporal differences in abundance and smoothed mean biomass among megabenthic fauna across the Barents Sea, the mean values per grid cell (N0.5°, E2°) were calculated both for early (2005–2011) and late (2012–2017) time periods of the study (see Figs 8 and 9).

Data smoothing. An examination of megabenthic biomass values in the Barents Sea indicated extensive inter-annual variations (Table 1). Therefore, the following steps were taken to minimize the chances of a possible sampling error and a distortion of results: 1) data collection was restricted to the area between N68–80°, E15–62° in order to exclude sectors covered only occasionally; 2) catches of > 1 ton were excluded; 3) shrimps of the Pandalidae family were excluded from the overall calculations and analyzed separately because all species of this family are benthopelagic, and the Campelen trawl possesses high catchability for such shrimps [51].

A smoothing function was constructed using a second-degree polynomial equation that was considered to minimize fluctuations in megafauna data. This was done for both Russian and Norwegian data samples, followed by a merge into a consolidated database. The smoothing procedure was conducted in three steps: 1) smoothing Pandalid data; 2) smoothing sessile epifauna data; 3) smoothing data of two other ecological groups (mobile epifauna and infauna).

The smoothing of Pandalid shrimp annual biomass data showed that the majority of shrimp biomass values had insignificant variations when compared to the smoothing curve. From the adjusted Pandalid values, correction coefficients were used to adjust the sampled biomass data of other taxa.

After this process, the megabenthic biomass was divided into three categories: “sessile epifauna”, “mobile epifauna”, and “infauna”. Because epifauna biomass fluctuated more than biomass of Pandalid shrimps, a second correction coefficient derived from the second-degree polynomial equation was calculated in the same way as for Pandalid shrimp biomass.

For mobile epifauna and infauna, the real values were divided by the second correction coefficient. Thereafter, modified biomass values of the mobile epifauna and infauna were smoothed in the same way. Smoothed data were used for further analysis in special cases, which are discussed below.

Production was calculated by multiplying taxon biomass by production to biomass (P/B) ratio. Two types of P/B ratio were used. The first was calculated for the major taxonomic groups from Degen *et al.* [11], and the second was calculated from the Manushin formula [37] (Table 2), except for taxa Porifera, Cnidaria, and Bryozoa, that were taken from Degen *et al.* [11]. Community production was calculated from the summarized production value of each taxon/species per station.

Table 2. Equations describing the dependence of the P/B ratio on mean body weight ($\overline{W}$, g of wet weight) for different taxa

Taxon	Equation
Annelida	$P / B = 0.365 \times \overline{W}^{-0.377}$
Arthropoda	$P / B = 2.190 \times \overline{W}^{-0.276}$
Chordata	$P / B = 0.073 \times \overline{W}^{-0.579}$
Echinodermata	$P / B = 0.730 \times \overline{W}^{-0.342}$
Total	$P / B = 0.694 \times \overline{W}^{-0.390}$

Biogeographical analysis. The biogeographical status of the Barents Sea can be assessed by determining the boundary lines between the Arctic and boreal communities at different points in time. The fluctuation of these boundary lines over time reflects the effects that water temperature changes have on benthic fauna. Here the Biogeographical Indices (hereinafter BGI) [38] are used to show the ratio between the boreal and Arctic components of the fauna:

$$BGI = \frac{Bb - Ba}{Bb + Ba}, \quad (1)$$

where Bb and Ba are biomasses of the boreal and Arctic species, respectively.

Each species from the stations was placed into one of three biogeographical categories: “boreal”, “Arctic”, or “boreal-Arctic” [50]. Afterwards, all species classified as “boreal-Arctic” were excluded from further analyses, leaving only pure “boreal” and “Arctic” species to be used in the calculation of the boreal-Arctic ratio per station [46]. The station value of the BGI varied from –1 (only Arctic species) to +1 (only boreal species). In the case of absence or equal amounts of boreal and Arctic species, the BGI for a station is zero. The stations with such BGI values represent the hypothetical boundary line between the Atlantic boreal and Arctic biogeographical regions.

To illustrate the BGI distribution, the Barents Sea and adjacent waters were divided into grid cells (10° long., 1° lat.), and the mean values of all stations per grid cell over a 3-year period were calculated and used as input for the map.

To show the distributional dynamics of borderlines between areas dominated by either boreal or Arctic species (*i. e.*, BGI = 0) 2005 to 2017, the centroid of each grid cell was used to plot the BGI in Map Viewer (Golden Software) [20]. The inverse distance to a power method was performed for gridding, and the moving average method was used for calculating the time series. Henceforth, the name **“boreal-Arctic boundary”** is used for the hypothetical boundary lines (BGI = 0) between the Atlantic boreal and Arctic biogeographical regions.

Dynamics of boundary shifts in the region of N69–76°, E20–55° 2005 to 2017 was described using the BGI per cell over a 3-year period and calculated using the moving average method. The area delimited by N69–76°, E20–55° was chosen for the analysis because it provided the most informative annual station coverage during the research period, with the exceptions being 2005 and 2014 due to the lack of data from the Norwegian participants of the study.

RESULTS

Biomass dynamics. The mean biomass 2006 to 2017 was estimated to be 31 kg·nm^{-1}. The mean biomass varied year to year, with the highest mean observed in 2012 (54 kg·nm^{-1}) and the lowest one registered in 2010 (22 kg·nm^{-1}) (Fig. 3A). The smoothed annual biomass reduced the maximum values of 2012 and 2017 considerably, resulting in a relatively stable curve, although variability increased after 2013, with the lowest biomass means observed in 2016 and 2017 (Fig. 3B). The average smoothed biomass 2006 to 2017 was estimated at 27 kg·nm^{-1}, with annual means varying –6 kg·nm^{-1} in 2016 to +7 kg·nm^{-1} in 2014.

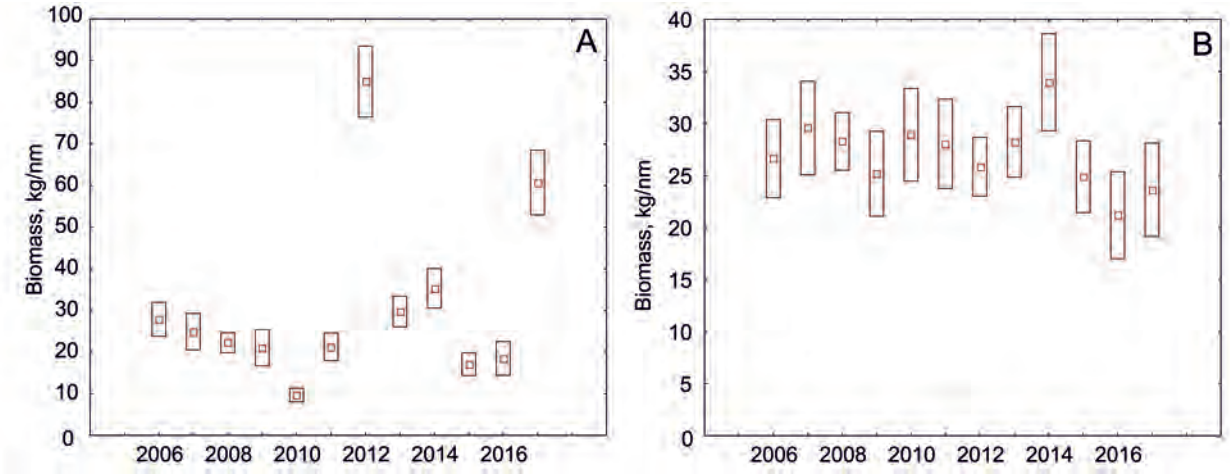

Fig. 3. Inter-annual variations in mean (± *SE*) biomass (kg·nm^{-1}) in the Barents Sea for observed (A) and smoothed (B) data (2006–2017)

Biomass of different taxa. The surveys in the Barents Sea have revealed patterns in the distribution of the megabenthic fauna. For the region as a whole, Porifera biomass dominated the fauna, followed by that of Arthropoda and Echinodermata (Fig. 4).

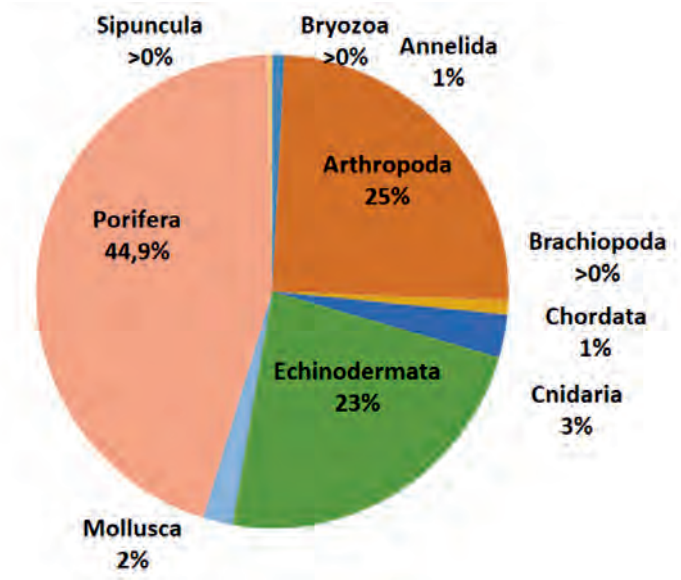

Fig. 4. Biomass distribution of the main megabenthic groups from 2005–2017 trawl surveys in the Barents Sea

Patterns were also noted in the spatial distribution in phyla biomass within the survey area (Fig. 5). Porifera was predominant in the western and northern peripheral areas; Arthropoda was predominant in the central and northwestern areas, while Echinodermata dominated mostly at the northern stations of the Barents Sea. Cnidaria dominated in the deep stations in the northern periphery but also had a noticeable presence in several locations in the central Barents Sea. Chordata (mainly Ascidiacea) biomass was dominant sporadically but with no apparent pattern. Areas with even phyla distribution were particularly prevalent in the shallow areas of the Novaya Zemlya Bank (eastern Barents Sea), Spitsbergen (northwestern Barents Sea) and other bank areas, due to the diversity of biotopes and environmental conditions there.

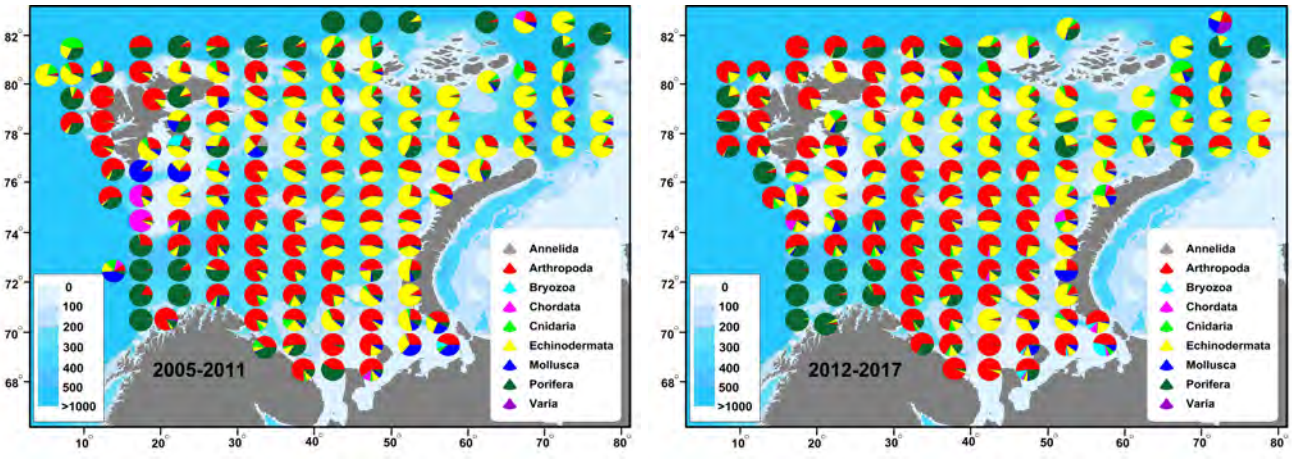

Fig. 5. Biomass distribution of the main phyla (Arthropoda, Echinodermata, Mollusca, and Porifera) and other groups (Annelida, Bryozoa, Sipuncula, Cnidaria, Chordata, and Brachiopoda) shown as mean values per grid cell (N1°, E5°) in 2005–2011 and 2012–2017

Several changes were observed in phyla dominance from the early period (2005–2011) to the late one (2012–2017). The northernmost stations, adjacent to the Arctic Ocean, shifted from being dominated by either Arthropoda or Echinodermata to becoming almost entirely dominated by Porifera. Along the west coast of Novaya Zemlya, the previously high diversity of phyla changed to domination by Arthropoda. Meanwhile, the central-eastern Barents Sea (N72–77°, E40–50°) has shifted from mostly Arthropoda to being dominated by Echinodermata.

Inter-annual variation in biomass (smoothed values) of five most dominant taxa revealed that Porifera remained relatively stable, except in 2017 when the biomass increased. The biomass of Cnidaria and Echinodermata experienced rapid decreases from 2015, while Arthropoda and Mollusca were more variable, ending with low values in 2017 (Fig. 6). Arthropoda and Echinodermata biomass were inversely related (linear regression is as follows: Echinoderm biomass = −1.4 × Arthropod biomass + 19.1; $R^2 = 0.64$).

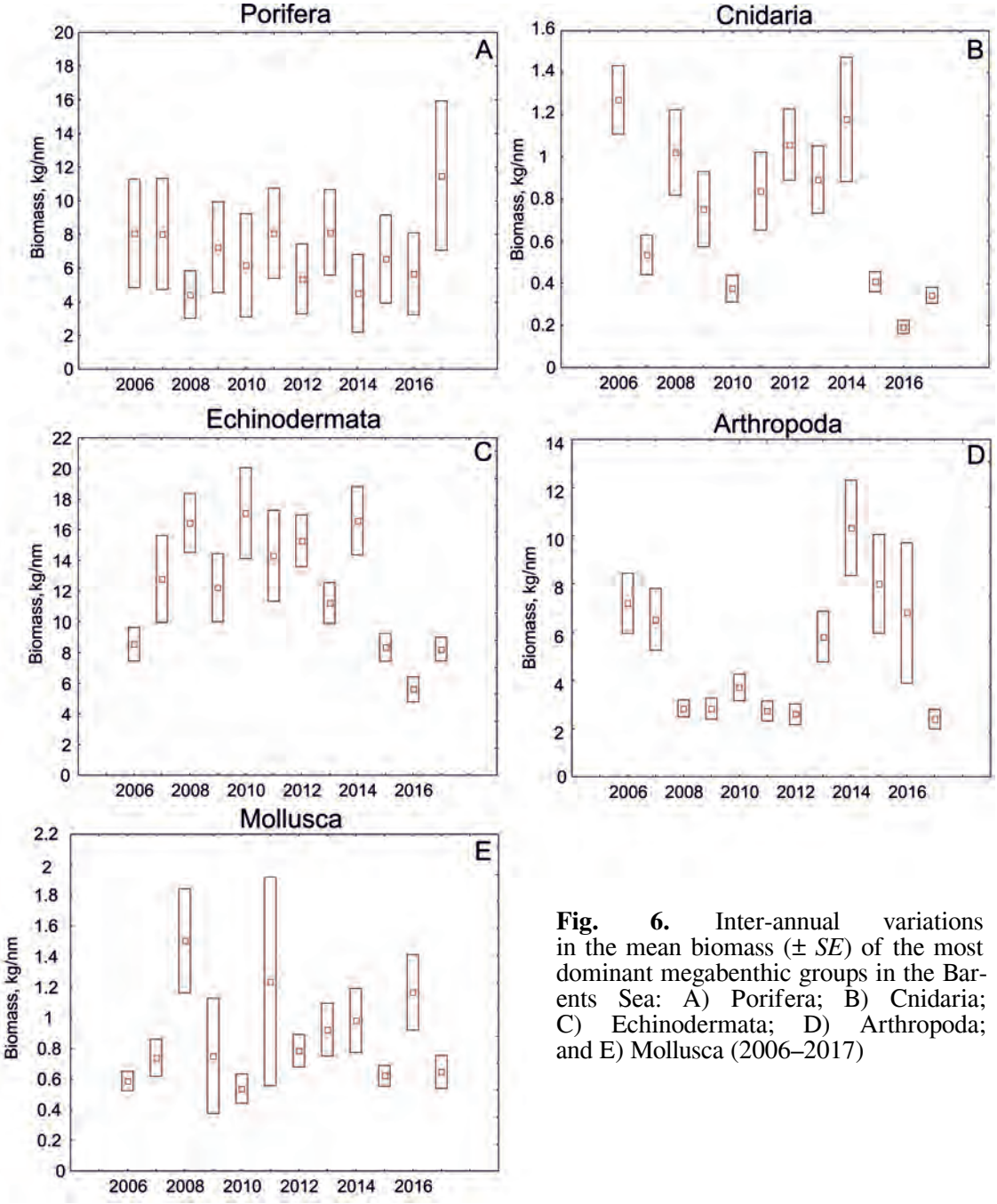

Fig. 6. Inter-annual variations in the mean biomass (± *SE*) of the most dominant megabenthic groups in the Barents Sea: A) Porifera; B) Cnidaria; C) Echinodermata; D) Arthropoda; and E) Mollusca (2006–2017)

The number of species. Species of the Barents Sea, presented as the mean number of species recorded during 2005–2017 (Fig. 7), had the highest values around Spitsbergen, while the lowest value was found in the northeastern region, which had the poorest coverage during the research period. However, low species diversity was also recorded in the southern areas of the Barents Sea that had experienced regular coverage as in the western and central areas of the sea.

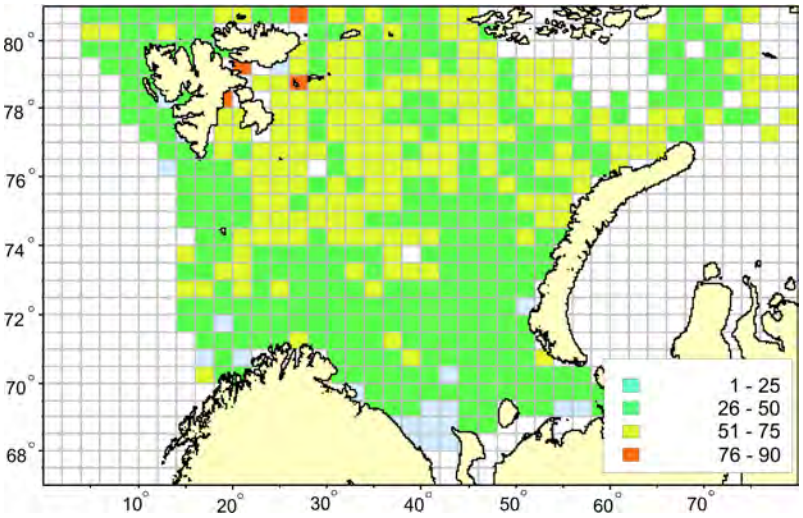

Fig. 7. Mean number of megabenthic species in the Barents Sea per grid cell (N0.5°, E2°) across the research period (2005–2017)

Abundance and biomass distribution during two time periods (2005–2011 and 2012–2017). The mean abundance was generally similar for both periods (the early one – (5489 ± 226) ind.·nm^{-1}; the late one – (5023 ± 363) ind.·nm^{-1}). However, the maximum catch nearly doubled between the early and late periods: 388,000 to 793,000 ind.·nm^{-1}. *F*-test shows that the differences between periods are statistically significant (F_{fact} (0.38) < F_{crit} (0.93); *p*-value = 0.0).

For both the early and late periods (Fig. 8), high mean abundances (up to 50,000 ind.·nm^{-1}) were recorded in the central region of the Barents Sea. However, in the late period, high abundances were also frequently noted in the northeastern region. The lowest abundances were observed in the southern area, particularly around Cape Kanin Nos that had regular coverage, but also in the northwest in the early period with poor coverage.

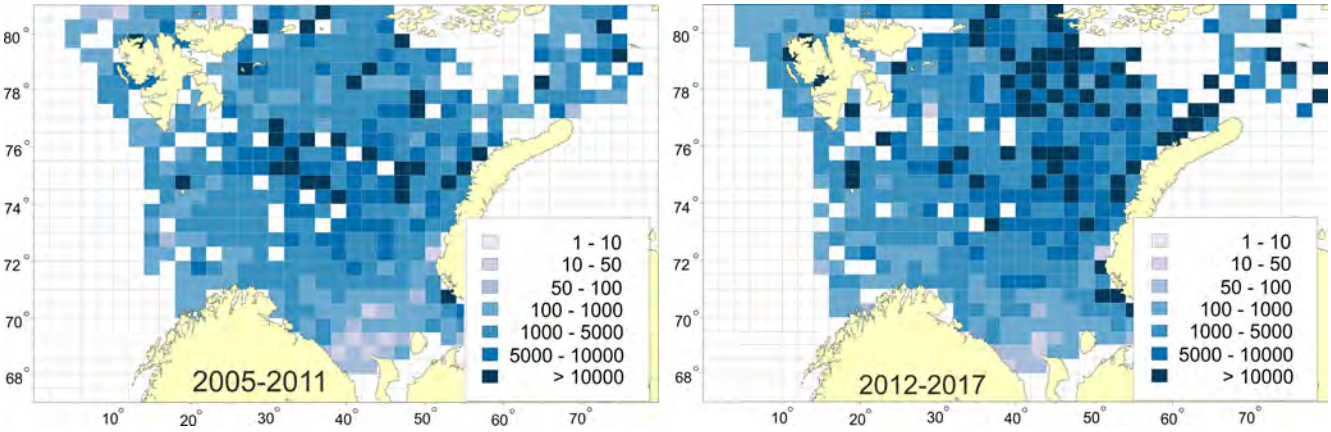

Fig. 8. Mean abundance (ind.·nm^{-1}) per grid cell (N0.5°, E2°) for the early (2005–2011) and late (2012–2017) research periods

The smoothed mean biomass decreased both in the early and late periods: (70.6 ± 6.6) kg·nm^{-1} in the earlier period to (63.0 ± 6.2) kg·nm^{-1} in the later one (Fig 9). *F*-test showed that these differences were statistically significant (F_{fact} (1.12) > F_{crit} (0.07); *p*-value = 0.0025). Meanwhile, the maximum catch increased 8.5 t·nm^{-1} in the early period to 9.8 t·nm^{-1} in the late one.

In the early period, the largest catches (> 1 ton) were obtained in the southwestern part of the Barents Sea (Fig. 9) due to the abundant sponge fields in this area; these were intentionally avoided in the late period due to the risk of damage to the bottom fauna and the gear. While relatively large catches have been made within a large area of the central Barents Sea in the early period, similar catches were mostly observed in the northeastern part of the Barents Sea during the late period. Late period data showed that large areas of the southeastern Barents Sea had the lowest biomass amounts (< 1 kg·nm^{-1}).

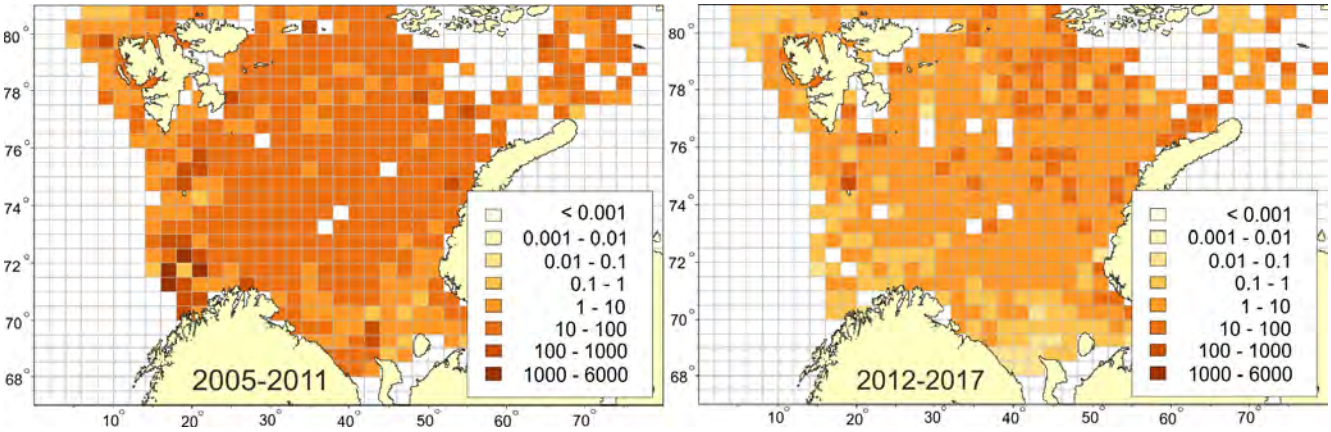

Fig. 9. Mean biomass (kg·nm^{-1}, smoothed values) per grid cell (N0.5°, E2°) across 2005–2011 and 2012–2017

The depth-related species richness, abundance, and biomass are shown in Fig. 10A, and a sampling frequency – in Fig. 10E. The highest sampling frequency and, therefore, more robust results were observed at 100–400-m depth. Stations shallower than 50 m or deeper than 600 m were less frequently sampled. In terms of species richness, the greatest diversity was seen at depths of 100–400 m (642 species), with lower richness on stations at ≤ 50 m (179 species) and a steady decline in richness at 500 m and deeper (≤ 347 species). The largest biomasses (average catch > 100 kg·nm^{-1}) were caught at 700-m depth, while the lowest biomasses (< 20 kg·nm^{-1}) – at ≥ 900 m. The highest abundances were noted at 200–300-m depth (more than 5000 ind.·nm^{-1}), while the lowest (less than 500 ind.·nm^{-1}) took place at ≤ 50 m and ≥ 700 m.

Production. When comparing the results for calculating production (see Fig. 11), the inter-annual variation showed similar trends between two methods, but at different scales, with the Manushin values being almost twice as large as those obtained with using the Degen *et al.* method (Fig. 11). Inter-annual variations of average megabenthic production in the Barents Sea in 2006–2017 reached the highest in 2008 and 2014 and the lowest in 2017. Most years showed a range 3–4 kg·nm^{-1}·year^{-1} (Fig. 11A) with a mean of (3.6 ± 0.6) kg·nm^{-1}·year^{-1} or 7–10 kg·nm^{-1}·year^{-1} with a mean of (8.1 ± 0.1) kg·nm^{-1}·year^{-1} (Fig. 11B).

The distribution of the Arctic *versus* boreal taxa of the Barents Sea. The distribution of the BGI values (see "Material and Methods") in the Barents Sea during 2005–2017 showed Arctic species dominating in the northern and eastern sectors of the Barents Sea, while the southern and western areas were dominated by the boreal species. These two regions are separated by a boreal-Arctic boundary line that has varied over time (Fig. 12).

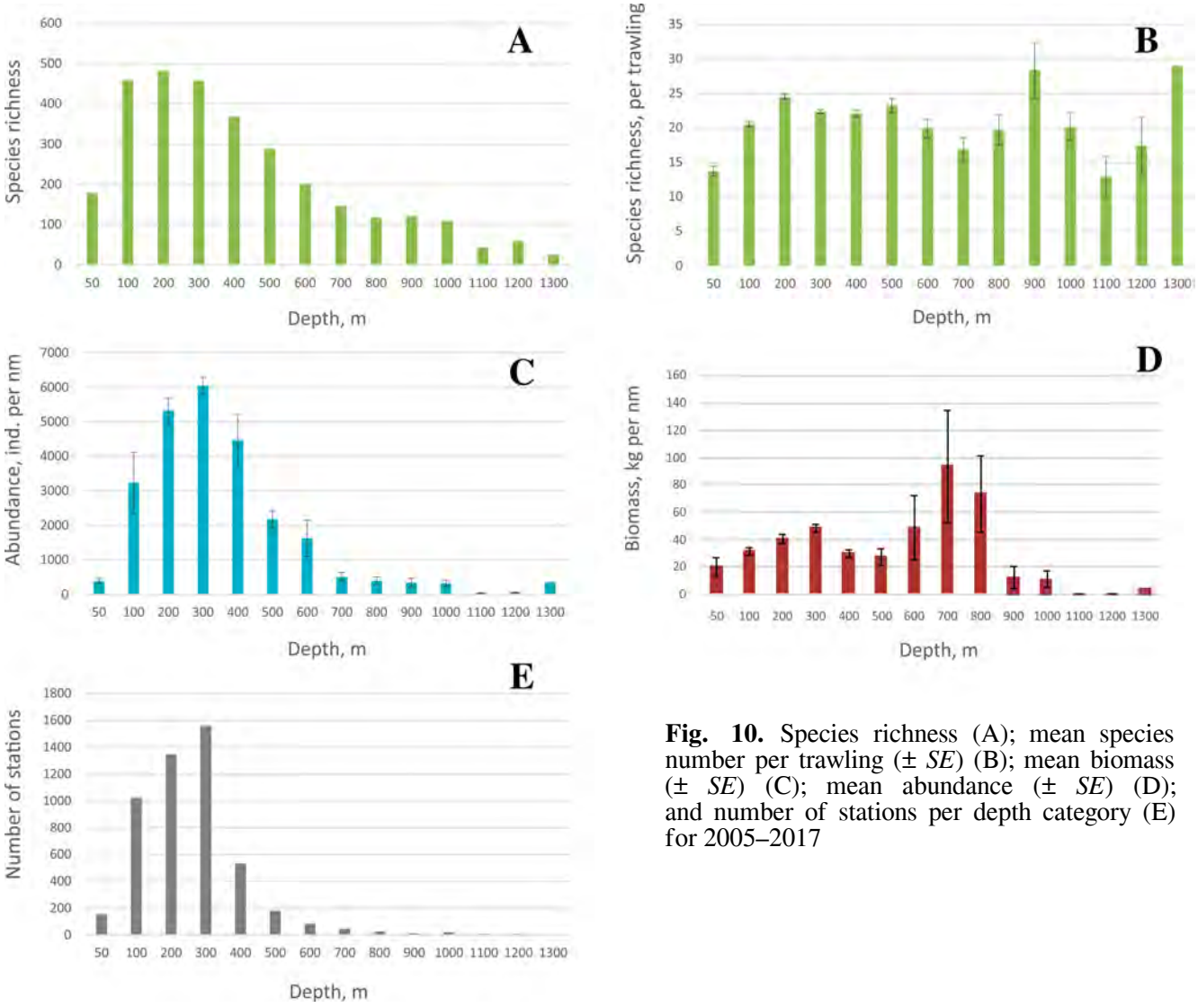

Fig. 10. Species richness (A); mean species number per trawling (± *SE*) (B); mean biomass (± *SE*) (C); mean abundance (± *SE*) (D); and number of stations per depth category (E) for 2005–2017

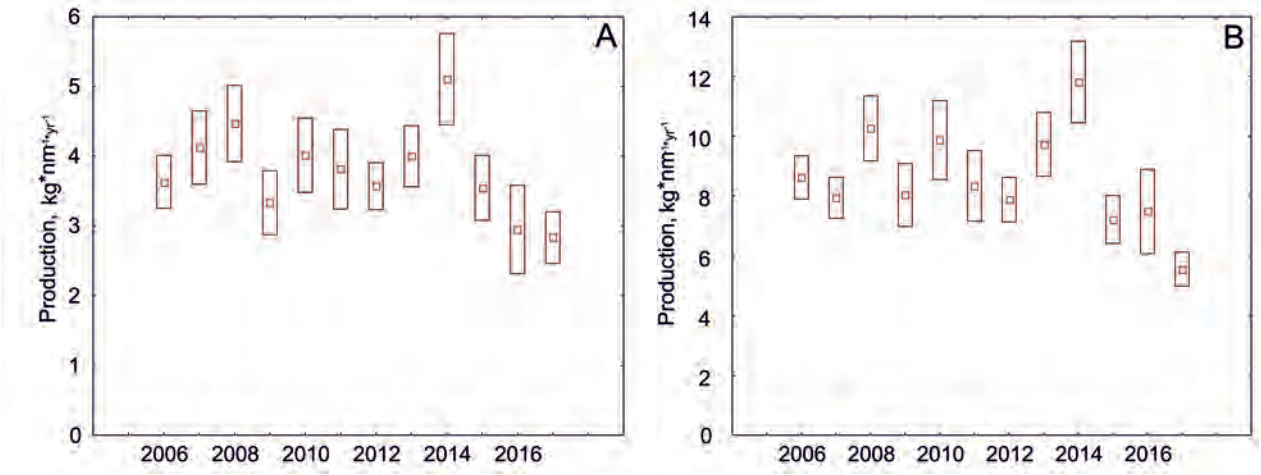

Fig. 11. Inter-annual variation of mean megabenthic production (± *SE*) in the Barents Sea in 2006–2017 calculated with two different P/B ratios: A) Degen *et al.* [11] and B) Manushin [37]

The location of the boreal-Arctic boundary line closely follows three main currents of Atlantic water in the Barents Sea: along the western slope of the Barents Sea shelf, to the Central Bank, and along the western shelf of the Novaya Zemlya archipelago (see also Fig. 1A).

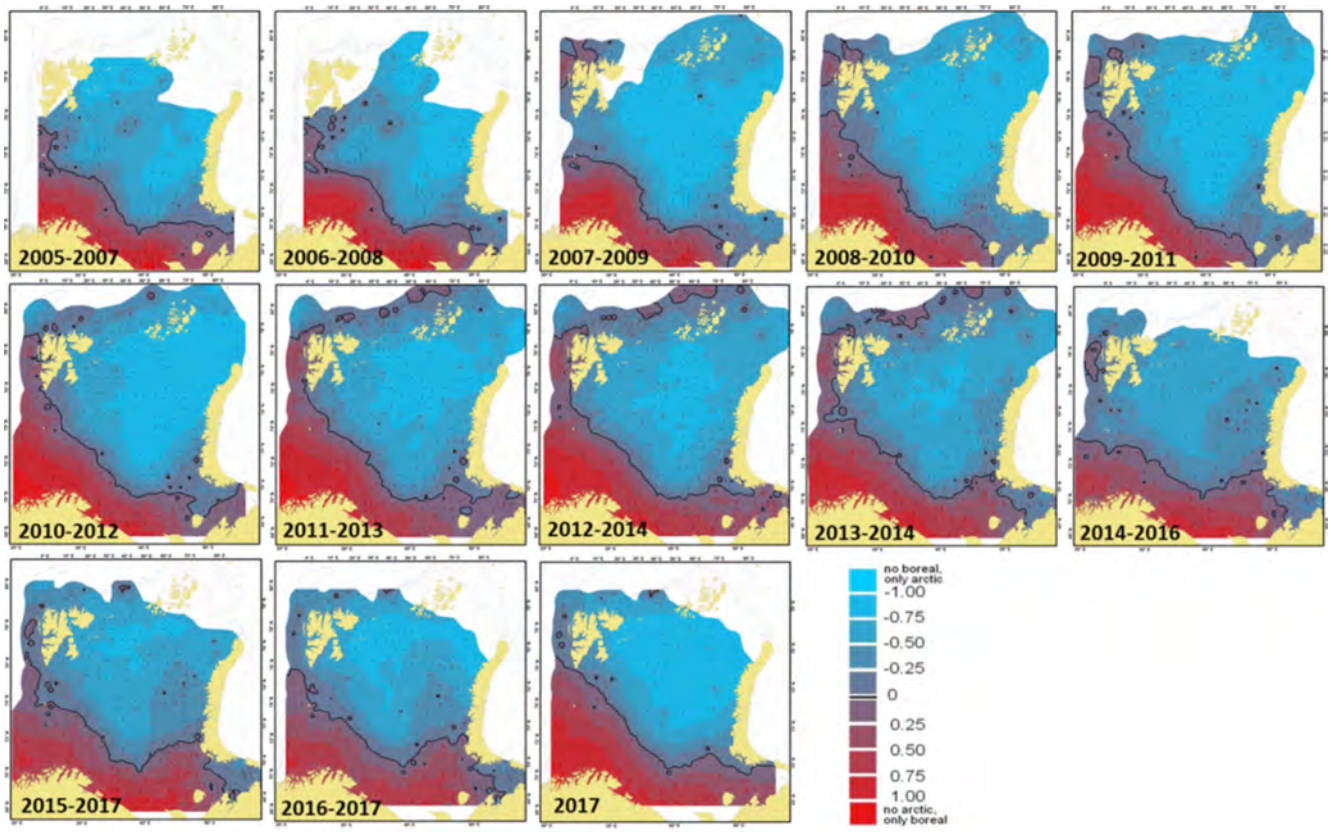

Fig. 12. Temporal distribution of the Arctic (blue) and boreal (red) areas of the Barents Sea (2005–2017). The black line shows the position of the boreal-Arctic boundary

The position of the boreal-Arctic boundary (BGI = 0) varied between years and locations (Fig. 13). In the southeastern part of the sea, the positions of the boundary have changed spatially by approximately 150–200 nm during 2005–2017, around 150 nm on the Spitsbergen Bank, and less than 50 nm in the central part of the sea.

The inter-annual fluctuation in the boreal-Arctic boundary position is most distinctive in the southeastern part of the Barents Sea. The results show that the boundary moved towards the southwest (upper five pictures in Fig. 12) during 2006–2010, indicating a prevalent distribution of Arctic species over boreal, while over the course of the next six years (2011–2016) it moved back in a northwards direction.

An area-based mean BGI for the central-southern part of the Barents Sea (Fig. 14) demonstrated a prevalence of Arctic species during 2007–2014, with a minimum value in 2010, followed by a prevalence of boreal species during 2014–2017. The years 2005 and 2014 are excluded from the calculation due to the lack of Norwegian data. The lowest and highest presence for boreal species in the constrained area is observed in 2010 and 2015–2016, respectively. Values below zero indicate the dominance of Arctic biomass, while values above zero indicate boreal dominance in the defined area (see embedded map in Fig. 14).

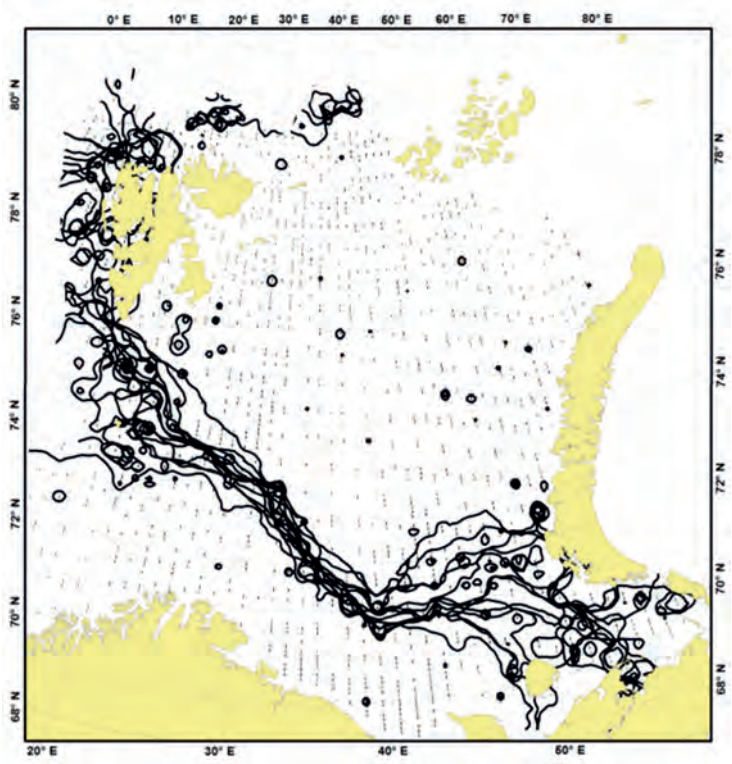

Fig. 13. Annual position of the boreal-Arctic boundary (BGI = 0) calculated 2005 to 2017

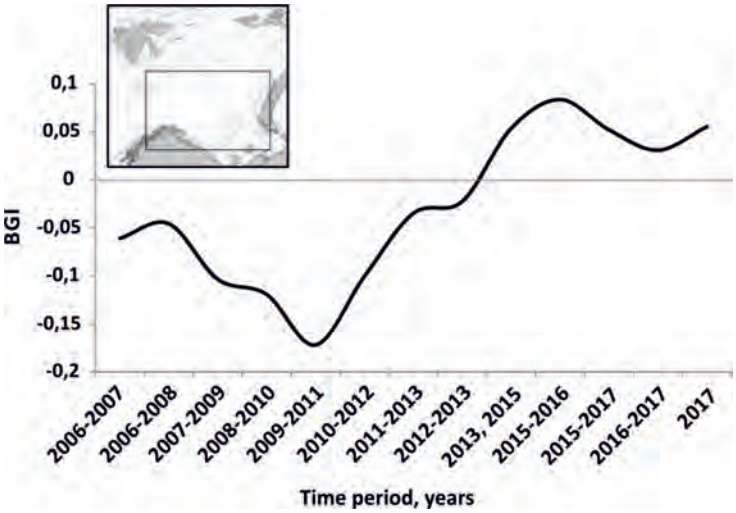

Fig. 14. Temporal variation of the mean BGI calculated for the central-southern Barents Sea constrained by N69–76°, E20–55° (map embedded) (2006–2017)

DISCUSSION

Throughout 13 years (2005–2017) of annual monitoring of the benthic megafauna, 21 % of 3245 species previously known [36] from Barents Sea, have been recorded. More than 5000 stations, 200 tons, and 14 million individuals of megafauna have been sampled. This achievement has become possible with using existing annual stock surveys, already being conducted by national governmental institutions, with the addition of benthic expertise, thereby making it possible to identify and evaluate the benthic by-catch from the commercial fish/shrimp trawl. It has proven to be a time- and cost-efficient approach for conducting long-term monitoring of the benthic habitats without additional seabed impact.

As the surveys were carried out using a trawl, animals in the catch were characterized by size as megabenthos [1]. Previous studies of zoobenthos mainly used material collected by grabs [15], but trawls and dredges of various design are better suited for sampling large invertebrates [17]. This was confirmed when studying the echinoderm fauna in the Kara Sea [2]. Taking into account the fact that the distribution, contribution to production, and gross biomass of 694 species (1058 taxa) studied here have been previously undervalued, it is therefore assumed that zoobenthos in previous studies had not been fully taken into account.

In 2005–2014 (the first nine years of investigation), the mean biomass and production values of the benthic megafauna were mostly stable, but they tended to decline after 2014.

The spatial distribution of the biomass showed that the highest values of megabenthos were recorded on the continental slope in the areas of hydrological fronts where water masses meet [39 ; 40 ; 42]. Similar results have previously been obtained for macrobenthos in the Barents Sea [2 ; 9 ; 14 ; 15 ; 34 ; 41], indicating that the same environmental factors are structuring these two faunal components. Prior to the ecosystem survey of the Barents Sea, however, there was no data on the distribution of megabenthic organisms in the Barents Sea, thus making it difficult to compare megabenthic and macrobenthic parts of the communities.

The depth range of 100–300 m accounted for 65 % of sea area [34] and included 79.5 % of the total number of stations used in the ecosystem survey, meaning that the investigated area was approximately evenly covered by bottom trawling. The highest species variety was observed in the 100–400-m depth layer, and a reduction in the number of species coincided with an increase in depth. This is also in accordance with prior investigations of macrobenthos [24], and has previously been explained by the depletion of food resources [34]. However, the mean numbers of species per trawling (Fig. 10B) show that species diversity in general is remarkably high in both shallow coastal areas and deep sea of the investigated parts of the Barents Sea.

The largest average catches of megabenthic fauna were taken at a depth range of 600–800 m, along the continental slope of the western and northern parts of the Barents Sea. Communities of high benthic biomass (predominantly sponges) have previously been reported [9 ; 34] in the area of the warm Atlantic Current of the West-Spitsbergen branch [39 ; 40 ; 42] and in Saint Anna Trough near Franz Josef Land [22] where they filtrate water current for food particles.

The average biomass of Arthropoda was at its highest in 2006–2007, coinciding with the introduction of red king crab (*Paralithodes camtschaticus*) to the southern part of the Barents Sea, and in 2013–2016, when the population of snow crab (*Chionoecetes opilio*) rose dramatically in the eastern part of the Barents Sea. The decrease in crustacean catches in recent years is most likely related to the spreading of snow crab over a larger area and the beginning of fishing in the areas of its maximum concentrations in the eastern part of the Barents sea in 2016 [48], where up to 8,000 tons of crab are caught annually.

It can be suggested that the decline observed in the biomass of Cnidaria and Echinodermata after 2014, was caused by predation and competition from the snow crab. Echinoderms and cnidarians are frequently found in crab stomachs [54], which may indicate feeding on these animals by large populations of snow crab.

Apart from a few exceptions, the Mollusca biomass tended to increase until 2016. Taking into account only the area populated by snow crab, the average biomass of Mollusca has increased, while across the Barents Sea as a whole, biomass was stable, which suggests that snow crabs may have only a small influence on the Mollusca biomass.

Molluscs are one of the main macrobenthic groups in snow crab diet [54]. However, large molluscs with strong shells, that could be caught by trawls, were not present in its diet, which suggests that the biomass of large molluscs is driven by other factors.

Both methods used to calculate the inter-annual variation of the megabenthic production in the Barents Sea showed similar trends; however, the use of Manushin formula doubled the resulting values of production. Using the mean biomass (27 kg·nm^{-1}), the annual P/B ratio was calculated to be 0.14 [11] and 0.3 [37]. There is a difference between the P/B ratio calculated by the Degen *et al.* method in this paper (0.14) and the value in the original article (0.15) [11]. This difference is explained by the selection of area of the Barents Sea (see "Material and Methods"), exclusion of catches > 1 ton, and the longer research period. It is assumed that the values obtained from the calculation with using the Manushin method [37] are more realistic because his formula is based on taxonomic status and an individual average body weight of ectothermic animals. It could be suggested that Degen *et al.* [11] calculations had not taken into account small-sized groups of animals, due to the low catchability of small animals by the Campelen trawl. In Manushin formula [37], this underestimation is minimized because both available materials and author's own data are used to create production equation for a wide size range of animals. Similar results were obtained in a study of scallop (*Chlamys islandica*) near the Kola Peninsula, being a similar megabenthos size group, where P/B ratio was estimated to be 0.25 [13]. Comparing P/B ratio of macrobenthos (0.2–5.3; mean (1.44 ± 0.06) [54]) and megabenthos (0.3), the level of megabenthic production seems to be realistic.

The boreal-Arctic boundary line in the Barents Sea (also called the biogeographical border between the Arctic and boreal regions) has been known since the mid-XIX century, but without general consensus of its position due to different criteria for setting the biogeographical boundaries [27].

The results from this research show that, in the current warm period, the majority of the Barents Sea is in an intermediate state between the Arctic and boreal regions due to the wide distribution of boreal species toward the north. Dynamics of BGI mean value within the central-southern part of the Barents Sea (see Fig. 14) suggests that since 2013, a larger part of the Barents Sea could be characterized as a predominantly boreal intermediate area. Moreover, it is suggested that the shift in the boundary line between the Arctic and boreal areas toward its most southern position in 2009–2011 may have been caused by the coldest year prior to the research period (2003, *i. e.*, six to eight years beforehand), resulting in the largest negative anomaly for the megabenthos biomass.

Acknowledgement. We acknowledge the joint Norwegian-Russian Ecosystem Survey of IMR and PINRO and all colleagues and staff on the ships, in the laboratories, and in the offices. We appreciate the help of Claude Nozères (Maurice Lamontagne Institute) and Stephen Long (Zoological Society of London) who made valuable corrections and remarks to the manuscript. We would like to thank the anonymous reviewers of the manuscript for useful comments.

REFERENCES

1. *Atlas of the megabenthic organisms of the Barents Sea and adjacent waters.* Murmansk : PINRO, 2018, 534 p. (in Russ.)
2. Anisimova N. A. Echinoderms of the southern part of the Kara Sea. In: *Fauna of the invertebrates of the Barents, the Kara and the White Seas* / G. G. Matishov (Ed.). Apatity : KSC RAS, 2003, pp. 111–130. (in Russ.)
3. Antipova T. V. Echinoderms of the southern part of the Kara Sea. *Trudy of the Knipovich Polar Research Institute of Marine Fisheries and Oceanography*, 1975, iss. 35, pp. 121–124. (in Russ.)
4. Årthun M., Eldevik T., Smedsrud L. H., Skagseth Ø., Ingvaldsen R. B. Quantifying the influence of Atlantic heat on Barents Sea ice variability and retreat. *Journal of Climate*, 2012, vol. 25,

iss. 13, pp. 4736–4743. https://doi.org/10.1175/JCLI-D-11-00466.1

5. Asplin L., Ingvaldsen R., Loeng H., Sætre R. *Transport of Atlantic Water in the western Barents Sea.* [Copenhagen : International Council for the Exploration of the Sea, 2001]. (ICES CM 2001/W:03).
6. Blacker R. W. Recent changes in the benthos of the West Spitsbergen fishing grounds. *Special Publication of the International Commission for the Northwest Atlantic Fisheries*, 1965, no. 6, pp. 791–794.
7. Bluhm B. A., Iken K., Hardy S. M., Sirenko B. I., Holladay B. A. Community structure of epibenthic megafauna in the Chukchi Sea. *Aquatic Biology*, 2009, vol. 7, no. 3, pp. 269–293. https://doi.org/10.3354/ab00198
8. Boitsov V. D., Karsakov A. L., Trofimov A. G. Atlantic water temperature and climate in the Barents Sea, 2000–2009. *ICES Journal of Marine Science*, 2012, vol. 69, iss. 5, pp. 833–840. https://doi.org/10.1093/icesjms/fss075
9. Brotskaya V. A., Zenkevich L. A. Quantitative evaluation of the bottom fauna of the Barents Sea. *Transactions of the Institute of Marine Fisheries and Oceanography of the USSR*, 1939, vol. 4, pp. 5–98. (in Russ.) ; pp. 99–126. (Summ. in Engl.)
10. Cheung W. W., Lam V. W., Sarmiento J. L., Kearney K., Watson R., Pauly D. Projecting global marine biodiversity impacts under climate change scenarios. *Fish and Fisheries*, 2009, vol. 10, iss. 3, pp. 235–251. https://doi.org/10.1111/j.1467-2979.2008.00315.x
11. Degen R., Jørgensen L. L., Lubin P., Ellingsen I. H., Pehlke H., Brey T. Patterns and drivers of megabenthic secondary production on the Barents Sea shelf. *Marine Ecology Progress Series*, 2016, vol. 546, pp. 1–16. https://doi.org/10.3354/meps11662
12. Denisenko S. G. Zoobentos Barentseva morya v usloviyakh izmenyayushchegosya klimata i antropogennogo vozdeistviya. In: *Dinamika morskikh ekosistem i sovremennye problemy sokhraneniya biologicheskogo potentsiala morei Rossii*. Vladivostok : Dal'nauka, 2007, pp. 418–511. (in Russ.)
13. Denisenko S. G. *Ekologiya i resursy islandskogo grebeshka v Barentsevom more.* Apatity : Kol'skii nauchnyi tsentr AN SSSR, 1989, 138 p. (in Russ.)
14. Denisenko S. G. Long-term changes of zoobenthos biomass in the Barents Sea. *Proceedings of the Zoological Institute of Russian Academy of Sciences*, 2001, vol. 289, pp. 59–66.
15. Denisenko S. G. *Bioraznoobrazie i bioresursy makrozoobentosa Barentseva morya: struktura i mnogoletnie izmeneniya.* Saint Petersburg : Nauka, 2013, 284 p. (in Russ.)
16. Dyer M. F., Cranmer G. J., Fry P. D., Fry W. G. The distribution of benthic hydrographic indicator species in Svalbard waters, 1978–1981. *Journal of the Marine Biological Association of the United Kingdom*, 1984, vol. 64, iss. 3, pp. 667–677. https://doi.org/10.1017/S0025315400030332
17. Filatova Z. A., Zenkevich L. A. Kolichestvennoe raspredelenie donnoi fauny Karskogo morya. *Trudy Vsesoyuznogo gidrobiologicheskogo obshchestva*, 1957, vol. 8, pp. 3–67. (in Russ.)
18. Fossheim M., Primicerio R., Johannessen E., Ingvaldsen R. B., Aschan M. M., Dolgov A. D. Recent warming leads to a rapid borealization of fish communities in the Arctic. *Nature Climate Change*, 2015, vol. 5, iss. 7, pp. 673–677. https://doi.org/10.1038/nclimate2647
19. Frainer A., Primicerio R., Kortsch S., Aune M., Dolgov A. V., Fossheim M., Aschan M. M. Climate-driven changes in functional biogeography of Arctic marine fish communities. *Proceedings of the National Academy of Sciences*, 2017, vol. 114, no. 46, pp. 12202–12207. https://doi.org/10.1073/pnas.1706080114
20. Franke R. Scattered data interpolation: Test of some methods. *Mathematics of Computations*, 1982, vol. 33, no. 157, pp. 181–200. https://doi.org/10.2307/2007474
21. Galkin Y. I. Long-term changes in the distribution of mollusks in the Barents Sea related to the climate. *Berichte der Polarforschung*, 1998, vol. 287, pp. 100–143.
22. Galkin S. V., Vedenin A. A., Minin K. V., Rogacheva A. V., Molodtsova T. N., Rajskiy A. K., Kucheruk N. V. Macrozoobenthos of southern part of St. Anna Trough and adjacent Kara Sea shelf. *Oceanology*, 2015, vol. 55, iss. 4, pp. 614–622. https://doi.org/10.1134/S0001437015040098

23. Grebmeier J. M., Smith W. O., Conover R. J. Biological processes on Arctic continental shelves: Ice-Ocean-Biotic interactions. In: *Arctic Oceanography: Marginal Ice Zones and Continental Shelves* / W. O. Smith, J. M. Grebmeier (Eds). Washington, DC : American Geophysical Union, 1995, pp. 231–261. (Coastal and Estuarine Studies ; vol. 49). https://doi.org/10.1029/CE049p0231
24. Herman Y. (Ed.) *The Arctic Seas: Climatology, Oceanography, Geology, and Biology*. Boston, MA : Springer, 1989, 888 p. https://doi.org/10.1007/978-1-4613-0677-1
25. Hoegh-Guldberg O., Bruno J. F. The impact of climate change on the world's marine ecosystems. *Science*, 2010, vol. 328, iss. 5985, pp. 1523–1528. https://doi.org/10.1126/science.1189930
26. *Interim Report of the Working Group on the Integrated Assessments of the Barents Sea (WGIBAR)*, 9–12 March, 2018, Tromsø, Norway. Copenhagen, Denmark : International Council for the Exploration of the Sea, 2018, 210 p. (WGIBAR 2018 Report ; ICES CM 2018/IEASG: 04).
27. Jirkov I. A. Biogeography of the Barents Sea benthos. *Invertebrate Zoology*, 2013, vol. 10, iss. 1, pp. 69–88.
28. Johannesen E., Høines Å. S., Dolgov A. V., Fossheim M. Demersal fish assemblages and spatial diversity patterns in the Arctic-Atlantic transition zone in the Barents Sea. *PLoS One*, 2012, vol. 7, iss. 4, art. E34924 (14 p.). https://doi.org/10.1371/journal.pone.0034924
29. Johannesen E., Jørgensen L. L., Fossheim M., Primicerio R., Greenacre M., Lubin P., Dolgov A. V., Ingvaldsen R. B., Anisimova N. A., Manushin I. E. Large-scale patterns in community structure of benthos and fish in the Barents Sea. *Polar Biology*, 2017, vol. 40, iss. 2, pp. 237–246. https://doi.org/10.1007/s00300-016-1946-6
30. Jørgensen L. L., Ljubin P., Skjoldal H. R., Ingvaldsen R. B., Anisimova N., Manushin I. Distribution of benthic megafauna in the Barents Sea: Baseline for an ecosystem approach to management. *ICES Journal of Marine Science*, 2015, vol. 72, iss. 2, pp. 595–613. https://doi.org/10.1093/icesjms/fsu106
31. Jørgensen L. L., Primicerio R., Ingvaldsen R. B., Fossheim M., Strelkova N., Thangstad T. H., Zakharov D. Impact of multiple stressors on sea bed fauna in a warming Arctic. *Marine Ecology Progress Series*, 2019, vol. 608, pp. 1–12. https://doi.org/10.3354/meps12803
32. Klages M., Boetius A., Christensen J. P., Deube H., Piepenburg D., Schewe I., Soltwedel T. The benthos of Arctic seas and its role for the organic carbon cycle at the seafloor. In: *The Organic Carbon Cycle in the Arctic Ocean* / R. Stein, R. W. Macdonald (Eds). Berlin ; Heidelberg : Springer, 2004, pp. 139–167. https://doi.org/10.1007/978-3-642-18912-8_6
33. Kortsch S., Primicerio R., Fossheim M., Dolgov A. V., Aschan M. Climate change alters the structure of arctic marine food webs due to poleward shifts of boreal generalists. *Proceedings of the Royal Society B: Biological Sciences*, 2015, vol. 282, iss. 1814, art. 20151546 (9 p.). https://doi.org/10.1098/rspb.2015.1546
34. Kuznetsov A. P. On the distribution of trophic groupings of bottom invertebrates in the Barents Sea. *Transactions of the P. Shirshov Institute of Oceanology*, 1970, vol. 88, pp. 5–80. (in Russ.)
35. Lind S., Ingvaldsen R. B. Variability and impacts of Atlantic water entering the Barents Sea from the north. *Deep Sea Research Part I: Oceanographic Research Papers*, 2012, vol. 62, pp. 70–88. https://doi.org/10.1016/j.dsr.2011.12.007
36. *List of Species of Free-living Invertebrates of Eurasian Arctic Seas and Adjacent Deep Waters* / B. I. Sirenko (Ed.). Saint Petersburg : Zoological Institute RAS, 2001, 129 p. (Explorations of the Fauna of the Seas ; iss. 51 (59)).
37. Manushin I. E. Srednyaya massa osobi kak pokazatel' skorosti oborota veshchestva v populyatsiyakh vodnykh ektotermnykh zhivotnykh. In: *Materialy X nauchnogo seminara "Chteniya pamyati K. M. Deryugina"*. Saint Petersburg : KopiServis, 2008, pp. 29–34. (in Russ.)
38. Manushin I. E., Anisimova N. A., Lyubin P. A., Dahle S., Cochrane S. Mnogoletnie izmeneniya v makrozoobentose yugo-vostochnoi chasti Barentseva morya. In: *Materialy XIV nauchnogo seminara "Chteniya pamyati K. M. Deryugina"*. Saint Petersburg : SpbGU, 2012, pp. 33–45. (in Russ.)

39. Matishov G. G., Volkov V. A., Denisov V. V. Structure of warm Atlantic water circulation in the Northern Barents. *Doklady Russian Academy of Sciences*, 1998, vol. 362, no. 4, pp. 553–556. (in Russ.)
40. Matishov G. G., Matishov D. G., Moiseev D. V. Inflow of Atlantic-origin waters to the Barents Sea along glacial troughs. *Okeanologia*, 2009, no. 51 (3), pp. 321–340.
41. Nesis K. N. Izmeneniya donnoi fauny Barentseva morya pod vliyaniem kolebanii gidrologicheskogo rezhima (na razreze po Kol'skomu meridianu). In: *Sovetskie rybokhozyaistvennye issledovaniya v moryah Evropeiskogo Severa*. Moscow : Pishchepromizdat, 1960, pp. 129–138. (in Russ.)
42. Ozhigin V. K., Ivshin V. A. *Vodnye massy Barentseva morya.* Murmansk : Izd-vo PINRO, 1999, 48 p. (in Russ.)
43. Ozhigin V. K., Ivshin V. A., Trofimov A. G., Karsakov A. L., Antsiferov M. Yu. *Waters of the Barents Sea: Structure, circulation, variability.* Murmansk : PINRO, 2016, 260 p. (in Russ.)
44. Oziel L., Sirven J., Gascard J.-C. The Barents Sea frontal zones and water masses variability (1980–2011). *Ocean Science*, 2016, vol. 12, iss. 1, pp. 169–184. https://doi.org/10.5194/os-12-169-2016
45. Roy V., Iken K., Archambault P. Regional variability of megabenthic community structure across the Canadian Arctic. *Arctic*, 2015, vol. 68, no. 2, pp. 180–192.
46. Shorygin A. A. Iglokozhie Barentseva morya. *Trudy Morskogo nauchno-issledovatel'skogo instituta*, 1928, vol. 3, no. 4, 128 p. (in Russ.)
47. Smedsrud L. H., Esau I., Ingvaldsen R. B., Eldevik T., Haugan P. M., Li C., Lien V. S., Abdirahman A. O., Omar M., Otterå O. H., Risebrobakken B., Sandø A. B., Semenov V. A., Sorokina S. A. The role of the Barents Sea in the Arctic climate system. *Reviews of Geophysics*, 2013, vol. 51, iss. 3, pp. 415–449. https://doi.org/10.1002/rog.20017
48. Sokolov K. M., Pavlov V. A., Strelkova N. A. et al. *Snow crab Chionoecetes opilio in the Barents and Kara seas.* Murmansk : PINRO, 2016, 242 p. (in Russ.)
49. Tantsyura A. I. On seasonal changes of currents in the Barents Sea. *Trudy of the Knipovich Polar Research and Designing Institute of Marine Fisheries and Oceanography*, 1973, iss. 34, pp. 108–112. (in Russ.)
50. Vassilenko S. V., Petryashov V. V. (Eds). *Illustrated Keys to Free-living Invertebrates of Eurasian Arctic Seas and Adjacent Deep Waters. Vol. 1: Rotifera, Pycnogonida, Cirripedia, Leptostraca, Mysidacea, Hyperiidea, Caprellidea, Euphausiacea, Dendrobranchiata, Pleocyemata, Anomura, and Brachyura.* Fairbanks, Alaska : Alaska Sea Grant College Program, University of Alaska Fairbanks ; Zoological Institute, Russian Academy of Sciences, 2009, 192 p. https://doi.org/10.4027/ikflieasadw.2009
51. Walsh S. J., McCallum B. R. Performance of the Campelen 1800 shrimp trawl during the 1995 Northwest Atlantic Fisheries Centre autumn groundfish survey. *Northwest Atlantic Fisheries Organization Scientific Council Studies*, 1997, no. 29, pp. 105–116.
52. Zakharov D. V., Anisimova N. A., Stepanenko A. M. First record of the sea star *Porania pulvillus* (O. F. Müller, 1776) in Russian part of the Arctic. *Russian Journal of Biological Invasions*, 2016, vol. 7, iss. 4, pp. 321–323. https://doi.org/10.1134/S207511171604010X
53. Zakharov D. V., Jørgensen L. L. New species of the gastropods in the Barents Sea and adjacent waters. *Russian Journal of Biological Invasions*, 2017, vol. 8, iss. 3, pp. 226–231. https://doi.org/10.1134/S2075111717030146
54. Zakharov D. V., Manushin I. E., Strelkova N. A., Pavlov V. A., Nosova T. B. Diet of the snow crab in the Barents Sea and macrozoobenthic communities in the area of its distribution. *Trudy VNIRO*, 2019, vol. 172, pp. 70–90. (in Russ.). https://doi.org/10.36038/2307-3497-2018-172-70-90

МЕГАБЕНТОС БАРЕНЦЕВА МОРЯ: ПРОСТРАНСТВЕННО-ВРЕМЕННОЕ РАСПРЕДЕЛЕНИЕ И ПРОДУКЦИОННАЯ ХАРАКТЕРИСТИКА

Д. В. Захаров[1,2], Л. Л. Йоргенсен[3], И. Е. Манушин[1], Н. А. Стрелкова[1]

[1]Полярный филиал ФГБНУ «ВНИРО» («ПИНРО» имени Н. М. Книповича), Мурманск, Российская Федерация

[2]Мурманский морской биологический институт РАН, Мурманск, Российская Федерация

[3]Институт морских исследований, Тромсё, Норвегия

E-mail: *zakharden@yandex.ru*

Представлены результаты программы мониторинга мегабентоса Баренцева моря и сопредельных акваторий, выполняемой Россией и Норвегией с 2005 г. Мегабентос является одним из важнейших компонентов донной составляющей экосистемы Баренцева моря, формируя значительную долю живого вещества, включённого в пищевые цепи и систему экологических взаимоотношений. В частности, организмы мегабентоса играют существенную, а зачастую и определяющую роль в питании донных рыб и ракообразных Баренцева моря, в том числе важнейших промысловых видов: трески, пикши, камчатского краба, краба-стригуна опилио и др. Нередко представители данной группы формируют специфические биотопы, определяющие условия существования множества других видов животных. Постепенное накопление знаний о мегабентосе позволит оценить его роль в экосистеме и в конечном итоге поспособствует рациональному управлению ресурсами Баренцева моря. Основная цель нашего исследования — описать пространственное распределение и выявить динамику биомассы и продукции мегабентоса в Баренцевом море. С 2005 г. в рамках оценки запасов промысловых видов рыб и беспозвоночных проводится обработка прилова мегабентоса из донных тралений. За 2005–2017 гг. выполнено 5016 траловых станций, обработано 238,4 т валовой биомассы мегабентоса, просмотрено около 14,9 млн экз. животных. Материал собирали с помощью донного трала Campelen 1800 — низкоселективного активного сетного орудия лова, выполненного из капроновой дели с шагом ячеи 125 мм, с мелкоячеистой сетной кутовой вставкой с размером ячеи 22 мм и резиновым грунтропом типа «рокхоппер» с диаметром катков 40 см. Для удобства сравнительного анализа количественные параметры, представленные в статье, рассчитывали на стандартную дистанцию траления в 1 морскую милю (nm). Обработку материала проводили на борту судна непосредственно между постановками тралов. В ходе исследования зарегистрировано 694 вида мегабентоса; высокое видовое разнообразие зафиксировано на глубинах 100–400 м, наибольшие средние значения биомассы и численности отмечены на глубинах 600–800 м. Биомасса (B) и продукция (P) мегабентоса были стабильны на протяжении первых девяти лет исследований, но после 2014 г. появилась тенденция к их снижению. Значение коэффициента P/B для мегабентоса оценивается на уровне 0,3. Предполагается, что предыдущие исследования бентоса в Баренцевом море недооценивали вклад как минимум 694 видов из группы мегабентоса в видовое богатство, валовую биомассу, численность и продукцию. Динамика биогеографического индекса (граница между бореальной и арктической зонами) в южной части Баренцева моря позволяет предположить, что с 2013 г. бóльшую часть моря можно охарактеризовать как бореальную промежуточную область.

Ключевые слова: Арктика, Баренцево море, мегабентос, климат, Атлантическое течение, продукция, видовое богатство

1871
ИнБЮМ – IBSS

Морской биологический журнал
Marine Biological Journal
2020, vol. 5, no. 2, pp. 38–49
https://doi.org/10.21072/mbj.2020.05.2.04

UDC 594.124:577.115:628.193(262.5)

FATTY ACID COMPOSITION IN TROCHOPHORES OF MUSSEL *MYTILUS GALLOPROVINCIALIS* GROWN UNDER CONTAMINATION WITH POLYCHLORINATED BIPHENYLS

© 2020 **L. L. Kapranova, L. V. Malakhova, M. V. Nekhoroshev, V. V. Lobko, and V. I. Ryabushko**

A. O. Kovalevsky Institute of Biology of the Southern Seas of RAS, Sevastopol, Russian Federation
E-mail: *lar_sa1980@mail.ru*

Received by the Editor 16.07.2019; after revision 14.04.2020;
accepted for publication 26.06.2020; published online 30.06.2020.

Status of *Mytilus galloprovincialis* populations in the natural habitat is known to directly depend on development of Black Sea mussel at all its stages, including initial stages of larval ontogenesis, which are very sensitive to environmental pollution. Organic pollutants adversely affect mussel larvae by inhibiting their growth and development. Patterns of mussel reproduction are well studied, which makes it possible to obtain larvae from artificially fertilized eggs of this mollusc species in controlled laboratory conditions. In this work, the fatty acid composition of *M. galloprovincialis* larvae at the trochophore stage on the 3rd day in the control experiment and under artificial contamination with polychlorinated biphenyls (PCBs) in different concentrations is studied for the first time. The fatty acid composition of total lipids in the biomass of larvae obtained on the 3rd day of the experiment was studied by means of gas chromatography – mass spectrometry. Totally, 14 fatty acids were identified in the samples; 59 % of them were saturated fatty acids, 24 % were monounsaturated fatty acids, and 17 % were polyunsaturated fatty acids. Statistical analysis was performed using Statistical Toolbox of MATLAB software (version 8.2). The totals of monounsaturated and polyunsaturated fatty acids significantly differed in lipids of *M. galloprovincialis* trochophores in the experiment with different PCB concentrations. The totals of saturated fatty acids did not significantly differ. The major saturated fatty acids in all mussel trochophores studied were palmitic (C16:0) and stearic (C18:0) acids. Their concentration did not significantly change under the exposure to PCBs. The main monounsaturated fatty acids were oleic (C18:1ω9), palmitoleic (C16:1ω7), and vaccenic (C18:1ω7) acids. The fraction of monounsaturated fatty acids was twice as low when exposed to the PCB concentrations 0.1 and 1.0 μg·L^{-1}. However, when the PCB concentration was 10 μg·L^{-1}, the total of these acids did not differ from the control. Among polyunsaturated fatty acids having biological essentiality, it was possible to identify arachidonic (C20:4ω6), eicosapentaenoic (C20:5ω3), and docosahexaenoic (C22:6ω3) acids. The total fraction of omega-3 and omega-6 acids in mussel larvae in the control did not exceed 12.8 %. With an increase of the PCB concentration in the growth medium 0.1 to 1.0 μg·L^{-1}, the fraction of polyunsaturated fatty acids increased 2.5-fold. At the PCB concentration 10 μg·L^{-1} and in the sample with pure acetone added, the total fraction of polyunsaturated fatty acids was comparable with that in the control. The results of the study indicate that fatty acid response is the highest when the medium is exposed to the PCB concentrations ranging 0.1 to 1.0 μg·L^{-1}. At the PCB concentrations equal to 10 μg·L^{-1} or higher, biochemical processes in larvae seem to slow down. The results of this study will contribute to a better understanding of biochemical rearrangements that allow molluscs at larval developmental stages to adapt to environmental pollution with organic xenobiotics.

Keywords: polychlorinated biphenyls, fatty acids, larvae, trochophore, mussel *Mytilus galloprovincialis*, Black Sea

The study of the effect of contamination of *Mytilus galloprovincialis* living in the natural conditions of Sevastopol marine area and being cultivated in coastal marine farms has been the subject of a number of works, focused mainly on adult mature individuals [11 ; 12 ; 19 ; 24 ; 31], as well as their gametes [7].

Mussels are known to be resistant to various types of pollution. Being filtrators, these molluscs actively accumulate pollutants in the organism. One of the most toxic environmental pollutants is organochlorine compounds (hereinafter OCC). The widespread prevalence of OCC in Black Sea water determined the pollution of natural mollusc populations in many marine areas off Sevastopol, since mussels accumulate hydrophobic OCC even with their relatively low concentration in seawater. In mussels from Martynova, Karantinnaya, and Golubaya bays, the total concentration of polychlorinated biphenyls ($\sum PCB_6$) varied from 3.8 ng·g^{-1} (hereinafter on wet weight) in gills to 459 ng·g^{-1} in hepatopancreas [6]. In Laspi Bay, where the anthropogenic impact is not so pronounced, OCC concentration was lower and ranged from 0.21 ng·g^{-1} in gills to 10.3 ng·g^{-1} in gonads [6]. OCC accumulation in mussel organs positively correlated with the content of total lipids in them [6]. Since embryos and larvae are the most sensitive stages of mussel ontogenesis, the influence of pollutants can lead to inhibition and arrest of their growth [8]. Under experimental conditions, chromosomal aberrations in cells under the influence of solutions of toxicants, such as surfactants, on fertilized eggs have already been established [9]. A few years ago, we showed *in vivo* a positive correlation of OCC concentration in water with pelagic eggs mortality and a negative correlation with the number of fish larvae at early stages of postembryonic development [23].

The aim of this work was to determine fatty acid composition of trophophores of the cultivated mussel *M. galloprovincialis*, grown under experimental contamination with polychlorinated biphenyls.

MATERIAL AND METHODS

The object of research was the bivalve mollusc *Mytilus galloprovincialis* Lamarck, 1819, taken in spring 2019 from collectors of a mussel-and-oyster farm located in Karantinnaya Bay water area (Sevastopol, Crimean Peninsula). To prepare for the study, 150 spec. of mussel with a shell length of 7–10 cm were selected. During that season, the molluscs were mainly at the spawning stage of development.

Larvae were obtained in laboratory conditions; the laboratory did not contain toxic fumes and gases. The ambient temperature in the laboratory was (20 ± 2) °C. The indoor lighting was combined [5]. To clear the digestive tract, 150 spec. of mussel were kept for 4 hours in filtered seawater, collected by a bathometer in Karantinnaya Bay water area. In the mussel-and-oyster farm area, the total polychlorinated biphenyls (hereinafter PCBs) concentration in water did not exceed 3 ng·L^{-1}, which corresponded to the average value for the open areas of the Black Sea [6 ; 10].

Each mollusc was placed the umbo down in a 0.5-L glass beaker. The glassware for the experiment was chemically clean. The seawater filtered through a membrane filter (with the pore size 3–5 μm) and heated to +25 °C was poured into each glass beaker, so as to cover the upper edge of the mussel cusps, thereby stimulating spawning [3]. The seawater, in which the larvae spawning and rearing took place, had the following physiochemical characteristics: temperature +23…+25 °C; pH 8.1–8.3; Ca^{2+} concentration 210–290 mg·L^{-1}; Mg^{2+} concentration 460–640 mg·L^{-1}; salinity 18 ‰; dissolved oxygen saturation in the surface water layer 100–110 %.

During the mollusc spawning, which occurred 4 hours after the stimulation, the eggs deposited on the bottom in the form of bright orange sediment, and sperm was released into the water in the form of a white cloud. After the isolation of gametes, the molluscs were removed from the glass beaker. The resulting solutions with eggs were joined and transferred to a 3-L container. The solutions with sperm were

collected in another 3-L container. Then, 10 mL of the mussel sperm solution was added to the egg containing solution. Since the fertilization process is fast [16], the solution with fertilized eggs was dispensed, 3 minutes after joining the solutions, in five separate 1-dm^3 reactors. A solution of PCB mixture in acetone (Aroclor 1254, Supelco, USA) was added to 3 reactors. PCB concentrations in water of the reactors affecting the larvae were 0.1, 1, and 10 $\mu g \cdot L^{-1}$. Acetone was added to the 4th reactor in the same amount as in the reactors with the PCBs. The 5th reactor was a control one. The experiment was carried out in triplicate.

The temperature in the reactors for larvae growing was (20 ± 2) °C. The light in the reactors was both artificial (fluorescent lamps) and natural. The combined illuminance measured with a Yu-116 lux meter did not exceed 750 lx. Mussel larvae were grown for 3 days when they were fed endogenously. At this stage, the development of the digestive system and the increase of the body cavity were only at the very beginning [16].

Lipid extraction and production of fatty acid methyl esters. The fatty acid composition was studied in total lipids isolated from the biomass of larvae obtained on the 3rd day of the experiment (*in vitro*). To obtain fatty acids, the larvae were separated from water by filtration through a filter with a pore size of 84 μm. The larvae were thoroughly washed from the filter with several 5-ml portions of a mixture of ethanol : chloroform (1 : 1). The resulting solution with 20 mL in volume was centrifuged for 10 minutes at 1500 rpm with a double volume of distilled water. The lower chloroform layer was collected with a capillary. The chloroform fraction was triply washed with water and evaporated on a rotary evaporator. After evaporation of chloroform to saponify lipid residues, 5 mL of an alkaline methanolic solution (10 mL of a 3 N solution of NaOH mixed with 90 mL of 90 % methanol) were added into the flask. The resulting solution was refluxed until complete saponification for two hours. After cooling, a few drops of a 1 % solution of phenolphthalein were added into the solution, and the extraction of unsaporifiable lipids was performed three times with hexane. The water-alcohol phase was acidified with hydrochloric acid by adding 300 μL of 6 N HCl. Then the repeated extraction of fatty acids was carried out with 3–4 portions of hexane, 5 mL each. The hexane fraction was evaporated to dryness on a rotary evaporator at a temperature +30…+35 °C; 5 mL of a 3 % solution of hydrogen chloride in methanol was added to the residue for methylation. The mixture was refluxed for 2 hours; after cooling, it was subjected to triple extraction with hexane (5 mL each portion). The hexane layer was filtered using an ashless filter. Before the determination of fatty acid methyl esters (hereinafter FAME), the hexane fraction was stored for no longer than a day at a temperature +5 °C [4].

Identification of fatty acid methyl esters. FAME identification was performed at IBSS “Spectrometry and Chromatography” core facility using a Crystal 5000.2 gas chromatograph (SKB “Chromatek”,Yoshkar-Ola, Russia) with a quadrupole mass detector and a capillary column DB-5ms (“Agilent Technologies”) 30 m long, with the inner diameter of 0.25 mm and the film phase thickness of 0.25 μm. The measurements were carried out in the electron impact ionization mode with a potential of 70 eV. The carrier gas was helium; the flow rate was 1 $ml \cdot min^{-1}$. The sample injection was carried out in the splitless mode. The injector temperature was +280 °C. The column temperature was as follows: initial temperature +60 °C; delay for 1 minute; temperature ramp 5 $°C \cdot min^{-1}$ to +180 °C; temperature ramp 5 $°C \cdot min^{-1}$ to +290 °C; final temperature +325 °C maintained for 10 minutes. The volume of the sample injected was 1.0 μl. The FAME identification was carried out in the total ion current. The FAME identification was carried out by comparing the relative retention time of the experimental chromatograms with that of the standard FAME mixture chromatogram (Supelco 37 component FAME mix) and by matching the obtained mass spectra of FAME – against the NIST 14 library counterparts with a degree of agreement exceeding 92 %. The calculation of FAME percentage in the sample was carried out by the normalization to the sum of the peak areas. The standard deviation of the output signal of the chromatograph did not exceed 6 % [15].

Statistical data processing. For the statistical analysis, we used Statistical Toolbox package embedded integrated in MATLAB software (version 8.2). Statistically significant differences between the samples were determined using one-way ANOVA and the Tukey – Kramer post-hoc test.

RESULTS AND DISCUSSION

It is known that the level of PCB accumulation by mussels depends on many factors such as tissue fat, mollusc size, and sexual maturation stage. It is individual differences of these factors that determine wide ranges of variation in the concentration of organochlorine toxicants in individuals collected in one region. Thus, PCB concentration in soft tissues of mussels in the sampling area varied 14 to 162 ng·g^{-1} and averaged 68 ng·g^{-1} ($n = 24$). A comparison of PCB levels in the mussels with the maximum permissible concentration (2000 ng·g^{-1} for the PCB according to the Technical Regulation of the Customs Union [13]), shows that there is no hazard for humans in case of consumption of the cultivated mussels from the farm. Moreover, according to the criteria established in the EU countries, the quality of mussels is ranked as very high, since the values do not exceed the established threshold for PCB concentration of 250 ng·g^{-1} [16].

In the experiments on the effect of environmentally significant PCB doses on mussel larvae, their response to this kind of pollution was revealed, which manifested itself in the variation of the fatty acid composition (Tables 1 and 2).

Table 1. Fatty acid fractions (% of the total) in trochophore lipids of mussel *M. galloprovincialis* grown in a medium with different concentrations of polychlorinated biphenyls

Identified fatty acid	Control	PCBs concentration, μg·L^{-1}			Acetone
		0.1	1	10	
Lauric (dodecanoic) (C12:0)	1.4 ± 0.6	0.6 ± 0.3	1.3 ± 0.4	1.0 ± 0.3	1.4 ± 0.5
Myristic (tetradecanoic) (C14:0)	6.2 ± 0.2	5.7 ± 0.6	7.7 ± 0.7	6.4 ± 0.4	6.5 ± 0.6
Pentadecanoic (C15:0)	4.4 ± 0.8	5.3 ± 1.1	8.5 ± 0.5	5.8 ± 0.2	4.7 ± 0.7
Palmitoleic (*cis*-9-hexadecenoic) (C16:1ω7)	11.0 ± 0.6	6.8 ± 0.6	7.0 ± 0.2	9.6 ± 0.4	10.8 ± 0.8
Palmitic (hexadecanoic) (C16:0)	29.3 ± 4.3	33.8 ± 0.4	30.1 ± 0.3	34.7 ± 0.6	31.7 ± 2.3
cis-10-heptadecenoic (C17:1ω7)	3.9 ± 1.5	1.2 ± 0.4	1.2 ± 0.2	1.4 ± 0.4	2.4 ± 1.5
14-methylhexadecanoic (*anteiso*-C17:0)	2.4 ± 0.5	1.8 ± 0.3	2.3 ± 0.2	2.0 ± 0.1	2.6 ± 0.8
Arachidonic (*cis*,*cis*,*cis*,*cis*-5,8,11,14-eicosatetraenic) (C20:4ω6)	1.3 ± 0.2	20.5 ± 1.5	12.8 ± 0.6	3.3 ± 0.3	1.0 ± 0.4
Linoleic (*cis*,*cis*-9,12-octadecadienoic) (C18:2ω6)	2,2 ± 0,6	3.0 ± 0.3	4.8 ± 0.6	1.3 ± 0.4	1.6 ± 0.7
Oleic (*cis*-9-octadecenoic) (C18:1ω9)	14.4 ± 1.5	1.5 ± 0.2	1.2 ± 0.2	15.3 ± 0.4	14.6 ± 1.1
Vaccenic (*cis*-11-octadecenoic) (C18:1ω7)	2.4 ± 0.3	5.8 ± 0.3	5.7 ± 0.2	2.4 ± 0.3	2.5 ± 0.7
Sum of two isomers of octadecenoic acids	16.8 ± 1.8	7.3 ± 0.5	6.9 ± 0.4	17.7 ± 0.7	17.1 ± 1.8
Stearic (octadecanoic) (C18:0)	14.4 ± 0.5	8.1 ± 0.4	10.3 ± 0.3	9.2 ± 0.3	13.3 ± 0.5
Eicosapentaenoic (*cis*,*cis*,*cis*,*cis*,*cis*-5,8,11,14,17-eicosapentaenoic, EPA) (C20:5ω3)	4.2 ± 0.6	3.0 ± 0.2	4.0 ± 0.1	4.6 ± 0.3	4.3 ± 0.3
Docosahexaenoic (*cis*,*cis*,*cis*,*cis*,*cis*,*cis*-4,7,10,13,16,19-docosahexaenoic, DHA) (C22:6ω3)	2.4 ± 1.0	2.9 ± 0.2	3.1 ± 0.2	2.8 ± 0.4	2.5 ± 0.5
Total saturated fatty acids (SFA)	58.2	55.3	60.2	59.1	60.3
Total monounsaturated fatty acids (MUFA)	31.6	15.3	15.1	28.8	30.3
Total polyunsaturated fatty acids (PUFA)	10.2	29.4	24.7	12.1	9.5
Total unsaturated fatty acids (UFA)	41.8	44.7	39.8	40.9	39.8
Total SFA / total UFA ratio	1.4	1.2	1.5	1.4	1.5

Table 2. Significant differences (denoted by pluses) in fatty acid composition of mussel *M. galloprovincialis* trochophores as found from one-way ANOVA (d*f* = 4) and Tukey – Kramer post-hoc test

Fatty acid	Pollutant concentration, μg·L^{-1}	Control	Pollutant concentration, μg·L^{-1}			*F*	*p*
			0.1	1	10		
Lauric	0.1	–		–	–	0.620	0.66
	1	–	–		–		
	10	–	–	–			
	acetone	–	–	–	–		
Myristic	0.1	–		–	–	1.81	0.20
	1	–	–		–		
	10	–	–	–			
	acetone	–	–	–	–		
Pentadecanoic	0.1	–		–	–	5.40	$1.4\cdot10^{-2}$
	1	+	–		–		
	10	–	–	–			
	acetone	–	+	–	–		
Palmitoleic	0.1	+		–	–	13.32	$5.1\cdot10^{-4}$
	1	+	–		–		
	10	–	–	–			
	acetone	–	+	+	–		
Palmitic	0.1	–		–	–	1.11	0.41
	1	–	–		–		
	10	–	–	–			
	acetone	–	–	–	–		
cis-10-heptadecenoic	0.1	–		–	–	1.48	0.28
	1	–	–		–		
	10	–	–	–			
	acetone	–	–	–	–		
14-methylhexadecanoic	0.1	–		–	–	0.58	0.68
	1	–	–		–		
	10	–	–	–			
	acetone	–	–	–	–		
Arachidonic	0.1	+		–	+	124	$1.8\cdot10^{-8}$
	1	+	–		+		
	10	–	+	+			
	acetone	–	+	+	–		
Linoleic	0.1	–		–	–	6.80	$6.6\cdot10^{-3}$
	1	–	–		+		
	10	–	–	+			
	acetone	–	–	+	–		
Oleic	0.1	+		–	+	71.3	$2.6\cdot10^{-7}$
	1	+	–		+		
	10	–	+	+			
	acetone	–	+	+	–		

Continue on the next page…

Fatty acid	Pollutant concentration, μg·L^{-1}	Control	Pollutant concentration, μg·L^{-1}			*F*	*p*
			0.1	1	10		
Vaccenic	0.1	+		–	+	23.1	$4.9 \cdot 10^{-5}$
	1	+	–		+		
	10	–	+	+			
	acetone	–	+	+	–		
Stearic	0.1	+		–	–	41.2	$3.5 \cdot 10^{-6}$
	1	+	–		–		
	10	+	–	–			
	acetone	–	+	+	+		
Eicosapentaenoic	0.1	–		–	–	3.52	$5.0 \cdot 10^{-2}$
	1	–	–		–		
	10	–	–	–			
	acetone	–	–	–	–		
Docosahexaenoic	0.1	–		–	–	0.344	0.84
	1	–	–		–		
	10	–	–	–			
	acetone	–	–	–	–		
Total SFA	0.1	–		–	–	1.00	0.45
	1	–	–		–		
	10	–	–	–			
	acetone	–	–	–	–		
Total MUFA	0.1	+		–	+	37.3	$5.6 \cdot 10^{-3}$
	1	+	–		+		
	10	–	+	+			
	acetone	–	+	+	–		
Total PUFA	0.1	+		–	+	65.5	$3.9 \cdot 10^{-7}$
	1	+	–		+		
	10	–	+	+			
	acetone	–	+	+	–		

Note: "+" indicates significant differences ($\alpha = 0.05$; $n = 3$); "–" indicates lack of significant differences ($\alpha = 0.05$; $n = 3$); *F* indicates Fisher's *F*-test; *p* indicates probability. The components with significant differences are in bold.

It was found that in lipids of *M. galloprovincialis* trochophores the totals of monounsaturated fatty acids (hereinafter MUFA) and polyunsaturated fatty acids (hereinafter PUFA) significantly differed. The total of saturated fatty acids (hereinafter SFA) did not statistically change. The main SFA were palmitic (C16:0) (35–39 %) and stearic (C18:0) (8–14 %) acids. Saturated acids with a carbon number of 14 and 15 ranged 4 to 7 %. A relatively high level of SFA in trochophores is associated with high metabolic activity of molluscs during the spring spawning [30]. For example, when studying a seasonal fatty acid composition of the pearl oyster *Pinctada fucata martensii*, it was determined that the major SFA were myristic (C14:0), palmitic (C16:0), and stearic (C18:0) acids. Myristic (C14:0) acid in animals is rarely the main component. In our studies, its percentage varied 5.7–7.7 %.

The most common MUFA are represented by palmitoleic (C16:1ω7), oleic (C18:1ω9), and vaccenic (C18:1ω7) acids. Palmitoleic (C16:1ω7) and oleic (C18:1ω9) acids are derivatives of palmitic (C16:0) and stearic (C18:0) acids [14]. Vaccenic (C18:1ω7) acid is an isomer of oleic (C18:1ω9) acid,

which is synthesized in animal cells (endoplasmic reticulum and mitochondria) from stearic (C18:0) acid by the double bond formation. The presence of *cis*-vaccenic (C18:1ω7) acid, which is characteristic of anaerobic bacteria [18], in trochophore samples indicates non-sterile experimental conditions.

The monounsaturated oleic (*cis*-9-octadecenoic) (C18:1ω9) acid, found by us in mussel trochophores, has two possible origins: exogenous (*via* the digestion of diatoms) and endogenous (*via* the conversion of palmitic (C16:0) and stearic (C18:0) acids) [20]. The increased content of irreplaceable oleic (C18:1ω9) acid in mollusc trochophores may be due to its additional synthesis under the toxic effects of pollutants in order to bind and detoxify xenobiotics [22]. An increase in the level of isomers of octadecenoic (C18:1) acids may indicate an enhanced metabolism in larval cells [14].

The following PUFA were identified in trochophore lipids: arachidonic (C20:4ω6), eicosapentaenoic (C20:5ω3), and docosahexaenoic (C22:6ω3) acids. The total fraction of omega-3 and omega-6 acids in mussel larvae of the control experiment did not exceed 12.8 %. The concentration of the essential arachidonic (C20:4ω6) acid in trochophores was not constant and varied over a wide range 1 to 21 %. For comparison, the concentration of arachidonic (C20:4ω6) acid in gastropods reached 5.73 % [25]. As is known, living organisms can synthesize arachidonic (C20:4ω6) acid from the essential omega-6-unsaturated linoleic acid [1]. The biosynthesis of linoleic (C18:2ω6) acid can be carried out only in plants. Then, it is transferred to animals through food chains. Since linoleic (C18:2ω6) acid was found in mussel larvae in almost every sample, it can be assumed that it is necessary for the biosynthesis of arachidonic (C20:4ω6) acid at further stages of the mollusc development. Arachidonic (C20:4ω6) acid is also a major component of membrane phospholipids in animals. In addition, it is necessary for prostaglandin biosynthesis [29]. Probably, higher levels of this fatty acid in trochophores are related to more intense synthesis of prostaglandins [21].

PUFA are involved in the adaptation of the organism to the environment. Most invertebrates are not able to synthesize PUFA and get them with food, satisfying their needs for these essential components to maintain normal functioning of the organism [28]. For example, docosahexaenoic (C22:6ω3) acid can affect the activity of Na^+/K^+-ATPase, an enzyme of cell membranes that selectively pumps out sodium ions from a cell and accumulates potassium ions in it. The difference in concentrations of monovalent cations created by the enzyme is used for key reactions of vital activity: excitation of a nerve impulse and water-salt metabolism and for the regulation of cellular metabolism [26]. In our study, the fraction of eicosapentaenoic (C20:5ω3) acid in all samples was low and did not exceed 4.5 %, and the percentage of docosahexaenoic (C22:6ω3) acid did not exceed 3.1 %. Since eicosapentaenoic (C20:5ω3) and docosahexaenoic (C22:6ω3) acids are produced by phytoplankton [27 ; 29 ; 30], their low levels can most likely be explained by the endogenous feeding of the larvae at the trochophore stage.

It is known that the environmental pollution by PCBs affects fatty acid composition [14]. Our experiments showed that the total fraction of SFA in larvae exposed to the PCBs varied in a rather narrow range 52.2 to 65.3 %. Accumulation of these acids indicates their participation in maintaining membrane structure integrity [14]. The lowest percentage of stearic (C18:0) acid in the larvae was observed when they were exposed to the PCB concentration 0.1 $\mu g \cdot L^{-1}$. Under the effect of the PCB concentrations 1 and 10 $\mu g \cdot L^{-1}$, the fractions of stearic (C18:0) acid practically did not differ, but became lower than in the control and in the sample with acetone. This fact suggests that larvae reaction to the PCB appearance in the medium was manifested in a decrease of the plasma membranes permeability, which could reduce the toxic effect of the PCBs.

MUFA fraction decreased about 2-fold at the PCB concentrations 0.1 and 1 $\mu g \cdot L^{-1}$, while PUFA fraction increased about 2.5–3-fold at the PCB concentrations 1 and 0.1 $\mu g \cdot L^{-1}$ and 1.3-fold at the PCB concentration 10 $\mu g \cdot L^{-1}$.

With a low PCB concentration 0.1 and 1 μg·L^{-1}, the proportion of octadecenoic acids (C18:1) decreased more than 2-fold compared to the control experiment; at 10 μg·L^{-1}, their percentage was equal to the proportions in the control. It is possible that at low PCB concentrations, a change in the MUFA proportion is caused by several catalytic mechanisms, including peroxidation, in addition to the P450 cytochrome monooxygenase pathway. Enzymes of cytochrome P450 system hydroxylate C-H bonds of substrates and catalyze omega-oxidation of saturated fatty acids and peroxidation of unsaturated fatty acids [14]. Prior to the development of digestive organs, trochophores are fed endogenously, while fatty acids are used mainly to form biomembranes and storage lipids [14 ; 16 ; 17 ; 25].

The change in MUFA and PUFA proportions with an almost constant fraction of SFA under the effect of PCBs is associated with the protective function of unsaturated fatty acids in the larval organism. It is explained by the fact that the synthesis of unsaturated fatty acids proceeds from SFA. PUFA, for example, have lower melting points compared to saturated acids and form a looser lipid bilayer structure. The asymmetric structure and melting point are two characteristics of polyenes, which increase fluidity of biological membranes and determine high metabolic activity of membrane enzymes [14]. The effect of pollutants can affect resistance and tolerance of cultivated organisms directly, especially at an early stage of ontogenesis, or indirectly, through changes in material and energy flows in the ecosystem [2].

An increase in the concentration of arachidonic (C20:4ω6) acid from 1.3 % in the control to 20.5 % when exposed to the PCB concentration 0.1 μg·L^{-1} is also explained by its ability to act as a hormone, activating cell receptors, while playing an important role in immune response. At higher PCB concentrations (1 and 10 μg·L^{-1}), the fraction of arachidonic (C20:4ω6) acid decreases, which indicates its intensive use in enzymatic processes [14].

Conclusion. The data obtained allow us to conclude that the type and composition of fatty acids in mussel trochophores changed depending on the level of PCB pollution of mollusc habitat. The fraction of SFA (for example, stearic (C18:0) acid) and octadecenoic (C18:1) acid isomers decreased sharply when exposed even to the PCB concentration 0.1 μg·L^{-1}, although the total SFA fraction was practically unchanged at the PCB concentrations 0 to 10 μg·L^{-1}, and the fraction of octadecenoic (C18:1) acid isomers increased almost 3-fold with an increase in PCB concentration to 10 μg·L^{-1}. This tendency is associated with structural features of both larvae cell membranes and SFA and MUFA molecules. On the contrary, the fraction of PUFA, for example, arachidonic (C20:4ω6) acid, increased under the effect of the PCB concentration 0.1 μg·L^{-1}, which is probably due to its ability to act as a hormone in immune response.

The results of the work can be used in the management of production processes in mollusc farms. A study of the dose-dependent effect of the PCBs on the ratio of SFA, MUFA, and PUFA in mussel larvae tissues can contribute to a better understanding of biochemical rearrangements that allow molluscs to adapt to the effects of adverse environmental factors.

This work was carried out within the frameworks of government research assignment of IBSS "Fundamental studies of the population biology of marine animals, their morphological and genetic diversity" (no. AAAA-A19-119060690014-5), "Molismological and biogeochemical fundamentals of homeostasis of marine ecosystems" (no. AAAA-A18-118020890090-2), and "Investigation of the mechanisms of controlling production processes in biotechnological complexes with the aim of developing the scientific foundations for the production of biologically active substances and technical products of marine genesis" (no. AAAA-A18-118021350003-6).

REFERENCES

1. Gavrisyuk V. K. Primenenie Omega-3 polinenasyshchennykh zhirnykh kislot v meditsine. *Ukrainskyi pulmonolohichnyi zhurnal*, 2001, no. 3, pp. 5–10. (in Russ.)
2. Zolotnitskii A. P. Sovremennoe sostoyanie, problemy i perspektivy razvitiya konkhiokul'tury v Ukraine. *Rybne hospodarstvo Ukrainy*, 2011, no. 4, pp. 45–48. (in Russ.)]
3. Karavantseva N. V., Pospelova N. V., Bobko N. I., Nekhoroshev M. V. Technique for collection of mussel *Mytilus galloprovincialis* Lam. gametes. *Sistemy kontrolya okruzhayushchei sredy*, 2012, no. 17, pp. 184–187. (in Russ.)
4. Kates M. *Tekhnika lipidologii.* Moscow : Izd-vo "Mir", 1975, 324 p. (in Russ.)
5. Kotelevtsev S. V., Matorin D. N., Sadchikov A. P. *Ekologicheskaya toksikologiya i biotestirovanie vodnykh ekosistem* : uchebnoe posobie. Moscow : Izd-vo "Infra-M", 2015, 252 p. (in Russ.)
6. Malakhova L. V., Malakhova T. V., Shchurova E. S., Karamyshev A. K. Monitoring khlororganicheskogo zagryazneniya Sevastopol'skoi akvatorii s ispol'zovaniem midii *M. galloprovincialis* v kachestve vida-indikatora. In: *Morskie biologicheskie issledovaniya: dostizheniya i perspektivy* : v 3-kh t. : sb. materialov Vseros. nauch.-prakt. konf. s mezhdunar. uchastiem, priuroch. k 145-letiyu Sevastopol'skoi biologicheskoi stantsii, Sevastopol, 19–24 Sept., 2016 / A. V. Gaevskaya (Ed.). Sevastopol : EKOSI-Gidrofizika, 2016, vol. 3, pp. 140–143. (in Russ.)
7. Nikonova L. L., Malakhova L. V., Nekhoroshev M. V., Ryabushko V. I. Organochlorine compounds in gonads and gametes of bivalve mollusk *M. galloprovincialis* Lam., cultivated near the shores of the Crimea (the Black Sea). *Voda: khimiya i ekologiya*, 2017, no. 3, pp. 40–45. (in Russ.)
8. Pirkova A. V., Ladygina L. V., Bobko N. I. Vozdeistvie zagryaznyayushchikh veshchestv v morskoi vode na razvitie lichinok midii *M. galloprovincialis* Lam. i ustritsy *Crassostrea gigas*. In: *Vodnye bioresursy, akvakul'tura i ekologiya vodoemov* : materialy Vseros. nauch. konf., Kaliningrad, 23–24 May, 2017. Kaliningrad : FGBOU VO "KGTU", 2017, pp. 135–138. (in Russ.)
9. Pirkova A. V., Ladygina L. V., Bobko N. I. Embriony midii *M. galloprovincialis* Lam. – indikatory zagryazneniya morskoi vody poverkhnostno-aktivnymi veshchestvami. In: *Zagryaznenie morskoi sredy: ekologicheskii monitoring, bioindikatsiya, normirovanie* : materialy Vseros. nauch. konf., Sevastopol, 28 May – 01 June, 2018. Sevastopol : OOO "Kolorit", 2018, pp. 205–209. (in Russ.)
10. PND F 14.1:2:3:4.204-04 *Metodika izmerenii massovykh kontsentratsii khlororganicheskikh pestitsidov i polikhlorirovannykh bifenilov v probakh pit'evykh, prirodnykh i stochnykh vod metodom gazovoi khromatografii* (izdanie 2018 g.). Utverzhdena direktorom FGBU "Federal'nyi tsentr analiza i otsenki tekhnogennogo vozdeistviya" V. Ch. Yuranets 31.07.2018 (in Russ.)
11. Pospelova N. V., Egorov V. N., Chelyadina N. S., Nekhoroshev M. V. The copper content in the organs and tissues of *Mytilus galloprovincialis* Lamarck, 1819 and the flow of its sedimentary deposition into bottom sediments in the farms of the Black Sea aquaculture. *Morskoj biologicheskij zhurnal*, 2018, vol. 3, no. 4, pp. 64–75. (in Russ.). https://doi.org/10.21072/mbj.2018.03.4.07
12. Ryabushko V. I., Kozintsev A. F., Toichkin A. M. Concentration of arsenic in the tissues of cultivated mussel *Mytilus galloprovincialis* Lam., water and bottom sediments (Crimea, Black Sea). *Morskoj biologicheskij zhurnal*, 2017, vol. 2, no. 3, pp. 68–74. (in Russ.). https://doi.org/10.21072/mbj.2017.02.3.06

13. TS T. R. 021/2011. *Tekhnicheskii reglament Tamozhennogo soyuza o bezopasnosti pishchevoi produktsii.* Moscow : Gosstandart Rossii, 2011, 242 p. (in Russ.)
14. Fokina N. N., Nefedova Z. A., Nemova N. N. *Lipidnyi sostav midii Mytilus edulis L. Belogo morya. Vliyanie nekotorykh faktorov sredy obitaniya.* Petrozavodsk : Izd-vo KarNTs RAN, 2010, 243 p. (in Russ.). http://doi.org/10.13140/2.1.2154.8322
15. Khasanov V. V., Ryzhova G. L., Dychko K. A., Kuryaeva T. T. Sostav zhirnykh kislot i steroidov rastitel'nykh masel. *Khimiya rastitel'nogo syr'ya*, 2006, no. 3, pp. 27–31. (in Russ.)
16. Kholodov V. I., Pirkova A. V., Ladygina L. V. *Cultivation of Mussels and Oysters in the Black Sea*. Voronezh : Izd-vo OOO "Izdat-Print", 2017, 508 p. (in Russ.). https://repository.marine-research.org/handle/299011/5523
17. Chebotareva M. A., Zabelinskii S. A., Shukolyukova E. P., Krivchenko A. I. Limit of change in unsaturation index of fatty acid composition of phospholipids at adaptation of molluscs to biogenic and abiogenic environmental factors. *Journal of Evolutionary Biochemistry and Physiology*, 2011, vol. 47, no. 5, pp. 448–453. (in Russ.). https://doi.org/10.1134/S0022093011050069
18. Cronan J. E., Thomas J. Bacterial fatty acid synthesis and its relationships with polyketide synthetic pathways. *Methods in Enzymology*, 2009, vol. 459, pp. 395–433. https://doi.org/10.1016/S0076-6879(09)04617-5
19. Egorov V. N., Lazorenko G. E., Mirzoeva N. Yu., Stokozov N. A., Kostova S. K., Malakhova L. V., Pirkova A. V., Arkhipova S. I., Korkishko N. F., Popovichev V. N., Plotitsyna O. V., Migal L. V. Content of ^{137}Cs, ^{40}K, ^{90}Sr, radionuclides, and some chemical pollutants in the Black Sea mussels *M. galloprovincialis* Lam. *Morskoj ekologicheskij zhurnal*, 2006, vol. 5, no. 3, pp. 70–78.
20. Ekin I., Başhan M. Fatty acid composition of selected tissues of *Unio elongatulus* (Bourguignat, 1860) (Mollusca: Bivalvia) collected from Tigris River, Turkey. *Turkish Journal of Fisheries and Aquatic Sciences*, 2010, vol. 1, no. 4, pp. 445–451. https://doi.org/10.4194/trjfas.2010.0402
21. Ekin I., Şeşen R. Investigation of the fatty acid contents of edible snails *Helix lucorum*, *Eobania vermiculata* and non-edible slug *Limax flavus*. *Records of Natural Products*, 2017, vol. 11, no. 6, pp. 562–567. https://doi.org/10.25135/acg.rnp.72.17.02.043
22. Fokina N. N., Ruokolainen T. R., Nemova N. N. Lipid composition modifications in the blue mussels (*Mytilus edulis* L.) from the White Sea. In: *Organismal and Molecular Malacology* / R. Bettencourt et al. (Eds). Intech, 2017, chap. 7, pp. 143–159. https://doi.org/10.5772/67811
23. Klimova T. N., Vdodovich I. V., Zagorodnyaya Yu. A., Ignatyev S. M., Malakhova L. V., Dotsenko V. S. Ichthyoplankton in the plankton community of the Crimean Peninsula shelf zone (Black Sea) in July 2010. *Journal of Ichthyology*, 2014, vol. 54, no. 6, pp. 409–421. https://doi.org/10.1134/S0032945214030060
24. Leonardos N., Lucas I. The use of larval fatty acids as an index of growth in *Mytilus edulis* L. larvae. *Aquaculture*, 2000, vol. 184, pp. 155–166. https://doi.org/10.1016/S0044-8486(99)00320-8
25. Leroy F., Meziane T., Riera P., Comtet T. Seasonal variations in maternal provisioning of *Crepidula fornicata* (Gastropoda): Fatty acid composition of females, embryos and larvae. *PLoS One*, 2013, no. 8, pp. 1–9. https://doi.org/10.1371/journal.pone.0075316
26. Nagy K., Tiuca I.-D. Importance of fatty acids in physiopathology of human body. In: *Fatty Acids* / A. Catala (Ed.). Intech, 2017, chap. 1, pp. 1–22. https://doi.org/10.5772/67407

27. Nelson M. M., Leighton D. L., Phleger C. F., Nichols P. D. Comparison of growth and lipid composition in the green abalone, *Haliotis fulgens*, provided specific macroalgal diets. *Comparative Biochemistry and Physiology Part B: Biochemistry and Molecular Biology*, 2002, vol. 131, no. 73, pp. 695–712. https://doi.org/10.1016/S1096-4959(02)00042-8
28. Peters J. Role of essential fatty acids on the reproductive success of the copepod *Temora longicornis* in the North Sea. *Marine Ecology Progress Series*, 2007, vol. 341, pp. 153–163. https://doi.org/10.3354/meps341153
29. Pettersen A. K., Turchini G. M., Jahangard S., Ingram B. A., Sherman C. D. Effects of different dietary microalgae on survival, growth, settlement, and fatty acid composition of blue mussel (*M. galloprovincialis*) larvae. *Aquaculture*, 2010, vol. 309, pp. 115–124. https://doi.org/10.1016/j.aquaculture.2010.09.024
30. Saito H. Lipid and FA composition of the pearl *Oyster pinctada*. *Lipids*, 2004, vol. 39, no. 10, pp. 997–1005. https://doi.org/10.1007/s11745-004-1322-3
31. Weis J. S. Delayed behavioral effects of early life toxicant exposures in aquatic biota. *Toxics*, 2014, vol. 2, no. 2, pp. 165–187. https://doi.org/10.3390/toxics2020165

СОСТАВ ЖИРНЫХ КИСЛОТ В ТРОХОФОРАХ МИДИЙ *MYTILUS GALLOPROVINCIALIS*, ВЫРАЩЕННЫХ В УСЛОВИЯХ ЗАГРЯЗНЁННОСТИ ПОЛИХЛОРБИФЕНИЛАМИ

Л. Л. Капранова, Л. В. Малахова, М. В. Нехорошев, В. В. Лобко, В. И. Рябушко

Федеральный исследовательский центр «Институт биологии южных морей имени А. О. Ковалевского РАН», Севастополь, Российская Федерация
E-mail: *lar_sa1980@mail.ru*

Состояние черноморских популяций *Mytilus galloprovincialis* в естественной среде обитания напрямую зависит от развития мидии на всех стадиях, в том числе на начальных стадиях личиночных форм, наиболее чувствительных к загрязнению окружающей среды. Поллютанты органического происхождения оказывают негативное влияние на личинки моллюска, проявляющееся в торможении их роста и развития. Закономерности размножения мидии хорошо изучены, что даёт возможность получать в контролируемых лабораторных условиях личинки из искусственно оплодотворённых яйцеклеток этого вида моллюсков. В работе впервые исследован жирнокислотный состав общих липидов, выделенных из биомассы тканей личинок *M. galloprovincialis* на стадии трохофоры в контроле и после их трёхдневной экспозиции в среде с добавлением различных концентраций полихлорбифенилов. Жирнокислотный состав суммарных липидов в биомассе личинок, полученных на третьи сутки эксперимента, исследовали методом хромато-масс-спектрометрии. Всего идентифицировано 14 жирных кислот: 59 % из них относились к насыщенным, 24 % — к моноеновым, 17 % — к полиеновым. Для статистического анализа использовали программу MATLAB (версия 8.2). В условиях проведённого эксперимента в липидах трохофор *M. galloprovincialis* достоверно отличались значения суммы мононенасыщенных и полиненасыщенных жирных кислот. Сумма насыщенных жирных кислот статистически значимо не изменялась. Основными насыщенными жирными кислотами во всех исследуемых трохофорах мидий являлись пальмитиновая (C16:0) и стеариновая (C18:0). Их концентрации значительно не изменялись под действием полихлорбифенилов. Наиболее значимые мононенасыщенные жирные кислоты — олеиновая (C18:1ω9), пальмитолеиновая (C16:1ω7) и вакценовая (C18:1ω7). Содержание мононенасыщенных жирных кислот понижалось вдвое при действии полихлорбифенилов с концентрациями 0,1 и 1 мкг·л$^{-1}$; при концентрации полихлорбифенилов 10 мкг·л$^{-1}$ суммарное содержание этих кислот было равно таковому в контроле. Среди полиненасыщенных жирных кислот, обладающих положительной биологической активностью, были идентифицированы арахидоновая (C20:4ω6), эйкозапентаеновая (C20:5ω3) и докозагексаеновая (C22:6ω3). Суммарное содержание Омега-3 и Омега-6 кислот в личинках мидий в контрольном опыте не превышало 12,8 %. С увеличением концентрации полихлорбифенилов

в среде выращивания трохофор с 0,1 до 1 мкг·л$^{-1}$ концентрация полиненасыщенных жирных кислот повышалась в 2,5 раза. При концентрации полихлорбифенилов 10 мкг·л$^{-1}$ и в пробе с ацетоном суммарное содержание полиненасыщенных жирных кислот было сопоставимо с таковым в контрольном опыте. Результаты исследования свидетельствуют о том, что жирнокислотный отклик трохофор мидий *M. galloprovincialis* максимален при воздействии концентраций полихлорбифенилов от 0,1 до 1 мкг·л$^{-1}$. При концентрации загрязнителей 10 мкг·л$^{-1}$ и выше биохимические процессы в личинках, по-видимому, замедляются. Результаты данного исследования могут способствовать лучшему пониманию перестроек, позволяющих моллюскам на личиночных стадиях развития адаптироваться к условиям загрязнения среды обитания органическими поллютантами.

Ключевые слова: полихлорбифенилы, жирные кислоты, личинки, трохофора, мидия *Mytilus galloprovincialis*, Чёрное море

1871
ИнБЮМ – IBSS

Морской биологический журнал
Marine Biological Journal
2020, vol. 5, no. 2, pp. 50–66
https://doi.org/10.21072/mbj.2020.05.2.05

UDC 593.1:591.1

EFFECTS OF LOW FREQUENCY RECTANGULAR ELECTRIC PULSES ON *TRICHOPLAX* (PLACOZOA)

© 2020 **A. V. Kuznetsov[1,3], O. N. Kuleshova[1], A. Yu. Pronozin[2], O. V. Krivenko[1], and O. S. Zavyalova[3]**

[1]A. O. Kovalevsky Institute of Biology of the Southern Seas of RAS, Sevastopol, Russian Federation
[2]Institute of Cytology and Genetics, Novosibirsk, Russian Federation
[3]Sevastopol State University, Sevastopol, Russian Federation
E-mail: *kuznet61@gmail.com*

Received by the Editor 24.09.2019; after revision 25.03.2020;
accepted for publication 26.06.2020; published online 30.06.2020.

The effect of extremely low frequency electric and magnetic fields (ELF-EMF) on plants and animals including humans is quite a contentious issue. Little is known about ELF-EMF effect on hydrobionts, too. We studied the effect of square voltage waves of various amplitude, duration, and duty cycle, passed through seawater, on *Trichoplax* organisms as a possible test laboratory model. Three Placozoa strains, such as *Trichoplax adhaerens* (H1), *Trichoplax* sp. (H2), and *Hoilungia hongkongensis* (H13), were used in experiments. They were picked at the stationary growth phase. Arduino Uno electronics platform was used to generate a sequence of rectangular pulses of given duration and duty cycle with a frequency up to 2 kHz. Average voltage up to 500 mV was regulated by voltage divider circuit. Amlodipine, an inhibitor of calcium channel activity, was used to check the specificity of electrical pulse effect on voltage-gated calcium channels in *Trichoplax*. Experimental animals were investigated under a stereo microscope and stimulated by current-carrying electrodes placed close to a *Trichoplax* body. Variations in behavior and morphological characteristics of *Trichoplax* plate were studied. Stimulating and suppressing effects were identified. Experimental observations were recorded using photo and video techniques. Motion trajectories of individual animals were tracked. Increasing voltage pulses with fixed frequency of 20 Hz caused H2 haplotype individuals to leave “electrode zone” within several minutes at a voltage of 25 mV. They lost mobility in proportion to voltage rise and were paralyzed at a voltage of 500 mV. Therefore, a voltage of 50 mV was used in further experiments. An animal had more chance to move in various directions in experiments with two electrodes located on one side instead of both sides of *Trichoplax*. Direction of motion was used as a characteristic feature. *Trichoplax* were observed to migrate to areas with low density of electric field lines, which are far from electrodes or behind them. Animals from old culture were less sensitive to electrical stimulus. H2 strain was more reactive than H1 strain and especially than H13 strain; it demonstrated stronger physiological responses at frequencies of 2 Hz and 2 kHz with a voltage of 50 mV. Motion patterns and animal morphology depended on the duration of rectangular stimulation pulses, their number, amplitude, and frequency. Effects observed varied over a wide range: from direct or stochastic migration of animals to the anode or the cathode or away from it to their immobility, an increase of optical density around and in the middle of *Trichoplax* plate, and finally to *Trichoplax* folding and detach from the substrate. Additional experiments on *Trichoplax* sp. H2 with pulse duration of 35 ms and pulse delay of 1 ms to 10 s showed that the fraction of paralyzed animals increased up to 80 % with minimum delay. Nevertheless, in the presence of amlodipine with a concentration of 25 nM, almost all *Trichoplax* remained fast-moving for several minutes despite exposure to voltage waves. Experimental animals showed a total discoordination of motion and could not leave an “electrode trap”, when amlodipine with a concentration of 250 nM was used. Further, *Trichoplax* plate

became rigid, which appeared in animal shape invariability during motion. Finally, amlodipine with a concentration of 50 μM caused a rapid folding of animal plate-like body into a pan in the ventral-dorsal direction and subsequent dissociation of *Trichoplax* plate into individual cells. In general, the electrical exposure applied demonstrated a cumulative but a reversible physiological effect, which, as expected, is associated with activity of voltage-gated calcium channels. Amlodipine at high concentration (50 μM) caused *Trichoplax* disintegration; at moderate concentration (250 nM), it disrupted the propagation of activation waves that led to discoordination of animal motion; at low concentration (25 nM), it prevented an electric shock.

Keywords: rectangular electric pulses, *Trichoplax*, Placozoa, voltage-gated calcium channels

Electromagnetic radiation in the range from units to several thousand Hz does not have a direct thermal effect on living tissue, but influences indirectly on certain cellular mechanisms and causes corresponding physiological effects [18 ; 29]. It was found that extremely low frequency electric and magnetic fields (hereinafter ELF-EMF) can induce gene expression [41 ; 48] and cause cell proliferation [43]. Laboratory studies showed that ELF-EMF affect cell membranes and ion channels [22], especially voltage-gated calcium channels [12].

It is of interest that calcium channel blockers significantly reduce various effects of ELF-EMF [26]. In addition, biophysical properties of voltage-gated channels can explain molecular mechanisms of ELF-EMF biological effects. For example, a downward regulatory cellular response to such effects can be mediated through Ca^{2+}/calmodulin stimulation of nitric oxide (NO) synthesis, while physiological reactions may be a result of stimulation of NO-dependent cGMP protein kinase G, and pathophysiological processes may result from NO-peroxynitrite oxidative stress. Other Ca^{2+}-mediated regulatory pathways, non dependent of nitric oxide, have been also described [11 ; 16 ; 25].

There are several types of calcium channels: high-, intermediate-, and low-voltage-activated calcium channels [27]. L-, P- and N-type calcium channels are activated at high values of membrane potential. Four proteins with many isoforms $Ca_v1.1$–$Ca_v1.4$ belong to L-type channels, encoded in humans by *CACNA1S*, *CACNA1C*, *CACNA1D*, and *CACNA1F* genes; they are expressed mainly in skeletal muscle and are responsible for the contraction of cardiac and smooth muscles [21]. P- and N-type channels are represented in neurons by $Ca_v2.1$ and $Ca_v2.2$ proteins, respectively; they are responsible for the release of neurotransmitters. R-type calcium channels, intermediate-voltage-activated ones, include $Ca_v2.3$ protein family [24 ; 35]. Low-voltage-activated channels are of T-type. Cells with pacemaker activity possess them, for example human pacemakers [5]. These channels are represented by $Ca_v3.1$–$Ca_v3.3$ proteins and are encoded by *CACNA1G*, *CACNA1H*, and *CACNA1I* genes, respectively [46]. The obvious role of T-type Ca_v3 channels is manifested in cellular excitability, where their low activation voltages make it easy to depolarize the membrane. T-type channels also play a role in triggering exocytosis mechanism in vertebrates and invertebrates [32 ; 45]. Ca_v3 channels are present in primitive animals and in unicellular organisms [23 ; 40].

Members of the phylum Placozoa, in particular *Trichoplax adhaerens* [30], can be a useful model for studying ELF-EMF effects. *Trichoplax* has a body of irregular shape (its size is about 1 mm); it is formed by two layers of epithelium with a doughy cell layer between them. This tiny marine animal is built of six basic cell types [7 ; 39]. *Trichoplax* aroused interest in terms of minimum requirements for metazoa after F. E. Schulze made an initial description in 1883 [31]. The lack of organs symmetry, nerve and muscle cells, basal plate, and extracellular matrix did not leave doubts about the anciend origin of *Trichoplax*. However, despite the primitive structure, these animals are able to coordinate motion activity during feeding [37] and demonstrate chemotaxis [13], confirming the existence of complex mechanisms of intercellular interaction and integration. Rapid rhythmic contractions of *Trichoplax* dorsal epithelium were found [30], and animal motion model based on Voronoi diagrams was proposed [38].

Structure, function, and ionic selectivity of a single T-type calcium channel from *Trichoplax* (TCa_v3) were characterized using the patch-clamp technique after cloning it in HEK-293T human kidney embryonic cells [36]. Taking into account the fact that Ca_v channels play a decisive role both in intracellular and intercellular signal transmission [23] and the fact that *Trichoplax* has in its genome a complete set of Ca_v1, Ca_v2, and Ca_v3 genes encoding Ca_v channels [15 ; 40], it became possible to study molecular targets and mechanisms underlying ELF-EMF effects on multicellular organisms.

The aim of this work was to study *Trichoplax* response to sequences of square-shaped pulses that simulate the effects necessary for opening the calcium channels *in vivo*. Rectangular pulses were chosen to influence *Trichoplax* because they cause greater effects on biological objects than vibrations of any another shape. We also found it appropriate to use square waves as an idealized, "discrete" model of electromagnetic radiation.

MATERIAL AND METHODS

Cultivation. Three Placozoa strains were used in experiments, such as *Trichoplax adhaerens* (haplotype H1), *Trichoplax* sp. H2 (haplotype H2), and *Hoilungia hongkongensis* (haplotype H13), of which the last strain can be attributed to a separate species [8 ; 9]. Animals were cultivated in glass Petri dishes with a diameter of 90 cm on mats of unicellular green alga *Tetraselmis marina* in artificial seawater (ASW, Red Sea Salt, Red Sea Fish Pharm LTD, Israel) with a salinity of 35 ‰ at a temperature of +25 °C according to the standard protocol [17]. Seawater was replaced at least once a week. The pH value was maintained in the range of 7.8 to 8.0. One hour before the start of the experiment, animals were placed in ASW on plastic dishes without algae.

Amlodipine preparation. Dihydropyridine derivative amlodipine ($C_{20}H_{25}ClN_2O_5$, 3-*O*-ethyl 5-*O*-methyl 2-(2-aminoethoxymethyl)-4-(2-chlorophenyl)-6-methyl-1,4-dihydropyridine-3,5-dicarboxylate as besylate, Teva) was added in 96 % ethanol or in water (ASW), and the concentration was calculated according to the solubility of this compound in those solvents.

Electrical stimulation. To generate a sequence of rectangular pulses of given duration and duty cycle, standard Arduino Uno R3 platform based on 8-bit AVR microcontroller ATmega328P was used. LED1 was used for visual control; a diode (D1, 1N4001) was connected in series with resistors R1 and R2 to prevent accidental short circuit. The average voltage value was adjusted from +10 mV to +1.5 V on voltage divider using potentiometer R2 (10 kΩ), as shown in Fig. 1. The electrodes were placed in seawater near the animal's body at a distance of about 1 mm from each other. We used plastic or wooden sticks, or metal electrodes disconnected from the controller as a base test of possible influence of foreign objects on animal behavior.

Software meander. Pulse duration and delay (duty cycle) were set by a program in the range of 0.5 ms to 10 s; the program was executed on the controller in an infinite loop (see supplementary file No. 1: https://doi.org/10.21072/mbj.2020.05.2.05). Conversion of time intervals (ms) into frequency (Hz) was carried out taking into account that 1 Hz corresponds to 1000 ms. To create packages of square-shaped pulses with changing duration and delay inside the package, incremental and decremental program cycles with a step of 1 ms were used (see supplementary file No. 2: https://doi.org/10.21072/mbj.2020.05.2.05).

Microscopy and data processing. The animals were stimulated with electric current under ZEISS Stemi 305 stereo microscope at magnifications ×8 and ×40. Variations in behavior (motion activity, direction, and trajectory) and morphological characteristics of the body (opalescence, shape) were evaluated. Stimulating and suppressing effects, *i. e.* leading to speed up of animal motion activity or to its retardation, shock, and paralysis, were identified. *Trichoplax* structure was studied under Nikon Eclipse Ts2R

inverted microscope with DIC optics at maximum magnification ×600. Images and behavioral activity of animals were documented using photo and video techniques. The video was processed using FFmpeg utility on Huawei FusionServer RH2288 V3. *Trichoplax* motion trajectories were tracked using ImageJ wrMTrck plugin (National Institutes of Health, USA) on Dell Precision T5810 graphics station.

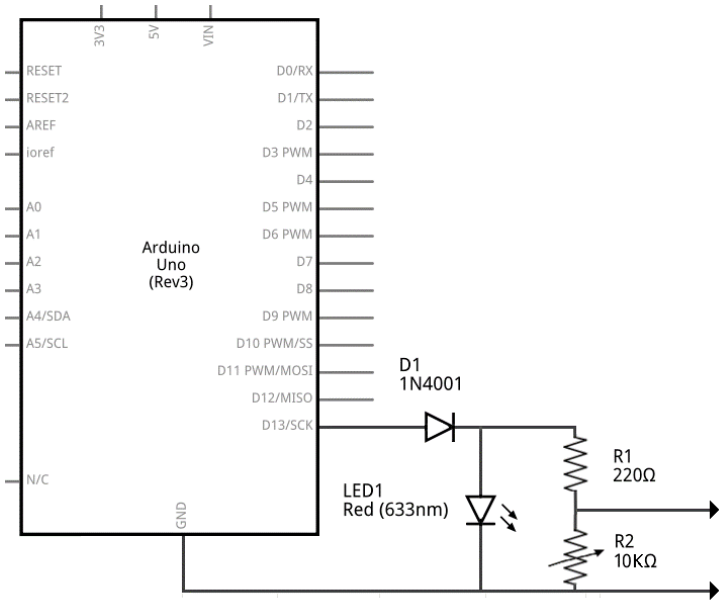

Fig. 1. Electronic circuit for *Trichoplax* electrical stimulation

RESULTS

Culture growth dynamics. *Trichoplax* culture was at the state of adaptation to new conditions for several days, showing no rise in number and size of individuals, after animals placement on fresh algal mats. *Trichoplax* began to grow with subsequent division after this lag phase. At the next stage, which corresponds to the exponential phase of the culture growth, *Trichoplax* grew actively and split in half once every 3–4 days by forming a constriction in cell division with a fall in the size of daughter individuals. Entry into the stationary phase of the culture growth was observed after 2–3 weeks, and it was accompanied by a twofold decrease in the average size of animals and by a sharp slowdown in the growth rate of their number. We observed decreasing size of individuals, change in their shape (elongation or, conversely, formation of small spheres detaching from the substrate and floating), as well as death of animals in old cultures. Therefore, *Trichoplax* were transplanted on fresh algal mats in the amount of 10–20 individuals per dish after 5–6 weeks of growth, and the cultivation process was repeated. In common, animals selected at the stationary phase of the culture growth were used.

Single electrode experiments. No pronounced reaction of animals to foreign objects was observed in tests in which small plastic, wood, or metal rods were applied. The animal usually moved away from an electric stimulus by a distance of one to three sizes of its body (1–3 mm) and continued to move slowly in a random direction, when electrodes connected to Arduino Uno controller, one of which (anode or cathode) setting near *Trichoplax* (H2 strain) and the other one at a considerable distance (more than 1 cm), were used. *Trichoplax* ran away immediately with pulse duration of 100 ms and a delay of 1 ms; they crawled away from the electrodes with a pause of several tens of seconds in the case of a delay of 1 s. It was noted that experimental animals taken from the old culture were less sensitive to an electric stimulus, which appeared in an increase in time of reaction delay and in a decrease in the distance they moved.

Two electrodes experiments. *Trichoplax* showed motion activity: it began to "explore" the space, approaching the electrodes and moving away from them, until it found a "comfortable" position in resulting weak electric field, when two rods made of metals with different electrochemical potential, forming a galvanic pair near the animal, were placed (Fig. 2).

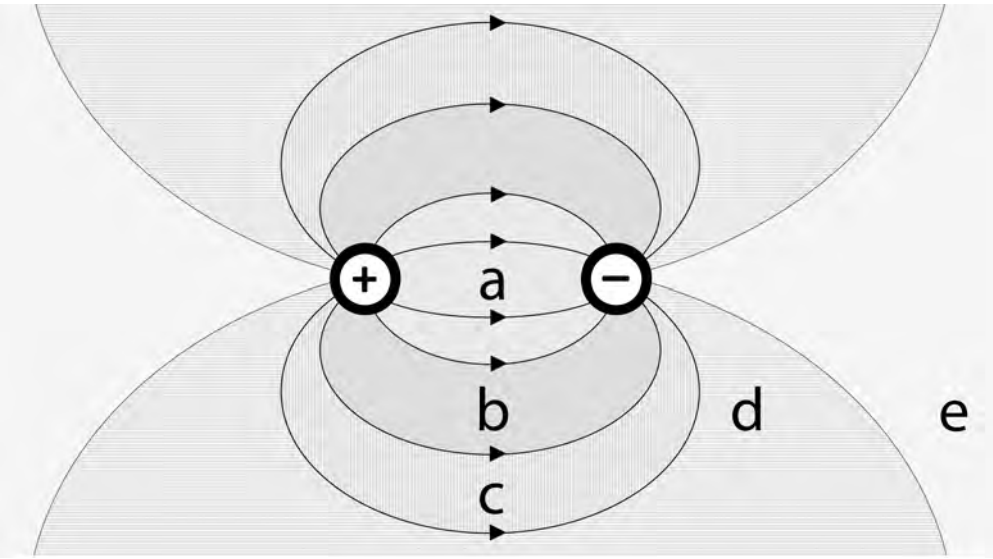

Fig. 2. Electric field lines in "electrode trap" for *Trichoplax*: (a) "electrode zone" with electrode gap no more than 1 mm; (b) immobilization zone corresponds to one *Trichoplax* body size (1 mm) from the center of the trap; (c) intermediate zone; (d) zone away from electrodes; (e) "comfort zone" just behind the electrodes (see the text for details)

Trichoplax avoided the cathode, when a direct current source (of 200 mV) was used, but did not approach the anode, crawling to the side and sometimes wandering between the electrodes. In case the animals crawled too close to the anode, they remained near it and wrinkled after a while. Reaction rate and motion direction depended largely on the initial position of the animal and the distance between the electrodes. A voltage of 1.2 V was lethal for the animals, *i. e.* they were paralyzed, radically changed their morphology, detached from the substrate, and subsequently desagregated.

Test studies were carried out in seawater with a salinity of 35 ‰, using pulse duration and delay of 35 ms (~ 30 Hz) with an average voltage of 50 mV. It is of interest that in the case of an industrial frequency (of 50 Hz), *Trichoplax* did not substantially change their morphology; they began to move, preferred the anode, crawled away from the electrodes, sometimes came back, and again moved away from the electrodes.

Voltage effect on *Trichoplax* was estimated by varying pulse amplitude using voltage divider at a fixed frequency of 20 Hz (see supplementary file No. 1: https://doi.org/10.21072/mbj.2020.05.2.05). The main evaluation criterion was the fraction of immobilized animals that did not leave the "electrode zone" within a few minutes. An additional criterion was pathological changes in the morphology of animals, such as the thickness of the rim of plate, rounding of the shape and reduction of opalescence. Their fraction increased in proportion to voltage rise (Fig. 3). Eventually, almost all animals left the "electrode zone" at a voltage of 25 mV, and they remained, on the contrary, within its boundaries, acquiring pathological signs at a voltage of 500 mV, although the intact features were recovered the next day after exposure withdrawal. A voltage of 50 mV was used in further experiments based on the results obtained.

We used mostly two active electrodes located in close proximity on both sides of *Trichoplax* plate. As one of effective options, pulses with a duration of 100 ms and a delay of 1 ms to 10 s were applied. For the experiments, 139 animals of H2 strain were used. We observed immobilization of animals, opacity

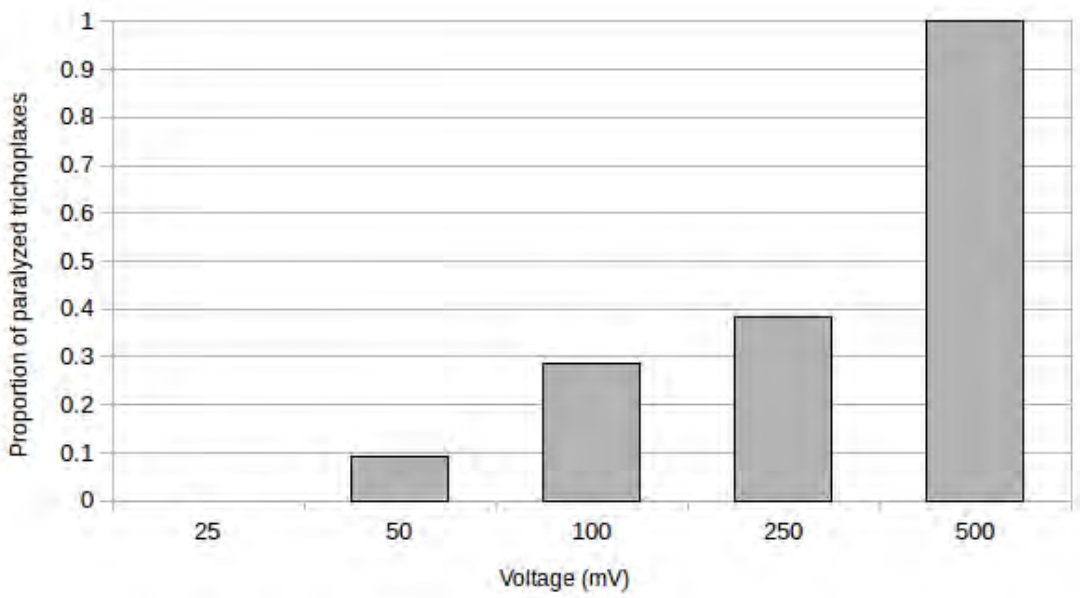

Fig. 3. Fraction of immobilized *Trichoplax* sp. H2 *versus* active animals at various voltage values of rectangular pulses at a frequency of 20 Hz. Totally 59 animals were used in the experiment

along the plate periphery and in its center with a subsequent reduction in size and wrinkling or folding of *Trichoplax* for different duty cycle values in 67 % of cases on average. These changes in physiological state and morphology of animal were not fatal. Trichoplaxes recovered several tens of minutes after the stimulus, which was became apparent in their flattening on the substrate and acquiring motion activity.

Probability of leaving the zone of stimulating electrodes increased in experiments with two electrodes located on one side of the plate. Moreover, the animal had the opportunity to move in different directions. This fact was later used as a characteristic feature for different strains. An average of 56 % of *Trichoplax* remained in immobilization zone near the electrodes.

In order to clarify the data obtained, an additional series of experiments was conducted on 121 animals using two significantly different duty cycle values, namely a delay of 1 ms and 1 s, with a pulse duration of 100 ms. In the case of placing the electrodes on both sides of *Trichoplax* plate, the fraction of animals crawled out from the zone of exposure was insignificant and amounted to 30 % with a delay of 1 ms and 52 % – with a delay of 1 s. The fraction of runaway animals was greater and amounted to 47 % for each pulse delay of 1 ms and 76 % – of 1 s, when the electrodes were placed on one side of *Trichoplax* plate (Fig. 4). It should be noted that in the experiments with two electrodes on both sides of the animal, *Trichoplax* took time to "decide" in which direction to crawl out of the "electrode trap". More often *Trichoplax* moved toward greater part of its body, located outside the electrodes.

Different *Trichoplax* strains testing. Various animal behavior patterns were revealed for different *Trichoplax* strains in comparative experiments on the effects of rectangular pulses with an average voltage value of 50 mV, a duty cycle of 0.5, and a frequency of 2 Hz and 2 kHz. The number of individuals moving from the anode to the cathode or *vice versa* – from the cathode to the anode – was counted. In the experiments, 143 individuals of *Trichoplax* were used. Of them: H1 strain – 51; H2 strain – 47; H13 strain – 45 individuals. The animal had to get out of the "electrode trap" – two electrodes on opposite sides of the body – in each experiment (Fig. 22). Long-term monitoring of shape change and *Trichoplax* trajectory was carried out (see supplementary file No. 3: https://doi.org/10.21072/mbj.2020.05.2.05).

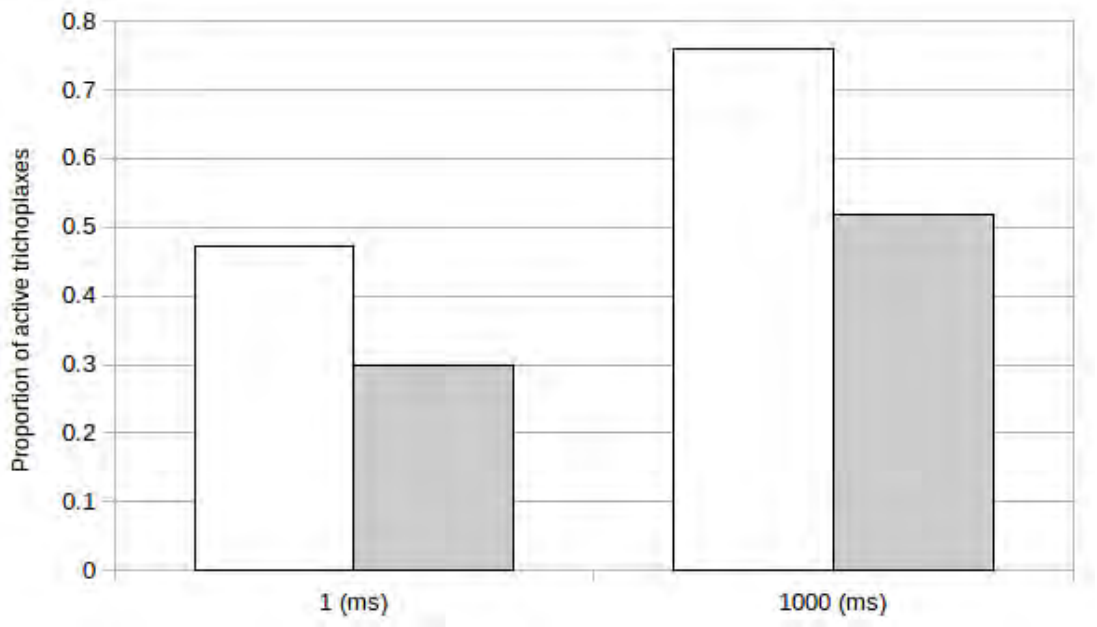

Fig. 4. Fraction of active *Trichoplax* sp. H2 *versus* immobilized animals at pulse duration of 100 ms and delay of 1 ms or 1 s; white color indicates the electrodes on one side of *Trichoplax* plate; gray color indicates the electrodes on opposite sides of *Trichoplax* plate. Totally 121 animals were used in the experiment

Trichoplaxes of H1 and H13 strains moved toward a low density of the lines of electric field intensity and sometimes stretched out along these imaginary lines (Fig. 5). Animals of H2 strain crawled to the opposite side of electrodes – to the "comfort zone" with a low density of lines of electric field strength – without significant moving away from the electrodes (Table 1). In most cases, individuals of H1 strain leaved the electrodes along an elongated path and often crawled behind one of the electrodes into the "comfort zone" at a low frequency (of 2 Hz). Animals of H2 strain preferred to move beyond the cathode, although sometimes they wandered between the electrodes and eventually crawled a short distance or left the anode. Representatives of H13 strain more often leaved the anode towards the cathode and moved beyond it. When using a high frequency (of 2 kHz), individuals of H1 strain preferred the anode, often remained in the "electrode zone", lost their motion activity, and wrinkled. Individuals of H2 strain quickly crawled to the anode or remained close to the electrodes, which often led to their immobilization. Individuals of H13 strain usually leaved the anode and moved to the cathode and crawled behind the cathode. Reaction lag, immobilization, and wrinkling at a frequency of 2 kHz were also observed for them.

Table 1. Behavioral patterns of *Trichoplax* between electrodes when exposed to rectangular pulses of various frequencies

Haplotype	**Rectangular pulse frequency**	
	2 Hz	**2 kHz**
H1	moves remotely behind one of the electrodes	moves away from the cathode towards the anode or remains in the area of the electrodes
H2	wanders between the electrodes, moves behind the cathode or anode, crawls away	approaches the anode quickly, wanders, stays close to the electrodes
H13	crawls off the anode and sometimes behind the cathode	distinctly leaves the anode, crawls behind the cathode

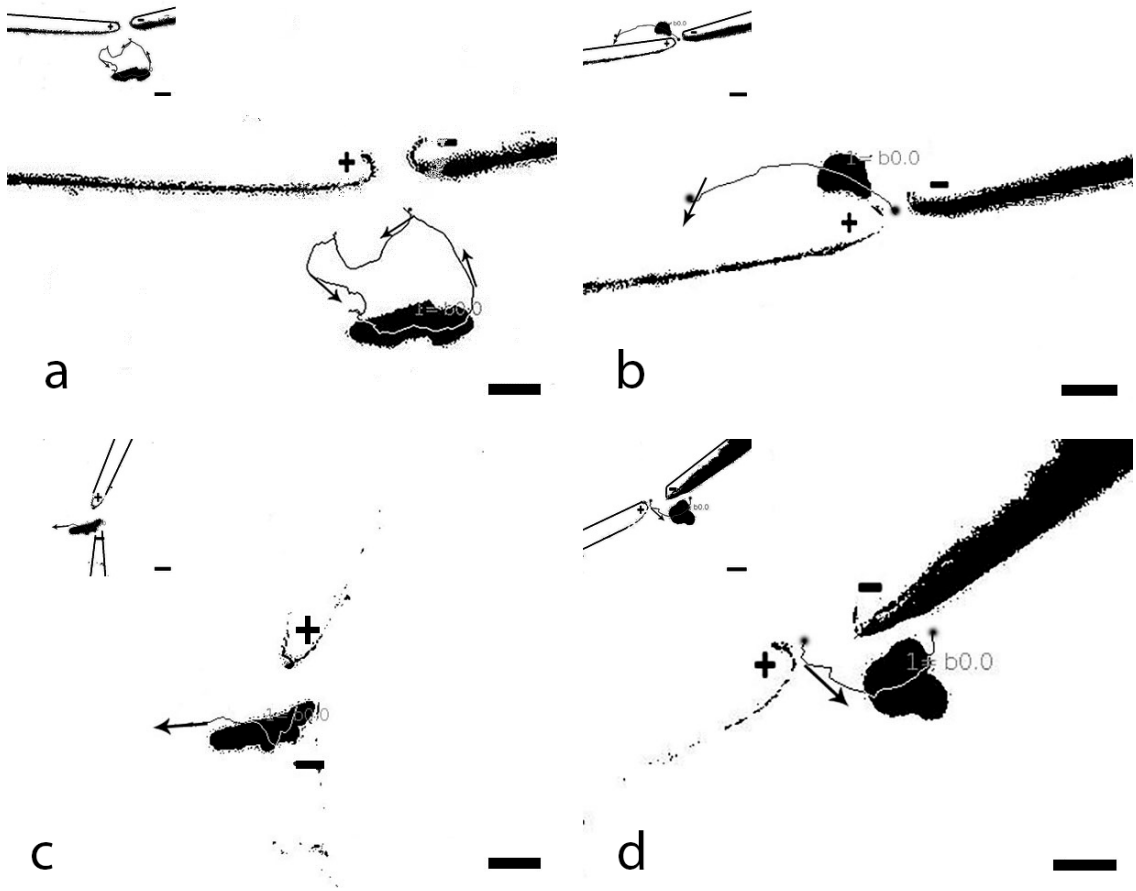

Fig. 5. Change of *Trichoplax adhaerens* H1 shape and motion trajectory from the "electrode trap": (a) seeking activity and elongation of *Trichoplax* along the line of electric field intensity; the directed motion of *Trichoplax* into the "comfort zone" located: (b) behind the anode, (c) far from the electrodes, and (d) behind the cathode. Arrows demonstrate *Trichoplax* motion direction; numbers in the figure indicate identification code assigned to the animal; "+" is the anode; "–" is the cathode; every bar length = 1 mm; graphic insert in the upper left corner explains the image

Experiments in the modes of calcium channels functioning. In order to presumably open *Trichoplax* calcium channels TCa_v3 *in vivo*, we used rectangular pulses with an average voltage of 50 mV, a duty cycle of 0.5, and frequencies of 2.5 Hz, 5 Hz, and 2 kHz. Frequencies are borrowed from [3 ; 20 ; 33]. Significant differences in the effects were found at frequencies of 2.5 Hz and 2 kHz. *Trichoplax* did not change the morphology, slowly crawled from the anode toward the cathode and moved beyond the cathode at a frequency of 2.5 Hz. On the contrary, *Trichoplax* mainly moved to the anode at a frequency of 2 kHz, but did not move far from the electrodes, changed the bulk tissue from transparent and shiny to opaque and dark, ultimately decreased in size, twisted, and detached from the substrate.

When applying the frequencies used in the patch-clamp technique [33], that is pulse duration and delay of 2 ms (500 Hz) or 500 ms (2 Hz), *Trichoplax* in the case of a frequency of 2 Hz did not change visible morphology and crawled from anode to the cathode, and in the case of a frequency of 500 Hz, they mainly moved from the cathode behind the anode or remained stationary and twisted.

In order to presumably open *Trichoplax* calcium channels TCa_v3 *in vivo*, we used rectangular pulses with average voltage of 10 to 120 mV, corresponding to delays of 10 s to 1 ms. Pulse duration was of 35 ms, as in [36]. To assess cumulative TCa_v3 channel-mediated effect of square-shaped pulses on *Trichoplax* sp. H2, delays of 1 ms to 10 s were used. Physiological effect of total pulses action was revealed after several

tens of seconds and looked like a dependence of animal mobility on the duty cycle in pulses sequence. The fractions of paralyzed animals were high – 78 and 80 % for delays of 1 and 10 ms, respectively, at low duty cycle, *i. e.* high frequency and large number of incoming signals (Fig. 6). As the duty cycle increased, the fractions of paralyzed *Trichoplax* decreased up to 44 % and 17 % in the case of one pulse per 1 s and one pulse per 10 s, respectively. Immobilized *Trichoplax* were absent in control experiments without electrical exposure.

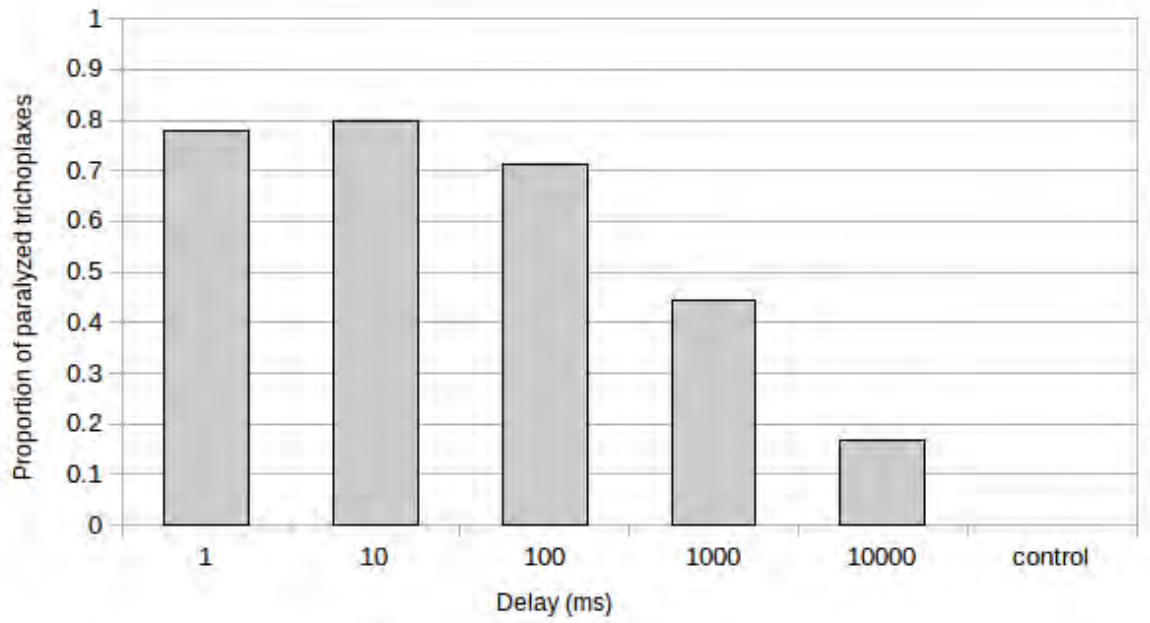

Fig. 6. Fraction of immobilized *Trichoplax* sp. H2 *versus* active animals at pulse duration of 35 ms and delay of 1 ms to 10 s. Totally 65 animals were used in the experiment

Calcium channels blocking. Amlodipine, an inhibitor of the activity of *Trichoplax* voltage-gated calcium channels TCa_v3, was used to prove the specificity of pulse currents effect on these channels.

In the presence of a small amount of amlodipine (25 nM), despite exposure to electric pulses of a duration of 35 ms with a delay of 10 ms, almost all *Trichoplax* (H2 strain) retained their native morphology and mobility for several minutes, preferring to move to the anode and then to leave it, which indicated the prevention of electric shock, observed at low duty cycle (Fig. 6). To identify possible targets, we exposed *Trichoplax* to rectangular pulse packages of variable width and duty cycle with a step of 1 ms, covering a frequency range of 1 Hz to 1 kHz (see supplementary file No. 2: https://doi.org/10.21072/mbj.2020.05.2.05). Immobilization of animals and formation of pans were observed, and their fraction decreased in the presence of 25 nM of amlodipine. However, all *Trichoplax* dissociated on individual cells under amlodipine treatment after several hours.

Effect of large doses of amlodipine on *Trichoplax* was studied in final series of experiments. Amlodipine at a concentration of 50 μM caused a rapid folding of *Trichoplax* plate-like body into a pan in the ventral-dorsal direction and subsequent dissociation of the plate into individual cells (Fig. 7). The pan formation continued for several minutes with amlodipine concentration reducing to 2.5 μM, which made it possible to register motion of the animals to the anode with a duration and a delay of pulses of 35 ms each [36] that corresponds to a frequency of 28.57 Hz. When using amlodipine with a concentration of 250 nM, gradual darkening of *Trichoplax* was observed – first along the periphery, then in the plate center. The outer rim thickened, *Trichoplax* rounded, forming a rugged scalloped edge, the blades of which were torn off the substrate, bent upward, and formed a rosette. Being in an “electrode trap”, animals moved discoordinated

and could not leave it. Further, rigidity of *Trichoplax* plate occurred, which was stated in the rigidity of the shape of the animals when moving. Nonetheless, motion patterns of individuals in electric field persisted: *Trichoplax* moved mainly to the anode. Later, plate rims resembling blades bent up and in. Animals dissociated into individual cells approximately 1 h after adding amlodipine, first along the periphery, then throughout the body.

Trichoplax H1 and H13 strains showed, like H2 strain, a change in morphology under the influence of 25 nM of amlodipine and a violation of amoeboid motion over time. In experiments without amlodipine, no similar phenomena were observed. Animals wandered between the electrodes, placed in the "comfort zone" or moved away at a safe distance from the electrodes in the absence of chemical effects. It should be noted that non-dihydropyridine Ca-channel blockers, such as verapamil and diltiazem with a concentration of 100 μM, did not significantly affect *Trichoplax* H2 strain, which remained viable in the presence of these substances within one day [data is not given].

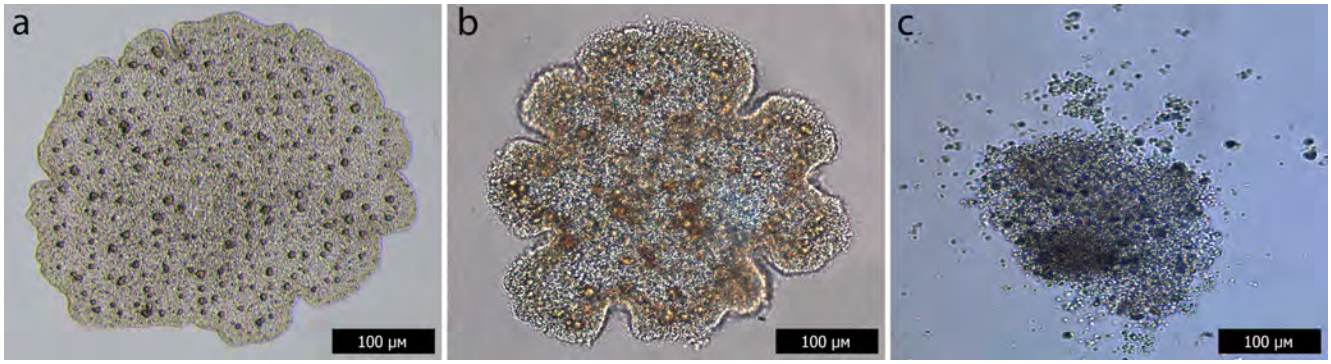

Fig. 7. Time-dependent effect of amlodipine (of 50 μM) on *Trichoplax* sp. H2: (a) intact animal; (b) folding into a pan after 30 minutes; (c) dissociation into individual cells after 60 minutes; bar length = 100 μm

DISCUSSION

Because of widespread distribution of extremely low frequency electric and magnetic fields, causing multiple physiological effects in humans [26 ; 44], the search for test objects for studying the mechanisms of ELF-EMF action is relevant. *Trichoplax adhaerens* was recently proposed as a test laboratory model [1]. We studied the effect of rectangular electric pulses of various amplitude, duration, and duty cycle on three laboratory *Trichoplax* strains (H1, H2, and H13).

In control tests using wood, plastic, or metal rods, no reaction of the animal to foreign objects placed near it was observed, except the cases of galvanic pair formation. Under the effect of a weak direct current with a voltage of 200 mV, *Trichoplax* H2 strain crawled away from the electrodes. However, reaction rate and motion trajectory were largely dependent on animal initial position in relation to the electrodes. When using active electrodes, one of which (the anode or the cathode) was placed near *Trichoplax*, the animal usually moved away from the stimulus. When placing both electrodes near *Trichoplax* plate, various motion patterns to the anode or the cathode were registered, depending on the stimulation mode and animal strain: "positive" migration to the anode, "negative" migration to the cathode, and "variable" migration when the animal changed preference anode – cathode several times. In the case of *Trichoplax* getting into the zone of close proximity to the electrodes, the animal was not always able to get out of the "electrode trap", which directly depended on the rise of amplitude and number of pulses. Far from the electrodes, *Trichoplax* sometimes stretched along the lines of electric field strength and headed to the hypothetical "comfort zone" with the lowest electric field intensity on back side of the electrodes.

In comparative experiments on the effect of rectangular pulses with a frequency of 2 Hz and 2 kHz on different *Trichoplax* strains, it was revealed that *Trichoplax* sp. H2 is more reactive and shows more pronounced physiological responses at frequencies of 2 Hz and 2 kHz compared with H1 strain and especially with H13 strain, which mainly migrates from the anode to the cathode. Therefore, most experiments were conducted with H2 strain. Despite preferable motion of *Trichoplax* H2 strain toward the cathode at low pulse current frequencies (about 2 Hz), a tendency was observed to gradually change a migration direction towards the anode with increasing pulse frequency (up to 2 kHz). Nevertheless, attention should be paid to unexpectedly wide individual variability in *Trichoplax* behavior, which complicates such interpretations and requires further research.

Sufficient attention was paid to time regimes previously used by other authors in detailed studies of L- and T-type calcium channels [3 ; 20 ; 33 ; 34 ; 36]. We investigated effects in frequency range of 2 Hz to 2 kHz. *Trichoplax* behavioral reactions were not unambiguous: extreme frequencies sometimes did not have an expected effect or led to an electric shock of the animal, which might be due to *Trichoplax* physiological state and/or initial position of the animal in the "electrode trap". The motion absence, plate clouding, size reduction, and wrinkling were reversible, and after a while or after the animal returned to the algal mat, *Trichoplax* revived their motion activity.

Depending on duration of stimulating pulses and their number, motion reactions and morphology of animals changed: from stochastic or directed migration to/from anode/cathode to immobilization of animals, optical density elevation, first along the periphery, then in plate center, to *Trichoplax* wrinkling, and even to separating it from the substrate. The effect applied was cumulative in its nature, which is probably related to the work of calcium channels and the activity of downstream regulatory cascades [10]. It is known that glandular cells located on *Trichoplax* periphery express voltage-gated calcium channels [32 ; 39]. Morphological changes observed in *Trichoplax* plate can be associated with calcium channel-mediated responses of secretory cells containing regulatory neuropeptides [42]. On the other hand, it was shown that ELF-EMF pathophysiological effects are associated at the molecular level with regulation of Ca^{2+}/nitric oxide/peroxynitrite, and positive ELF-EMF physiological effect is explained by the alternative pathway of Ca^{2+}/nitric oxide/cGMP/protein kinase G [19]. Mutually exclusive *Trichoplax* behavioral reactions, such as positive and negative electromigration, to varying modes of electrical exposure (Table 1) may be due to the various signaling pathways involving calcium ions in behavioral reactions.

It is believed that amlodipine, when binding to dihydropyridine receptors, blocks L- and T-type calcium channels, which leads to a drop-off in Ca^{2+} transfer to the cell. Amlodipine also has antioxidant properties and contributes to the production of the neurotransmitter nitric oxide due to regulation of Ca^{2+} ions concentration in the cell [4 ; 11 ; 14 ; 16 ; 25]. Additional experiments with amlodipine showed that this calcium channel blocker at low concentrations (of 25 nM) is capable of briefly neutralizing the shock effect of rectangular electric pulses in a duration of 35 ms and a delay of 10 ms, which usually leads to immobilization of *Trichoplax* sp. H2 without amlodipine. We also scanned potential cellular targets in frequency range of 1 Hz to 1 kHz and studied *Trichoplax* responses to packages of rectangular pulses using a software meander with a step of 1 ms. A decline in ELF-EMF negative effect within this range with amlodipine at a concentration of 25 nM may indicate that ELF-EMF affects L- and/or T-type calcium channels of *Trichoplax*.

In addition to silencing the effect of electric stimulus on the animals with amlodipine, we observed other effects. Thus, use of this calcium antagonist in high concentration (of > 2.5 μM) resulted in *Trichoplax* dissociation into individual cells, which is directly caused by the destruction of calcium bridges [28].

When using this calcium blocker in moderate concentration (of < 250 nM), a violation of amoeboid motion of *Trichoplax* was noted, which can result from a decrease in the functional activity of the cells initiating motion, a distortion of activation waves propagation, or a violation of nitric oxide synthesis, which may play a role in rapid contractions of the dorsal epithelium [2 ; 11 ; 16 ; 25]. It should be noted that at the same time, the residual mobility of rigid animals provided by the cilia was observed, which indicates independence of the mentioned process from regulation by calcium ions.

Our data show that amlodipine inhibits *Trichoplax* calcium channels functioning, which is manifested both in a decrease in animals' reactivity at a low concentration of Ca^{2+} channel blocker and in the dissociation of the cells, that make up the animal, at a high concentration of calcium antagonist. It should be noted that amlodipine effect is similar to that of a compound ML218 – a specific blocker of T-type calcium channels in humans. Thus, electrophysiological studies of neurons of the subthalamic nucleus in the presence of ML218 revealed the inhibitory effect of ML218 on T-type calcium channels, suppression of the low-voltage-activated response, and inhibition of neuron activity burst [47].

The assumption in favor of T-type Ca^{2+} channels was confirmed in additional experiments on *Trichoplax* H2 strain, where besides amlodipine, one of dihydropyridine calcium channel blockers, non-dihydropyridine calcium channel blockers, such as verapamil and diltiazem, were tested. Amlodipine led to *Trichoplax* dissociation into individual cells, while verapamil and diltiazem did not have such an effect on animals. This fact confirms that amlodipine blocks *Trichoplax* low-voltage-activated Ca^{2+} channel TCa_v3, because amlodipine is a blocker of L- and T-type calcium channels, while verapamil and diltiazem are only blockers of high-voltage-activated L-type calcium channels.

It should be noted that *Trichoplax* motion was not strictly targeted, but resembled a "stochastic" taxis [38], kinesis, or motion to a target by trial and error. It points out that *Trichoplax* has no central regulator and indicates, possibly, distributed control and collective decision making between cells, which leads in some cases to a delay in system response to stimulus [6].

Conclusion. The study of *Trichoplax* electrophysiology is important in connection with the prevalence of ELF-EMF and is of interest because of simple structure of the animal and ease of cultivation, which makes it possible to understand the mechanisms of its behavior and motion in the future. The diverse responses of *Trichoplax* to electrical stimulus discovered in our experiments indicate latent possibilities of this organism, based on the collective action of its cells.

This work was carried out within the frameworks of government research assignment of IBSS RAS "Patterns of formation and anthropogenic transformation of biodiversity and biological resources of the Sea of Azov – the Black Sea basin and other parts of the World Ocean" (No. AAAA-A18-118020890074-2) and with the support of a grant by the Resolution of the Government of the Russian Federation No. 220 (agreement No. 14.W03.31.0015 of 02.28.2017).

Acknowledgement. K. A. V. expresses gratitude to Gorbunov R. V. and Moroz L. L. for the opportunity to work in the laboratory of biodiversity and functional genomics of the World Ocean at IBSS RAS; to custodians of collections – for *Trichoplax* strains; to laboratory staff – Baiandina Yu. S., Vodiasova E. A., and Kirin M. P. – for help and support; to Romanova D. Yu., Chelebieva E. S., Ponomareva A. A., Kolesnikova E. E., and Kartashov L. E. – for consultations. The authors are grateful to anonymous reviewers for useful comments, which helped to improve the manuscript.

REFERENCES

1. Albertini M. C., Fraternale D., Semprucci F., Cecchini S., Colomba M., Rocchi M. B. L., Sisti D., Di Giacomo B., Mari M., Sabatini L., Cesaroni L., Balsamo M., Guidi L. Bioeffects of *Prunus spinosa* L. fruit ethanol extract on reproduction and phenotypic plasticity of *Trichoplax adhaerens* Schulze, 1883 (Placozoa). *PeerJ*, 2019, vol. 7, article e6789 (22 p.). https://doi.org/10.7717/peerj.6789
2. Armon S., Bull M. S., Aranda-Diaz A., Prakash M. Ultrafast epithelial contractions provide insights into contraction speed limits and tissue integrity. *Proceedings of the National Academy of Science of the USA*, 2018, vol. 115, no. 44, pp. E10333–E10341. https://doi.org/10.1073/pnas.1802934115
3. Bers D. M., Perez-Reyes E. Ca channels in cardiac myocytes: Structure and function in Ca influx and intracellular Ca release. *Cardiovascular Research*, 1999, vol. 42, iss. 2, pp. 339–360. https://doi.org/10.1016/S0008-6363(99)00038-3
4. Catterall W. A. Voltage-gated calcium channels. *Cold Spring Harbor Perspectives in Biology*, 2011, vol. 3, iss. 8, article 003947 (23 p.). https://doi.org/10.1101/cshperspect.a003947
5. Chandler N. J., Greener I. D., Tellez J. O., Inada S., Musa H., Molenaar P., Difrancesco D., Baruscotti M., Longhi R., Anderson R. H., Billeter R., Sharma V., Sigg D. C., Boyett M. R., Dobrzynski H. Molecular architecture of the human sinus node: Insights into the function of the cardiac pacemaker. *Circulation*, 2009, vol. 119, no. 12, pp. 1562–1575. https://doi.org/10.1161/CIRCULATIONAHA.108.804369
6. d'Alessandro J., Mas L., Aubry L., Rieu J. P., Rivière C., Anjard C. Collective regulation of cell motility using an accurate density-sensing system. *Journal of the Royal Society Interface*, 2018, vol. 15, iss. 140, article 20180006 (11 p.). https://doi.org/10.1098/rsif.2018.0006
7. DuBuc T. Q., Ryan J. F., Martindale M. Q. "Dorsal-Ventral" genes are part of an ancient axial patterning system: Evidence from *Trichoplax adhaerens* (Placozoa). *Molecular Biology and Evolution*, 2019, vol. 36, iss. 5, pp. 966–973. https://doi.org/10.1093/molbev/msz025
8. Eitel M., Francis W. R., Varoqueaux F., Daraspe J., Osigus H. J., Krebs S., Vargas S., Blum H., Williams G. A., Schierwater B., Wörheide G. Correction: Comparative genomics and the nature of placozoan species. *PLoS Biology*, 2018, vol. 16, no. 9, article e3000032 (1 p.). https://doi.org/10.1371/journal.pbio.2005359
9. Eitel M., Francis W. R., Varoqueaux F., Daraspe J., Osigus H. J., Krebs S., Vargas S., Blum H., Williams G. A., Schierwater B., Wörheide G. Comparative genomics and the nature of placozoan species. *PLoS Biology*, 2018, vol. 16, no. 7, article E2005359 (36 p.). https://doi.org/10.1371/journal.pbio.2005359
10. Gao R., Zhao S., Jiang X., Sun Y., Zhao S., Gao J., Borleis J., Willard S., Tang M., Cai H., Kamimura Y., Huang Y., Jiang J., Huang Z., Mogilner A., Pan T., Devreotes P. N., Zhao M. A large-scale screen reveals genes that mediate electrotaxis in *Dictyostelium discoideum*. *Science Signaling*, 2015, vol. 8, iss. 378, pp. ra50 (10 p.). https://doi.org/10.1126/scisignal.aab0562
11. Godfraind T. Discovery and development of calcium channel blockers. *Frontiers in Pharmacology*, 2017, vol. 8, article 286 (25 p.). https://doi.org/10.3389/fphar.2017.00286
12. Grassi C., D'Ascenzo M., Torsello A., Martinotti G., Wolf F., Cittadini A., Azzena G. B. Effects of 50 Hz electromagnetic fields on voltage-gated Ca^{2+} channels and their role in modulation of neuroendocrine cell proliferation and death. *Cell Calcium*, 2004, vol. 35, iss. 4, pp. 307–315. https://doi.org/10.1016/j.ceca.2003.09.001
13. Heyland A., Croll R., Goodall S., Kranyak J., Wyeth R. *Trichoplax adhaerens*, an enigmatic basal metazoan with potential. In: *Developmental Biology of the Sea Urchin and Other Marine. Invertebrates: Methods and Protocols* / D. J. Carroll, S. A. Stricker (Eds). New York : Humana Press, 2014, chap. 4, pp. 45–61. https://doi.org/10.1007/978-1-62703-974-1_4

14. Iftinca M. C. Neuronal T-type calcium channels: What's new? *Journal of Medicine and Life*, 2011, vol. 4, iss. 2, pp. 126–138.
15. Kamm K., Osigus H. J., Stadler P. F., DeSalle R., Schierwater B. *Trichoplax* genomes reveal profound admixture and suggest stable wild populations without bisexual reproduction. *Scientific Reports*, 2018, vol. 8, iss. 1, article 11168 (11 p.). https://doi.org/10.1038/s41598-018-29400-y
16. Kopecky B. J., Liang R., Bao J. T-type calcium channel blockers as neuroprotective agents. *Pflügers Archiv – European Journal of Physiology*, 2014, vol. 466, iss. 4, pp. 757–765. https://doi.org/10.1007/s00424-014-1454-x
17. Kuznetsov A. V., Halaimova A. V., Ufimtseva M. A., Chelebieva E. S. Blocking a chemical communication between *Trichoplax* organisms leads to their disorderly movement. *International Journal of Parallel, Emergent and Distributed Systems*, 2020, vol. 35, iss. 4, pp. 473–482. https://doi.org/10.1080/17445760.2020.1753188
18. Lawrence A. F., Adey W. R. Nonlinear wave mechanisms in interactions between excitable tissue and electromagnetic fields. *Neurological Research*, 1982, vol. 4, iss. 1–2, pp. 115–153. https://doi.org/10.1080/01616412.1982.11739619
19. Ledoigt G., Belpomme D. Cancer induction molecular pathways and HF-EMF irradiation. *Advances in Biological Chemistry*, 2013, vol. 3, pp. 177–186. https://doi.org/10.4236/abc.2013.32023
20. Linz K. W., Meyer R. Control of L-type calcium current during the action potential of guinea-pig ventricular myocytes. *Journal of Physiology*, 1998, vol. 513, pt. 2, pp. 425–442. https://doi.org/10.1111/j.1469-7793.1998.425bb.x
21. Lipscombe D., Andrade A. Calcium channel $Ca_V\alpha_1$ splice isoforms – Tissue specificity and drug action. *Current Molecular Pharmacology*, 2015, vol. 8, iss. 1, pp. 22–31. https://doi.org/10.2174/1874467208666150507103215
22. Marchionni I., Paffi A., Pellegrino M., Liberti M., Apollonio F., Abeti R., Fontana F., D'Inzeo G., Mazzanti M. Comparison between low-level 50 Hz and 900 MHz electromagnetic stimulation on single channel ionic currents and on firing frequency in dorsal root ganglion isolated neurons. *Biochimica et Biophysica Acta (BBA) – Biomembranes*, 2006, vol. 1758, iss. 5, pp. 597–605. https://doi.org/10.1016/j.bbamem.2006.03.014
23. Moran Y., Barzilai M. G., Liebeskind B. J., Zakon H. H. Evolution of voltage-gated ion channels at the emergence of Metazoa. *Journal of Experimental Biology*, 2015, vol. 218, pt. 4, pp. 515–525. https://doi.org/10.1242/jeb.110270
24. Nanou E., Catterall W. A. Calcium channels, synaptic plasticity, and neuropsychiatric disease. *Neuron*, 2018, vol. 98, iss. 3, pp. 466–481. https://doi.org/10.1016/j.neuron.2018.03.017
25. Pall M. L. Electromagnetic fields act *via* activation of voltage-gated calcium channels to produce beneficial or adverse effects. *Journal of Cellular and Molecular Medicine*, 2013, vol. 17, iss. 8, pp. 958–965. https://doi.org/10.1111/jcmm.12088
26. Pall M. L. Microwave frequency electromagnetic fields (EMFs) produce widespread neuropsychiatric effects including depression. *Journal of Chemical Neuroanatomy*, 2016, vol. 75, pt. B, pp. 43–51. https://doi.org/10.1016/j.jchemneu.2015.08.001
27. Ritter J. M., Flower R. J., Henderson G., Loke Y. K., MacEwan D., Rang H. P. *Rang & Dale's Pharmacology*. 9th edition. Elsevier, 2019, 808 p.
28. Ruthmann A., Terwelp U. Disaggregation and reaggregation of cells of the primitive metazoon *Trichoplax adhaerens*. *Differentiation*, 1979, vol. 13, iss. 3, pp. 185–198. https://doi.org/10.1111/j.1432-0436.1979.tb01581.x
29. Santini M. T., Rainaldi G., Indovina P. L. Cellular effects of extremely low frequency (ELF) electromagnetic fields. *International Journal of Radiation Biology*, 2009, vol. 85, iss. 4, pp. 294–313. https://doi.org/10.1080/09553000902781097
30. Schierwater B. My favorite animal, *Trichoplax adhaerens*. *BioEssays*, 2005, vol. 27, iss. 12, pp. 1294–1302. https://doi.org/10.1002/bies.20320
31. Schulze F. E. *Trichoplax adhaerens*, nov. gen., nov. spec. *Zoologischer Anzeiger*, 1883, vol. 6, pp. 92–97.
32. Senatore A., Raiss H., Le P. Physiology and evolution of voltage-gated calcium channels in early diverging animal phyla: Cnidaria, Placozoa, Porifera, and Ctenophora. *Frontiers in Physiology*, 2016, vol. 7, article 481. https://doi.org/10.3389/fphys.2016.00481

33. Shiels H. A., Vornanen M., Farrell A. P. Temperature dependence of cardiac sarcoplasmic reticulum function in rainbow trout myocytes. *Journal of Experimental Biology*, 2002, pt. 23, pp. 3631–3639.
34. Shiels H. A., Vornanen M., Farrell A. P. Temperature-dependence of L-type Ca^{2+} channel current in atrial myocytes from rainbow trout. *Journal of Experimental Biology*, 2000, pt. 18, pp. 2771–2780.
35. Simms B. A., Zamponi G. W. Neuronal voltage-gated calcium channels: Structure, function, and dysfunction. *Neuron*, 2014, vol. 82, iss. 1, pp. 24–45. https://doi.org/10.1016/j.neuron.2014.03.016
36. Smith C. L., Abdallah S., Wong Y. Y., Le P., Harracksingh A. N., Artinian L., Tamvacakis A. N., Rehder V., Reese T. S., Senatore A. Evolutionary insights into T-type Ca^{2+} channel structure, function, and ion selectivity from the *Trichoplax adhaerens* homologue. *Journal of General Physiology*, 2017, vol. 149, iss. 4, pp. 483–510. https://doi.org/10.1085/jgp.201611683
37. Smith C. L., Pivovarova N., Reese T. S. Coordinated feeding behavior in *Trichoplax*, an animal without synapses. *PLoS One*, 2015, vol. 10, iss. 9, article e0136098 (15 p.). https://doi.org/10.1371/journal.pone.0136098
38. Smith C. L., Reese T. S., Govezensky T., Barrio R. A. Coherent directed movement toward food modeled in *Trichoplax*, a ciliated animal lacking a nervous system. *Proceedings of the National Academy of Science of the USA*, 2019, vol. 116, no. 18, pp. 8901–8908. https://doi.org/10.1073/pnas.1815655116
39. Smith C. L., Varoqueaux F., Kittelmann M., Azzam R. N., Cooper B., Winters C. A., Eitel M., Fasshauer D., Reese T. S. Novel cell types, neurosecretory cells, and body plan of the early-diverging metazoan *Trichoplax adhaerens*. *Current Biology*, 2014, vol. 24, iss. 14, pp. 1565–1572. https://doi.org/10.1016/j.cub.2014.05.046
40. Srivastava M., Begovic E., Chapman J., Putnam N. H., Hellsten U., Kawashima T., Kuo A., Mitros T., Salamov A., Carpenter M. L., Signorovitch A. Y., Moreno M. A., Kamm K., Grimwood J., Schmutz J., Shapiro H., Grigoriev I. V., Buss L. W., Schierwater B., Dellaporta S. L., Rokhsar D. S. The *Trichoplax* genome and the nature of placozoans. *Nature*, 2008, vol. 454, no. 7207, pp. 955–960. https://doi.org/10.1038/nature07191
41. Sun Z. C., Ge J. L., Guo B., Guo J., Hao M., Wu Y. C., Lin Y. A., La T., Yao P. T., Mei Y. A., Feng Y., Xue L. Extremely low frequency electromagnetic fields facilitate vesicle endocytosis by increasing presynaptic calcium channel expression at a central synapse. *Scientific Reports*, 2016, vol. 6, article 21774 (11 p.). https://doi.org/10.1038/srep21774
42. Varoqueaux F., Williams E. A., Grandemange S., Truscello L., Kamm K., Schierwater B., Jékely G., Fasshauer D. High cell diversity and complex peptidergic signaling underlie placozoan behavior. *Current Biology*, 2018, vol. 28, iss. 21, pp. 3495–3501 (10 p.). https://doi.org/10.1016/j.cub.2018.08.067
43. Vianale G., Reale M., Amerio P., Stefanachi M., Di Luzio S., Muraro R. Extremely low frequency electromagnetic field enhances human keratinocyte cell growth and decreases proinflammatory chemokine production. *British Journal of Dermatology*, 2008, vol. 158, iss. 6, pp. 1189–1196. https://doi.org/10.1111/j.1365-2133.2008.08540.x
44. Warille A. A., Altun G., Elamin A. A., Kaplan A. A., Mohamed H., Yurt K. K., El Elhaj A., Skeptical approaches concerning the effect of exposure to electromagnetic fields on brain hormones and enzyme activities. *Journal of Microscopy and Ultrastructure*, 2017, vol. 5, iss. 4, pp. 177–184. https://doi.org/10.1016/j.jmau.2017.09.002
45. Weiss N., Zamponi G. W. Control of low-threshold exocytosis by T-type calcium channels. *Biochimica et Biophysica Acta (BBA) – Biomembranes*, 2013, vol. 1828, iss. 7, pp. 1579–1586. https://doi.org/10.1016/j.bbamem.2012.07.031
46. Weiss N., Zamponi G. W. Genetic T-type calcium channelopathies. *Journal of Medical Genetics*, 2019, vol. 57, iss. 1, pp. 1–10. https://doi.org/10.1136/jmedgenet-2019-106163
47. Xiang Z., Thompson A. D., Brogan J. T., Schulte M. L., Melancon B. J., Mi D., Lewis L. M., Zou B., Yang L., Morrison R., Santomango T., Byers F., Brewer K., Aldrich J. S., Yu H., Dawson E. S., Li M., McManus O., Jones C. K., Daniels J. S.,

Hopkins C. R., Xie X. S., Conn P. J., Weaver C. D., Lindsley C. W. The discovery and characterization of ML218: A novel, centrally active T-type calcium channel inhibitor with robust effects in STN neurons and in a rodent model of Parkinson's disease. *ACS Chemical Neuroscience*, 2011, vol. 2, iss. 12, pp. 730–742. https://doi.org/10.1021/cn200090z

48. Zalata A., El-Samanoudy A. Z., Shaalan D., El-Baiomy Y., Mostafa T. *In vitro* effect of cell phone radiation on motility, DNA fragmentation, and clusterin gene expression in human sperm. *International Journal of Fertility and Sterility*, 2015, vol. 9, iss. 1, pp. 129–136. https://doi.org/10.22074/ijfs.2015.4217

ДЕЙСТВИЕ ПРЯМОУГОЛЬНЫХ ЭЛЕКТРИЧЕСКИХ ИМПУЛЬСОВ НИЗКОЙ ЧАСТОТЫ НА ТРИХОПЛАКСА (ТИП PLACOZOA)

А. В. Кузнецов[1,3], О. Н. Кулешова[1], А. Ю. Пронозин[2], О. В. Кривенко[1], О. С. Завьялова[3]

[1]Федеральный исследовательский центр «Институт биологии южных морей имени А. О. Ковалевского РАН», Севастополь, Российская Федерация

[2]Институт цитологии и генетики СО РАН, Новосибирск, Российская Федерация

[3]Севастопольский государственный университет, Севастополь, Российская Федерация

E-mail: *kuznet61@gmail.com*

Влияние низкочастотного электромагнитного излучения (НЭМИ) на растения и животных, включая человека, достаточно спорно. Мало известно и о воздействии НЭМИ на гидробионтов. Мы изучили действие прямоугольных импульсов напряжения различной амплитуды, длительности и скважности, пропущенных через морскую воду, на трихоплакса (тип Placozoa) как на возможную тестовую лабораторную модель. В опытах использовали три штамма Placozoa, *Trichoplax adhaerens* (H1), *Trichoplax* sp. (H2) и *Hoilungia hongkongensis* (H13), отобранных на стационарной стадии роста культуры. Для генерации последовательности прямоугольных импульсов заданной длительности и скважности с частотой до 2 кГц применяли аппаратную платформу Arduino Uno. Среднее значение напряжения до 500 мВ регулировали с помощью схемы делителя напряжения. Для доказательства специфичности действия электрических импульсов на потенциалзависимые кальциевые каналы трихоплакса использовали ингибитор активности кальциевых каналов амлодипин. Животных стимулировали электрическим током под стереомикроскопом. Электроды располагали в непосредственной близости от животного. Исследовали сопутствующие изменения поведения и морфологии пластинки трихоплакса. Выделяли стимулирующие и подавляющие воздействия. Наблюдения документировали с помощью фото- и видеосъёмки. Отслеживали траектории движения отдельных особей. Увеличение напряжения на электродах при фиксированной частоте 20 Гц приводило к тому, что животные штамма H2 покидали «зону электродов» в течение нескольких минут при 25 мВ, однако теряли подвижность пропорционально росту напряжения и обездвиживались при 500 мВ. Именно поэтому в дальнейших опытах применяли напряжение 50 мВ. В экспериментах с двумя электродами, находящимися с одной стороны трихоплакса, у животного было больше возможностей перемещаться в разных направлениях, чем в случае расположения электродов по обеим сторонам пластинки. Направление движения использовали как характеристический признак. Отмечено, что трихоплаксы мигрируют в области с низкой плотностью линий электрического поля, которые расположены вдали или за электродами. Животные из старой культуры отличались меньшей чувствительностью к электрическому раздражителю. Штамм H2 был наиболее чувствительным и демонстрировал более выраженные физиологические реакции на частотах 2 Гц и 2 кГц с напряжением 50 мВ, чем штамм H1 и особенно штамм H13. В зависимости от длительности стимулирующих прямоугольных импульсов, их числа, амплитуды и варьирующей частоты менялись двигательные реакции и морфология животных: от направленной или стохастической миграции в сторону анода/катода или от него до обездвиживания животных, увеличения оптической плотности по периферии и в центре пластинки и до сворачивания трихоплакса и отделения его от субстрата. В дополнительных опытах на *Trichoplax* sp. H2 показано, что при длительности импульсов 35 мс и задержке импульсов

от 1 мс до 10 с доля обездвиженных животных увеличивается до 80 % при минимальной задержке. Тем не менее в случае применения амлодипина в концентрации 25 нМ практически все трихоплаксы в течение нескольких минут сохраняли подвижность несмотря на обработку электрическими импульсами. Между тем при использовании амлодипина в концентрации 250 нМ животные двигались дискоординированно и не могли покинуть «электродную ловушку». Далее пластинка трихоплакса становилась ригидной, что выражалось в неизменности формы животного при движении. Наконец, амлодипин в концентрации 50 мкМ вызывал быстрое сворачивание краёв трихоплакса в розетку в вентрально-дорсальном направлении и последующую диссоциацию пластинки на отдельные клетки. В целом применяемое электрическое воздействие имело кумулятивный, но обратимый эффект, который, как предполагается, может быть связан с работой потенциалзависимых кальциевых каналов. Амлодипин в большой концентрации (50 мкМ) вызывал разрушение трихоплакса, в умеренной (250 нМ) он нарушал, вероятно, распространение волн активации, что приводило к дискоординации движений животного, а в малой (25 нМ) предотвращал электрошок.

Ключевые слова: прямоугольные электрические импульсы, трихоплакс, пластинчатые, потенциалзависимые кальциевые каналы

1871
ИнБЮМ – IBSS

Морской биологический журнал
Marine Biological Journal
2020, vol. 5, no. 2, pp. 67–75
https://doi.org/10.21072/mbj.2020.05.2.06

UDC 591.148:574.583(262.5)

INFLUENCE OF INVADER CTENOPHORES ON BIOLUMINESCENCE VARIABILITY OFF THE COAST OF WESTERN CRIMEA

© 2020 **A. V. Melnik, V. V. Melnikov, L. A. Melnik, and O. V. Mashukova**

A. O. Kovalevsky Institute of Biology of the Southern Seas of RAS, Sevastopol, Russian Federation
E-mail: *melnikalexsand@gmail.com*

Received by the Editor 21.11.2019; after revision 26.03.2020;
accepted for publication 26.06.2020; published online 30.06.2020.

In the second half of the XX century, Black Sea ecosystem has undergone significant changes: a number of storm winds and upwellings decreased, precipitation abundance increased, coastal waters salinity decreased, temperature increased; moreover, ctenophores invaded. As a result, in the late 1980s, Black Sea pelagic ecosystem abruptly got restructured. This research is based on the studies performed in 1965–1966 and 2007–2012 near Sevastopol (Western Crimea) using the remote sensing data. Analysis of satellite data over the past 20 years showed the presence of positive dynamics in surface water temperature in Sevastopol water area. In the mid-1960s, the annual bioluminescence was characterized by seasonal peaks of dinophytes luminescence. In recent years, this rhythm has changed due to ctenophores invasion. The increase in *Mnemiopsis leidyi* abundance leads to a decrease in bioluminescence of luminous microalgae being consumed by these ctenophores. Due to *Beroe ovata* invasion and reproduction, *M. leidyi* biomass decreased; as a result, bioluminescence increased.

Keywords: Black Sea, bioluminescence, ctenophores, salinity, monitoring

Biophysical studies in the Black Sea began in the 1960s when D. Sc. E. Bityukov (IBSS) made the first annual measurements of bioluminescence in Sevastopol area [2]. Thus, in 1965–1966, 18 expeditions were carried out for instrumental measurements, and 72 net samplings of plankton were taken. Continuation of these works was initiated by D. Sc. Yu. Tokarev (IBSS); the studies were carried out in 2008–2015. So, it became possible to evaluate the long-term changes of coastal water bioluminescence under conditions of climate changes.

The climate changes in Black Sea ecosystem have led to the invasion of huge number of new luminous species: they were brought in with ballast waters from other regions. Therefore, all past experience and knowledge about Black Sea bioluminescence are subject to minor adjustments.

Before ctenophores invasion, bioluminescence field in Black Sea photic layer was formed by luminous dinoflagellates [4]. In the early 1980s, ctenophore *Mnemiopsis leidyi* A. Agassiz, 1865 invaded the Black Sea, which led to a significant reduction in plankton base and fish food [18]. In the late 1990s, another ctenophore, *Beroe ovata* Mayer, 1912, invaded the Black Sea and began to consume *Mnemiopsis leidyi* [6]. Now, the system is balanced: when the number of one species increases, the number of other species decreases. Therefore, it was suggested that these invader species should make a significant contribution to changing the seasonal dynamics of coastal water bioluminescence.

The aim of this work is to determine influence of these two species on the seasonal dynamics of coastal water bioluminescence.

MATERIAL AND METHODS

The fieldwork was carried out at the 10-mile station off the Kruglaya Bay (No. 1) and at two stations in the Sevastopol Bay (No. 2 and 3) (Western Crimea) (Fig. 1). The research was based on the real-time instrumental measurements of bioluminescence amplitude-frequency parameters, as well as on the determination of their spatial conjugacy with biological and hydrophysical characteristics of water masses.

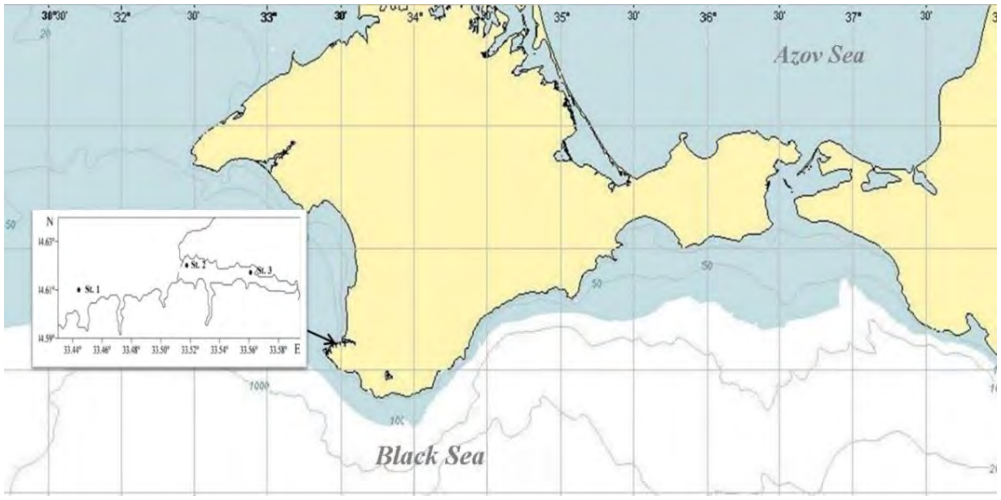

Fig. 1. Map of stations

Station No. 1, located near the Kruglaya Bay (depth of 60 m), has water exchange with the open sea and is characterized by a fairly stable stratification of water column, which determines the vertical structure of temperature and salinity. Stations No. 2 and 3 are located in the Sevastopol Bay, and water exchange with the open sea is limited. In addition, the Sevastopol Bay includes the mouth of the Chernaya River, which is the flow of fresh water into the bay; this results in mixing of river water and seawater [15]. Depending on the volume of river flow, the impact of fresh water extends to different zones of the bay, which significantly affects region ecological conditions. Water area of Konstantinovskaya Bay (station No. 2, depth of 19 m) is relatively clean. Gollandiya Bay (station No. 3, depth of 18 m) is located in the central part of the Sevastopol Bay in the zone of active mixing of river water and seawater [8].

Bioluminescence intensity and background parameters were recorded using a submersible complex "Salpa-M" [21]. It allows taking simultaneous measurements of bioluminescent potential, temperature, hydrostatic pressure, turbidity, and photosynthetically active radiation. "Salpa-M" has four rows of blackened impellers, consisting of two groups of rows mutually perpendicular to attack angles and forming a moving light trap. This ensures the attenuation of light energy by $2 \cdot 10^7$ times, which is especially important during the daytime. The weight of the submersible complex does not exceed 15 kg; it is designed for autonomous power supply of 24 V.

Discreteness of the measurements during the "down" operation at a speed of 1.2 $m \cdot s^{-1}$ was about 0.25 m. To construct graphs of vertical profiles, the data were integrated up to 1 m. The method of collecting and processing the data using the "Salpa-M" complex was previously described in details [21]. On processing its data, profiles of bioluminescence, temperature, salinity, and conditional density of water were calculated. Results of the measurements were processed and added to a database [13].

Simultaneously with measurements with the "Salpa-M" complex, phytoplankton samples were taken using a bathometer. The fieldwork was carried out both at night (the period of maximum bioluminescence)

and at daytime (the period of minimum bioluminescence). At each station, measurement with the "Salpa-M" complex was carried out twice. During several cruises of RV "Professor Vodyanitsky", 10 to 30 continuous soundings were made by the "Salpa-M" complex at station No. 1.

Changes in sea surface temperature (hereinafter SST) in Sevastopol area were analyzed for 2008–2017 based on the analysis of remote sensing data. Under the conditions of a sea expedition, methodological approaches described in this article were tested, which will be applied in the scientific researches in the Antarctic region.

RESULTS

Mean annual SST values (°C) have a negative trend since 1982 reaching its minimum in 1987; then, the period until 2017 is characterized by a significant positive trend (Fig. 2). Since trend lines were constructed by least squares calculation, the accuracy of the approximation was estimated by the coefficient of determination. This graph clearly shows that during the period of ctenophores invasion in the area studied, substantial warming of surface waters occurred.

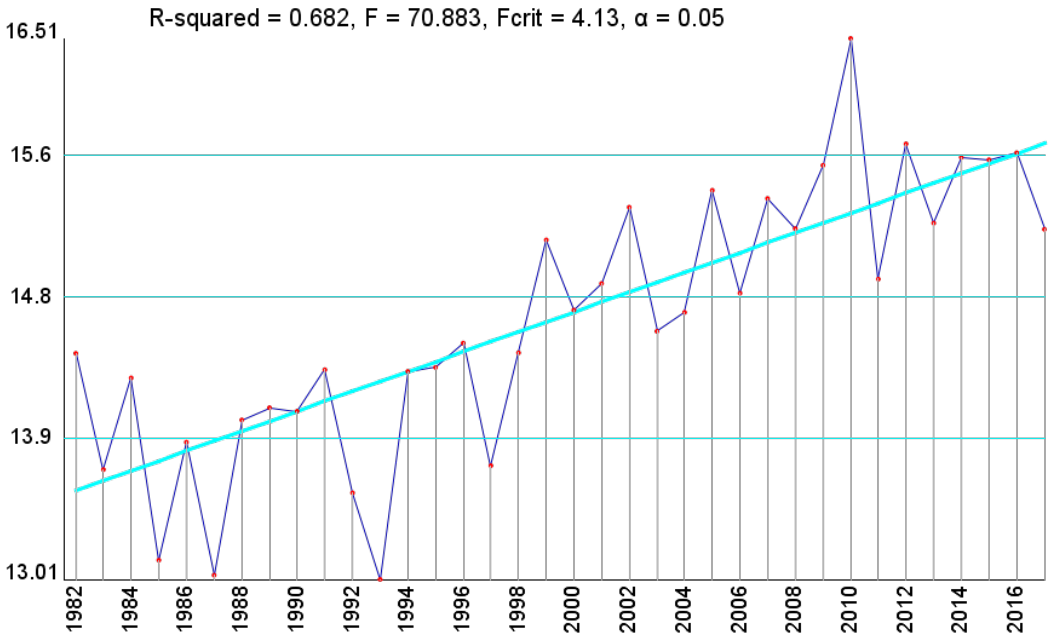

Fig. 2. Mean annual sea surface temperature values (°C) calculated for 1982–2017 with a spatial resolution of 0.0417° in latitude and longitude. *R*-squared (R^2) is the coefficient of determination; *F* is Fisher's *F*-test; *Fcrit* is the critical value of Fisher's *F*-test for the data considered at the accepted confidence probability α [14]

Data analysis showed that in 1965–1966, two seasonal peaks of bioluminescence were observed (Fig. 3A), which were associated with spring and autumn phytoplankton blooming [5]. In recent years, global warming has changed this rhythm. Thus, in 2008–2012, the seasonal dynamics of bioluminescence on Sevastopol coast was characterized by the appearance of additional peaks in the warm season, associated with the outbreaks of warm-water invader ctenophores – *M. leidyi* and *B. ovata* (Fig. 3A). Under favorable conditions, abrupt outbreaks of *B. ovata* abundance are possible, often alternating with recessions up to its complete disappearance (this, for example, is typical of North America coast [11]). It resulted in significant imbalance in the seasonal dynamics of the coastal water bioluminescence near Sevastopol.

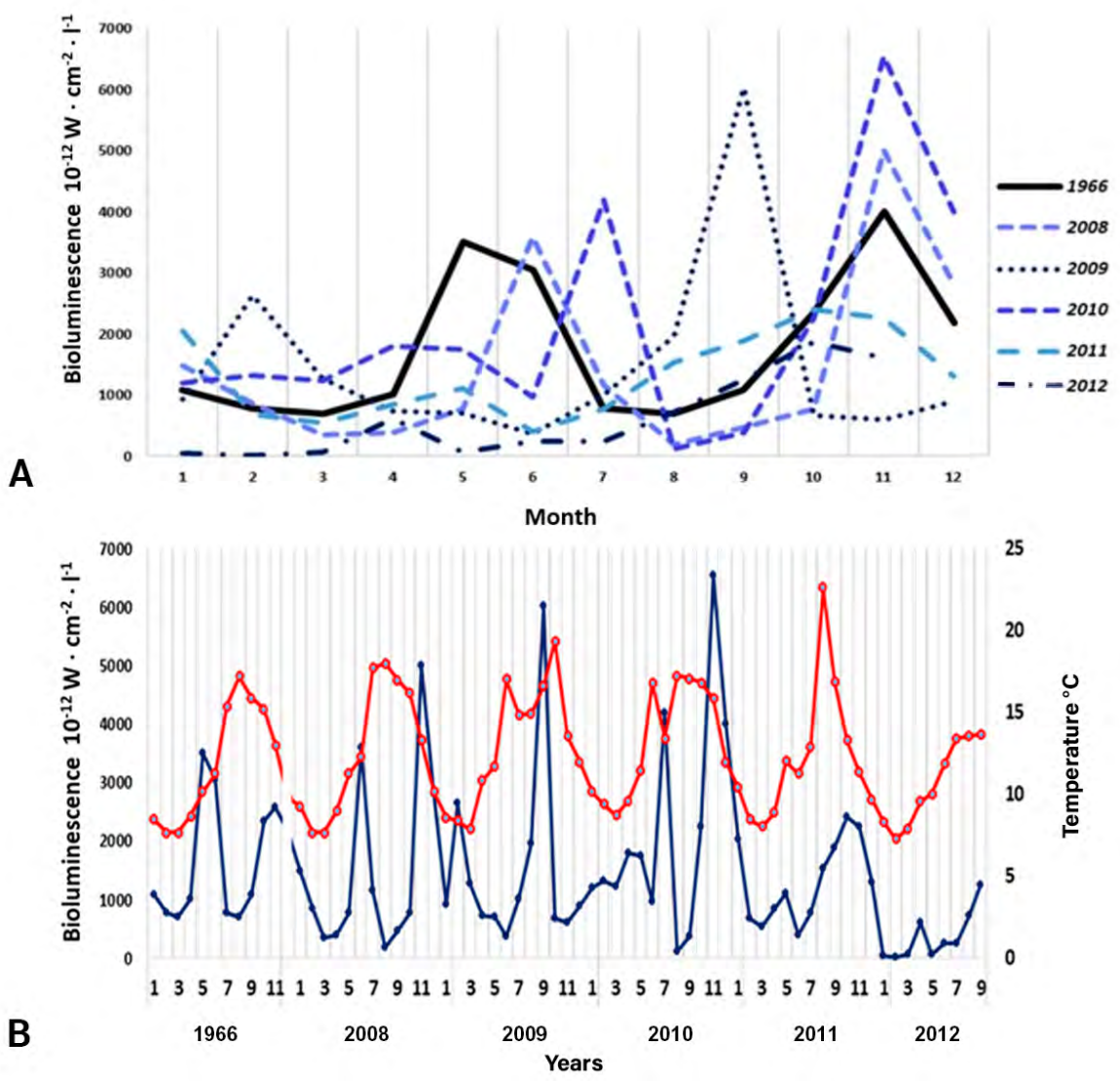

Fig. 3. A – seasonal dynamics of bioluminescence intensity; B – inter-annual dynamics of bioluminescence (mean values are indicated by a blue line) and water temperature (red line) in Sevastopol coastal waters in 55-m layer (1966, 2008–2012)

The inter-annual dynamics of temperature and bioluminescence (Fig. 3B, Table 1) was characterized by the presence of a positive annual mean trend – an increase in mean values of water temperature in 0–55-m layer from +12.11 °C (2008) to +12.89 °C (2010). The maximum summer values of the mean temperature increased from +18.00 °C (August 2008) to +22.62 °C (August 2011).

The peaks of bioluminescence (Fig. 3B) were observed in June 2008 ($3594 \cdot 10^{-12}$ W·cm^{-2}·L^{-1}), in July 2009 ($4200 \cdot 10^{-12}$ W·cm^{-2}·L^{-1}), and in September 2009 ($6029 \cdot 10^{-12}$ W·cm^{-2}·L^{-1}), as well as in spring and autumn regularly due to phytoplankton blooming (Table 1).

The vertical structure of bioluminescence in all the seasons was determined by hydrological conditions, especially thermocline layer location. Bioluminescence is mainly represented by a structure of two maxima separated by a water column where bioluminescence is reduced. The upper stationary layer was almost always observed at a depth of 0–6 m; the lower layer with a higher luminosity migrated within 15–64 m and was located in thermocline area.

Table 1. Mean values of water temperature (T, °C) and bioluminescence (B, $\cdot 10^{-12}$ W·cm^{-2}·L^{-1}) at station No. 1 (I–XII indicate months January till December)

Year	1966		2008		2009		2010		2011		2012	
Index	T	B	T	B	T	B	T	B	T	B	T	B
I	8.5	1094	9.3		8.62	929	10.16	1204	10.45	2048	8.35	42
II	7.7	781	7.7	859	8.38	2643	9.42	1326	8.5	691	7.29	17
III	7.7	703	7.7	352	7.9	1274	8.72	1233	8.07	544	7.94	68
IV	8.7	1016	9.0	391	10.84	733	9.62	1801	8.92	850	9.58	618
V	10.2	3516	11.3	781	11.75	700	11.48	1754	12.04	1104	10.06	76
VI	11.3	3047	12.3	3594	17.03	371	16.81	974	11.27	412	11.88	249
VII	15.4	781	17.7	1172	14.9	1011	13.43	4200	12.89	772	13.46	248
VIII	17.2	703	18.0	195	14.91	1970	17.24	126	22.62	1534		
IX	15.9	1094	17.0	469	16.62	6029	17.07	386	16.92	1898	13.71	1254
X	15.2	2344	16.2	781	19.36	675	16.81	2257	13.30	2410		
XI	13.0	2574	13.3	5000	13.57	608	15.87	6545	11.37	2256		
XII	9.8	2188	10.2	2813	12.00	900	12.00	4000	9.70	1304		

Studies of the inter-annual dynamics of invader ctenophores abundance near Sevastopol in 2009–2010 [1] showed that seasonal peaks for *M. leidyi* and *B. ovata* do not coincide (Fig. 3) due to differences in diets of these species. Increase in *B. ovata* abundance leads to decrease in *M. leidyi* abundance, which restores the number of luminous dinoflagellates. Recently it has been found out [20] that even *M. leidyi* larvae and post-larvae are likely to consume significant amounts of microphyto- and zooplankton including dinoflagellates, ciliated infusoria, and other flagellates.

B. ovata is the main consumer of *M. leidyi* in the Black Sea. Peaks of its seasonal abundance occur at the end of summer, when *M. leidyi* biomass reaches its maximum value. After density of food resource reduces, *Beroe* populations continue to persist due to a decrease in the mean body size of individuals [12].

Using the statistical analysis (Pearson's correlation coefficient, r) on the data on invader ctenophore abundance and bioluminescence dynamics showed that correlation between *M. leidyi* traits studied and the bioluminescence is low (–0.49) (Figs 4, 5). Correlation between *B. ovata* traits studied and the bioluminescence was assessed as strong (0.71). It can be concluded that in cases of $r = -0.49$, the increase in *M. leidyi* biomass moderately affects the decrease in bioluminescence intensity. In cases of $r = 0.71$, the increase in *B. ovata* biomass significantly affects the increase in bioluminescence intensity. Correlation between these data was measured by the Chaddock scale. Criteria for evaluation were as follows: $0.1 < r < 0.3$ (weak); $0.3 < r < 0.5$ (moderate); $0.5 < r < 0.7$ (noticeable); $0.7 < r < 0.9$ (strong); $0.9 < r < 1$ (very strong).

DISCUSSION

Because of the global warming, intensive distribution and development of gelatinous plankton has occurred in various marine areas of the world in recent decades. Significant secular trends of increasing air temperature (by 0.4–0.8 °C per 100 years) are observed along Black Sea coast, which corresponds to global warming estimates [9]. During the second half of the XX century, the recurrence of strong winds and upwellings decreased three times; a significant increase in precipitation and a decrease in evaporation were observed [10 ; 14]. This created the conditions for the resettlement of invader species, which have radically changed Black Sea ecosystem.

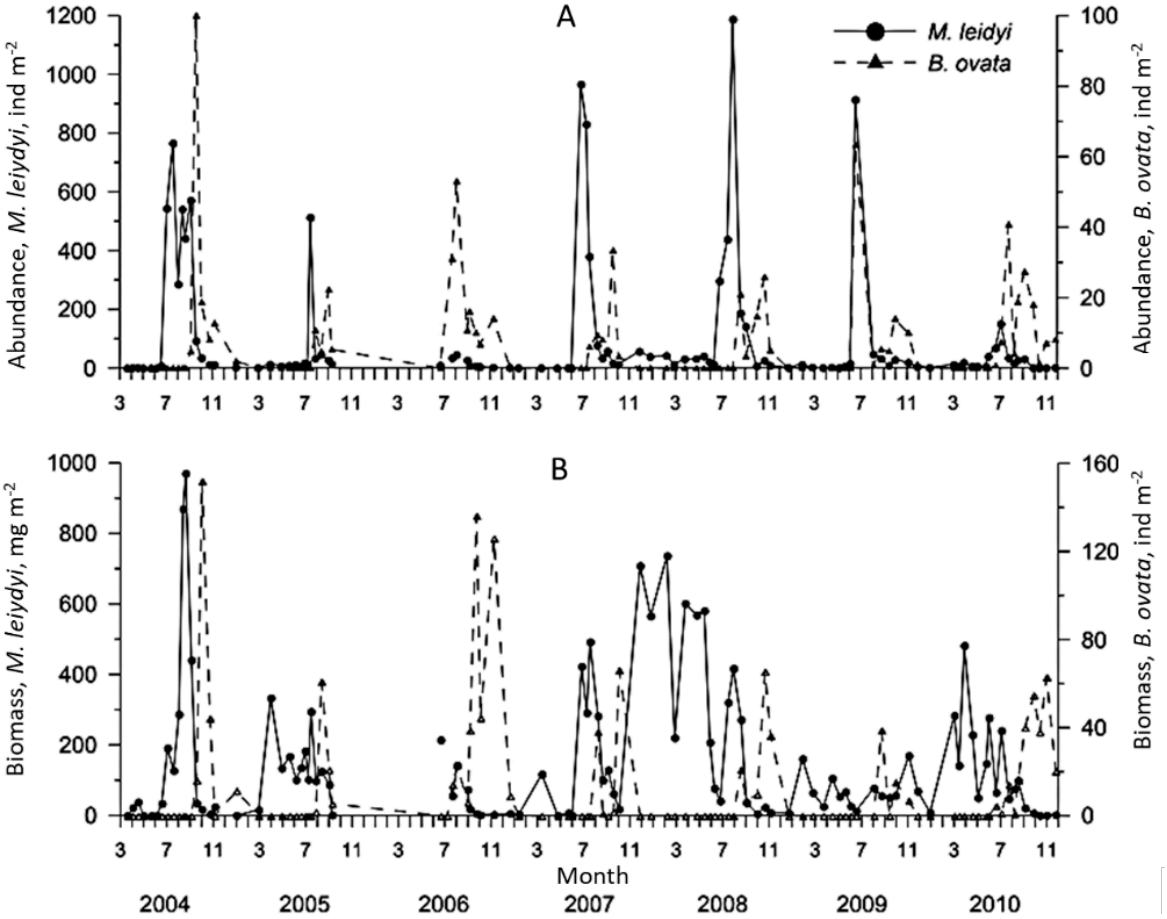

Fig. 4. Inter-annual dynamics of *Mnemiopsis leidyi* and *Beroe ovata* abundance (A) and biomass (B) [1]

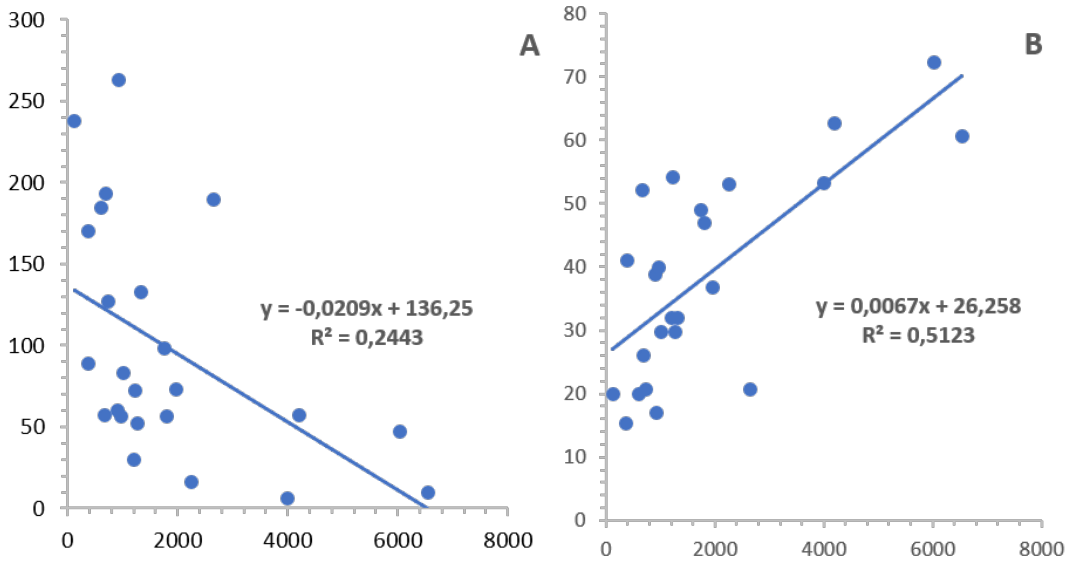

Fig. 5. Dependence of bioluminescence on ctenophores biomass: A – *Mnemiopsis leidyi*; B – *Beroe ovata* (for 0–10-m layer)

In the Black Sea, warm-water ctenophores appeared about 40 years ago [17 ; 18], as well as in the Sea of Azov [12] and the Caspian Sea [19]. Everywhere, *M. leidyi* invasion led to catastrophic changes in marine ecosystems [23]. For a decade, due to the absence of natural predators, *M. leidyi* development in the Black Sea was controlled only by temperature and food availability [7]. In 1997, its consumer, new carnivorous ctenophore *B. ovata*, was firstly discovered in the Black Sea; in 1999 and 2000, *Mnemiopsis* population density began to decline rapidly due to *Beroe* mass development [22]. Before the invasion of this predatory ctenophore, *Mnemiopsis* had abundance peaks in warm season. Now, in the summertime, the second minimum of its abundance is formed, due to *B. ovata* intensive development.

Till now, there are practically no studies on the effect of these invaders on the overall variability of Black Sea bioluminescence. Prior to their invasion, the total luminosity of coastal waters was determined by seasonal peaks of dinoflagellates development [2 ; 3 ; 4 ; 5]. Invader ctenophores do not only actively luminesce on their own, but also have a decisive influence on species composition and abundance of other bioluminescents.

According to the results of the detailed study of the long-term variability of bioluminescence in 2009–2012 in the research area [16], seawater luminescence in winter occurs due to the development of microalgae *Ceratium fusus* Ehrenb., *C. tripos* Ehrenb., *C. furca* Ehrenb., *Protoperidinium divergens* (Ehrenb.) Balech, *P. crassipes* (Kof.) Balech, *P. pallidum* (Ostenf.) Balech, *P. depressum* (Bailey), and *Balech oblongum* (Auriv.) Parke & J. D. Dodge. The second peak of the development of microalgae, Gonyaulax, *Scrippsiella trochoidea* (F. Stein), *Scrippsiella* Balech ex A. R. Loeblich III, 1965, and *Lingulodinium polyedrum* (F. Stein) J. D. Dodge, was observed during the springtime. This study has shown that the seasonal variability of total bioluminescence occurs in spring and autumn till now, as it was observed in the 1970s. Meanwhile, now bioluminescence peaks are sometimes twice as high as they were 50 years ago. It is likely that, in addition to microalgae contribution, in certain seasons of the year, the total area of luminous water increases due to ctenophores bioluminescence contribution. The authors of the present study very often register rapid increases of bioluminescence level in areas of ctenophores swarms in Sevastopol coastal waters. However, the incompleteness of these data does not allow one to estimate direct ctenophores contribution to the total water luminosity. On the other hand, ctenophores abundance is not comparable with that of phytoplankton determining the total bioluminescence of coastal waters.

Thus, the results of this study showed that differences in food modes of ctenophores have a significant impact on the seasonal dynamics of the bioluminescence of Black Sea coastal waters. The invasion of a new predatory species has led to the emergence of a balance, that depends on the nature of regional climatic and seasonal changes in the aquatic environment.

This work was carried out within the framework of government research assignments of IBSS "Superposition of physical, chemical, and biological processes in the formation of the quality of the marine environment and the functional state of aquatic organisms in the Sea of Azov – Black Sea basin" (No. AAAA-A18-118020790154-2) and "Functional, metabolic, and toxicological aspects of the existence of hydrobionts and their populations in biotopes with different physical and chemical regimes" (No. AAAA-A18-118021490093-4) and partly supported by the grant of the Russian Foundation for Basic Research (No. 18-45-920015). Method development was carried out within the framework of the project "Comprehensive studies of the current state of the ecosystem of the Atlantic sector in the Antarctic" (No. AAAA-A19-119100290162-0).

Acknowledgement. We are grateful to M. Biryukova and L. Eremeev for their invaluable contribution during this study. We would like to thank the anonymous reviewers for the constructive and useful comments that greatly contributed to improving the final version of the paper.

REFERENCES

1. Abolmasova G. I., Finenko G. A., Romanova Z. A., Datsyk N. A., Anninsky B. E. State of gelatinous macrozooplankton in inshore waters off Crimean coast of the Black Sea in 2009–2010. *Morskoj ekologicheskij zhurnal*, 2012, vol. 11, no. 3, pp. 17–24. (in Russ.)
2. Bityukov E. P., Rybasov V. P., Shayda V. G. Annual variations of the bioluminescence field intensity in the neuritic zone of the Black Sea. *Okeanologiya*, 1967, vol. 7, no. 6, pp. 1089–1099. (in Russ.)
3. Bityukov E. P. Biolyuminestsentsiya *Noctiluca miliaris* v raznykh temperaturnykh usloviyakh. *Biologiya morya*, 1971, iss. 24, pp. 70–77. (in Russ.)
4. Bityukov E. P., Evstigneev P. V., Tokarev Yu. N. Luminescent Dinoflagellata of the Black Sea as affected by anthropogenic factors. *Gidrobiologicheskii zhurnal*, 1993, vol. 29, no. 4, pp. 27–34. (in Russ.)
5. Bityukov E. P., Vasilenko V. I., Serikova I. M., Tokarev Yu. N. Results and prospects of the bioluminescent investigation at the Black Sea. *Ekologiya morya*, 1996, iss. 45, pp. 19–24. (in Russ.)
6. Datsyk N. A., Romanova Z. A., Finenko G. A., Abolmasova G. I., Anninskiy B. E. Zooplankton community structure in the inshore waters of the Crimean coasts (Sevastopol area) and trophic relations in the food chain zooplankton – *Mnemiopsis* in 2004–2008. *Morskoj ekologicheskij zhurnal*, 2012, vol. 11, no. 2, pp. 28–38. (in Russ.)
7. Finenko G. A., Abolmasova G. I., Romanova Z. A., Datsyk N. A., Anninskiy B. E. Sovremennoe sostoyanie populyatsii grebnevikov *Mnemiopsis leidyi* kak pishchevykh konkurentov promyslovykh ryb v pribrezhnykh raionakh krymskogo poberezh'ya Chernogo morya. In: *Promyslovye biologicheskie resursy Chernogo i Azovskogo morey* / V. N. Eremeev, A. V. Gaevskaya, G. E. Shul'man, Yu. A. Zagorodnyaya (Eds). Sevastopol : ECOSI-Gidrofizika, 2011, chap. 9, pp. 271–276. (in Russ.)
8. Ivanov V. A., Mikhailova E. N., Repetin L. N., Shapiro N. B. A model of the Sevastopol'skaya Bay. Reproduction of the vertical structure of temperature and salinity fields in 1997–1999. *Physical Oceanography*, 2003, vol. 13, iss. 4, pp. 201–222. https://doi.org/10.1023/A:1025850016768
9. *IPCC, 2007: Climate Change 2007: Synthesis Report. Contribution of Working Groups I, II, and III to the Fourth Assessment Report of the Intergovernmental Panel on Climate Change* / [Core Writing Team ; R. K. Pachauri, A. Reisinger (Eds)]. Geneva, Switzerland : IPCC, 2007, 104 p.
10. Lipchenko A. E., Il'in Yu. P., Repetin L. I., Lipchenko M. M. Reduction of evaporation from the Black Sea surface in the second half of the XX century as consequence of the global climate change. In: *Ekologicheskaya bezopasnost' pribrezhnoi i shel'fovoi zon i kompleksnoe ispol'zovanie resursov shel'fa* : sbornik nauchnykh trudov. Sevastopol : EKOSI-Gidrofizika, 2006, iss. 14, pp. 449–461. (in Russ.)
11. Luppova N. E. *Beroe ovata* Mayer, 1912 (Ctenophora, Atentaculata, Beroida) in the nearshore waters of the North-Eastern Black Sea. *Ekologiya morya*, 2002, iss. 59, pp. 23–25. (in Russ.)
12. Luppova N. E. Abundance dynamics and population structure of the invasive ctenophore *Mnemiopsis leidyi* A. Agassiz, 1865 (Mnemiopsida, Tentaculata) in the coastal zone of the northeastern Black Sea. *Povolzhskii ekologicheskii zhurnal*, 2014, no. 4, pp. 537–543. (in Russ.)
13. Melnikov V. V., Melnik A. V., Melnik L. A., Belogurova Yu. B., Zhuk V. F. Marine bioluminescence historical database. *Sistemy kontrolya okruzhayushchei sredy*, 2018, iss. 12 (32), pp. 44–51. (in Russ.)
14. Melnik A. V., Melnikov V. V., Serebrennikov A. N., Melnik L. A., Mashukova O. V. Biooceanographic characteristics of the bioluminescence fields in the Sevastopol coastal waters: Results of long-term monitoring. *Sistemy kontrolya okruzhayushchei sredy*, 2019, iss. 1 (35), pp. 79–88. (in Russ.). https://doi.org/10.33075/2220-5861-2019-1-79-87
15. Repetin L. N., Gordina A. D., Pavlova E. V., Romanov A. S., Ovsyanyi E. I. Affect of oceanographic factors upon the ecological state of the Sevastopol Bay (the Black Sea). *Morskoi gidrofizicheskii zhurnal*, 2003, no. 2, pp. 66–80. (in Russ.)
16. Serikova I. M., Bryantseva Yu. V., Tokarev Yu. N., Stanichnyi S. V., Suslin V. V., Vasilenko V. I.

Response of phytoplankton of the Sevastopol coastal zone to climate peculiarities of the years 2009–2012. *Gidrobiologicheskii zhurnal*, 2015, vol. 51, no. 5. pp. 40–51. (in Russ.)

17. Shushkina E. A., Musayeva E. I., Anokhina L. L., Lukasheva T. A. The role of the gelatinous macroplankton jellyfish *Aurelia* and invading ctenophores *Mnemiopsis* and *Beroe* in the plankton communities of the Black Sea. *Okeanologiya*, 2000, vol. 40, no. 6, pp. 859–866. (in Russ.)
18. Shushkina E. A., Musaeva E. I. Structure of epipelagic zooplankton community and its changes related to the invasion of *Mnemiopsis leidyi* in the Black Sea. *Okeanologiya*, 1990, vol. 30, no. 2, pp. 306–310. (in Russ.)
19. Sokolskiy A. F., Kamakin A. M. Raspredelenie grebnevika *Mnemiopsis* sp. v Kaspiiskom more v 2001 g. In: *Fisheries Researches in the Caspian : scientific-research works results for 2000*. Astrakhan : KaspNIIRKh Publ., 2001, pp. 105–110. (in Russ.)
20. Sullivan J., Gifford L. Diet of the larval ctenophore *Mnemiopsis leidyi* A. Agassiz (Ctenophora, Lobata). *Journal of Plankton Research*, 2004, vol. 26, iss. 4, pp. 417–431. https://doi.org/10.1093/plankt/fbh033
21. Tokarev Yu. N., Vasilenko V. I., Zhuk V. F. Novyi gidrobiofizicheskii kompleks dlya ekspressnoi otsenki sostoyaniya pribrezhnykh ekosistem. In: *Sovremennye metody i sredstva okeanologicheskikh issledovanii* : materialy XI Mezhdunar. nauch.-tekhn. konf., Moscow, 25–27 Nov., 2009. Moscow : Izd-vo RAN, 2009, pt. 3, pp. 23–27. (in Russ.)
22. Vinogradov M. E., Shushkina E. A., Anokhina L. L., Vostokov S. V., Kucheruk N. V., Lukasheva T. A. Massovoe razvitie grebnevika *Beroe ovata* u severo-vostochnogo poberezh'ya Chernogo morya. *Okeanologiya*, 2000, vol. 41, no. 1, pp. 52–55. (in Russ.)
23. Vinogradov M. E., Shushkina E. A., Vostokov S. V., Vereshchaka A. L., Lukasheva T. A. Population dynamics of the ctenophores *Mnemiopsis leidyi* and *Beroe ovata* near the Caucasus shore of the Black Sea. *Okeanologiya*, 2002, vol. 42, no. 5, pp. 693–701. (in Russ.)

ВЛИЯНИЕ ГРЕБНЕВИКОВ-ВСЕЛЕНЦЕВ НА ИЗМЕНЧИВОСТЬ БИОЛЮМИНЕСЦЕНЦИИ У БЕРЕГОВ ЗАПАДНОГО КРЫМА

А. В. Мельник, В. В. Мельников, Л. А. Мельник, О. В. Машукова

Федеральный исследовательский центр «Институт биологии южных морей имени А. О. Ковалевского РАН», Севастополь, Российская Федерация

E-mail: *melnikalexsand@gmail.com*

Во второй половине XX века произошли значительные изменения в экосистеме Чёрного моря. Так, число штормовых ветров и апвеллингов уменьшилось, осадки стали обильнее, солёность прибрежных вод снизилась, температура водных масс повысилась. Кроме того, произошло вселение гребневиков. В итоге в конце 1980-х гг. пелагическая экосистема Чёрного моря резко перестроилась. Данная работа основана на исследованиях, выполненных при помощи дистанционного зондирования в 1965–1966 и 2007–2012 гг. в районе г. Севастополя (Западный Крым). Анализ спутниковых данных за последние 20 лет показал наличие положительной динамики температуры поверхностных вод в акватории Севастополя. В середине 1960-х гг. годовая динамика биолюминесценции характеризовалась сезонными пиками свечения динофитовых микроводорослей. В последние годы этот ритм изменился из-за вселения гребневиков. Увеличение численности *Mnemiopsis leidyi* приводит к уменьшению биолюминесценции светящихся микроводорослей, которых этот гребневик потребляет. Вселение и размножение *Beroe ovata* обусловило резкое уменьшение биомассы *M. leidyi* и, как следствие, рост биолюминесценции.

Ключевые слова: Чёрное море, биолюминесценция, гребневик, солёность, мониторинг

1871
ИнБЮМ – IBSS

Морской биологический журнал
Marine Biological Journal
2020, vol. 5, no. 2, pp. 76–87
https://doi.org/10.21072/mbj.2020.05.2.07

UDC 574.64:582.261.1

ESTIMATION OF CELL DISTRIBUTION HETEROGENEITY AT TOXICOLOGICAL EXPERIMENTS WITH CLONAL CULTURES OF BENTHIC DIATOMS

© 2020 **A. N. Petrov and E. L. Nevrova**

A. O. Kovalevsky Institute of Biology of the Southern Seas of RAS, Sevastopol, Russian Federation
E-mail: *alexpet-14@mail.ru*

Received by the Editor 17.09.2019; after revision 23.04.2020;
accepted for publication 26.06.2020; published online 30.06.2020.

An increase in anthropogenic pressure on coastal water areas requires regular monitoring of marine ecosystems. The appropriate bioindicators for indirect assessment of the quality of the near-shore environment are benthic diatom algae, which are a key element of coastal communities and are highly sensitive to environmental impact. Changes in the development of diatoms under the influence of various toxicants may be used as relevant tool for monitoring of marine environment quality. However, scientific and methodological approaches to application of benthic diatom algae as test objects remain unstudied. One of the important methodological problems is the assessment of the significance of the samples in experimental vessels when counting cells abundance at different stages of toxicological test. The study is focused on assessment of the statistical significance of the equality of the initial mean number of cells of clonal culture inoculum placed into each of the replicates, as well as the statistical uniformity of cell distribution over the entire bottom area of Petri dishes. We used clonal cultures of three benthic diatom species belonging to different classes of Bacillariophyta: *Thalassiosira excentrica* Cleve, 1903 (Coscinodiscophycea), *Ardissonea crystallina* (C. Agardh) Grunow, 1880 (Fragilariophyceae), and *Pleurosigma aestuarii* (Bréb. in Kütz.) W. Smith, 1853 (Bacillariophyceae). They significantly differ in valve morphology and life history (floating in water mass, attached to substrate, and motile). The results of statistical comparison of cell number variability in the experiment for all studied species confirmed the absence of significant differences between the mean values of the tested parameter at a standard significance level (0.05). It was shown that despite specific differences in cell growth rate during the experiment, the variability in cell number in the microscope viewing fields varies irregularly. The highest value of the variability coefficient was observed on the 5th day for the small-sized species *T. excentrica* (*Cv* = 42…55 %), and the lowest variability – for the large-cell species *A. crystallina* (*Cv* = 27…31 %). The absence of significant differences in cell number between three replicates (for each species) was established both during the initial placing of inoculum into the dishes and on the following days of the experiment. The conclusion is applicable for each of diatom species studied, which allows to consider all replicates as subsamples of the replicate sample and to average the results obtained at different stages of the toxicological experiment. The uniformity of cell distribution throughout experimental dishes bottom, which does not depend on species and absolute cell number, was statistically proven. The results obtained allow to statistically reliably estimate the changes in cell number at different stages of toxicological experiment according to replicate sampling, based on cell counting in a limited number of viewing fields.

Keywords: toxicological experiment, methodology, statistical estimation, Bacillariophyta, *Thalassiosira excentrica*, *Ardissonea crystallina*, *Pleurosigma aestuarii*, Black Sea

Due to the significant anthropogenic pressure on the Black Sea, which is especially evident in coastal waters off the coast of Crimea, it is necessary to monitor changes in the state of planktonic and benthic communities. As one of the most appropriate objects for bioassay and bioindication, planktonic microalgae are widely used, and there are numerous methodological developments for their applying [3 ; 8 ; 12 ; 19].

Extensive literature on the effect of different toxicants on microalgae is mainly devoted to Chlorophyta [10] and Cryptophyta [17 ; 25], while the contribution of these phyla (they include 23 and 2 species, respectively) to Black Sea benthic microalgae cenoses is quite insignificant, in contrast to the contribution of the phylum Bacillariophyta (1094 species and intraspecific taxa) [13], representatives of which bring up 99 % of the abundance and biomass in the World Ocean microphytobenthos [29]. The fact mentioned above indicates an insufficient level of knowledge for obtaining a comprehensive data of the effect of toxicants on microphytobenthos communities.

Many mass benthic diatom species (Bacillariophyta), being important structural components of marine ecosystems, are characterized by development only within the certain microbiotopes and high sensitivity to the influence of adverse environmental factors [14]. This allows to apply benthic diatoms as appropriate test objects, and the changes in their physiological parameters (specific growth rate, mortality, and chloroplast state) under the impact of different pollutants can be a convenient tool for indirect assessment of environmental quality [3 ; 10 ; 12 ; 18 ; 24 ; 25 ; 27].

Within the tasks of hydrobiological monitoring of coastal water areas, the use of benthic diatoms as test objects is a poorly developed scientific and methodological problem [9 ; 23]. Its solution allows to obtain new experimental data on the tolerance ranges of various marine diatom species when exposed to model toxicants (copper sulfate, synthetic surfactants, pesticides, etc.) during subacute and chronic experiments [1 ; 10 ; 11 ; 24 ; 25]. In addition, it becomes possible to solve a number of issues of a methodological nature, which affects the reliability of conclusions based on the results of toxicological tests [19].

One of the main methodological problems is to check the significance of sample assessment when counting cell number in experimental vessels (in our case, Petri dishes) at different stages of a multi-day toxicological experiment. The accuracy of results may be affected by the uneven number of cells initially contained in the inoculum aliquot (1 ml) input in Petri dishes at the beginning of each experiment, as well as by possible uneven cell distribution on dishes bottom in the following days of exposure.

Due to small size and high abundance of diatom algae, direct total cell counting in each dish at different stages of experiment is hardly possible. Therefore, cell number is counted under a microscope in a certain number of discrete viewing fields of known area, and then the numerical data obtained are recounted for the entire bottom area of experimental vessel. In case of such indirect counting of the total cell number in dishes, the final results can vary greatly, which can lead to distortion of conclusion about the degree of toxicant impact on cell number changes. These difficulties determined the need for special methodological study, the results of which can be used to optimize the carrying out of toxicological experiments on benthic diatoms and to provide reliable conclusion when interpreting the quantitative data obtained.

The purpose of the work carried out using clonal cultures of three benthic diatom species is to verify the validity of the following methodological hypotheses based on an assessment of the statistical significance of the results obtained:

1) the mean number of clonal culture inoculum cells, input into each Petri dish at the beginning of the experiment, should be approximately equal, *i. e.* the initial cell numbers in each of three replicates, that are put in each line, should not statistically differ from each other;

2) cell distribution in each dish, controlled during repeated counting in viewing fields over the entire bottom area, is relatively uniform, *i. e.* there is no statistically significant spatial heterogeneity in cell numbers *in vitro*.

The possible aggregation of cell distribution when counting a certain number of viewing fields (their sum area is not more than 4–5 % of Petri dish total bottom area), when recounting on experimental vessel entire bottom area, can lead to a significant overestimation (or underestimation) of the total cell number. Thus, such results may distort the conclusion concerning the degree of impact of different toxicant concentrations as well as the time of exposure on the total changes in cell numbers.

MATERIAL AND METHODS

Research objects. To assess microalgae distribution in experimental vessels, three benthic diatom species were used: *Thalassiosira excentrica* Cleve, 1903 (Coscinodiscophycea), *Ardissonea crystallina* (C. Agardh) Grunow, 1880 (Fragilariophyceae), and *Pleurosigma aestuarii* (Bréb. in Kütz.) W. Smith, 1853 (Bacillariophyceae). The choice of species was based on the following reasons: 1) significant differences in valve morphology (diskoid, linear, and sigmoid); 2) different life history (planktonic – floating in water mass, benthic – attached to substrate, and motile – moving on substrate); 3) ability to form colonies; 4) species-specific rate of reproduction, and therefore, the presumably different nature of cell distribution on dishes bottom, as well as growth rate of cell numbers during a long-term experiment; 5) affiliation with three different taxonomic classes of Bacillariophyta (according to taxonomic system [28]). A comparative statistical assessment of cell distribution features, having cardinal differences in life history, allows us to verify the reliability of results when conducting further toxicological experiments using representatives of different classes of Bacillariophyta.

According to the results of molecular genetic studies and experiments on sexual reproduction, the systematic position of *A. crystallina*, previously transferred from the class Fragilariophyceae to Coscinodiscophycea, is questioned. It is assumed that *Ardissonea* (and other representatives of Toxariales) can represent a unique evolutionary group isolated from the pennate diatoms [22]. Taking into account the fact that this species is more similar to Fragilariophyceae in terms of its valve outline and ability to form bundle-shaped colonies attached to substrate, we consider *A. crystallina* as belonging to this class for the purposes of our experiment.

Selected diatom algae species were isolated into clone lines by micropipetting and 7-fold single cell washing under MBS-10 binocular at magnification ×40 [2 ; 5 ; 18].

Thalassiosira excentrica strain was isolated from microphytobenthos of soft substrate, sampled in Laspi Bay in September 2017 at a 9-meter depth. The species is marine, bento-planktonic, and able to float in water column or dip to bottom. It is characterized by high abundance in Black Sea sublittoral zone. Cells form chain-shaped colonies of 4–6 individuals connected by a thin transparent filament [13 ; 15]. The valves are flat-cylindrical; disk diameter is of 25 μm*; height is of 3 μm (Fig. 1A, D).

Ardissonea crystallina strain was isolated from phytoperiphyton of artificial substrate, sampled in Kazach'ya Bay in April 2018 at a 5-meter depth. The species is marine, benthic, often found in coastal areas. Cells attach to substrate, forming bundle-shaped colonies of 4–30 individuals [4 ; 13]. Valves are narrowly linear; length is of 410 μm; width is of 18 μm (Fig. 1B, E).

*Hereinafter, cell sizes are indicated as they were at the beginning of the experiment.

Pleurosigma aestuarii strain was isolated from microphytobenthos of rocky substrate, sampled from Cape Aya in July 2018 at a 3-meter depth. The species is marine, benthic, often found in the Black Sea sublittoral zone. Cells are single, motile; they quickly move along substrate surface [13 ; 16]. Valves are narrow-lanceolate, sigmoid curved at the ends; length is of 135 μm; width is of 22 μm (Fig. 1C, F).

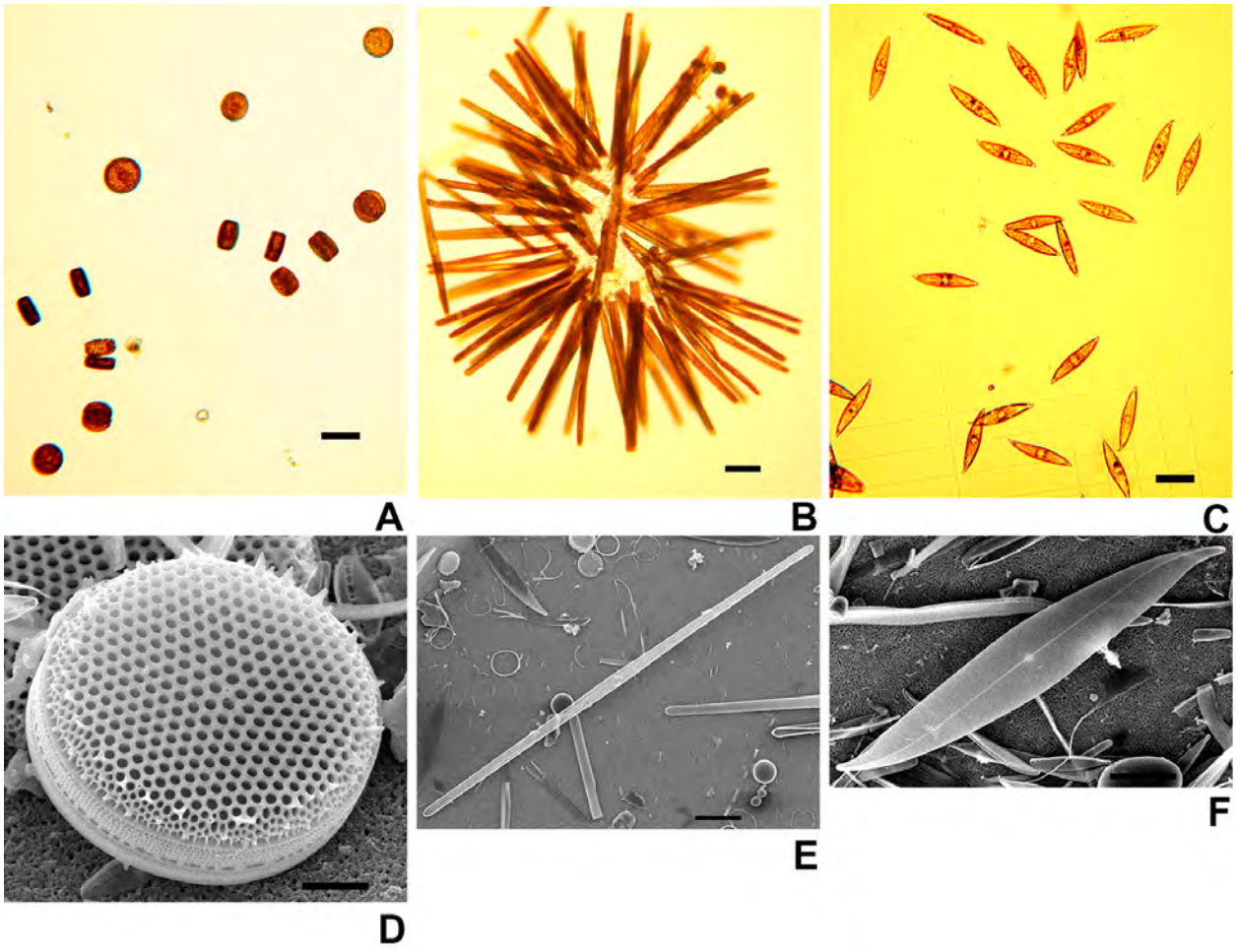

Fig. 1. Benthic diatoms used in experiment: A, D – *Thalassiosira excentrica*; B, E – *Ardissonea crystallina*; C, F – *Pleurosigma aestuarii*. Light microscope – A, B, C (scale bar = 10 μm); scanning electronic microscope – D (scale bar = 5 μm), E (scale bar = 50 μm), F (scale bar = 20 μm)

Cultural media maintenance. Clonal cultures were maintained in natural seawater media by Goldberg [7 ; 21] modified for the cultivation of marine benthic diatoms, at a constant temperature of (22 ± 2) °C in ambient light on the north window of IBSS laboratory. To prepare the medium, seawater was taken in a 12-mile off-coast zone and filtered through a 0.45-μm filter, then pasteurized three times at a temperature of +75 °C and enriched with nutrients according to the protocol (Table 1).

Experiment design. Possible discrepancies between three replicates in mean cell number in each Petri dish after 1 day and 5 days of exposure were assessed in an experiment with clonal cultures of three diatom species. For each species, the experiment was carried out using modified natural seawater media by Goldberg, without adding a toxicant. Totally, 30 ml of natural medium and 1 ml of clonal culture inoculum were added to each dish (inner diameter of 85 mm; bottom area about 5700 mm^2); then the contents were thoroughly mixed, and the dish was sealed with Parafilm film to prevent medium evaporation.

Table 1. Recipes for modified natural seawater media by Goldberg

No. of solution	Substance	Amount of substance per 100 ml of dH_2O	Quantity of solution used per 1 L of seawater, ml
1	KNO_3	10.1 g	2.0
2	$NaH_2PO_4 \times 2H_2O$	1.421 g	0.5
3	$MnCl_2 \times 4H_2O$ $CoCl_2 \times 6H_2O$	0.01979 g 0.02379 g	1.0
4	$Na_2EDTA \times 2H_2O$ $FeCl_3 \times 6H_2O$	0.244 g 0.144 g	1.0
5	$FeNH_4$-citrate	0.072 g	0.5
6	$Na_2SiO_3 \times 5H_2O$	1.5 g	2.0
7	Thiamine (vitamin B_1)	0.05 mg	0.5
8	Cyanocobalamin (vitamin B_{12})	0.5 mg	5.0

To control distribution uniformity of random viewing fields over the entire area, dish bottom was divided by lines into 8 equal parts (Fig. 2). Within the boundaries of each sector, photographies of 8–9 viewing fields were carried out. Viewing fields were selected randomly over the whole bottom area; so, 64–72 fields were taken into account in each dish. Microphotography was carried out under Carl Zeiss Axiostar Plus light microscope with an Achroplan ×10 lens using Canon PowerShot A640 digital camera (IBSS RAS, Sevastopol) and under JEOL JSM-6390LA scanning electron microscope (Komarov Botanical Institute RAS core facility, Saint Petersburg). Taxonomic identification was carried out according to species guides [6 ; 15 ; 16 ; 26].

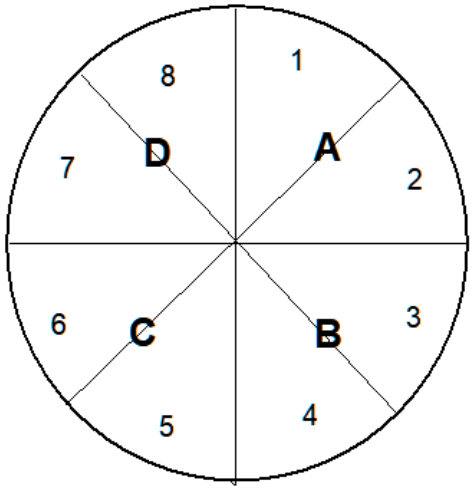

Fig. 2. Estimation of distribution heterogeneity of random viewing fields over the entire Petri dish bottom area in the experiment

Cell counting was performed using photographs of each sector. The area of one viewing field was about 4.0 mm^2, *i. e.* during the viewing, 4.5–4.9 % of bottom area of each dish was counted. Further, when assessing distribution uniformity of diatom cells over dish bottom at different stages of the experiment, the mean values of cell number in viewing fields in 4 sectors of dish bottom (A, B, C, and D) were compared, and the previously obtained calculation data for viewing fields from 8 adjacent parts were combined in pairs: 1 + 2, 3 + 4, 5 + 6, and 7 + 8. These methodical features were related to the fact that the absolute

variation in cell number, when comparing individual viewing fields even within one of 8 sectors, could be significant, especially on the 5th day of exposure. For example, for *A. crystallina* the range of variation was 16÷41 cells, for *T. excentrica* – 11÷48, for *P. aestuarii* – 36÷91. The coefficient of variation, when counting cell numbers in individual sectors separated by lines, could also reach 70–78 %. When making comparative estimation for 4 sectors (A–D) with combined data from adjacent parts of dishes bottom, the variability indexes of cell number (variance and standard error) were significantly lower due to taking into account the doubled number of measurements for each replicate. To assess discrepancy degree between the replicates (dishes), the statistical significance of pairwise differences in mean cell number was counted both between 4 sectors of the same dish (*i. e.* the degree of cell aggregation within the bottom of one dish was assessed) and between sectors belonging to different dishes.

Since these diatom species are characterized by different growth rates of cell number during the experiment, for the correct assessment of statistical differences by the mean number, the relative cell growth rate (V) for all studied species was calculated using the formula [19 ; 20]:

$$V = (N_{(t+\Delta t)} - N_t) / (\Delta t \cdot N_t) ,$$

where N_t is the mean cell number in a culture in a Petri dish at time t (the 1st day of the experiment);

$N_{(t+\Delta t)}$ is the mean cell number in a culture at time t+Δt (the 5th day of the experiment);

Δt is the period of exposure (four days).

Statistical data processing. Statistical processing of the experimental results was carried out using standard routines of parametric and rank analysis included in the statistical analysis platform "SigmaPlot 12.5" [30].

Normality of cell distribution mode in the sample (cell number in 64–72 viewing fields in each Petri dish) was estimated according to Shapiro – Wilk or Kolmogorov – Smirnov criterion with preliminary data testing and exclusion from calculations of sharply differed values in each sample estimated by quintile method. Such aggregations with an abnormally high cell abundance are not the result of a natural increase in their number during the experiment, but occur sometimes either as a result of the initial placing into the Petri dish of inoculum, which already contains cell aggregation linked by polysaccharides, or as a result of fluctuations of dish contents while photographing.

Comparison of variances for 3 and more independent subsamples was carried out using the Fisher criterion (ANOVA), as well as the Kruskal – Wallis test by ranks (in case of the non-normal distribution mode) for significance level $P = 0.05$. The following comparison of the statistical significance of differences in mean feature values (mean cell number in random viewing fields in 4 sectors of dishes taking into account various exposure stages) was performed using Student's *t*-test (in case of normality of the distribution mode in samples and the equality of variances). To compare independent samples, in which the distribution mode differed from the normal one, non-parametric Holm – Šidák test (for samples equal in amount) and Dunn's test (when different-sized samples were compared) were applied [30].

RESULTS AND DISCUSSION

The results of the analysis showed that the variability of data, when counting cell number in viewing fields, can significantly differ both when comparing different species and in one species but at different exposure stages (Table 2).

Table 2. Variation characteristics for three benthic diatom species reflecting the changes in mean cell number in Petri dishes (3 replicates) on the 1st and 5th days of the experiment

Species	Replicate	The 1st day			The 5th day		
		n	*N* ± *SE*	*Cv*, %	n	*N* ± *SE*	*Cv*, %
Ardissonea crystallina	I	65	6.16 ± 0.41	51.3	63	22.70 ± 0.82	31.4
	II	63	6.82 ± 0.41	44.8	62	24.71 ± 0.90	32.2
	III	62	6.79 ± 0.42	46.2	68	24.65 ± 0.76	26.7
Thallassiosira excentrica	I	63	9.19 ± 0.39	34.1	63	20.68 ± 1.42	54.6
	II	64	9.67 ± 0.44	37.3	63	20.91 ± 1.21	46.1
	III	62	11.45 ± 0.41	28.3	62	24.00 ± 1.26	41.6
Pleurosigma aestuarii	I	65	17.37 ± 0.38	29.6	72	63.44 ± 1.37	22.3
	II	67	18.55 ± 0.54	24.0	72	60.78 ± 1.71	23.9
	III	72	19.79 ± 0.52	22.8	72	61.83 ± 1.80	24.7

Note: n – total number of examined viewing fields in each Petri dish minus the sharply distinguished values (statistical outliers); *N* ± *SE* – mean cells number ± sampling standard error; *Cv* – coefficient of variation.

Possible statistical differences in distribution pattern of diatom cells on dish bottom at different stages of the experiment could be caused by the fact that on the 1st day cell distribution was mainly determined by thorough mechanical mixing of the inoculum before and after placing it into a dish, which theoretically caused a more uniform cell distribution in viewing fields. On the 5th day of exposure, distribution pattern of diatom cells on dish bottom could be mainly determined by individual motility of cells and by tendency to attach to substrate and to form aggregations or to soar passively in the cultural medium. The factors mentioned above could influence the non-uniformity of values when counting cell numbers in random viewing fields.

The highest coefficient of variation was observed in *A. crystallina* samples on the 1st day of the experiment (45–51 %), as well as in *T. excentrica* samples on the 5th day (42–54 %), although the mean cell number in viewing fields of these species differed by 3.5 times. The high variability of the data could be caused by distribution heterogeneity of these species, when along with single cells in viewing fields there are aggregations, in which cells are bound by polysaccharide secretions (*T. excentrica*) or form bundle-shaped colonies (*A. crystallina*) attached to dish bottom at single point. Thereby, *P. aestuarii* samples in viewing field are characterized by minimal variability (23–29 %) in terms of abundance, regardless of exposure stage, which was explained by cell motility of this species that freely move throughout dish bottom during the experiment and do not concentrate in one point.

The results of analysis for studied diatom species showed that the variances between the samples did not differ statistically, when comparing three replicates: the probability (*P*) of the accepting the null-hypothesis is much higher than the critical one (0.05) and ranges 0.27–0.49 on the 1st day and 0.16–0.47 on the 5th day. The results of a pairwise comparison of the mean values of cell number in each Petri dish (comparison between replicates) at different stages of the experiment are shown in Table 3.

For *A. crystallina*, all pairwise differences in the mean cell number between replicates on both the 1st and 5th days of exposure were insignificant ($P_{exp} >> 0.05$).

For *T. excentrica*, on the 1st day, significant differences in the mean cell number in viewing fields were identified between pairs of replicates I – III and II – III ($P_{exp} \leq 0.003$). The differences were unreliable when comparing the pair I – II ($P_{exp} = 0.416$). On the 5th day, there were no significant differences in the mean cell number values between all pairs of replicates.

Table 3. Results of testing the differences between the mean cell numbers in Petri dishes under pairwise comparison of three replicates for diatom species at different stages of experiment

Species	Pair of replicates	Mean value (the 1st day)		*P*	Mean value (the 5th day)		*P*
Ardissonea crystallina	I – II	6.16	6.82	0.252	22.70	24.71	0.090
	I – III	6.16	6.79	0.283	22.70	24.65	0.092
	II – III	6.82	6.79	0.951	24.71	24.65	0.747
Thallassiosira excentrica	I – II	9.19	9.67	0.416	20.68	20.91	0.906
	I – III	9.19	11.45	**0.000**	20.68	24.00	0.084
	II – III	9.67	11.45	**0.003**	20.91	24.00	0.080
Pleurosigma aestuarii	I – II	17.37	18.55	0.163	63.44	60.78	0.077
	I – III	17.37	19.79	**0.001**	63.44	61.83	0.200
	II – III	18.55	19.79	0.135	60.78	61.83	0.671

Note: *P* – probability of acceptance of the null-hypothesis that there are no differences between the mean values of cell number in samples compared ($P_\alpha = 0.05$). Statistically significantly different results are indicated in bold.

For *P. aestuarii*, on the 1st day, there were no reliable mean differences under the pairwise comparison between replicates I – II and II – III. Only when comparing the pair I – III, the differences in mean cell number values were reliable ($P_{exp} \leq 0.001$). On the 5th day, there were no significant differences in mean cell number values when comparing all replicates ($P_{exp} > 0.05$).

The rate of relative increase in cell number was in average higher in *P. aestuarii* (0.59) and *T. excentrica* (0.40), than in *A. crystallina* (0.37), which could affect the variability indexes, although the resulting differences in cell number between replicates of the experiment turned out to be not significant for both species (see Table 3).

Thus, it can be assumed that the variability range of the mean cell number for each species in different replicates in most cases does not exceed the statistical error. This fact gives reason to consider all replicates (random subsamples of cells) as corresponding to one initially taken sample (inoculum of each species cells) with a similar degree of variability.

The results of assessment of cell number distribution uniformity in 4 sectors of Petri dishes bottom showed the following.

The 1st day. For all diatom species studied, there were no statistically significant differences ($P >> 0.05$) between the mean values of parameter (cell number in 16–18 viewing fields) at pairwise comparison of 12 sectors, *i. e.* three replicates (4 sectors in each dish – A, B, C, and D). Consequently, at the initial stage of experiment, cell distribution over dishes bottom was statistically uniform, and there were no noticeable differences between dishes in the results of counting the total cell number by the mean values from selected viewing fields.

The 5th day. Considering that the distribution of cell number in samples in many sectors differs from the normal one (Kolmogorov – Smirnov test: 0.125–0.210) and has significantly different variances, the testing of significance of possible differences between dish sectors was carried out using rank criteria (Kruskal – Wallis test).

Ardissonea crystallina. The results of 66 pairwise rank comparisons of the mean cell number values in each sector of Petri dish bottom showed the absence of statistically significant differences ($P_{exp} = 0.067$) both between sectors of the bottom of one dish and between dishes (replicates).

Thallassiosira excentrica. The results of 66 pairwise rank comparisons of the mean cell number values in each sector indicate the absence of statistically significant differences ($P_{exp} = 0.071$) both between sectors of the bottom of one dish and between dishes.

Pleurosigma aestuarii. In all 66 pairwise rank comparisons of 12 sectors from three replicates, only in pairs of sectors where the data from 1D sector were considered (1D *vs* 2A; 1D *vs* 2B; 1D *vs* 3B), the differences in the mean cell number values were significant (P_{exp} was of 0.001, 0.003, and 0.008, respectively). For the other pairwise rank comparisons of the mean values, performed by the Dunn's test, differences between sectors were not significant ($P_{exp} > 0.05$). In case of exclusion of sector 1D (the only one with abnormally high cell number in the viewing fields) from the analysis, no statistically significant differences were identified both between sectors of the bottom of one dish and between dishes ($P_{exp} = 0.272$).

The data obtained confirm statistical uniformity of cell distribution pattern of benthic diatoms through bottom of experimental vessels even in case when not more than 5 % of dish bottom area is considered by direct visual counting. The results remain valid regardless of microalgae species used, their morphological structure, and life history, as well as differences in the values of their absolute number in dishes at different stages of experiment.

Conclusion. The results of statistical comparison of degree of variation in cell number in experimental dishes of three marine benthic diatom species belonging to three different classes of Bacillariophyta (*Thalassiosira excentrica*, *Ardissonea crystallina*, and *Pleurosigma aestuarii*) confirmed that overwhelmingly there were no statistically significant differences between the mean values of the studied parameter at standard significance level (0.05). It was shown that despite species-specific differences in cell number growth rate during the experiment, the variability of parameter varied irregularly. After a 5-day exposure, the highest variability coefficient in cell number in viewing fields (Cv = 42…55 %) was observed for the bentoplanktonic small-sized species *T. excentrica*, mainly soaring in water mass, and the lowest (Cv = 27…31 %) was noted for large-cell species *A. crystallina*, that attaches to dish bottom.

It was found that the counted mean diatom cell number did not differ significantly between three replicates both on the 1st day, after the initial placing of inoculum into the dishes, and at the final stage of experiment. The conclusion is valid for all studied diatom species used as test objects, and this allows us to consider all replicates as subsamples of one sample and to average the results obtained on them at different stages of toxicological experiments.

Cell distribution uniformity within experimental dishes bottom was statistically proven (even when counting not more than 5 % of bottom area). The uniformity of distribution pattern is not species-specific and does not depend on the absolute number of diatom cells in the dishes. The results obtained make it possible to statistically reliably assess the changes in cell number of studied species at different stages of toxicological experiment according to replicate samples, obtained on the base of cell counting in a limited number of viewing fields.

This work was carried out within the framework of government research assignment of IBSS "Patterns of formation and anthropogenic transformation of biodiversity and biological resources of the Sea of Azov – the Black Sea basin and other parts of the World Ocean" (No. AAAA-A18-118020890074-2).

REFERENCES

1. Aizdaicher N. A., Reunova Yu. A. The effect of detergents on growth of the diatom *Thalassiosira pseudonana* in culture. *Biologiya morya*, 2002, vol. 28, no. 5, pp. 362–365. (in Russ.)
2. Gaisina L. A., Fazlutdinova A. I., Kabirov R. R. *Sovremennye metody vydeleniya i kultivirovaniya vodoroslei* : uchebnoe posobie. Ufa : Izd-vo BGPU, 2008, 152 p. (in Russ.)
3. Gelashvili D. B., Bezel' V. S., Romanova E. B., Bezrukov M. E., Silkin A. A., Nizhegorodtsev A. A. *Printsipy i metody ekologicheskoi toksikologii.* Nizhnii Novgorod : Nizhegorodslii gosuniversitet, 2015, 742 p. (in Russ.)
4. Guslyakov N. E., Zakordonets O. A., Gerasimyuk V. P. *Atlas diatomovykh vodoroslei bentosa severo-zapadnoi chasti Chernogo morya i prilegayushchikh vodoemov.* Kiev : Naukova dumka, 1992, 115 p. (in Russ.)
5. Davidovich N. A., Davidovich O. I., Podunay Yu. A. Diatom culture collection of the Karadag scientific station (Crimea). *Morskoj biologicheskij zhurnal*, 2017, vol. 2, no. 1, pp. 18–28. (in Russ.). https://doi.org/10.21072/mbj.2017.02.1.03
6. *Diatomovyi analiz.* Kn. 3. *Opredelitel' iskopaemykh i sovremennykh diatomovykh vodoroslei. Poryadok Pennales* / A. I. Proshkina-Lavrenko (Ed.). Moscow ; Leningrad : Gosgeolitizdat, 1950, 398 p. (in Russ.)
7. Kabanova Yu. G. *Organicheskii fosfor kak istochnik pitaniya fitoplanktona* : avtoref. dis. … kand. biol. nauk : 03.00.18. Moscow, 1958, 13 p. (in Russ.)
8. Krainyukova A. N. Biotestirovanie i okhrana vod ot zagryazneniya. In: *Metody biotestirovaniya vod*. Chernogolovka : GK OP SSSR, 1988, pp. 4–21. (in Russ.)
9. Markina Zh. V. *Primenenie mikrovodoroslei dlya otsenki kachestva morskoi vody i deistviya detergentov* : avtoref. dis. … kand. biol. nauk : 03.00.18 ; 03.00.16. Vladivostok, 2008, 21 p. (in Russ.)
10. Markina Zh. V. Influence of detergents and surface-active substances on unicellular algae growth, physiological and biochemical parameters (review). *Izvestiya TINRO*, 2009, vol. 156, pp. 125–134. (in Russ.)
11. Markina Zh. V., Aizdaicher N. A. The influence of detergents on the abundance dynamics and physiological state of the benthic microalgae *Attheya ussurensis* (Bacillariophyta) in laboratory culture. *Biologiya morya*, 2007, vol. 33, no. 6, pp. 432–439. (in Russ.)
12. Markina Zh. V., Aizdaicher N. A. *Phaeodactylum tricornutum* Bohlin bioassay of water quality of Amur Bay (the Sea of Japan). *Sibirskii ekologicheskii zhurnal*, 2011, vol. 18, no. 1, pp. 99–105. (in Russ.)
13. Nevrova E. L. *Bentosnye diatomovye vodorosli (Bacillariophyta) Chernogo morya: raznoobrazie i struktura taksotsenov razlichnykh biotopov.* [dissertation]. Moscow, 2015, 445 p. (in Russ.). https://dlib.rsl.ru/01005555099
14. Nevrova E. L., Snigireva A. A., Petrov A. N., Kovaleva G. V. *Guidelines From Quality Control of the Black Sea. Microphytobenthos* / A. V. Gaevskaya (Ed.). Sevastopol ; Simferopol : N. Orianda, 2015, 176 p. (in Russ.). https://doi.org/10.21072/978-5-9907290-2-5
15. Proshkina-Lavrenko A. I. *Diatomovye vodorosli planktona Chernogo morya.* Moscow ; Leningrad : Izd-vo AN SSSR, 1955. 222 p. (in Russ.). https://repository.marine-research.org/handle/299011/6623
16. Proshkina-Lavrenko A. I. *Diatomovye vodorosli bentosa Chernogo morya.* Moscow ; Leningrad : Izd-vo AN SSSR, 1963, 243 p. (in Russ.)
17. Reunova Yu. A., Aizdaicher N. A. Vliyanie detergenta na soderzhanie khlorofilla *a* i dinamiku chislennosti u mikrovodorosli *Chroomonas salina* (Wils.) Butch. (Cryptophyta). *Al'gologiya*, 2004, vol. 14, no. 1, pp. 32–38. (in Russ.)
18. Romanova D. Yu., Petrov A. N., Nevrova E. L. Copper sulphate impact on growth and cell morphology of clonal strains of four benthic diatom species (Bacillariophyta) from the Black Sea. *Morskoj biologicheskij zhurnal*, 2017, vol. 2, no. 3, pp. 53–67. (in Russ.). https://doi.org/10.21072/mbj.2017.02.3.05
19. Spirkina N. E. *Issledovanie kul'tury zelenoi mikrovodorosli Monoraphidium arcuatum kak novogo*

test-ob"ekta dlya otsenki kachestva vodnoi sredy. [dissertation]. Moscow, 2016, 172 p. (in Russ.)
20. Schlegel H. G. *Allgemeine Mikrobiologie.* Moscow : Mir, 1987, 567 p. (in Russ.)]
21. Andersen R. A., Berges J. A., Harrison P. J., Watanabe M. M. Recipes for freshwater and seawater media. In: *Algal culturing techniques* / R. A. Andersen (Ed.). San Diego : Elsevier Academic Press, 2005, pp. 429–538.
22. Davidovich N. A., Davidovich O. I., Podunay Yu. A., Gastineau R., Kaczmarska I., Poulíčková A., Witkowski A. *Ardissonea crystallina* has a type of sexual reproduction that is unusual for centric diatoms. *Scientific Reports*, 2017, vol. 7, article 14670 (16 p.). http://www.nature.com/articles/s41598-017-15301-z
23. Kim J. W., Price N. M. The influence of light on copper-limited growth of an oceanic diatom, *Thalassiosira oceanica* (Coscinodiscophyceae). *Journal of Phycology*, 2017, vol. 53, iss. 5, pp. 938–950. https://doi.org/10.1111/jpy.12563
24. Markina Z. V., Aizdaicher N. A. Content of photosynthetic pigments, growth, and cell size of microalga *Phaeodactylum tricornutum* in the copper-polluted environment. *Russian Journal of Plant Physiology*, 2006, vol. 53, no. 3, pp. 305–309. https://doi.org/10.1134/S1021443706030034
25. Markina Zh. V., Aizdaicher N. A. Influence of the ariel detergent on the growth and physiological state of the unicellular algae *Dunaliella salina* (Chrorophyta) and *Plagioselmis protonga* (Cryptophyta). *Hydrobiological Journal*, 2010, vol. 46, iss. 2, pp. 49–56. https://doi.org/10.1615/HydrobJ.v46.i2.60
26. Reid G. *A revision of the family Pleurosigmataceae* / A. Witkowski (Ed.). Ruggell : A. R. G. Gantner Verlag K. G., 2012, 163 p. (Diatom Monographs ; vol. 14).
27. Rijstenbil J. W., Gerringa L. J. A. Interactions of algal ligands, metal complexation and availability, and cell responses of the diatom *Ditylum brightwellii* with a gradual increase in copper. *Aquatic Toxicology*, 2002, vol. 56, iss. 2, pp. 115–131.
28. Round F. E., Crawford R. M., Mann D. G. *The Diatoms. Biology and Morphology of the Genera.* Cambridge : Cambridge University press, 1990, 747 p.
29. Seckbach J., Kociolek J. P. (Eds). *The Diatom World.* Berlin ; Heidelberg ; New York : Springer Verlag, 2011, 533 p. (Book series : Cellular Origin, Life in Extreme Habitats and Astrobiology ; vol. 19). https://doi.org/10.1007/978-94-007-1327-7
30. *SigmaPlot 12.5 User's Guide.* USA : Systat Software Inc., 2013, 455 p.

ОЦЕНКА НЕОДНОРОДНОСТИ РАСПРЕДЕЛЕНИЯ КЛЕТОК ПРИ ТОКСИКОЛОГИЧЕСКИХ ЭКСПЕРИМЕНТАХ С КЛОНОВЫМИ КУЛЬТУРАМИ БЕНТОСНЫХ ДИАТОМОВЫХ ВОДОРОСЛЕЙ

А. Н. Петров, Е. Л. Неврова

Федеральный исследовательский центр «Институт биологии южных морей имени А. О. Ковалевского РАН», Севастополь, Российская Федерация
E-mail: *alexpet-14@mail.ru*

Увеличение антропогенной нагрузки на прибрежные акватории требует постоянного отслеживания состояния их экосистем. Удобными биоиндикаторами для опосредованной оценки качества морской среды служат донные диатомовые водоросли, являющиеся ключевым звеном морских прибрежных сообществ и обладающие высокой чувствительностью к влиянию экологических факторов. Изменение показателей развития микроводорослей под воздействием различных токсикантов может быть подходящим инструментом при мониторинге качества морской среды, однако научно-методические подходы использования бентосных диатомовых как тест-объектов остаются недостаточно разработанными. Одной из важных проблем является оценка достоверности выборок при подсчёте обилия клеток в сосудах на разных этапах токсикологического эксперимента. Цель работы — провести статистическую оценку достоверности равенства среднего

исходного числа клеток инокулята клоновой культуры, вносимого в каждую из повторностей, а также достоверности равномерного распределения клеток по всей площади дна чашек Петри. Использованы клоновые культуры трёх видов бентосных диатомовых водорослей — *Thalassiosira excentrica* Cleve, 1903 (Coscinodiscophycea), *Ardissonea crystallina* (C. Agardh) Grunow, 1880 (Fragilariophyceae) и *Pleurosigma aestuarii* (Bréb. in Kütz.) W. Smith, 1853 (Bacillariophyceae). Эти виды относятся к разным классам Bacillariophyta и значительно различаются по морфологии панциря и образу жизни (парящие в водной массе, прикреплённые, подвижные). Статистическое сравнение вариативности числа клеток в эксперименте подтвердило отсутствие достоверных различий между средними значениями исследуемого параметра у всех видов при стандартном уровне значимости (0,05). Показано, что, несмотря на видоспецифические отличия в темпе приращения числа клеток, вариативность числа клеток в полях зрения микроскопа в ходе эксперимента меняется незакономерно. Наибольшая вариативность отмечена на 5-е сутки у мелкоразмерного вида *T. excentrica* (*Cv* = 42…55 %), а наименьшая — у крупноклеточного вида *A. crystallina* (*Cv* = 27…31 %). Установлено отсутствие достоверных различий в численности клеток между тремя повторностями (для каждого из видов) как при исходном внесении инокулята в чашки, так и в последующие дни опыта. Вывод справедлив для каждого из изученных видов диатомовых, что позволяет рассматривать все повторности как выборки одной совокупности и осреднять результаты, полученные на разных стадиях токсикологического эксперимента. Статистически доказана равномерность распределения клеток по дну экспериментальных чашек, которая не зависит от видовой принадлежности клеток и их абсолютной численности. Результаты позволяют надёжно оценивать изменения численности клеток тестируемых видов диатомовых водорослей на разных этапах эксперимента по выборкам, полученным на основе подсчёта клеток в ограниченном числе полей зрения.

Ключевые слова: токсикологический эксперимент, методика, статистическая оценка, Bacillariophyta, *Thalassiosira excentrica*, *Ardissonea crystallina*, *Pleurosigma aestuarii*, Чёрное море

1871
ИнБЮМ – IBSS

Морской биологический журнал
Marine Biological Journal
2020, vol. 5, no. 2, pp. 88–104
https://doi.org/10.21072/mbj.2020.05.2.08

UDC 582.261.1:678.7

FEATURES OF FORMATION OF COLONIAL SETTLEMENTS OF MARINE BENTHIC DIATOMS ON THE SURFACE OF SYNTHETIC POLYMER

© 2020 **Ph. V. Sapozhnikov[1], A. I. Salimon[2], A. M. Korsunsky[2,3], O. Yu. Kalinina[1,4], F. S. Senatov[5], E. S. Statnik[2], and Ju. Cvjetinovic[2]**

[1]P. P. Shirshov Institute of Oceanology, Moscow, Russian Federation
[2]Skolkovo Institute of Science and Technology, Moscow, Russian Federation
[3]University of Oxford, Oxford, United Kingdom
[4]Lomonosov Moscow State University, Moscow, Russian Federation
[5]National University of Science and Technology "MISIS", Moscow, Russian Federation
E-mail: *fil_aralsky@mail.ru*

Received by the Editor 10.10.2019; after revision 28.04.2020;
accepted for publication 26.06.2020; published online 30.06.2020.

The topic of interactions between plastic and natural communities is now more relevant than ever before. Gradual accumulation of artificial polymer products and their fragments in the natural environment has reached a level at which it is already impossible to ignore the affect of these materials on living organisms. First and foremost, microorganism colonies inhabiting different biotopes, both aquatic and terrestrial, have been affected. These species are at the front-end of interaction with plastic, including those present in marine ecosystems. Nevertheless, in order to understand these processes, it is necessary to take into account several aspects of such interactions: the impact of different types of plastic on microbial community through the release of their decomposed products into the environment, the forms of plastic usage by microorganisms themselves, including mechanisms for surface colonization, as well as possible biodegradation processes of polymers due to the actions of microorganisms. At the same time, types of plastic may differ not only in mechanical strength, but also in their resistance to biodegradation caused by microorganisms. Experiments with surface colonization of types of plastic, which are different in composition and mechanical strength, provide a wide range of results that are not just relevant for understanding modern natural processes involving plastic: these results are also important for application in certain areas of technology development (for example, when creating composite materials). In particular, researches into the forms and mechanisms of sustainable colonization of particularly strong polymers by diatoms from natural communities are of great interest. Due to the fouling of surface of particularly strong synthetic polymers by diatoms, it is possible to form a single diatom-polymeric composite with general properties being already substantially different from those of the polymer itself. For example, when a polymer is fouled with diatoms that are firmly held on its surface due to physiological mechanisms that ensure their reliable fixation, total surface area of the composite increases by 2–3 orders of magnitude compared with this of bare polymer. Such composites and their properties are formed due to mechanisms of substrate colonization used by diatoms from natural marine cenoses – during the transfer of these mechanisms to a new material being prospective for diatom settlement. The practical applications of these composites lie in the sphere of heat and sound insulation, as well as in the field of creating prosthetic tissues for bone operations. In our experiments, we tracked the sequence of development of a stable composite when diatoms colonized the surface of samples of a particularly strong synthetic polymer being resistant to corrosion. In this case, the sample population process took place on the basis of colonies formed in accumulative cultures from the natural marine environment. Samples of ultra-high molecular weight polyethylene (UHMWPE)

with a smooth and porous surface structure (with an open cell, bulk porosity up to 80 %) were colonized by diatoms *Karayevia amoena* (Hust.) Bukht., 2006, *Halamphora coffeaeformis* (C. Agardh) Levkov, 2009, and *Halamphora cymbifera* (W. Greg.) Levkov, 2009. These laboratory experiments lasted for three weeks. Accumulative microphyte cultures, on the basis of which the experiments were conducted, were obtained from the Baltic Sea (Baltiysk area, Russia) and the Arabian Sea (Mumbai area, India). The types and stages of development of colonial settlements on various elements of the frontal surface microrelief and in the underlying caverns were studied using a scanning electron microscope on samples subjected to stepwise thermal drying. Individual cells of *K. amoena*, *H. coffeaeformis*, and *H. cymbifera*, their chain-like aggregates, and outstretched colonial settlements occupied varying in degree non-homogeneous microrelief surface elements, forming structures with a thickness of 1–2 layers with an average settlement height of 1–1.3 single specimen height. *K. amoena* cells were tightly fixed to the polymer substrate using the pore apparatus of the flap of the frustule. Observations using scanning electron microscope revealed shell imprints on the substrate, which were signs of a polymer substrate introduction into hypotheca areoles. The spread mechanisms of diatoms of three mentioned species on various elements of UHMWPE surface were explored, as well as the formation of the characteristic elements of colonial settlements, including for *K. amoena* – consecutively in the form of "pots" and spheres, by means of interaction with polymer surface and its extension with the increase in the number of tightly attached cells in the colonial settlement.

Keywords: diatoms, diatom algae, Bacillariophyta, plastic colonization, UHMWPE, sustainable materials, plastic in the marine environment, aquaculture

For many decades, diatoms attract the attention of a wide range of scientists because of their role in the ecology of the biosphere as a whole: as producers of about ¼ of terrestrial organic matter and almost ⅓ of all oxygen generated on the planet. More recently, in the field of materials science, the study of a hierarchical multilevel organization observed in diatom shells structure and, as a consequence, of their biomechanical characteristics has begun. Many issues of cell interaction with various substrates have been studied in detail [6 ; 7 ; 14 ; 15 ; 16 ; 17 ; 24], but a number of questions still have no adequate response. A deeper understanding of these aspects is expected to be obtained using modern FIB-SEM methods (focused ion beam scanning electron microscopy) [6 ; 20 ; 25]. The use of aquaculture technologies can expand the use of diatoms as a sustainable resource for biofuels, biomineralization, and material production. The potential biodegradation of hydrosphere-contaminating polymers by fouling with diatoms is also considered as an important environmental problem [2 ; 6 ; 22 ; 23 ; 26].

Ultra-high molecular weight polyethylene (hereinafter UHMWPE) commercialized by Celanese [9] is a polymer with high mechanical properties that has been used in marine practice for the manufacture of ropes and sails since the 1990s. Due to bioinertness, as well as acceptable mechanical properties and wear resistance, the field of UHMWPE application in surgery is growing: when creating implants for bones and joints and, more recently, in reconstruction processes at the cellular level, as scaffolds for tissue engineering [13]. Being colonized by mesenchymal stromal cells, UHMWPE scaffolds with open porosity demonstrate a high ability to osseointegration and vascularization [21].

The main idea of this study is as follows: if certain diatom species from natural marine communities are able to colonize the surface of various types of plastic [4 ; 5 ; 6], including UHMWPE, in some cases this process can be classified as a way to create a new class of biocorrosion- and strain-resistant materials – diatom-polymer hybrids. Theoretically, a number of processes accompanying synthetic polymer colonization can be considered:

A. "Surface single-layer colonization" will take place without significant proliferation of diatoms in the depth of the substrate due to the lack of porosity. If the colonized surface is destroyed as a result of biodegradation, over time this process will end with disintegration of polymer products into fragments of various size, and it can be used as a technology for combating environmental pollution with macroscopic plastic.

B. In contrast to “surface single-layer colonization”, formation of a sufficiently thick, dense, and mechanically strong multilayer coating with barrier or other properties, valuable for practical application, is possible on the surface of biostable polymers.

C. “Colonization of volume” due to intensive proliferation in depth of the porous (cellular) polymer is expected to create a stable bulk diatom-polymer composite with a wide range of technical characteristics, that are important for solving structural, tribological, filtration, and thermal problems, as well as for use in the field of vibration- and sound insulation. The expansion of the spectrum of possible applications is due to a significant increase of the total surface of the composite – by 2–3 orders of magnitude compared with the non-colonized surface of the polymer.

Since UHMWPE has significant chemical and biological stability, it is an important candidate material for studying the process of colonization of its surface and volume. In this article, we discuss the first results on the structural aspects of the interaction of marine diatoms from natural microphytobenthos communities with porous UHMWPE surface.

MATERIAL AND METHODS

UHMWPE samples of two types were used to study the surface colonization process: smooth and porous ones. Samples of both types were exposed in the accumulative cultures of diatoms isolated from the sandy littoral: I – in Mumbai area (the Arabian Sea); II – in Baltiysk area (the Kaliningrad Bay, the Baltic Sea). In both accumulative cultures, diatoms grew under natural diffused light, in the conditions of alternating day and night (on the windowsill in the laboratory of P. P. Shirshov Institute of Oceanology), in the temperature range of +5 to +30 °C (from the coldest winter months to the warmest summer ones), covering the walls of 1-L laboratory vessels of polyethylene terephthalate (hereinafter PET) and high density polyethylene (hereinafter HDPE). Culture growth occurred without additional aeration, in the same volume of water into which they were transferred from natural biotopes. The salinity of seawater in the first vessel was of 30 ‰, in the second – of 5 ‰. The age of culture I at the time colonization experiments began was of 21 months, of culture II – of 20 months. In culture I, representatives of the genus *Halamphora* (Cleve) Levkov dominated: *Halamphora coffeaeformis* (C. Agardh) Levkov, 2009 (Fig. 1c–e) and *Halamphora cymbifera* (W. Greg.) Levkov, 2009 (Fig. 1f); in culture II – *Karayevia amoena* (Hust.) Bukht., 2006 (Fig. 1a, b).

The choice of cultivation conditions – sufficiently rigid for marine benthic diatoms taken from the natural environment – was dictated by the need to obtain mixed accumulative cultures from several species, maximally adapted for joint development over a long period of time with no additional aeration and no feeding with biogenes from the outside, as well as with significant changes of lighting conditions and ambient temperature. The act of colonization of vessel walls surface by different diatom species deserved special attention and became the basis for experiments with UHMWPE colonization.

Samples of smooth UHMWPE were obtained by thermal cutting of a dense (non-porous) cylinder with a diameter of 26 mm into 2–3-mm high “tablets” with surfaces smoothed due to reflow.

Samples of porous UHMWPE were prepared in accordance with the method presented in [12]. UHMWPE powder (4120 GUR Ticona®) was mixed with edible rock salt (NaCl) with a particle size of 80–700 μm. The dry mixture with a weight ratio of 1 : 9 was carefully mixed using planetary ball mill Fritsch Pulverisette 5 (Fritsch GmbH, Germany) in 500-ml agate centrifuge filled with corundum balls with diameter of 8 mm. Thermal pressing was carried out under a load of 70 MPa at +180 °C. Salt removal was then carried out using distilled water at +60 °C, using an ultrasonic cleaner. This process resulted in the formation of porous structures with open pores, with a bulk porosity of about 80 %.

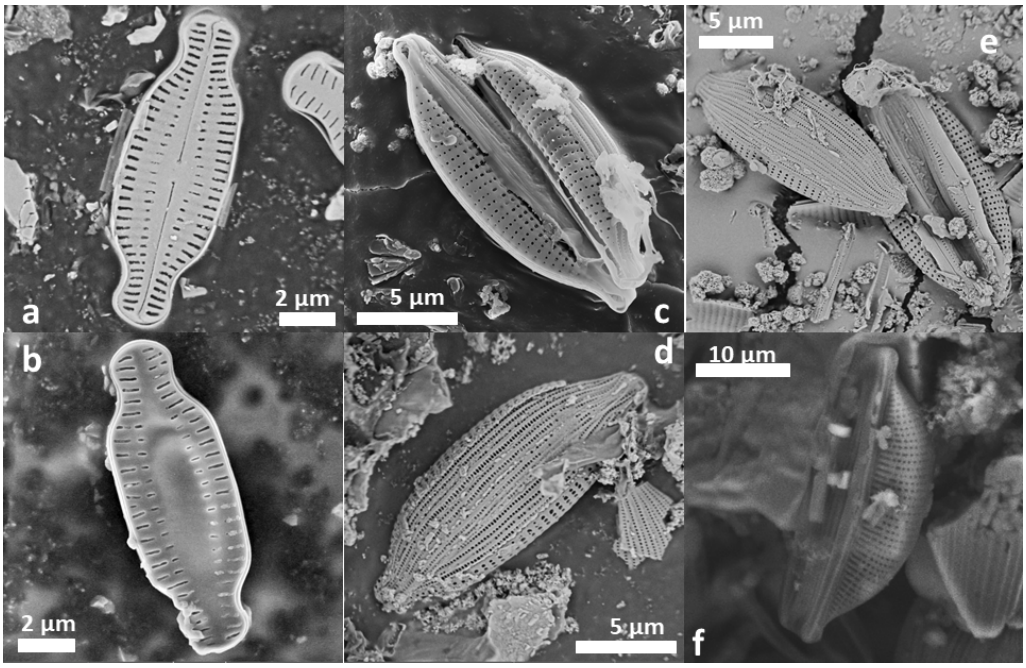

Fig. 1. The most common diatom species that formed fouling on the surface of porous UHMWPE samples: a, b – *Karayevia amoena* (in storage culture II); c–e – *Halamphora coiffeaeformis*; f – *Halamphora cymbifera* (in storage culture I)

To obtain experimental fouling of smooth and porous UHMWPE surface (with different surface microreliefs), various samples of this material – three replicates for each sample – were exposed in accumulative cultures over a period of 21 days under constant diffused light with LED1106 G2 2.3 W, 18 mA, 35 lm/W. The dimensions of rectangular samples of porous UHMWPE were of 40×19×3 mm, and the diameter of smooth samples was of 25 mm. Laboratory vessels made of colorless PET and HDPE with a capacity of 1 L (2 pieces each) with accumulative cultures were located at a distance of 45 cm from the light source. Light intensity was of 135 lx.

Three-week duration of the experiment is explained by the fact that by the end of this period, extensive placers of brown fouling spots had formed on the surface of porous UHMWPE samples, which were clearly visible to the naked eye. This allowed us to proceed to the stage of material microscopy.

Colonial settlements of diatoms from accumulative culture II grew on the walls of vessels 1 and 2 (PET); on the walls of vessels 3 and 4 (HDPE) – colonial settlements of diatoms from accumulative culture I. In vessel 1, samples of porous UHMWPE No. 8 and 9 were exposed in three replicates, in two rows, three in a row. In vessel 2, sample of porous UHMWPE No. 10 were exposed in three replicates, the upper row, and "tablets" of smooth UHMWPE – three replicates, the lower row. In vessel 3, samples of porous UHMWPE No. 1 and 2 were exposed, by analogy with vessel 1. In vessel 4, a sample of porous UHMWPE No. 3, in three replicates, and three "tablets" of smooth UHMWPE, by analogy with vessel 2, were exposed. General scheme of the experiment is shown in Fig. 2.

During the experiment, UHMWPE samples were suspended in water column, on threaded loops made of copper wire (Glorex, 20 m × 0.4 mm, with anti-corrosion coating) at a distance of 5–10 mm from aquarium walls covered with diatom fouling, at an angle of 30–40° to light source. Fouling of *Halamphora* species was obtained on samples No. 1, 2, and 3 (three replicates for each), and of *Karayevia amoena* – on samples No. 8, 9, and 10 (also in triplicate). During the experiments, control extracts of samples were not performed in 21 days of exposure; therefore, it is not possible to determine time and place of appearance of the first diatom cells on specific samples.

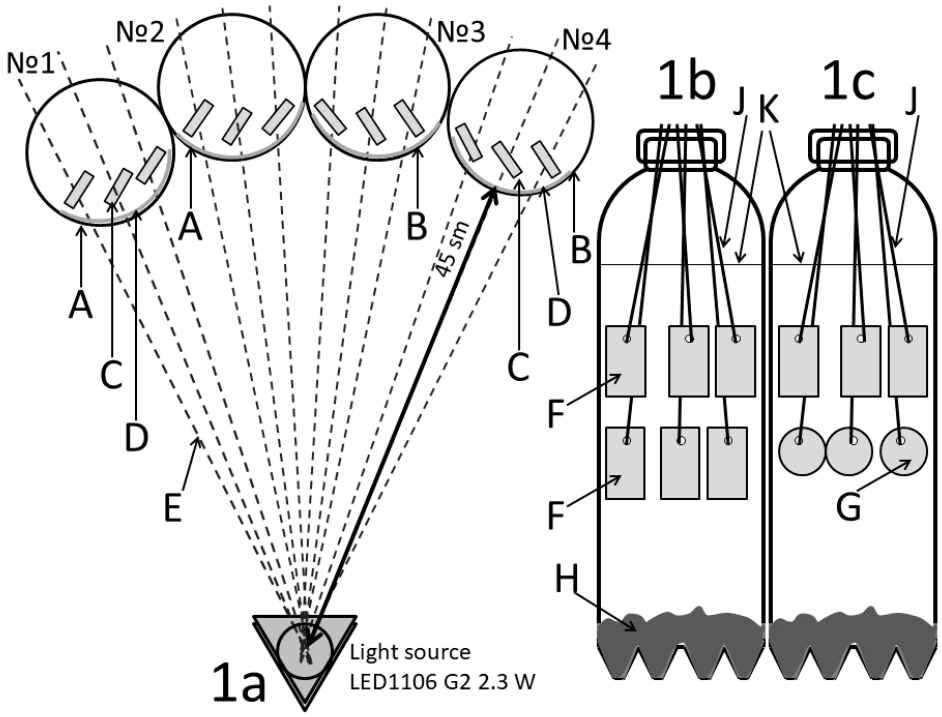

Fig. 2. General scheme of the experiment with colonization of the surface of porous and smooth UHMWPE samples by marine diatoms from various storage polycultures. **1a** – scheme of the experiment, top view: A – PET-mini-aquariums (1-L bottles); B – HDPE-mini-aquariums (1-L bottles); C – samples located at an angle to light source; D – layer of diatom colonial settlements on the bottle wall; E – vector of the direction of the light flux from the source. **1b** – layout of samples in bottles No. 1 and 3: F – porous UHMWPE samples; H – sea soil; J – copper wire fixing UHMWPE sample in water, near the bottle wall; K – sea water level. **1c** – layout of samples in bottles No. 2 and 4: G – smooth UHMWPE samples

When preparing samples for microphotography using a scanning electron microscope, we used a new author's method of three-stage drying: exposure in a drying cabinet at +50 °C for 8 hours, at +80 °C – for 3 hours, and at +100 °C – for 1 hour. The methodology proposed, never published before, was based:

1) on the results of Ph. V. Sapozhnikov for drying diatom periphyton on filamentous algae in a drying cabinet, obtained in 1996 at Belomorsky Biological Station of Moscow State University, whose goal was to create permanent preparations from dried diatom shells on filamentous algae surface without loss of periphyton spatial organization;

2) on the data on changes in UHMWPE properties upon heating, which made it possible to estimate the degree of density of shell association with sample surface.

The temperature of +80 °C is the limit, beyond which UHMWPE begins to soften, acquiring the properties of thick resin. However, small diatoms, such as *K. amoena* (up to 15 μm long), cannot immerse into the thickness of this polymer due to their own weight, since their mass is too small, the specific surface area of wide ovaloids of revolution, which geometrically are their frustules, is quite large, and the softness of the substrate itself is insufficient for this. This is also evidenced by the fact that larger cell diatom species used in the experiments (*Halamphora coffeaeformis* and *H. cymbifera* having length of less than 30 and 50 μm, respectively, and the geometric shape of a wide ovaloid of revolution) did not immerse in the polymer thickness when heated above +80 °C. Moreover, at +90 °C UHMWPE samples begin to be affected by the shape memory effect (common materials science designation of this process is "cylinder narrows and extends"), due to which small objects, immersed in it under their own weight, are pushed out.

Thus, after the final stage of drying for one hour at +100 °C, one should not expect the effect of spontaneous fusion of diatom shells into the surface of this polymer. Rather, if loosely associated with the polymer, they would separate from the surface due to buoyancy shape memory effect.

After primary drying, the samples exhibited in accumulative culture I were heavily coated with salt; therefore, they were additionally washed by two-day exposure in the distillate, and then dried again for 4 hours at +60 °C. Microphotography of diatom fouling was carried out at a magnification ×500 to ×700 using three different scanning electron microscopes: Hitachi TM 1000, Tescan LYRA, and Tescan MAIA3.

Counting of the shells on the surface of UHMWPE samples was carried out manually using microphotographs, marking the specimens counted as a part of both chains and "cloak-like" settlements. When isolating discrete spots, markers of different colors were used. The number of intervals when separating the size classes of spots was approximately calculated using the formula:

$$h = 2(IQ)n^{-1/3},$$

where h is the length of the interval;

(IQ) is the difference between the upper and lower quartiles (according to Freedman – Diaconis formula [8]).

RESULTS AND DISCUSSION

Surface colonization of smooth UHMWPE samples did not occur in any of diatom accumulative cultures. The result obtained is important because of its potential application in the design of marine antifouling underwater structures of UHMWPE with a smooth surface.

Experiments with surface colonization of porous UHMWPE samples showed a number of important features of this process, including common ones, for various diatom species. So, in accumulative cultures, where many diatom species developed on a sandy substrate, and only a few species settled on the walls of experimental vessels (with the predominance of mentioned above), only certain taxa transferred to UHMWPE samples.

In particular, accumulative culture II consisted of 10 species of benthic diatoms. Of them, *Karayevia amoena* formed numerous and dense colonial settlements on the walls of PET vessels and sparse settlements – on grains of sand at the bottom of the vessel; *Melosira nummuloides* C. Agardh formed few short chains; other species from the genera *Amphora* Ehr. ex Kütz., *Diploneis* (Ehr.) Cleve, *Nitzschia* Hassall, and *Fallacia* Stickle et D. G. Mann were often found in the sand and occasionally – on the walls of the vessel. Only the first two species mentioned – *K. amoena* and *M. nummuloides* – have moved on to living on a new substrate (porous polyethylene).

Scanning electron microscope studies did not reveal the development of bacterial colonies on UHMWPE samples. In turn, *K. amoena* formed different types of colonial settlements on the surface of various UHMWPE samples.

In accumulative culture I, three species from the genus *Halamphora* were noted, two – from *Karayevia* Round et Bukhtiyarova ex Round, two – from *Nitzschia*, and one – from *Navicula* Bory. All benthic diatoms lived not only in sand at the bottom of the vessel, but also on the walls, forming on them dense spots of colonial settlements with a predominance of *H. coffeaeformis*. Only *H. cymbifera*, *H. coffeaeformis*, and *K. amoena* settled on porous UHMWPE samples. The third species in culture I had morphological differences from that in culture II; it was seen rarely and by separate cells, while the first two species formed

colonial settlements of various types. The dominant species forming the most extensive colonial settlements on the porous UHMWPE was *H. coffeaeformis*. No bacterial colonies were observed on the surface of UHMWPE samples in this experiment either, but individual cells of rod-shaped bacteria were found.

All three species that showed active growth on porous UHMWPE (*K. amoena*, *H. coffeaeformis*, and *H. cymbifera*) are benthic ones and lead an attached lifestyle in nature, colonizing various substrates (surface of mineral grains of sand and plant debris, chitinous shells of dead invertebrates). Moreover, according to shell macro- and micromorphology, ability to move actively, and way of fixing on the substrate, representatives of the genus *Karayevia* differ significantly from those of *Halamphora* [3 ; 10 ; 11 ; 19]. Extremely inactive *K. amoena* attaches very tightly to substrate surface, and all movements of its cells are reduced to upper daughter cell crawling away from the lower one after division over a distance not exceeding, as a rule, its length. To date, no independent movement of *K. amoena* over distances significantly exceeding its shell length has been reported. The transfer of cells of this species to new habitats, significantly remote from the previous ones, occurs solely due to action of external factors during water movement or during the movement of substrate particles already populated by them. In particular, we assume the possibility of transferring cells to UHMWPE surface (from the composition of colonial settlements on the walls of the vessels and from the surface of sandy soil) using bubbles of oxygen released by microphytes, because the walls of these bubbles, being separated from the fouling, often had a brownish color. On the contrary, *H. coffeaeformis* and *H. cymbifera* cells, although they lead an attached lifestyle and are inactive, are still able to transfer over distances many times larger than the length of their shell, which can affect the nature of the settlements formed by them [18].

We observed three main types of colonial settlements with transitional forms between them. This suggests that the process of populating porous UHMWPE with *K. amoena* occurs in three successive stages. First, the cells of this diatom propagate along the substrate, forming primary colonization chains (Fig. 3). To do this, they use the tops (ridges) or the edge areas of folds and surface flocculent fragments. Chains of this type are characterized by terminal (apical) growth; they are formed as a result of cell division and the subsequent movement of each upper daughter cell from the lower one over a small distance along the surface of the highest protruding microrelief elements of the sample. Intercalar doubling of cells in such a chain occurs locally, and only in places of microrelief "branching": lateral processes are added to the main growth direction, also elongating terminally. It can be assumed that the formation of these chains is not only the primary surface colonization, but also the process of searching for areas, where the formation of more compact colonial settlements is possible.

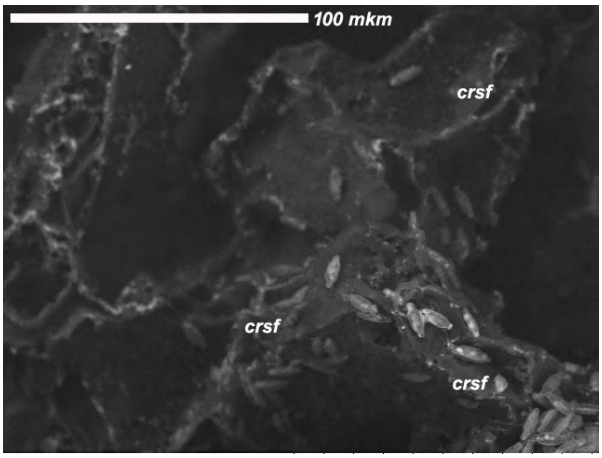

Fig. 3. Primary colonization chains of porous UHMWPE by *Karayevia amoena* cells. In the foreground, the chains pass along the crests of substrate folds (*crsf*)

When such chains reach relief areas characterized by either a high density of folds (especially on hill-shaped elevations), or, conversely, by the relative surface smoothness (including the bottom of small gaps), the formation of secondary colonization chains begins. These structures are formed due to the doubling of not only the terminal cell in the chain, but also of all its other cells that have reached such an area. As a result, oblong sinuous or branching structures are formed from cells arranged in two rows according to the "herringbone principle" (parquet "herringbone") (Fig. 4). If primary colonization chain has significant

intervals (gaps) (at least of 1–1.5 cells long) then several secondary colonization chains can form from it. Given the quasihomogeneous nature of the microrelief, primary and then secondary colonization chains are able to cover substrate surface with a rather dense net (Fig. 4).

Secondary colonization chains give rise to "nuclei", or to the most dense, initial groups of cells, during the growth of colonial settlements. Continuing to double frequently in secondary colonization chains, *K. amoena* cells efficiently spread over an area with a high density of folds (often along a "hill") or over a limited area on a relatively flat surface, filling its entire available area. This forms the third stage of colonization, or "cloak-like" settlement (Fig. 5).

The area covered by such a settlement depends on the space scale of the elements of microrelief, that ensures its development. Such vast settlements, often formed from hundreds and thousands of cells, consist of smaller fragments of mosaics, or "spots" of a similar configuration [1]. "Spots" can be clearly distinguished by narrow winding gaps between them, as well as by the direction of the axes of the cells of which they consist. As a rule, these "spots" look like tubercles in the composition of the settlement, are located at different angles in relation to each other, and correspond to centers of intense cell division. With the development of a particularly dense "cloak-like" settlement, they reflect the features of microrelief surface on which they are formed. On UHMWPE samples of different porosity, such "spots" differ in the abundance of cells. When the maximum packing density is reached and the cells of the settlement already cover the substrate in 1–1.3 dense layers and begin to rise above it in the form of a knoll, they cease to massively divide, as noted in the composition of extensive open "cloak-like" settlements. It was also registered that periodically, in conditions of a small area of accessible relatively flat surface, the cells continue doubling and begin to actively transform the substrate, as it will be described below.

On the surface areas of sample No. 8, represented mainly by relatively smooth 20(30)–80 μm wide flakes being torn along the edges, the size of primary

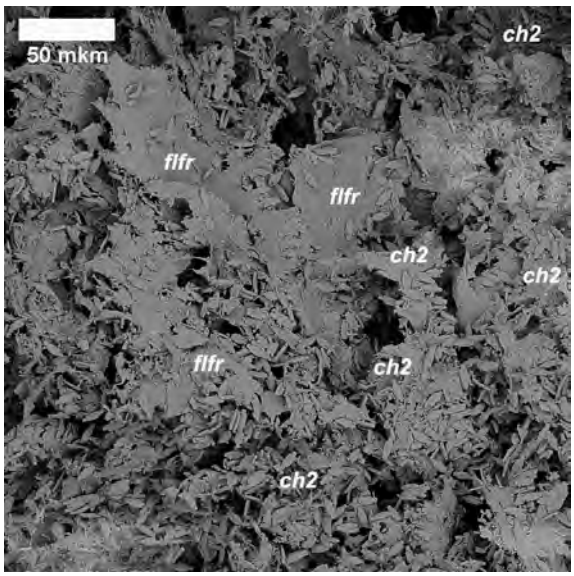

Fig. 4. Secondary colonization chains (*ch2*) of porous UHMWPE by diatom *K. amoena*: cell structures arranged in two rows according to "herringbone principle" ("herringbone" parquet). The substrate is represented by small flocculent fragments (*flfr*) of a relatively flat surface

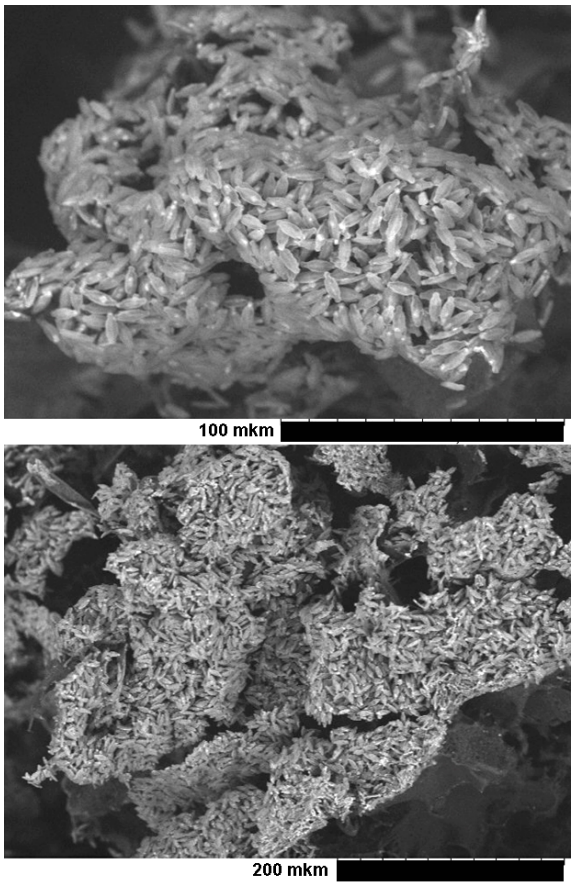

Fig. 5. View of "cloak-like" areas of *K. amoena* settlements on the surface of porous UHMWPE (at different magnification)

colonization chains ranged from 2 to 12 cells (3 on average), with a predominance of chains of 3–4 cells. The size of secondary colonization chains at the stage of the abundant formation of “herringbones” and the coating of the substrate with a dense net varied from 3 to 23 cells (9.94 on average), with a predominance of chains of 6–11 cells (they accounted for a total of 48.75 %) (Fig. 6). In turn, the size of “spots” ranged from 9 to 73 cells (31.01 on average), and the largest of them had branched outlines.

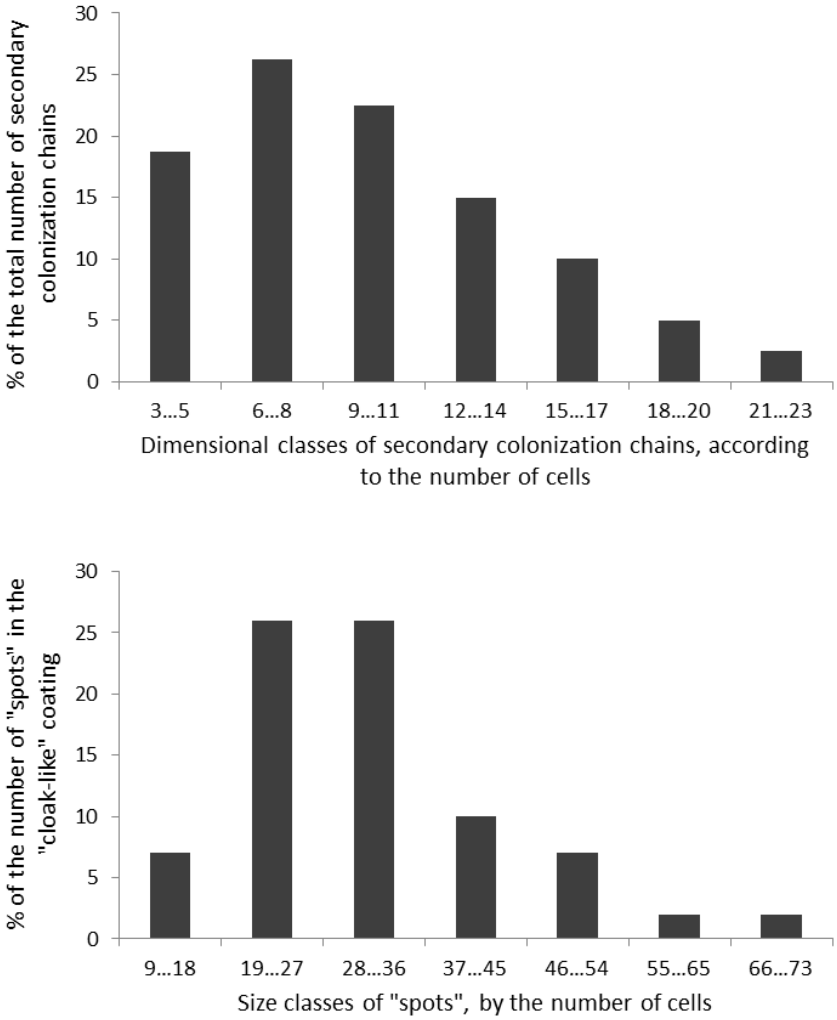

Fig. 6. Frequency distribution of size classes of “spots” in “cloak-like” colonial settlements on the surface of sample No. 8

However, in the structure of “cloak-like” settlements, “spots” with a size of 19–35 cells prevailed (65 % in total) (Fig. 6). Totally, location of 12,404 shells in 400 “spots” was taken into account.

On the surface of sample No. 10, the folding was significantly higher: the microrelief was sinuous and finely folded; it consisted of three-dimensionally branching structures covered with a mosaic of small flat sections (of 40–60 μm along the largest axis), located in different planes and separated by thin low folds-barriers. Primary colonization chains were 2–8 cells long (3–4 cells on average); secondary colonization chains consisted of 3–15 cells (5–8 cells on average; chains of this size accounted for 60 %) (Fig. 7). “Spots” consisted of 5–26 cells (17 on average), but structures of two types prevailed among them: formed of 14–16 and 19–21 cells, depending on characteristics of the surface microrelief (Fig. 7). In this sample, 9520 shells in 560 “spots” were taken into account.

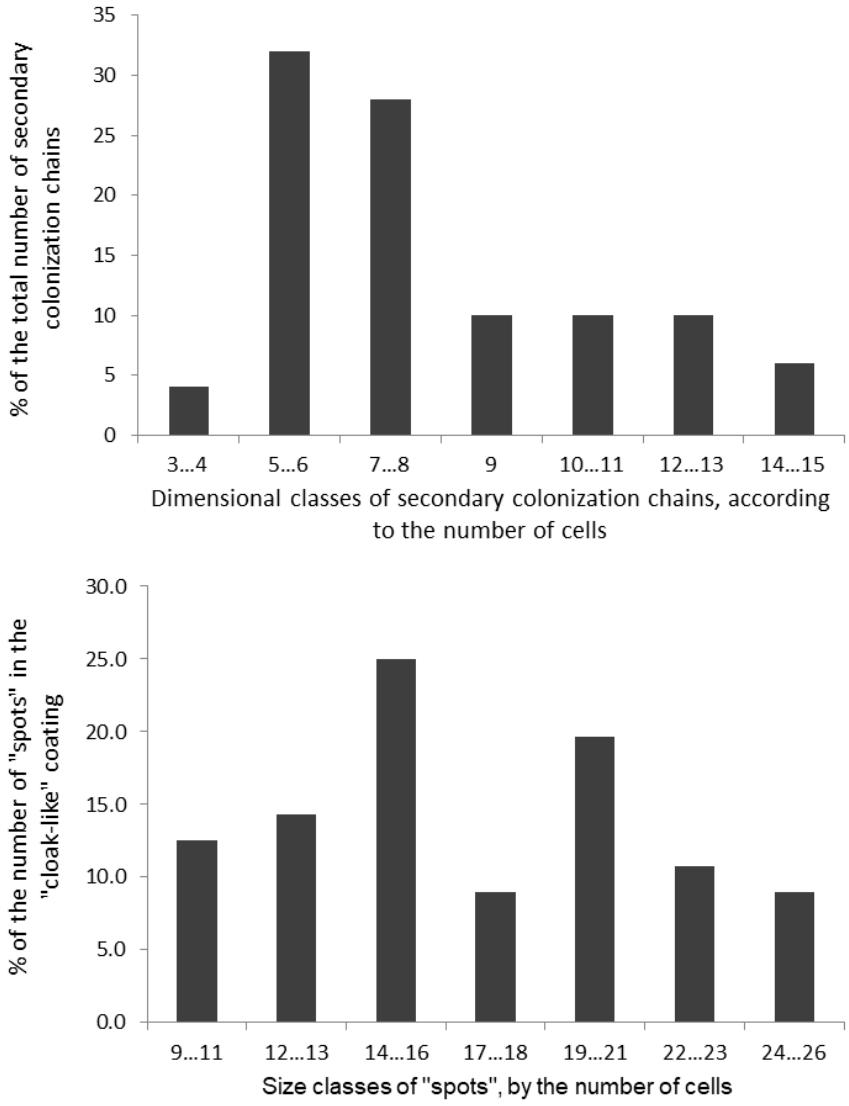

Fig. 7. Frequency distribution of size classes of “spots” in “cloak-like” colonial settlements on the surface of sample No. 10

It is important to note the ability of *K. amoena*, which we established, to modify UHMWPE microrelief: on the one hand, due to a very tight attachment of cells to sample surface, and on the other, due to their synchronous division in rows. When examing fragments of the developed fouling at a magnification ×3000, the following types of deformation of polyethylene surface by diatom cells were noted.

The first type consisted of ridges with a length of 20–30 μm, squeezed out by diatom shells due to fouling compaction on both fold sides. Successive doubling of cell rows tightly attached to the substrate, on both sides of a low but wide fold, with the integration of newly formed rows between them, led to stretching of the substrate itself: the fold was stretched into a narrow ridge. On such ridges, several cells grew, which were in the substrate in the wells depicting the outlines of the shell (Fig. 8). The wells could be formed due to the compression of these cells, which continue to hold tightly in place, while raising the edges of the crest apex due to its extension in height, accompanied by squeezing the edge into the fold.

The second type was formed by squeezed and thinned edges of flat surface areas, along the edges of which there were diatoms in the wells in the shape of a shell (Fig. 8).

Both types of elements of large (in relation to the shells) deformation were formed due to the growth of cell chains in width (doubling), and due to the fact that the shells were tightly attached to the surface, and the newly formed cell rows were embedded between already attached rows, thus stretching the substrate.

Absolutely special secondary structures formed by *K. amoena* from UHMWPE were noted on the surface of sample No. 8 (Fig. 9). Upon reaching the maximum population density of an even and relatively small area, the cells began to transform its surface using tight attachment to the substrate, as well as increasing of the number of adjacent rows, thereby stretching the polymer substrate.

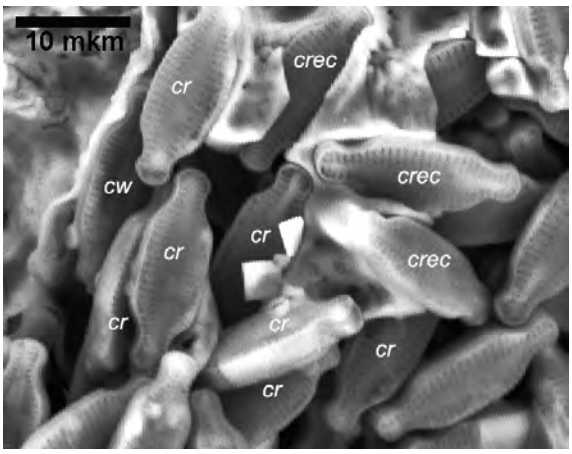

Fig. 8. UHMWPE surface deformations by *K. amoena* cells during the formation of a "cloak-like" settlement. Cells on the edge of the crest (*crec*), squeezed from a wide fold of the substrate in dense cell rows (*cr*), sit in the wells formed by extruding the brow in the form of a fold. The cell in the well (*cw*) is visible on the left in the wrung-out part of the marginal area (the squeezed fold frames the cell on the left)

First, an annular row located along the area edge was formed (Fig. 9a), and its doubling began on both sides with a gradual extrusion of the substrate surface into a low annulated fold. Then, separating more and more new rows in both directions – in and out of the annular row – the diatoms squeezed the fold already into the annular wall (Fig. 9b). Rows inside such a "well" under construction received obviously less light and biogens than rows outside, because a semi-enclosed space was formed. As a result, the number of rows outside grew faster, including due to their intercalary doubling up and down along the entire height of the "well". Because of this, the walls of the "well" bent outward, forming a "pot" (Fig. 9c).

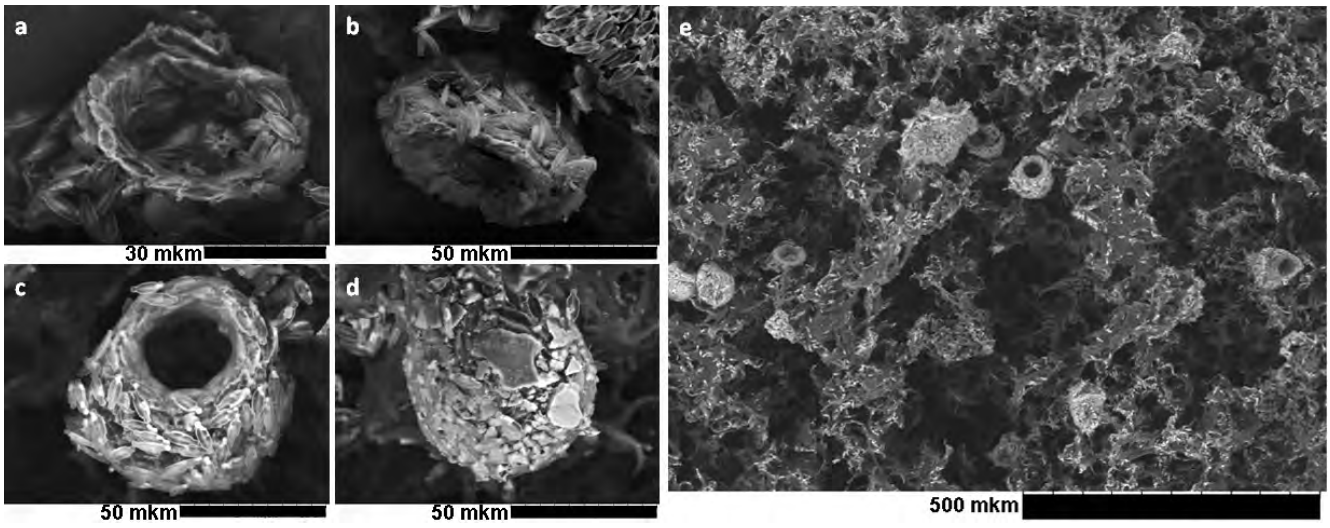

Fig. 9. Deep deformation of the surface of porous UHMWPE by the growing *K. amoena* colonial settlement: a – formation of an annular fold; b – stage of fold extrusion in the annular wall; c – stage of the "pot"; d – formation of a fragment of a "cloak-like" settlement in the form of a sphere, inside the fouling there is a fragment of UHMWPE surface extruded by dense cell rows in the form of a "pot"; e – location of the protruding fragments of the "cloak-like" settlement in the form of "pots" and balls on frontal surface of porous UHMWPE

In the late stages of the formation of such a structure, light and biogens almost ceased to enter its internal space through a narrow gap. During this period, the increase in the number of cells continued only outside, and the diatoms in the rows already formed short sequences of 3–4 cells, forming "end-specks" of the membrane. Such "end-specks" were located at different angles to each other. In the final stage, a similarity of a sphere was formed (Fig. 9d): the terminal hole of the bloated "pot" covered the "spot" of the diatoms of the outer membrane. The diameter of these extruded structures was of ≈ 60 μm at the stage of fold and of ≈ 80 μm at the stage of "pot"; the volume formed was of ≈ 270–290 μm^3. The distance between the "pots" on the front surface of the sample reached 300(400)–600(700) μm with their rare location and 10(40)–700 μm – with frequent location, including doubles (Fig. 9e).

The surface of porous UHMWPE in sample thickness was colonized up to a depth of 150–200 μm – both in the form of primary colonization chains along the bottom of the caverns and due to the wide "cloak-like" settlements in the areas of deep folding of the front surface.

The successive formation of the same three stages of the colonization of porous UHMWPE was noted for *H. coffeaeformis*, but with its own characteristics. Firstly, primary colonization chains of this species were significantly sparser (due to the movement of daughter cells over longer distances after division). Secondly, intercalular cell division was more often observed in their composition, and this was not always accompanied by the growth of lateral "branches" along suitable microrelief areas. Thirdly, primary colonization occurred not only in the protruding, multi-folded areas (on samples No. 1 and 2), but also in concave relief elements – as on the surface of sample No. 3 (Fig. 10). Here, wide, being devoid of additional folding, and smoothly curving "blades" (with the width of 200–400 μm) often interspersed with wide caverns (of 200–700 μm along the largest axis), the depth of which reached 200–500 μm. In turn, the blades themselves, due to their bends, could reach a height of 300–700 μm. Nevertheless, the formation of secondary colonization chains occurred along "ridges" and edges of caverns in the front UHMWPE surface according to the same principle of parquet row doubling as for *K. amoena*, or by an increase in the number of cells in the chain in the form of bundles. Fourthly, the development of particularly large "cloak-like" *H. coffeaeformis* settlements was most often observed along the edges of large caverns (Fig. 11), and of smaller ones – along the upper edges of the "blades" (on sample No. 3) or along the "hills" (on samples No. 1 and 2) (Fig. 12). Due to the sparseness of the chains of primary and secondary colonization, as well as the net nature of "spots", it is not possible to reliably distinguish their characteristic sizes for *H. coffeaeformis*.

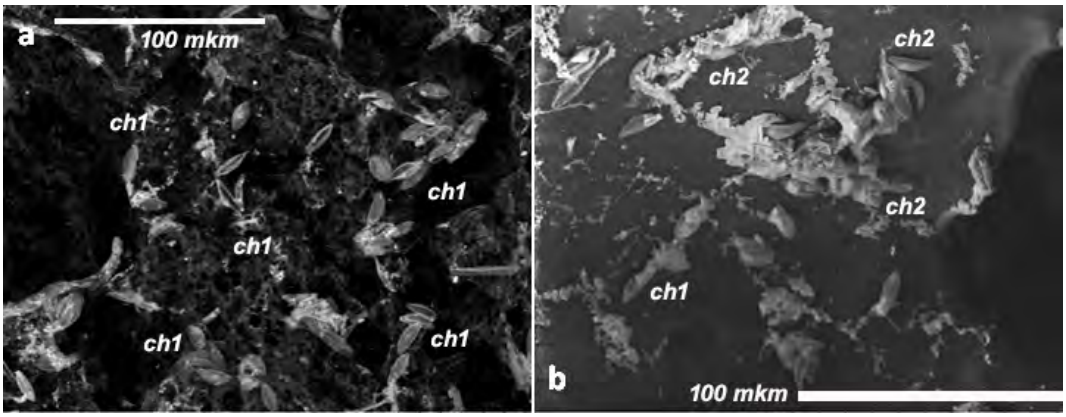

Fig. 10. Primary (*ch1*) and secondary (*ch2*) colonization chains of surface of porous UHMWPE by *Halamphora coffeaeformis* cells

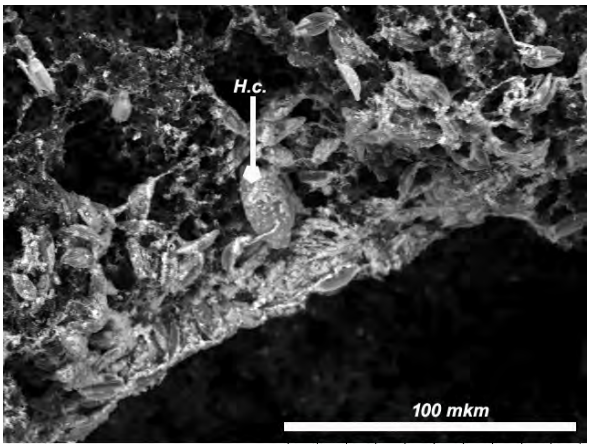

Fig. 11. Large "cloak-like" settlement of *Halamphora coffeaeformis* along the edge of a large cavern on the frontal surface of porous UHMWPE. In the center of the image there is a separate large cell of *H. coffeaeformis* (*H.c.*)

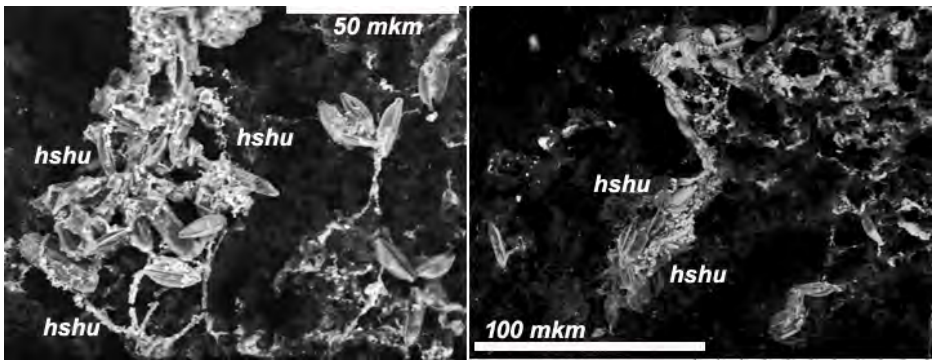

Fig. 12. Small "cloak-like" *Halamphora coffeaeformis* settlements along the tops of hill-shaped uplifts (*hshu*) of the densely folded surface of porous UHMWPE

Finally, *H. cymbifera* did not form primary colonization chains at all to search for topologically suitable surface areas. Large cells of this species either settled on shaded microrelief areas and gave rise there to very dense, compact colonial settlements (on sample No. 3) (Fig. 13), or settled alone along the edges of caverns, among dense *H. coffeaeformis* settlements (on samples No. 1 and 2) (Fig. 11).

The size of compact *H. cymbifera* populations varied from 6 to 32 cells (17.08 on average). Groups of 14–18 cells prevailed (a total of 32 %).

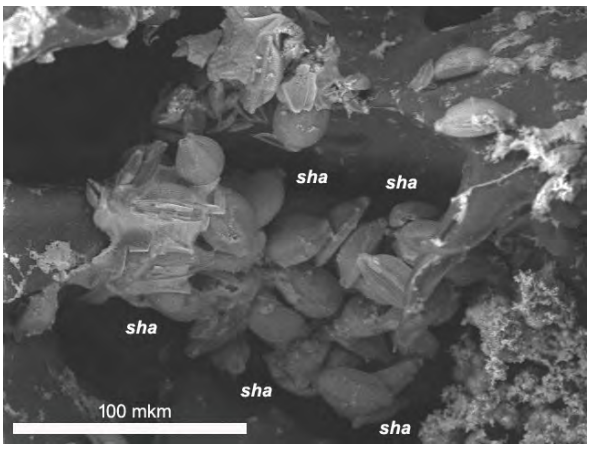

Fig. 13. Dense and compact *Halamphora cymbifera* colonial settlement in the shaded ("cavernous") area (*sha*) of porous UHMWPE microrelief

Conclusion. The results of the experiments on the study of diatom fouling of UHMWPE samples with different surface microrelief structures revealed a number of general characteristics of the process. Surface fouling of smooth UHMWPE did not occur. Samples of porous UHMWPE were colonized by cells with different morphologies: achnantoids (*Karayevia amoena*) and amphoraids (*Halamphora* spp.), which have different mechanisms of adhesion to the substrate surface, but have shown common strategies for accustoming samples differing in microrelief. For species of similar sizes (*K. amoena* and *H. coffeaeformis*, size class of ≈ 10–18 μm), three common successive stages of colonial settlements formation were revealed: 1) primary colonization chains, with the help of which the cells settled on the substrate; 2) secondary, or planar, colonization chains; 3) open, or "cloak-like", settlements formed from "spots".

The first and second stages of colonization spread mainly along the protruding elements of the microrelief, and the third stage – in relatively flat areas or areas speckled with tiny, densely arranged folds, where each cell was attached immediately to two or three folds. In the areas with the densest folding or with a relatively smooth surface, both species formed extensive "cloak-like" settlements, being the most abundant on the "hills" and "lobes" rising above the general level of the frontal surface. In all samples, where the minimum repeating area of the folded surface was comparable with the size of the cells [from ≈ 10 : 1 to ≈ (50…100) : 1], the formation of "spots" from a more or less certain number of cells was noted, with their location repeating microrelief features and forming "cloak-like" settlements.

For *K. amoena*, the ability to modify UHMWPE surface was noted for the first time – due to extremely tight attachment of cells to the substrate and, as a result, due to stretching of this surface with an increase in the number of cell rows. In some cases, the modification was expressed in point stretching of marginal zones of the smallest flat areas suitable for the growth of open settlements. In other cases, the transformation consisted of squeezing of area surface in the form of a ring and of further formation of a "pot" with convex walls. On the surface of the sample with minimal folding, *H. coffeaeformis* (size class of ≈ 10–18 μm) used shaded areas for large compact settlements – along cavern edges, in dents along the bends of the "blades", and on narrow isthmuses between the caverns. In this case, minimum relatively homogeneous area significantly exceeded the area of the cells of this size class, and they preferred the areas protected from water movement and direct lighting. Larger *H. cymbifera* cells (size class of ≈ 30–35 μm) with minimal folding also went into "shadow", but used more comparable areas at the bottom of shallow caverns.

Thus, it was revealed that during the colonization of various samples of porous UHMWPE, diatoms form stable settlements, tightly associated with the surface, the morphology of which is closely related to the features of surface microrelief. With appropriate processing of composites obtained, which allows us to get rid of the organic content of diatom cells and to clean their shells, it becomes possible to obtain UHMWPE samples with a stably biomineralized surface, the total area of which is several orders of magnitude larger than that of the original surface.

This work was partially supported by the grants of the Royal Society of London (No. IEC/R2/170223) and of the Russian Foundation for Basic Research (No. 19-55-80004).

REFERENCES

1. Azovsky A. I. *Prostranstvenno-vremennye masshtaby organizatsii morskikh donnykh soobshchestv*. [dissertation]. Moscow : MGU, 2003, 291 p. (in Russ.)
2. Artham T., Doble M. Biodegradation of aliphatic and aromatic polycarbonates. *Macromolecular Bioscience*, 2008, vol. 8, iss. 1, pp. 14–24. https://doi.org/10.1002/mabi.200700106
3. Bukhtiyarova L. N. Additional data on the diatom genus *Karayevia* and a proposal to reject the genus

Kolbesia. *Nova Hedwigia, Beiheft*, 2006, vol. 130, pp. 85–96.

4. Carson H. S., Nerheim M. S., Carroll K. A., Eriksen M. The plastic-associated microorganisms of the North Pacific Gyre. *Marine Pollution Bulletin*, 2013, vol. 75, iss. 1–2, pp. 126–132. https://doi.org/10.1016/j.marpolbul.2013.07.054
5. Dussud C., Hudec C., George M., Fabre P., Higgs P., Bruzaud S., Delort A.-M., Eyheraguibel B., Meistertzheim A.-L., Jacquin J., Cheng J., Callac N., Odobel Ch., Rabouille S., Ghiglione J.-F. Colonization of non-biodegradable and biodegradable plastics by marine microorganisms. *Frontiers in Microbiology*, 2018, vol. 9, article 1571 (13 p.). https://doi.org/10.3389/fmicb.2018.01571
6. Eich A., Mildenberger T., Laforsch C., Weber M. Biofilm and diatom succession on polyethylene (PE) and biodegradable plastic bags in two marine habitats: Early signs of degradation in the pelagic and benthic zone? *PLoS ONE*, 2015, vol. 10, no. 9, article e0137201 (16 p.). https://doi.org/10.1371/journal.pone.0137201
7. Fisher J., Dunbar M. J. Towards a representative periphytic diatom sample. *Hydrology and Earth System Sciences*, 2007, vol. 11, iss. 1, pp. 399–407. https://doi.org/10.5194/hess-11-399-2007
8. Freedman D., Diaconis P. On the histogram as a density estimator: L_2 theory. *Zeitschrift für Wahrscheinlichkeitstheorie und Verwandte Gebiete*, 1981, vol. 57, iss. 4, pp. 453–476.
9. *GUR® UHMW-PE ultra high molecular weight polyethylene.* URL: https://www.celanese.com/engineered-materials/products/gur-uhmw-pe.aspx (accessed 01.06.2020).
10. Kingston J. C. Araphid and monoraphid diatoms. In: *Freshwater Algae of North America. Ecology and Classification* / J. D. Wehr, R. G. Sheath (Eds). San Diego : Academic Press, 2003, pp. 595–636.
11. Levkov Z. *Amphora* sensu lato. In: *Diatoms of Europe* / H. Lange-Bertalot (Ed.). Ruggell : A. R. G. Gantner Verlag K. G., 2009, vol. 5, 916 p.
12. Maksimkin A. V., Kaloshkin S. D., Tcherdyntsev V. V., Chukov D. I., Stepashkin A. A. Technologies for manufacturing ultrahigh molecular weight polyethylene based porous structures for bone implants. *Biomedical Engineering*, 2013, vol. 47, no. 2, pp. 73–77. https://doi.org/10.1007/s10527-013-9338-5
13. Maksimkin A. V., Senatov F. S., Anisimova N. Yu., Kiselevskiy M. V., Zalepugin D. Yu., Chernyshova I. V., Tilkunova N. A., Kaloshkin S. D. Multilayer porous UHMWPE scaffolds for bone defects replacement. *Materials Science and Engineering: C*, 2017, vol. 1, no. 73, pp. 366–372. https://doi.org/10.1016/j.msec.2016.12.104
14. Mejdandžić M., Ivanković T., Pfannkuchen M., Godrijan J., Pfannkuchen D. M., Hrenović J., Ljubešić Z. Colonization of diatoms and bacteria on artificial substrates in the northeastern coastal Adriatic Sea. *Acta Botanica Croatica*, 2015, vol. 74, iss. 2, pp. 407–422. https://doi.org/10.1515/botcro-2015-0030
15. Nenadović T., Šarčević T., Čižmek H., Godrijan J., Pfannkuchen D. M., Pfannkuchen M., Ljubešić Z. Development of periphytic diatoms on different artificial substrates in the Eastern Adriatic Sea. *Acta Botanica Croatica*, 2015, vol. 74, iss. 2, pp. 377–392. https://doi.org/10.1515/botcro-2015-0026
16. Penna A., Magnani M., Fenoglio I., Fubini B., Cerrano C., Giovine M., Bavestrello G. Marine diatom growth on different forms of particulate silica: Evidence of cell/particle interaction. *Aquatic Microbial Ecology*, 2003, vol. 32, iss. 3, pp. 299–306. https://doi.org/10.3354/ame032299
17. Richard C., Mitbavkar S., Landoulsi J. Diagnosis of the diatom community upon biofilm development on stainless steels in natural freshwater. *Scanning*, 2017, article 5052646 (13 p.). https://doi.org/10.1155/2017/5052646
18. Round F. E., Crawford R. M., Mann D. G. *Diatoms: Biology and Morphology of the Genera.* Cambridge : Cambridge University Press, 1990, 747 p.
19. Sala S. E., Sar E. A., Hinz F., Sunesen I. Studies on *Amphora* subgenus *Halamphora* (Bacillariophyta): The revision of some species described by Hustedt using type material. *European Journal of Phycology*, 2006, vol. 41, iss. 2, pp. 155–167. https://doi.org/10.1080/09670260600556609
20. Sheik S., Chandrashekar K. R., Swaroop K., Somashekarappa H. M. Biodegradation of gamma irradiated low density polyethylene and polypropylene by endophytic fungi. *International Biodeterioration*

& Biodegradation, 2015, vol. 105, pp. 21–29. https://doi.org/10.1016/j.ibiod.2015.08.006
21. Senatov F. S., Anisimova N. Yu., Kiselevskiy M. V., Kopylov A. N., Tcherdyntsev V. V., Maksimkin A. V. Polyhydroxybutyrate/Hydroxyapatite highly porous scaffold for small bone defects replacement in the nonload-bearing parts. *Journal of Bionic Engineering*, 2017, vol. 14, iss. 4, pp. 648–658. https://doi.org/10.1016/S1672-6529(16)60431-6
22. Shah A. A., Hasan F., Hameed A., Ahmed S. Biological degradation of plastics: A comprehensive review. *Biotechnology Advances*, 2008, vol. 26, iss. 3, pp. 246–265. https://doi.org/10.1016/j.biotechadv.2007.12.005
23. Tokiwa Y., Calabia B. P., Ugwu C. U., Aiba S. Biodegradability of plastics. *International Journal of Molecular Sciences*, 2009, vol. 10, iss. 9, pp. 3722–3742. https://doi.org/10.3390/ijms10093722
24. Totti C., Cucchiari E., De Stefano M., Pennesi C., Romagnoli T., Bavestrello G. Seasonal variations of epilithic diatoms on different hard substrates, in the northern Adriatic Sea. *Journal of the Marine Biological Association of the United Kingdom*, 2007, vol. 87, iss. 3, pp. 649–658. https://doi.org/10.1017/S0025315407054665
25. Xing Y., Yu L., Wanga X., Jiaa J., Liua Y., Hec J., Jia Z. Characterization and analysis of *Coscinodiscus* genus frustule based on FIB-SEM. *Progress in Natural Science: Materials International*, 2017, vol. 27, iss. 3, pp. 391–395. https://doi.org/10.1016/j.pnsc.2017.04.019
26. Zettler E. R., Mincer T. J., Amaral-Zettler L. A. Life in the “plastisphere”: Microbial communities on plastic marine debris. *Environmental Science and Technology*, 2013, vol. 47, iss. 13, pp. 7137–7146. https://doi.org/10.1021/es401288x

ОСОБЕННОСТИ ФОРМИРОВАНИЯ КОЛОНИАЛЬНЫХ ПОСЕЛЕНИЙ МОРСКИХ БЕНТОСНЫХ ДИАТОМЕЙ НА ПОВЕРХНОСТИ СИНТЕТИЧЕСКОГО ПОЛИМЕРА

Ф. В. Сапожников[1], А. И. Салимон[2], А. М. Корсунский[2,3], О. Ю. Калинина[1,4], Ф. С. Сенатов[5], Е. С. Статник[2], Ю. Цветинович[2]

[1]Институт океанологии имени П. П. Ширшова РАН, Москва, Российская Федерация
[2]Сколковский институт науки и технологии, Москва, Российская Федерация
[3]Оксфордский университет, Оксфорд, Соединённое Королевство
[4]Московский государственный университет имени М. В. Ломоносова, Москва, Российская Федерация
[5]Национальный исследовательский технологический университет «МИСиС», Москва, Российская Федерация
E-mail: *fil_aralsky@mail.ru*

Тема взаимодействий пластика и природных сообществ к настоящему времени актуальна как никогда прежде. Постепенное накопление изделий из искусственных полимеров и их фрагментов в природной среде достигло того уровня, при котором уже невозможно не считаться с влиянием этих материалов на живые организмы. В первую очередь воздействию подвергаются сообщества микроорганизмов, населяющих разные биотопы (как водные, так и наземные). Эти существа находятся на переднем крае взаимодействия с пластиком, в том числе в морских экосистемах. Тем не менее для понимания данных процессов необходимо принимать во внимание несколько аспектов таких взаимодействий: влияние разных видов пластика на сообщества микроорганизмов через выделение в среду продуктов их разложения, формы использования пластика самими микроорганизмами, в том числе механизмы колонизации его поверхности, а также возможные процессы биодеструкции полимеров за счёт деятельности микроорганизмов. При этом разные виды пластика могут отличаться не только механической прочностью, но и устойчивостью к биодеструкции, вызываемой микроорганизмами. Эксперименты с колонизацией поверхности видов пластика, разных по составу и механической прочности, позволяют получить широкий спектр

результатов, актуальных не только для понимания современных природных процессов с участием пластика: эти результаты важны и для применения в некоторых областях развития технологий (например, при создании композитных материалов). В частности, представляют большой интерес исследования форм и механизмов устойчивой колонизации особо прочных полимеров видами диатомовых водорослей из состава природных сообществ. За счёт обрастания поверхности особо прочных синтетических полимеров диатомеями возможно формирование единого диатомово-полимерного композита, общие свойства которого уже существенно отличаются от свойств полимера как такового. Например, при обрастании полимера диатомеями, плотно удерживающимися на его поверхности за счёт физиологических механизмов, обеспечивающих им надёжную фиксацию, суммарная площадь поверхности композита возрастает на 2–3 порядка по сравнению с таковой голого полимера. Такие композиты и их свойства формируются за счёт механизмов колонизации субстратов, используемых диатомеями из естественных морских ценозов, — при перенесении этих механизмов на новый, перспективный для заселения диатомеями материал. Возможности практического применения этих композитов лежат в сфере тепло- и звукоизоляции, а также в области создания протезирующей ткани при операциях на костях. В наших экспериментах отслежены последовательности развития устойчивого композита при колонизации диатомеями поверхности образцов особо прочного синтетического полимера, стойкого к коррозии. Процесс заселения образцов происходил на базе сообществ, сформированных в накопительных культурах из природной морской среды. Образцы сверхвысокомолекулярного полиэтилена низкого давления (СВМПЭ) с гладкой и пористой структурой поверхности (с открытой ячейкой, до 80 объёмных % пористости) были подвергнуты колонизации диатомовыми водорослями *Karayevia amoena* (Hust.) Bukht., 2006, *Halamphora coffeaeformis* (C. Agardh) Levkov, 2009 и *Halamphora cymbifera* (W. Greg.) Levkov, 2009. Лабораторные эксперименты продолжались три недели. Накопительные культуры микрофитов, на базе которых проводили эксперименты, были получены из Балтийского моря (район г. Балтийска, Россия) и Аравийского моря (район г. Мумбаи, Индия). Типы и стадии развития колониальных поселений на различных элементах микрорельефа фронтальной поверхности и в подлежащих полостях изучали с помощью сканирующего электронного микроскопа на образцах, подвергнутых постадийной термической сушке. Отдельные клетки *K. amoena*, *H. coffeaeformis* и *H. cymbifera*, их цепочковидные агрегаты и распростёртые колониальные поселения занимают различные по степени неоднородности элементы поверхности микрорельефа, образуя структуры мощностью в 1–2 слоя со средней высотой поселения 1–1,3 высоты единичной особи. Клетки *K. amoena* плотно фиксируются на полимерном субстрате, используя поровый аппарат нижней створки панциря. При этом наблюдения с помощью сканирующего электронного микроскопа выявили отпечатки панцирей на субстрате, являющиеся признаками внедрения полимерной подложки в ареолы гипотеки. Рассмотрены механизмы распространения диатомей трёх указанных видов по различным элементам поверхности СВМПЭ, а также формирования характерных элементов колониальных поселений, в том числе для *K. amoena* — последовательно в форме «горшков» и сфер, посредством взаимодействия с поверхностью полимера и её растяжения по мере нарастания количества плотно прикреплённых клеток в колониальном поселении.

Ключевые слова: диатомеи, диатомовые водоросли, Bacillariophyta, колонизация пластика, СВМПЭ, устойчивые материалы, пластик в морской среде, аквакультура

1871
ИнБЮМ – IBSS

Морской биологический журнал
Marine Biological Journal
2020, vol. 5, no. 2, pp. 105–108
https://doi.org/10.21072/mbj.2020.05.2.09

NOTES

UDC 593.8:535

RESPONSE OF *MNEMIOPSIS LEIDYI* LARVAE TO LIGHT INTENSITY CHANGES

© 2020 **Iu. S. Baiandina**

A. O. Kovalevsky Institute of Biology of the Southern Seas of RAS, Sevastopol, Russian Federation
E-mail: *sepulturka@mail.ru*

Received by the Editor 24.12.2019; after revision 24.12.2019;
accepted for publication 26.06.2020; published online 30.06.2020.

A possible response to light of larvae of Black Sea ctenophore *Mnemiopsis leidyi* of two age groups (first to fourth day and one-two weeks after hatching) was experimentally studied. The larvae were placed in a Petri dish with seawater, in which two areas (light and dark) were created using a light source and a black opaque background. The number of larvae in each area was recorded for an hour after the start of the experiment. It was found that on average 77 % of the early stage larvae (first to fourth day) migrated to the dark area after an hour. We hypothesized that *Mnemiopsis leidyi* early stage larvae have negative phototaxis. Similar response of the older larvae (one-two weeks) was not recorded.

Keywords: *Mnemiopsis leidyi*, ctenophore, larvae, phototaxis, migration

Ctenophores are planktonic predatory gelatinous marine animals. The species *Mnemiopsis leidyi* belongs to the order Lobata. The animals of this order move using ctenes of cilia, which create water current. Synchronous movement of the cilia is coordinated by the nervous system [6]. The complex of the aboral organ is the main sensory structure of the animal; it controls movement and, possibly, is a light sensor.

The development of *Mnemiopsis leidyi* is direct. However, after hatching, the larva passes the cydippid planktonic stage (body length 0.3 cm (when hatching) to 3 cm); the larva has a pair of long branching tentacles and actively moves in a water column (Fig. 1). During development of *Mnemiopsis* larva, its body structure becomes similar to an adult sexually mature individual (3 to 15 cm): tentacles are reduced, and typical long lobes appear [4].

Modern taxonomists consider that Ctenophora are a “sister taxon” in relation to all other Metazoa; the development of their nervous and muscular systems is unique [3]. Identification of the presence of behavioral reactions to light intensity changes of ctenophore larvae is important for understanding the operation of these systems.

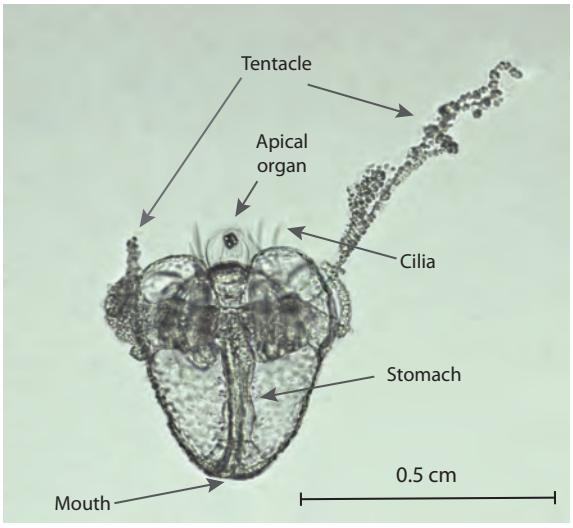

Fig. 1. *Mnemiopsis leidyi* larvae on the first day after hatching

Previously, Schnitzler *et al.* [5] performed a comprehensive analysis of the genes involved in the production and absorption of light in *Mnemiopsis leidyi* larvae; it was shown that the expression of opsin genes, which are involved in light perception, occurs in the apical sensory organ, namely, in nerve ciliary cells. A joint localization of the expression of photoprotein genes and two opsin genes in developing *Mnemiopsis leidyi* photocytes was also revealed. The authors suggested that there is a connection between bioluminescence and phototaxis in ctenophores, and photocytes probably not only emit, but also perceive light [5].

According to the results of the study [1], it was suggested that one of the factors stimulating *Mnemiopsis leidyi* to perform vertical migrations is the avoidance of bright light (over 10 $\mu E \cdot m^{-2} \cdot sec^{-1}$). It was found that only small animals (up to 22 mm) perform migrations. The authors consider the animals swim to the upper layers following food objects only in the night, while in the daytime they swim down avoiding sunlight.

Information on laboratory experiments aimed at studying the response of ctenophores to the light has not been found in the literature.

The aim of this work is to study the effect of light intensity changes on the behavior of ctenophore larvae.

MATERIAL AND METHODS

Adult *Mnemiopsis leidyi* individuals were collected from the sea from IBSS mooring (Karantinnaya Bay, Sevastopol) in September 2019. The animals were brought to the laboratory, placed in 5-L containers with seawater (5–7 animals per container) and left overnight in a darkened room. In the morning, the appearance of eggs and larvae was observed. On the first day after hatching, the larvae were moved with a pipette into separate 0.5-L glass beakers. The experiments were carried out on larvae in the early stages of development (first to fourth day). They were kept in room temperature seawater (+22 °C); food objects were not introduced. For each subsequent experiment, we selected larvae, which were not involved in previous ones.

A small Petri dish (10 cm in diameter, 1 cm high) filled with filtered seawater was placed on the frosted glass above a light source – a LED element installed at a distance, at which the water in the dish did not heat up. A black opaque background was placed under the dish, so that one its half was darkened, and the other one remained completely illuminated (Fig. 2). An impenetrable plastic partition was installed at the light – dark border. Totally, 20 *Mnemiopsis* larvae were placed on the side of the illuminated area, and then the partition was removed. We observed larvae behavior for an hour after the start of the experiment and counted larvae number in dark and illuminated dish areas. The experiments were carried out within four days after larvae hatching, 5 replicates per day; in total, 20 experiments.

During the 110th cruise of RV “Professor Vodyanitsky” (4–20 October, 2019), in the Sea of Azov 1-cm to 2-cm larvae were sampled (the estimated larvae age is one to two weeks). The reactions to light were studied under the same experimental conditions in the laboratory of biodiversity and functional genomics of the World Ocean (hereinafter BiFGWO) onboard the vessel. Totally, 10 experiments were conducted.

RESULTS AND DISCUSSION

Observations of the behavior of early stage larvae within an hour after the start of the experiment showed that within the first 30 minutes, the larvae migrate throughout the entire dish volume, and after 1 hour about 77 % move into the dark area, avoiding bright light (Table 1).

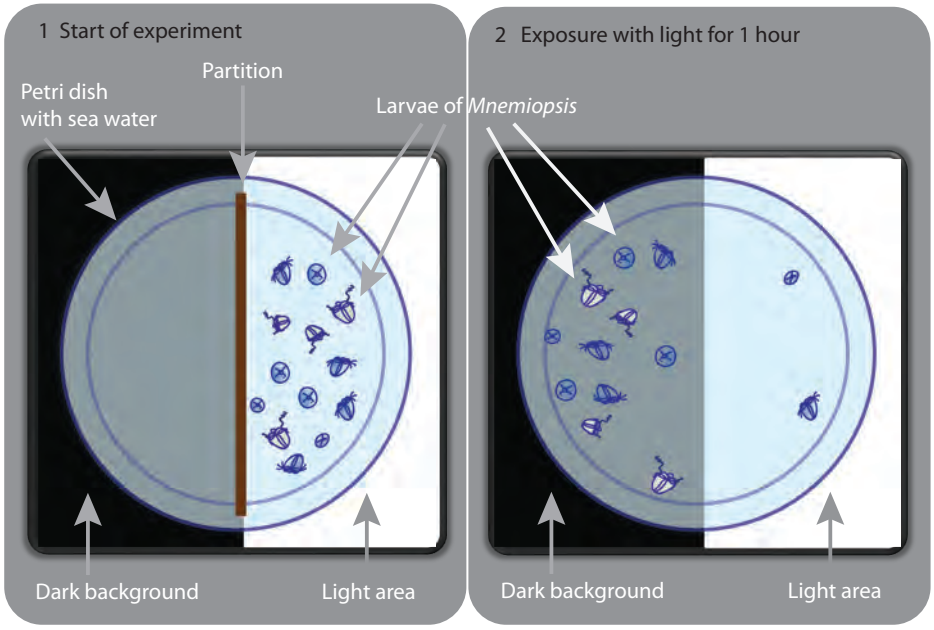

Fig. 2. Scheme of the experiment.
1 – start of the experiment: the Petri dish with seawater is placed above the light source, a black opaque background is placed under one half of the dish, a partition is installed at the light – dark border, *Mnemiopsis* larvae are placed in the light area.
2 – exposure of larvae in a dish without partition for one hour after the start of the experiment

Table 1. Percentage of larvae in the dark area of the Petri dish within one hour after the start of the experiments

Age of larvae, days	*n*	Percentage of larvae in the dark area, %
1	5	85
2	5	64
3	5	76
4	5	83
For all the time	**20**	**77**

The response of early stage larvae to light intensity change does not manifest itself immediately, but over time. A rapid light intensity change triggers a cascade of internal processes of the animal, which takes a certain time. It is known that phototaxis mechanism of all eukaryotes includes three main stages [2]:

1) light absorption and primary reactions in photoreceptors;

2) transformation of stimuli and transmission of signals to the motor apparatus;

3) change in movement.

Thus, it can be assumed that *Mnemiopsis leidyi* larvae in the early stages of development have negative phototaxis.

For older larvae, it was not possible to reliably establish the presence of a response to light. In some experiments, almost all the larvae migrated to the dark area of the dish within an hour; in others, they occupied the entire dish volume and did not move even two hours after the start of the experiment.

Due to the fact that *Mnemiopsis leidyi* larvae perform vertical migrations in water column, the larger larvae may not have enough water in the Petri dish to move freely. To identify their possible response to light intensity changes, other experimental conditions are necessary.

This work was carried out within the framework of government research assignment of IBSS "Structural and functional organization, productivity, and sustainability of marine pelagic ecosystems" (No. AAAA-A18-118020790229-7) and "Patterns of formation and anthropogenic transformation of biodiversity and biological resources of the Sea of Azov – the Black Sea basin and other parts of the World Ocean" (No. AAAA-A18-118020890074-2).

Acknowledgement. The author thanks leading engineer of IBSS laboratory of BiFGWO Kirin M. P. for adult ctenophores sampling and delivery to the laboratory; IBSS plankton department employee Dotsenko V. S. – for *Mnemiopsis* larvae sampling in the 110th cruise of RV "Professor Vodyanitsky"; senior researcher of IBSS laboratory of BiFGWO PhD Krivenko O. V. – for valuable recommendations while writing this scientific note.

REFERENCES

1. Haraldsson M., Båmstedt U., Tiselius P., Titelman J., Aksnes D. L. Evidence of diel vertical migration in *Mnemiopsis leidyi*. *PLoS One*, 2014, vol. 9, iss. 1, article e86595 (10 p.). https://doi.org/10.1371/journal.pone.0086595
2. Jekely G. Evolution of phototaxis. *Philosophical Transactions of the Royal Society B: Biological Sciences*, 2009, vol. 364, iss. 1531, pp. 2795–2808. https://doi.org/10.1098/rstb.2009.0072
3. Moroz L., Kevin L., Kocot M., Citarella M. R. et al. The ctenophore genome and the evolutionary origins of neural systems. *Nature*, 2014, vol. 510, no. 7503, pp. 109. https://doi.org/10.1038/nature13400
4. Rapoza R., Novak D., Costello J. H. Life-stage dependent, *in situ* dietary patterns of the lobate ctenophore *Mnemiopsis leidyi* Agassiz, 1865. *Journal of Plankton Research*, 2005, vol. 27, no. 9, pp. 951–956. https://doi.org/10.1093/plankt/fbi065
5. Schnitzler C. E., Pang K., Powers M. L., Reitzel A. M., Ryan J. F., Simmons D., Tada T., Park M., Gupta J., Brooks S. Y., Blakesley R. W., Yokoyama S., Haddock S. H. D., Martindale M. Q., Baxevanis A. D. Genomic organization, evolution, and expression of photoprotein and opsin genes in *Mnemiopsis leidyi*: A new view of ctenophore photocytes. *BMC Biology*, 2012, vol. 10, pp. 107. https://doi.org/10.1186/1741-7007-10-107
6. Tamm S. L. Cilia and the life of ctenophores. *Invertebrate Biology*, 2014, vol. 133, iss. 1, pp. 1–46. https://doi.org/10.1111/ivb.12042

РЕАКЦИЯ ЛИЧИНОК *MNEMIOPSIS LEIDYI* НА ИЗМЕНЕНИЕ ОСВЕЩЁННОСТИ

Ю. С. Баяндина

Федеральный исследовательский центр «Институт биологии южных морей имени А. О. Ковалевского РАН», Севастополь, Российская Федерация

E-mail: *sepulturka@mail.ru*

Экспериментально изучены возможные реакции на свет личинок черноморского гребневика *Mnemiopsis leidyi* двух возрастных групп (первые-четвёртые сутки и одна-две недели после вылупления). Личинок помещали в ёмкость с морской водой, в которой с помощью источника света и непрозрачного фона создавали две световые зоны (свет и тень); количество личинок регистрировали в каждой зоне в течение часа после начала эксперимента. Показано, что в среднем 77 % личинок, находящихся на ранних стадиях развития (первые-четвёртые сутки), через час мигрируют в тёмную область. Высказано предположение о наличии отрицательного фототаксиса у ранних личинок *Mnemiopsis leidyi*. Подобные реакции у более взрослых личинок (одна-две недели) не обнаружены.

Ключевые слова: *Mnemiopsis leidyi*, гребневик, личинки, фототаксис, миграции

1871
ИнБЮМ – IBSS

Морской биологический журнал
Marine Biological Journal
2020, vol. 5, no. 2, pp. 109–111
https://doi.org/10.21072/mbj.2020.05.2.10

UDC 595.142.2(262.5)

THE FINDING OF A RARE IN THE BLACK SEA POLYCHAETE *CTENODRILUS SERRATUS* (SCHMIDT, 1857) (ANNELIDA, CIRRATULIDAE)

© 2020 **E. V. Lisitskaya and N. A. Boltachova**

A. O. Kovalevsky Institute of Biology of the Southern Seas of RAS, Sevastopol, Russian Federation
E-mail: *e.lisitskaya@gmail.com*

Received by the Editor 21.11.2019; after revision 13.02.2020;
accepted for publication 26.06.2020; published online 30.06.2020.

In July 2019, three polychaetae specimens of the genus *Ctenodrilus* were found in oyster cages on silted oyster shells. The cages from a mussel-and-oyster farm located at the outer roadstead of Sevastopol Bay were suspended at a depth of 6–8 m. The bottom soil under the mussel-and-oyster farm is silted sand, and the depth is of 16 m. During the sampling, water temperature was of +23 °C, and the salinity was of 17.7 ‰. Thus, according to morphological characteristics, polychaetae we found should be classified as *Ctenodrilus serratus* (Schmidt, 1857). Photographs of alive and fixed polychaetae, chaetae patterns, and a schematic representation of their number by segments are presented. At the beginning of the XX century, a single specimen of this species was found in the Black Sea.

Keywords: polychaetae, *Ctenodrilus serratus* (Schmidt, 1857), Black Sea

There is only one known representative of the subfamily Ctenodrilinae of the family Cirratulidae in the Black Sea – *Ctenodrilus serratus* (Schmidt, 1857) [2 ; 3]. At the beginning of the XX century, a single specimen of this species was found in Sevastopol Bay in the fouling of a pipe near the military hospital at a depth of 1 m [1]. The respective specimen was probably lost. There were no further observations of this species in the Black Sea. All references to its presence in Black Sea fauna [2 ; 3] have been based on the first mention.

In July 2019, three specimens of polychaetae genus *Ctenodrilus* were found in oyster cages on silted oyster shells. The cages from the mussel-and-oyster farm located at the outer roadstead of Sevastopol Bay (44°37′13.3″N, 33°30′07.1″E) were suspended at a depth of 6–8 m. The substrate under the farm is silted sand, and the depth is of 16 m. During the sampling, water temperature was of +23 °C, and the salinity was of 17.7 ‰. Optical microscopes Mikmed-5, MBS-9, and Olympus CX-41 were used to identify these specimens. The photographs were taken by cameras Canon Digital IXUS 90 IS and Sony Cyber-Shot 16.2. Gathered material is lodged in IBSS RAS collection (IBSS-POL / Cirratulidae / No. 7).

The polychaetes have 11–12 segments; their body width is of 0.12–0.13 mm, and the length is of 1.25–1.5 mm (Fig 1A, B). Alive specimens: translucent body with a greenish tint; black-purple dots throughout the body; red intestines visible. Fixed specimens in 4 % formalin solution: light-green; with red stomach.

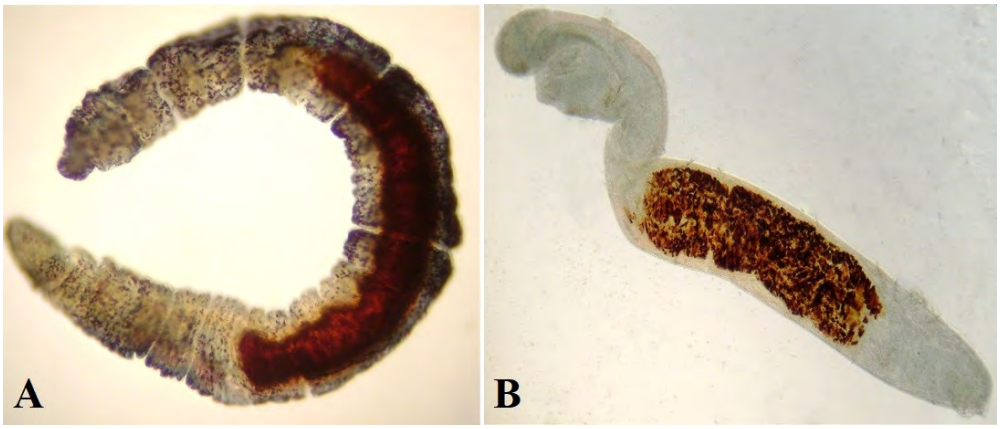

Fig. 1. *Ctenodrilus serratus* (IBSS-POL / Cirratulidae / No. 7): A – alive specimen; B – formalin-fixed specimen

Prostomium round-conical. Eyes, head appendages, and gills absent. Prostomium and peristomium ciliated ventrally. Peristomium and last segment without chaetae. Parapodia not developed; chaetae in two bundles come directly from body side. All chaetae simple, of the same shape – distally expanded. Expanded part of hooks on one side has 5–6 large triangular teeth; all teeth of nearly the same size (Fig. 2A). Variable number (1 to 4) of chaetae is in the noto- and neuropodial bundles in different chaetigers (Fig. 2B). Intestine with an expansion from chaetiger 3 to the beginning of chaetiger 6. Pygidium rounded, without cirri.

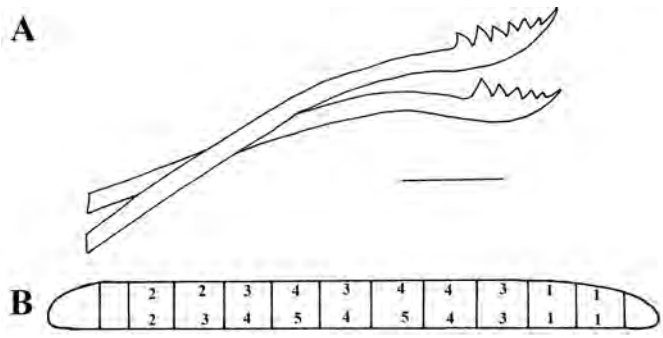

Fig. 2. A – chaetae of observed speciemen *Ctenodrilus serratus*, scale bar 10 μm; B – schematic representation of the number of chaetae in chaetigers of *C. serratus* in notopodia (upper row) and neuropodia (lower row)

Morphological characteristics of the polychaetes we have found fit the description of *Ctenodrilus serratus* (Schmidt, 1857) [5]. The subfamily Ctenodrilinae includes two genera – *Aphropharynx* Wilfert, 1974 and *Ctenodrilus* Claparède, 1863. The main difference between these genera is chaetal morphology. *Aphropharynx* representatives have three types of simple chaetae: trichoid, serrated with small teeth, and serrated with large teeth, whereas *Ctenodrilus* representatives have only one type of chaetae – hooks [7 ; 8].

The genus *Ctenodrilus* includes four species. Validity of one of them (*Ctenodrilus paucidentatus* Ben-Eliahu, 1976) is doubtful. *Ctenodrilus parvulus* Scharff, 1887 is characterized by the presence of only smooth chaetae without teeth [4]. Recently described species *Ctenodrilus pacificus* Magalhães, Weidhase, Schulze & Bailey-Brock, 2016 from the Pacific Ocean (Hawaii) is morphologically quite similar to *C. serratus*, and main differences between these species are found at the molecular level [4].

C. serratus is the most common species of the genus *Ctenodrilus*. According to numerous indications of its presence in various water areas (Pacific, Atlantic oceans to Mediterranean Sea, English Channel, and Helgoland), this species appears to be spread worldwide. Due to lack of molecular data in most reports, it is not known whether this species is a cosmopolitan one or a complex of potentially cryptic species. Representatives of the genus *Ctenodrilus* found in oyster cages of a farm in South Africa and identified as *C. serratus* according to molecular studies were identical to *C. serratus* from the North Sea [6].

Taking into account that molecular studies of Black Sea *Ctenodrilus* have not been carried out, the specimens we found can be tentatively classified as *C. serratus*.

This work was carried out within the framework of government research assignments of IBSS "Investigation of the mechanisms of controlling production processes in biotechnological complexes with the aim of developing the scientific foundations for the production of biologically active substances and technical products of marine genesis" (No. AAAA-A18-118021350003-6) and "Patterns of formation and anthropogenic transformation of biodiversity and biological resources of the Sea of Azov – the Black Sea basin and other parts of the World Ocean" (No. AAAA-A18-118020890074-2).

REFERENCES

1. Jakubova L. I. List of Archannelidae and Polychaeta of the Sevastopol Bay of the Black Sea. *Izvestiya Akademii nauk SSSR*, 1930, no. 9, pp. 863–881. (in Russ.)
2. Kisseleva M. I. *Polychaetes (Polychaeta) of the Black and Azov Seas* / Russian Academy of Sciences, Murmansk Marine Biological Institute, Kola Science Centre. Apatity, 2004, 409 p. (in Russ.)
3. Kurt-Şahin G., Çinar M. E. A check-list of polychaete species (Annelida: Polychaeta) from the Black Sea. *Journal of the Black Sea / Mediterranean Environment*, 2012, vol. 18, no. 1, pp. 10–48. https://doi.org/10.3906/zoo-1405-72
4. Magalhães W. F., Weidhase M., Schulze A., Bailey-Brock J. H. Taxonomic remarks on the genus *Ctenodrilus* (Annelida: Cirratulidae) including description of a new species from the Pacific Ocean. *Zootaxa*, 2016, vol. 4103, no. 4, pp. 325–343. https://doi.org/10.11646/zootaxa.4103.4.2
5. Schmidt O. Zur Kenntnis der Turbellaria, Rhabdocoela und einiger anderer Wuermer des Mittelmeeres. *Sitzungsberichte der Kaiserliche Akademie der Wissenschaften, Wien, Mathematisch-Naturwissenschaftliche Klasse*, 1857, vol. 23, no. 2, pp. 347–366.
6. Weidhase M., Bleidorn Ch., Simon C. A. On the taxonomy and phylogeny of *Ctenodrilus* (Annelida: Cirratulidae) with a first report from South Africa. *Marine Biodiversity*, 2016, vol. 46, no. 1, pp. 243–252. https://doi.org/10.1007/s12526-015-0355-3
7. Wilfert M. Ein Beitrag zur Morphologie, Biologie und systematischen Stellung des Polychaeten *Ctenodrilus serratus*. *Helgoländer wissenschaftliche Meeresuntersuchungen*, 1973, vol. 25, iss. 2–3, pp. 332–346.
8. Wilfert M. *Aphropharynx heterochaeta* nov. gen. nov. spec., ein neuer polychaet aus der familie Ctenodrilidae Kennel 1882. *Cahiers de Biologie Marine*, 1974, vol. 15, no. 4, pp. 495–504.

ОБНАРУЖЕНИЕ РЕДКОГО ДЛЯ ЧЁРНОГО МОРЯ ВИДА ПОЛИХЕТ *CTENODRILUS SERRATUS* (SCHMIDT, 1857) (ANNELIDA, CIRRATULIDAE)

Е. В. Лисицкая, Н. А. Болтачева

Федеральный исследовательский центр «Институт биологии южных морей имени А. О. Ковалевского РАН», Севастополь, Российская Федерация
E-mail: *e.lisitskaya@gmail.com*

В июле 2019 г. в устричных садках на заиленных створках устриц обнаружены 3 экземпляра полихет рода *Ctenodrilus*. Садки с мидийно-устричной фермы, расположенной на внешнем рейде бухты Севастопольская, были подвешены на глубине 6–8 м. Грунт под фермой — заиленный песок, глубина — 16 м. Температура воды во время отбора материала составляла +23 °С, солёность — 17,7 ‰. Найденные полихеты по морфологическим признакам отнесены к виду *Ctenodrilus serratus* (Schmidt, 1857). Представлены фотографии живой и фиксированной полихеты, рисунки щетинок и схема их количества по сегментам. Данный вид в Чёрном море был отмечен единственный раз в начале XX века.

Ключевые слова: полихеты, *Ctenodrilus serratus* (Schmidt, 1857), Чёрное море

1871
ИнБЮМ – IBSS

Морской биологический журнал
Marine Biological Journal
2020, vol. 5, no. 2, pp. 112–114
https://mbj.marine-research.org

CHRONICLE AND INFORMATION

TO THE ANNIVERSARY OF ACADEMICIAN OF THE RAS VIKTOR EGOROV

This year, Viktor Egorov, IBSS Supervisor, Academician of the Russian Academy of Sciences, D. Sc., Prof., Editor-in-Chief of "Marine Biological Journal", celebrates the anniversary. He developed the theory of mineral metabolism between marine organisms and the aquatic environment, discovered jet methane gas emissions from the bottom of the Black Sea, and created the basics of the biophysical theory of the ecological capacity of the marine environment in relation to pollutants. Viktor Egorov is the author of more than 360 articles and 6 monographs.

Staff of IBSS radiation and chemical biology department congratulates Viktor Egorov on his jubilee! We are proud to work in a team with the author of scientific discoveries and the outstanding scientist who has made a significant theoretical and practical contribution to the study of homeostasis of marine ecosystems.

At present, V. Egorov, D. Sc., Prof., Academician of the Russian Academy of Sciences (since 2016) and the National Academy of Sciences of Ukraine (since 2012), is the Supervisor of A. O. Kovalevsky Institute of Biology of the Southern Seas of RAS.

From the age of 18, attention of Viktor Egorov, native of Sevastopol, was riveted to the sea: at the beginning while working on fishing vessels in the Caspian Sea, then while modeling the dynamics of the movement of atomic submarines in the Sevastopol Higher Naval Engineering School, and since 1968 – in IBSS. Through competitive selection, V. Egorov first entered functioning of marine ecosystems department headed by Corresponding Member of the Academy of Sciences of the Ukrainian SSR Tamara Petipa, and later – radiation and chemical biology department headed by Gennady Polikarpov.

Over the years of work, Viktor Egorov has been steadily growing professionally. In 1968–1970, he was a senior engineer; then, until 1980, – a junior researcher. In 1975, he defended his candidate dissertation brilliantly and became a PhD with a degree in geophysics (sea physics). Then, he worked as a senior researcher; in 1983, he became the head of the laboratory of dynamic radiochemoecology. In 1988, he defended his doctoral dissertation in radiobiology. In 1989–1993, he was IBSS deputy director. At the same time (1991), he received a ship's wheel (a symbol of the head of RCBD) from G. Polikarpov, Academician of the National Academy of Sciences of Ukraine. Heading the department at the difficult time (1990s), V. Egorov always made strategically correct decisions and overcame difficulties.

Gennady Polikarpov passes the ship's wheel (a symbol of the head of RCBD) to his student, scientific follower, and successor Viktor Egorov

During those difficult years, he proved himself to be a talented organizer of international marine research and the head of a creative scientific team. Thanks to him, 16 international grants were received for studying the Black Sea, and expeditionary work, financed by the European Union, the International Atomic Energy Agency, and intergovernmental funds, was realized. As a result of such cooperation, the scientific using of RV "Professor Vodyanitsky" was provided, and up to 70 % of marine expeditionary work of the NAS of Ukraine on the Black Sea was organized for the fulfilling in 1992–2005.

In the World Ocean science, Viktor Egorov has priority in several directions. These are the development of the theory of mineral metabolism between marine organisms and the aquatic environment, the management of research and the generalization of their results on the response of the Black Sea to the Chernobyl disaster, the discovery of jet methane gas emissions from the bottom of the Black Sea in the late 1980s, which caused a sensation in the scientific world and laid the foundation for many years of research on this phenomenon. He created the basics of the biophysical theory of the ecological capacity of the marine environment in relation to pollutants. The conditions of the stability of the system of biotic self-purification of the photic layer of seawaters were studied using mathematical models. It was shown that water anthropogenic pollution increase can lead to a change from the first to zero order of the metabolic rate of pollutant exchange by marine organisms, as well as to saturation of the sorbing surfaces of inert and bioinert substances. At the same time, the system of complex biogeochemical self-purification of waters can lose stability, which results in an increase in the content of pollutants in the aquatic environment up to levels leading to toxic effects on marine organisms.

The results of V. Egorov's scientific research are recognized worldwide. He is the author of 365 articles (more than 70 of them are published abroad) and 6 monographs highly valued and regularly cited by colleagues. Under his supervision, the students defended seven PhD dissertations on biogeochemistry of pollutants of different nature in marine ecosystems, as well as the methane problem. In the arsenal of pedagogical influences of Viktor Egorov, a talented teacher and a delicate person, there are no methods of coercion. He involves in work, sets a personal example, conveys not only his knowledge, but also his life experience, skills and abilities, shows interest in the work of students on all the stages, and contributes to their professional growth.

V. Egorov is an unrivalled storyteller. His memories of sea expeditions always cause genuine interest and amaze with lots of vivid details. He participated in 45 research cruises, of which he headed 22 (16 international). During scientific expeditions and business trips, he visited 53 countries of the world, was in 24 seas of the Atlantic, Indian and Pacific oceans, and completed a circumnavigation.

Since his childhood, Viktor Egorov was fond of fishing, and years later he became the owner of a boat, on which, for many years, together with colleagues from RCBD and other departments of IBSS, he took samples of water, hydrobionts, and benthic sediments in Sevastopol coastal areas from Cape Lucullus to Cape Fiolent. In one of "Antares" expeditions, jet methane gas emissions in Sevastopol coastal waters were discovered by the hydroacoustic method.

"Antares" boat crew after an expedition to Sevastopol coastal waters. Left to right: V. Popovichev, S. Gulin, N. Stokozov, "Antares" skipper V. Egorov, L. Malakhova, I. Moseychenko

We are pleased to have the opportunity to study Viktor Nikolaevich's colossal capacity for work, scientific intuition, and his brilliant human qualities – steadfast optimism and amazing sense of humor. With all our hearts, we wish good health to the hero of the day and his loved people, prosperity, happiness, new achievements in scientific work, and worthy students and followers!

Staff of IBSS radiation and chemical biology department

К ЮБИЛЕЮ АКАДЕМИКА РАН ВИКТОРА НИКОЛАЕВИЧА ЕГОРОВА

В мае 2020 г. исполнилось 80 лет Виктору Николаевичу Егорову — и. о. научного руководителя ФИЦ ИнБЮМ, академику Российской академии наук, доктору биологических наук, профессору, главному редактору «Морского биологического журнала». В. Н. Егоров разработал теорию минерального обмена между морскими организмами и водной средой, открыл струйные метановые газовыделения со дна Чёрного моря, создал основы биофизической теории экологической ёмкости морской среды в отношении загрязняющих веществ. Виктор Николаевич — автор более чем 360 статей и 6 монографий.

ISSN 2499-9768
20002
9 772499 976005 >

Вниманию читателей!

Институт биологии южных морей имени А. О. Ковалевского РАН, Зоологический институт РАН

издают научный журнал

Морской биологический журнал
Marine Biological Journal

- МБЖ — периодическое издание открытого доступа. Подаваемые материалы проходят независимое двойное слепое рецензирование. Журнал публикует обзорные и оригинальные научные статьи, краткие сообщения и заметки, содержащие новые данные теоретических и экспериментальных исследований в области морской биологии, материалы по разнообразию морских организмов, их популяций и сообществ, закономерностям распределения живых организмов в Мировом океане, результаты комплексного изучения морских и океанических экосистем, антропогенного воздействия на морские организмы и экосистемы.
- Целевая аудитория: биологи, экологи, биофизики, гидро- и радиобиологи, океанологи, географы, учёные других смежных специальностей, аспиранты и студенты соответствующих научных и отраслевых профилей.
- Статьи публикуются на русском и английском языках.
- Периодичность — четыре раза в год.
- Подписной индекс в каталоге «Пресса России» — Е38872. Цена свободная.

Заказать журнал

можно в научно-информационном отделе ИнБЮМ. Адрес: ФГБУН ФИЦ «Институт биологии южных морей имени А. О. Ковалевского РАН», пр. Нахимова, 2, г. Севастополь, 299011, Российская Федерация.
Тел.: +7 8692 54-06-49.
E-mail: *mbj@imbr-ras.ru*.

A. O. Kovalevsky Institute of Biology of the Southern Seas of RAS, Zoological Institute of RAS

publish scientific journal

Морской биологический журнал
Marine Biological Journal

- MBJ is an open access, peer reviewed (double-blind) journal. The journal publishes original articles as well as reviews and brief reports and notes focused on new data of theoretical and experimental research in the fields of marine biology, diversity of marine organisms and their populations and communities, patterns of distribution of animals and plants in the World Ocean, the results of a comprehensive studies of marine and oceanic ecosystems, anthropogenic impact on marine organisms and on the ecosystems.
- Intended audience: biologists, ecologists, biophysicists, hydrobiologists, radiobiologists, oceanologists, geographers, scientists of other related specialties, graduate students, and students of relevant scientific profiles.
- The articles are published in Russian and English.
- The journal is published four times a year.
- The subscription index in the “Russian Press” catalogue is E38872. The price is free.

You may order the journal

in the Scientific Information Department of IBSS. Address: A. O. Kovalevsky Institute of Biology of the Southern Seas of RAS, 2 Nakhimov avenue, Sevastopol, 299011, Russian Federation.
Tel.: +7 8692 54-06-49.
E-mail: *mbj@imbr-ras.ru*.